

**APPLICATION OF RECOMBINANT ANTIBODY
TECHNOLOGY FOR THE DEVELOPMENT OF ANTI-LIPID
ANTIBODIES FOR TUBERCULOSIS DIAGNOSIS**

CONRAD CHAN EN ZUO

NATIONAL UNIVERSITY OF SINGAPORE

2013

APPLICATION OF RECOMBINANT ANTIBODY
TECHNOLOGY FOR THE DEVELOPMENT OF ANTI-LIPID
ANTIBODIES FOR TUBERCULOSIS DIAGNOSIS

CONRAD CHAN EN ZUO
BSc. (Hons.), MRes. Imperial College London

A THESIS SUBMITTED
FOR THE DEGREE OF DOCTOR OF PHILOSOPHY


DEPARTMENT OF MICROBIOLOGY

NATIONAL UNIVERSITY OF SINGAPORE
2013

DECLARATION

I hereby declare that this thesis is my original work and it has been written by me in its entirety. I have duly acknowledged all the sources of information which have been used in the thesis.

This thesis has also not been submitted for any degree in any university previously



Conrad Chan En Zuo

5th August 2013

Acknowledgements

The work here would not have been possible without the assistance of so many people. Firstly, to A/Prof Paul MacAry and Dr. Brendon Hanson, my co-supervisors, thank you for your encouragement, advice, support and the opportunity to carry out research in a very exciting field. Also to my collaborators with whom I had the privilege of working with over these five years; From NUS: Dr Timothy Barkham, Dr Seah Geok Teng, Prof Markus Wenk, Dr Anne Bendt, Dr Amaury Cazenave-Gassiot; From FIND: Dr Gerd Michel, From Max Planck Institute Berlin: Prof Peter Seeberger & Sebastian Gotze, From Georgia: Dr Nestan Tukvadze and the staff of the TB Institute, Dr Mason Soule and Dr Mzia Kutateladze, I really appreciate the sharing of your scientific expertise and efforts. A special note of thanks to those in Georgia, who made my trip a real pleasure. To all my fellow colleagues at DSO National Laboratories, Annie, Steve, Angeline, Shyue Wei, De Hoe, Grace and Shirley, thanks for all your assistance and encouragement and for covering all the stuff I could not do. The same to my fellow students & colleagues in PAM Lab especially those in the Lipid Squad: Omedul and Yanting, as well as Fatimah for doing all those admin stuff that we hate to do. I would also like to acknowledge the support of DSO National Laboratories for providing the scholarship to support my studies. Finally, to God, for His innumerable blessings and provision along the way; and to my family and especially my wife Sally, this is as much your success as it is mine.

Table of Contents

Acknowledgements	1
Table of Contents	ii
Summary	viii
List of Tables	x
List of Figures	xi
List of Abbreviations	xiv
List of Publications & Patents	xvii
Chapter 1: Introduction	1
1.1 Tuberculosis pathology, epidemiology, prevention and treatment	2
1.2 Methods for TB diagnosis	7
1.2.1 Detection of host immune responses- X-rays, TST and IGRA	8
1.2.2 Direct microbiological detection – Acid-fast stain, microbial culture and Nucleic acid amplification tests	9
1.3 TB diagnostics in resource-poor settings	12
1.3.1 Improving current diagnostics for resource-poor countries	13
1.3.2 Potential point-of care diagnostics for resource-poor countries.....	15
1.4 Anti-lipid antibodies.....	18
1.4.1 Lipids as disease biomarkers	18
1.4.2 Recombinant phage display	20
1.4.3 Recombinant antibody expression	21

1.5 Lipid biomarkers for TB diagnostics.....	23
1.5.1 Lipoarabinomannan	25
1.5.2 LAM diagnostics.....	29
1.5.3 Mycolic acid.....	31
1.6 Aims of this thesis.....	35
1.6.1 Optimize expression of full length IgG in <i>E. coli</i>	36
1.6.2 Develop antibodies targeting the <i>Mtb</i> lipids Lipoarabinomannan and mycolic acid	36
1.6.3 Thoroughly characterize anti-LAM/anti-mycolic acid antibodies.....	37
1.6.4 Determine the diagnostic utility of the antibodies	37
Chapter 2: Materials and methods	38
2.1 Buffers and solutions	39
2.2 Construction of antibody expression vectors	42
2.2.1 Construction of mammalian expression vectors.....	42
2.2.2 Construction of bacterial expression vectors.....	43
2.2.3 Construction of chimeric antibody constructs	43
2.2.4 Sub-cloning of antibody heavy and light chains by restriction digest and ligation.....	46
2.3 Expression and purification of bacterial IgG.....	46
2.3.1 Initial periplasmic expression in BL21 or HB2151	46
2.3.2 Small scale optimization of bacterial IgG expression conditions	47
2.3.3 Large-scale expression and purification of bacterial IgG.....	47

2.4 Expression and purification of mammalian IgG and Fab	48
2.5 Polyacrylamide gels and western blot.....	50
2.6 Measurement of protein concentration	50
2.7 Bacterial strains and culture	51
2.8 Phage display	52
2.8.1 Negative selection panning against ManLAM	52
2.8.2 Lipid panning against mycolic acid.....	53
2.8.3 Phage recovery after each round of panning	54
2.8.4 Screening of phage libraries.....	55
2.9 Carbohydrate microarrays	57
2.10 Immunofluorescence and acid fast-staining.....	58
2.11 Collection and processing of bacterial cultures for ELISA	59
2.11.1 Bacterial supernatants and whole cell suspension for LAM ELISA	59
2.11.2 Lipid extraction from bacterial cultures for mycolic acid ELISA	60
2.12 Collection of clinical samples for ELISA.....	61
2.12.1 Spiked whole blood and serum samples for LAM ELISA	61
2.12.2 TB patient selection criteria and sample collection procedure.....	62
2.12.3 Clinical patient serum samples for LAM ELISA	63
2.12.4 Clinical patient urine samples for LAM ELISA	63
2.12.5 Clinical patient sputum samples for LAM ELISA	63
2.12.6 Clinical patient sputum samples for mycolic acid ELISA	64

2.13 ELISAs.....	64
2.13.1 Comparison of functional IgG levels in bacterial lysate and determination of purified bacterial IgG affinity curves by indirect ELISA.....	64
2.13.2 Indirect phage polyclonal and monoclonal ELISAs	66
2.13.3 Indirect monoclonal IgG ELISA against LAM or lipids	67
2.13.4 Determination of chimeric antibody affinity binding curves.....	68
2.13.5 Determination of limit of sensitivity for anti-mycolic acid antibodies	69
2.13.6 Indirect sandwich ELISA on purified LAM, bacterial suspensions and culture supernatants.....	69
2.13.7 Determination of anti-LAM antibody titres in healthy serum samples.....	70
2.13.8 Indirect sandwich ELISA on spiked or patient clinical samples	71
2.13.9 Indirect ELISA on patient lipid extracts.....	71
2.14 Mass spectrometric profiling and quantification of mycolic acids.	72
2.15 Data analysis and statistics.....	73
Chapter 3: Optimization of IgG expression in bacteria	74
3.1 Introduction	75
3.2 Preliminary expression in two common <i>E. coli</i> bacterial strains.....	76
3.3 Optimization of expression in small scale culture	78
3.4 Comparison of yield by large scale expression.....	83
3.5 Comparison of bacterial and mammalian expressed IgG	85
3.6 Discussion	87
Chapter 4: Generation of anti-ManLAM antibodies by phage display	91

4.1 Introduction	92
4.2 Panning of the Humanyx phage library	93
4.3 Monoclonal screening and identification of my2F12	95
4.4 Characterization of my2F12 specificity	97
4.5 Expression of my2F12 in bacteria.....	101
4.6 Discussion	105
Chapter 5: Optimization of my2F12 antibody and sample processing for diagnostic use	108
5.1 Introduction	109
5.2 Design and expression of my2F12 chimeric antibodies.....	111
5.3 Characterization of my2F12 chimeric antibody avidity	114
5.4 Identification of pathogenic mycobacteria with chimeric my2F12 by immunofluorescence microscopy	115
5.5 Identification of pathogenic mycobacteria with chimeric my2F12 by sandwich ELISA	120
5.6 Enhancing the sensitivity of my2F12 ELISA on spiked serum samples.....	122
5.7 Discussion	127
Chapter 6: Generation of anti-mycolic acid antibodies by phage display	131
6.1 Introduction	132
6.2 Isolation of mycolic acid-specific antibodies	133
6.3 Characterization of mycolic acid antibody specificity and sensitivity	137
6.4 Optimization of mycolic acid extraction protocol	142
6.5 Determination of species specificity.....	146

6.6 Determination of CFU limit of detection	147
6.7 Discussion	149
Chapter 7: Validation of antibodies on clinical samples.....	155
7.1 Introduction.....	156
7.2 Optimization of assay antibody concentration.....	158
7.3 Testing of clinical samples for ManLAM	159
7.4 Analysis of results by individual patient groups	164
7.5 Analysis of combined data.....	166
7.6 Conversion of mc3 to chimeric antibody for diagnostic use	170
7.7 Testing of clinical patient samples for mycolic acid.....	173
7.8 Discussion	174
Chapter 8: Discussion & Conclusion	180
Bibliography	190

Summary

Tuberculosis (TB) is the most significant infectious disease afflicting human populations (1). The causative agent is *Mycobacterium tuberculosis* (*Mtb*), a bacterium capable of surviving in an intracellular niche after uptake by phagocytic cells in the respiratory system (2,3). Infection can be asymptomatic, resulting in latent TB infection (LTBI), with a 10% chance of re-activation throughout life (4). Active disease can occur in any organ in the body but typically presents as a persistent pulmonary infection which is also the principle site of pathogen entry (2). The burden of disease falls disproportionately on low- and middle-income countries, primarily in Asia and Africa, which account for 85% of all cases worldwide (1). Nevertheless, TB remains a treatable disease although it requires a prolonged course of antibiotic therapy-over six months, with an 85% success rate (1). In high-income countries, a combination of diagnostic methodologies including the tuberculin skin test (TST, also known as Mantoux test), chest X-rays, sputum culture and the ubiquitous sputum smear acid-fast stain, Interferon-gamma release assay (IGRA) and nucleic acid amplification test (NAAT), has enabled medical authorities to assess infection accurately and initiate treatment rapidly, hence preventing spread of infection (5,6). With additional resources to carry out contact tracing and treat LTBI, tuberculosis incidence is extremely low (5).

However, in low-income countries, a lack of funding, infrastructure, and trained medical personnel severely limits the ability of their health care systems to deliver efficient and accurate diagnostic services and currently an estimated third of new TB infections are undiagnosed (1). This translates into a vital requirement for a

low-cost, infrastructure-independent, point-of-care diagnostic that requires minimal training to use and hence can be easily deployed in resource-poor settings. It has been estimated that such a diagnostic with 100% sensitivity and specificity could save 625000 lives annually (7). Antibody-based detection of *Mtb* derived biomarkers is ideal, but the utility of antibody based assays targeting *Mtb* proteins remains unproven (8). *Mtb* lipid biomarkers are another suitable class of targets due to their resistance to degradation and presence in a variety of clinical samples, but the lack of T cell help required for an effective B cell immune response and the insolubility of many lipid antigens has made the generation of highly specific, high affinity antibodies using traditional hybridoma technology challenging (9). The advent of recombinant antibody phage display allows for the selection of such antibodies *in vitro* without a requirement for an immune response (10,11). We have therefore explored antibody phage display for the generation of high affinity, highly specific antibodies against two potential TB lipid biomarkers: lipoarabinomannan (LAM), a soluble highly branched glycolipid reportedly found in patient urine; and mycolic acid, an insoluble long chain fatty acid present in high quantities in TB patient sputum samples (12,13). High affinity antibodies with diagnostic potential were generated against both targets. In this study, we detail their derivation and thorough characterization. Testing against clinical samples indicated that our anti-LAM antibody had significant sensitivity in the smear-negative, HIV negative cohort. We also describe our efforts to develop novel inexpensive production methodologies for these antibodies in *E. coli* as current methods rely primarily upon expensive mammalian expression.

List of Tables

Table 4-1: Binding characteristics of monoclonals from 3rd Pan.....	96
Table 4-2: CDR sequences of isolated monoclonal my2F12.....	97
Table 6-1: Binding characteristics of monoclonals from 4 th Pan.....	134
Table 6-2: CDR sequences of isolated anti-mycolic antibodies.....	135
Table 7-1: Specificity and sensitivity from combination of assay results on different clinical sample types.	166

List of Figures

Figure 1-1: Location of the various current direct detection TB diagnostics in a typical health care system.	13
Figure 1-2: Structure of the mycobacterial cell wall.....	24
Figure 1-3: Structure of lipoarabinomannan	26
Figure 1-4: Structure of the three main classes of mycolic acid in <i>Mtb</i>	32
Figure 3-1: Design of the bacterial IgG expression vector.....	76
Figure 3-2: Periplasmic extract of bacterial IgG expressed in two different <i>E. coli</i> strains.....	77
Figure 3-3: Variations in wet cell mass under different inductions conditions.....	80
Figure 3-4: Levels of fully assembled or functional bacterial IgG obtained under different induction conditions.....	82
Figure 3-5: Purification of bacterial IgG on Protein A and Protein L.....	84
Figure 3-6: Coomassie gel of purified bacterial IgG	86
Figure 3-7: Comparison of mammalian and bacterial culture expressed IgG affinity	87
Figure 4-1: Panning of Humanyx antibody phage library against ManLAM.....	94
Figure 4-2: Diversity of monoclonals from the enriched 3 rd Pan.....	96
Figure 4-3: ManLAM-specificity of isolated monoclonal my2F12	97
Figure 4-4: Mycobacterial specificity of ManLAM specific antibody my2F12.....	98
Figure 4-5: my2F12 specificity for α 1-2 mannose linkages	100
Figure 4-6: Lack of my2F12 binding to other oligosaccharides	101
Figure 4-7: Wet cell mass obtained during expression of my2F12 bacterial IgG....	102
Figure 4-8: Levels of fully assembled or functional my2F12 bacterial IgG obtained under different induction conditions.....	103
Figure 4-9: Large scale expression and purification of my2F12 bacterial IgG	104
Figure 5-1: Design and expression of my212 chimeric variants	113
Figure 5-2: Variation in binding affinity of different my2F12 chimeric antibodies....	115

Figure 5-3: Phylogenetic distribution and diagnostic characteristics of various mycobacterial species	116
Figure 5-4: my2F12 immunofluorescent staining for slow-growing mycobacteria ..	118
Figure 5-5: Lack of my2F12 immunofluorescent staining for fast-growing mycobacteria or non-mycobacterial species	119
Figure 5-6: Lack of my2F12 immunofluorescent staining for common throat bacteria	120
Figure 5-7 Specificity of chimeric my2F12 for various mycobacterial species	122
Figure 5-8: Influence of serum anti-LAM antibodies on my2F12 assay sensitivity .	124
Figure 5-9: Improvement in assay sensitivity by heat and proteinase K denaturation of serum anti-LAM antibodies.....	126
Figure 6-1: Panning of Humanyx antibody phage library against mycolic acid.....	134
Figure 6-2: Expression of four unique antibodies from the 4 th Pan.....	136
Figure 6-3: Confirmation of mycolic acid specificity of four isolated monoclonal IgGs	136
Figure 6-4: Lipid specificity of four anti-mycolic acid antibodies	139
Figure 6-5: Limit of detection for various classes of mycolic acids	141
Figure 6-6: Determination of optimal lipid extraction method	143
Figure 6-7: Identification of mycolic acids in lipid extract by mass spectrometry	145
Figure 6-8: Bacterial species specificity of anti-mycolic acid antibodies.....	146
Figure 6-9: Sensitivity of anti-mycolic acid antibodies for whole mycobacteria	148
Figure 7-1: Optimization of capture and detector antibody concentration	159
Figure 7-2: Detection of ManLAM in TB patient sputum samples	161
Figure 7-3: Detection of ManLAM in TB patient serum samples	162
Figure 7-4: Detection of ManLAM in TB patient urine samples	163
Figure 7-5: Sensitivity of optimized my2F12 sandwich assay for individual patient groups	165

Figure 7-6: Sensitivity and specificity rates obtained using combination of absorbance values (OD) from different clinical sample types.....	168
Figure 7-7: Sensitivity and specificity rates obtained from combination of absorbance from urine (100µl sample at 15min TMB) and serum (100µl sample at 30min TMB)	169
Figure 7-8: Design and expression of mc3 chimeric variants	171
Figure 7-9: Avidity and specificity of engineered chimeric mc3	172
Figure 7-10: Detection of mycolic acid in TB patient sputum.....	173

List of Abbreviations

AraLAM	arabinose-capped lipoarabinomannan
ATCC	American Type Culture Collection
BCG	<i>Mycobacterium bovis</i> strain Bacille Calmette-Guérin
CDR	complementarity determining region
CFP-10	Culture filtrate protein-10kDa
CFU	colony forming units
CH1	antibody constant domain-1
DAPI	4',6-diamidino-2-phenylindole (DNA binding fluorescent dye)
DC	dendritic cell
DIC	differential interference contrast
DMPA	dimyristoyl phosphatidic acid
DMPC	dimyristoyl phosphocholine
DNA	deoxyribonucleic acid
DOTS	Directly Observed Therapy- Short Course
EBNA-1	Epstein-Barr virus nuclear antigen -1
EDTA	ethylenediaminetetraacetic acid (chelating agent)
ELISA	enzyme-linked immunosorbent assay
ESAT-6	Early secreted antigen-6kDa
Fab	Fragment antigen binding
FcR(n)	Fc (fragment crystallisable) receptor (neonatal)
FcγR	Fc (fragment crystallisable) gamma receptor
HEPES	4-(2-hydroxyethyl)-1-piperazineethanesulfonic acid (buffering reagent)
HIV	Human Immunodeficiency Virus
HR-MS/MS	High resolution tandem mass spectrometry

HRP	horseradish peroxidase
IF	immunofluorescence
IGRA	Interferon-gamma (γ) release assay
IHC	immunohistochemistry
IMAC	Immobilized metal affinity chromatography
LAM	lipoarabinomannan
LAMP	loop-mediated isothermal amplification
LED	Light emitting diode
LTBI	Latent tuberculosis infection
ManLAM	mannose-capped lipoarabinomannan
MDR-TB	Multi-drug resistant tuberculosis
MOI	multiplicity of infection
MHC	major histocompatibility complex
MRM	multiple reaction monitoring
<i>Mtb</i>	<i>Mycobacterium tuberculosis</i>
NAAT	Nucleic acid amplification test
OD	optical density
PAGE	polyacrylamide gel electrophoresis
PBS	phosphate buffered saline
PCR	polymerase chain reaction
PDIM	phthiocerol dimycocerosate
PEG	polyethylene glycol
PILAM	phosphoinositide capped lipoarabinomannan
PIM	phosphatidylinositol mannoside
PMSF	phenylmethylsulfonyl fluoride (protease inhibitor)

PPD	Purified protein derivative (of mycobacterium tuberculosis)
RNA	ribonucleic acid
ROC	receiver operating characteristic
SDS	sodium dodecyl sulphate (protein denaturing agent)
SNR	signal-to-noise ratio
TB	Tuberculosis
TBS	Tris-buffered saline
TDM	trehalose dimycolate
TEMED	tetramethylethylenediamine (polymerizing agent)
TMB	3,3',5,5'-Tetramethylbenzidine (colour developer for ELISA)
TST	Tuberculin skin test
UV	ultraviolet
WHO	World Health Organization
XDR-TB	Extensively-drug resistant tuberculosis

List of Publications & Patents

Chan, C. E., Lim, A. P., Chan, A. H., MacAry, P. A., Hanson, B. J. (2010) Optimized expression of full-length IgG1 antibody in a common *E. coli* strain. *PloS One*. 5(4):e10261.

Islam, M. O., Lim, Y. T., **Chan, C. E.**, Cazenave-Gassiot, A., Croxford, J. L., Wenk, M. R., MacAry, P. A. and Hanson, B. J. (2012) Generation and characterization of a novel recombinant antibody against 15-ketocholestane isolated by phage-display. *Int J Mol Sci*. 13(4): p. 4937-48.

Chan, C. E., Zhao, B. Z., Cazenave-Gassiot, A., Pang, S. W., Bendt, A. K., Wenk, M. R., MacAry, P. A. and Hanson, B. J. (2013) Novel phage display-derived mycolic acid-specific antibodies with potential for tuberculosis diagnosis. *Journal of lipid research*. Epub 2013/06/26

Chan, C. E., Gotze, S., Seah, G. T., Seeberger, P., Wenk, M. R., Hanson, B. J. and MacAry, P. A. Targeting the α -1,2 mannose capping motif on lipoarabinomannan for improved detection of pathogenic mycobacteria. (manuscript in preparation)

Provisional US Patent: Pathogenic mycobacteria-derived mannose-capped lipoarabinomannan antigen binding proteins. Authors: **Chan, C.E.**, Wenk, M.R., Hanson, B.J. and MacAry, P. A.

Provisional US Patent: Recombinant human antibodies specific for mycobacterial methoxy mycolic acid. Authors: **Chan, C.E.**, Wenk, M.R., Hanson, B.J. and MacAry, P. A.

Chapter 1: Introduction

1.1 Tuberculosis pathology, epidemiology, prevention and treatment

Tuberculosis (TB) is one of the oldest diseases known to man, with archaeological evidence from ancient Egypt and historical written records from classical Greece attesting to its presence in the ancient Near East; and in its most common form presents itself as a persistent pulmonary infection (14). It is currently the second most common cause of death due to an infectious disease, with an estimated 1.4 million deaths in 2011, and thus is a major public health concern (1). The causative agent, the bacteria *Mycobacterium tuberculosis* (*Mtb*) was discovered in the late 19th century by Robert Koch, and a number of species of the same genus have subsequently been associated with various skin and lung diseases (14). Pathogenic species of note include *M. avium* and *kansasii*, which are the two species frequently found in non-tuberculous pulmonary infections while *M. marinum* and *ulcerans* typically cause granulomatous lesions and chronic ulcerations of the soft tissue of the skin respectively (15,16). *M. leprae* on the other hand is well known for its association with the historical disease leprosy (17). However, there is a large group of mycobacterial species that are non-pathogenic as well e.g. *M. smegmatis* (18).

Mtb is a non-motile, non-spore forming, aerobic rod-shaped bacillus and is an intracellular pathogen that infects humans as its primary host (2). It cannot be classified as either a true Gram-positive or negative bacteria but is generally termed acid-fast, due to its ability to resist decolourisation with mild acid after staining with various dyes (2). TB is typically acquired via inhalation of *Mtb* contaminated aerosol droplets generated by the coughing of patients with active infection. Once inhaled

into the lung, the invading bacteria are taken up by resident phagocytic cells such as macrophages and dendritic cells. *Mtb* has evolved various methods for evading phagocytic killing including the prevention of phagosome maturation by inhibiting lysosome fusion or acidification, escaping into the cytosol or inactivation of host generated reactive oxygen and nitrogen species by enzymatic breakdown (19). This enables the survival and replication of *Mtb* in this intracellular niche. As the bacilli replicate, the growing infection with associated inflammation attracts additional mononuclear phagocytes which in turn can be infected. Sustained intracellular infection results in the formation of granulomas, which are aggregates of primarily macrophages, but also other immune cells such as neutrophils, monocytes, dendritic cells (DCs), B and T cells and natural killer cells, at the site of infection which seal off the infection and prevent further spread of the bacteria (20). The granuloma, while protecting the host from disseminated disease, also appears to provide the invading pathogen with an environment within which it can survive shielded from further host immune responses. It also impacts upon the penetrance and hence efficiency of antimycobacterial drugs (3).

In most immunocompetent individuals, granuloma formation is the end stage of disease, producing an asymptomatic latent TB infection (LTBI), which is the case for over 90% of infections (4). Currently, it is estimated that one-third (approximately 2 billion individuals) of the world's population has LTBI (1). However, there is a 5% chance of active disease within the first 18 months of infection and a further 5% chance of disease reactivation over the person's remaining lifetime (21). The symptoms of active TB include prolonged coughing, weight loss, fever and night sweats (2,4). Active disease can occur in both immunocompromised and healthy

individuals and is due to release of bacilli from containment in the granuloma (22). This enables further spread in the body and aerosol transmission to other individuals by coughing and expectoration of infectious bacteria. It is unclear what the contributing immunological mechanisms are but two known triggers are depletion of CD4 helper T cells due to HIV infection and TNF α blocking therapy with monoclonal antibodies; and is also associated with anti-inflammatory steroid treatment, malnutrition and diabetes (22).

Prior to the development of antimycobacterial drugs, treatment of tuberculosis was limited to providing rest, good nutrition and fresh air in various spas and sanatoriums (15). Drug treatment of tuberculosis started with the development of streptomycin in 1946, although frequent use has led to drug resistance and hence its discontinuation from first-line usage (23). Currently, four drugs are recommended by the World Health Organization (WHO) for first line use: rifampicin, which interferes with bacterial RNA synthesis; isoniazid, which interferes with mycolic acid synthesis; pyrazinamide, which accumulates in and acidifies the interior of the bacterium; and ethambutol, which inhibits cell wall synthesis by blocking of arabinosyl transferase (23). A combination of all four is given for the first two months and subsequently only rifampicin and isoniazid for next four months to treat active infection(4). Isoniazid is given alone for nine months to treat LTBI. With such a long treatment regime, compliance is important to limit the development of drug resistance; therefore patients are usually required to take their drugs in the presence of an observer, which is termed DOTS (Directly Observed Therapy- Short Course).

Due to lack of compliance, various multi-drug resistant TB (MDR-TB) strains have appeared which are defined as resistance to at least rifampicin and isoniazid. Nonetheless, MDR-TB remains treatable through the careful use of a combination of at least four second line antimycobacterial drugs, which include aminoglycosides (Kanamycin/Amikacin) and fluoroquinolones (ofloxacin/levofloxacin/moxifloxacin) (24). Of greater concern has been the recent appearance of extensively-drug resistant TB (XDR-TB), which is defined by resistance to both rifampicin and isoniazid plus at least one drug in each of the two classes of second line drugs above. XDR-TB is harder to detect and treat due to the need to test for resistance to multiple drugs and find appropriate drugs combinations that are effective, which has led to poorer outcomes associated with such infections (25). It also raises the possibility of the development of TB strains that are totally resistant to current therapy.

The principle vaccine available for TB is based on an attenuated strain of *Mycobacterium bovis*, Bacille Calmette-Guérin (BCG) which is injected as a live vaccine into new-borns and children (26). While moderately protective (73-77% reduction in risk) against severe disseminated TB infection in infants and young children, it offers poor protection (50% average reduction in risk) against pulmonary infection in adults with a wide variation in efficacy from nil to 80% (27,28). The geographic latitude where the individual vaccination studies were conducted accounted for a significant (66%) proportion of the variation, with vaccine efficiency decreasing towards the equator (28). This has been attributed to exposure to environmental non-tuberculosis bacteria, which is more prevalent in lower latitudes, conferring broad anti-mycobacterial immunity and hence minimizing the additional

effect of BCG immunization, or alternatively, limiting the multiplication of the live BGC vaccine and hence development of specific immunity to TB (29,30).

Despite the apparent treatability of both active and latent TB infection, disease transmission remains significant, with an estimated 8.7 million new cases alone in 2011 (1,31). This can primarily be attributed to delayed or missed diagnosis due to the inadequacy of current diagnostic tests, resulting in sustained spread of disease by untreated TB sufferers. A systematic review of TB cases from the pre-antibiotic era indicated an estimated average mortality rate of 70% and 20% within 10 years of infection for sputum smear-positive and negative cases respectively, indicating the deadly outcome of non-treatment which arises from missed diagnosis (32). The World Health Organization (WHO) and other groups have estimated the number of undetected cases, based on actual reported cases and estimated incident rates to be one-third *of all* TB cases, suggesting that there is an urgent requirement for improvement in TB diagnosis particularly in the early stages of active disease (1,33). An additional confounding factor is the increasing proportion of TB patients co-infected with HIV (Human Immunodeficiency Virus), which is estimated to be 13% globally and above 50% in parts of sub-Saharan Africa (1). TB/HIV co-infection leads to a more rapid progression to the fatal disease manifestations and thus requires better early diagnosis; it also reduces the efficacy of a number of widely used diagnostic tools such as sputum smear, X-ray and tests relying on immunological responses such as the tuberculin skin tests (34). As a result, deaths due to TB/HIV make up approximately half of all deaths due to TB despite only comprising a fraction of the total TB infected cohort (1).

1.2 Methods for TB diagnosis

A wide variety of methods are currently used and recommended for the diagnosis of TB or LTBI and can be divided into two general categories: firstly, direct microbiological detection of the pathogen via acid-fast staining, microbial culture or more recently nucleic acid amplification tests (NAATs). Alternatively, diagnosis can be made via detection of specific immune responses, either measuring T cell responses to TB antigen with the tuberculin skin test (TST, also known as Mantoux test) or interferon gamma release assay (IGRA), or formation of granulomatous lesions via chest X-ray (31,35-37). Detection of T cell responses are more typically used to screen for LTBI, as they cannot distinguish between active disease and latent infection (4,38). In resource-rich first world countries, a combination of the above tests have been successfully used to detect and treat both active disease and latent infection and incidence rates are typically in the order of less than 25 per 100,000 in North America and Western Europe in contrast to rates greater than 300 per 100,000 in the most severely afflicted regions of sub-Saharan Africa (1). However, each method has drawbacks in terms of cost, requirements for infrastructure and trained manpower, rapidity and accuracy. While this has minimal effect in resource-rich countries due to well-developed medical infrastructure and manpower, availability of funds for medical diagnostics and ready medical access for the vast majority of the population, these drawbacks, which we describe in detail below, has severely impacted the ability of resource-poor countries to detect, control and treat TB.

1.2.1 Detection of host immune responses- X-rays, TST and IGRA

Chest X-rays are only useful for the detection of the pulmonary form of TB and relies on radiographic visualization of lung granulomatous lesions which appear opaque on film. While X-rays have long been used in first-world countries due to its rapidity and reasonable sensitivity in HIV negative individuals, they have a high false positive rate especially in low burden populations due to its lack of specificity and vulnerability to observer error (31,39). This is evidenced by a cross-sectional study in which 36% of patients with X-rays suggestive of TB could not have their diagnosis confirmed by microbial culture, the most sensitive direct detection method, and 20% of culture-positive patients were not picked up by X-rays (40). This has led to recommendations that any radiological diagnosis of TB be confirmed by direct microbiological detection (35,36).

The tuberculin skin test (TST) is the oldest test that is capable of detecting LTBI, in addition to active TB, and is based on measuring the skin hypersensitivity reaction to subcutaneously injected purified protein derivative (PPD) of *Mtb*. However, as the antigens which are used to trigger the skin reaction can also be found in related mycobacteria, populations vaccinated with BCG often have high false-positive rates (31,41). Also, due to its dependence on a functional immune system, responses are depressed in the HIV positive cohort resulting in a higher false negative rate (42,43). It also requires a repeat visit within a short timeframe to assess the degree of skin response.

A recent improvement is the IGRA, which measures the cytokine response of patients' T cells to TB specific protein antigens based on interferon gamma secretion. Unlike the TST, it relies on TB specific antigens such as ESAT-6 (Early Secreted Antigenic Target-6kDa) and CFP-10 (Culture filtrate protein-10kDa) and so is not likely to trigger a response from individuals vaccinated with BCG or exposed to other mycobacteria. It has shown promise especially on extra-pulmonary samples from which T cells can be isolated, where sensitivity in other rapid assays such as acid-fast staining and NAATs are low (44). However, similar to the TST, it cannot distinguish between latent TB and active disease and also exhibits the same reduced response in the HIV cohort (41,45). Due to these drawbacks, WHO has recommended that the TST and IGRA not be used to diagnose active TB in low and medium income countries, where HIV incidence is higher, although IGRAs remain widely used in high income countries to detect latent TB infection due to their better performance characteristics versus TSTs (38).

1.2.2 Direct microbiological detection – Acid-fast stain, microbial culture and Nucleic acid amplification tests

Direct microbiological detection is regarded as the only means for confirming a case of TB and highly recommended before deciding to initiate therapy (1). This is primarily due to the logistical difficulty and toxicity of treatment (six months of antibiotic therapy) and the lack of specificity for active TB for diagnosis on the basis of symptomology, X-rays or TST/IGRAs alone (35). This is evidenced by the low proportion of microbiologically confirmed TB cases (7-15%) present in a population sample identified by persistent cough alone, the most common symptom (46). The

direct microbiological detection test most widely employed globally (and also the oldest TB diagnostic in use for over 100 years) is the acid-fast stain, where collected specimens are smeared directly onto a slide and stained with Ziehl-Neelsen or Auramine-O dyes to highlight mycobacterial bacilli which are counted under an optical microscope (31). The dyes employed for this assay stain surface mycolic acids—a family of hydrophobic long chain fatty acids highly enriched in mycobacterial cell walls (47). Staining of sputum samples (sputum smear) is the most common form of this assay and is used to confirm a diagnosis of pulmonary TB. However, due to the presence of mycolic acids in all mycobacteria as well as a variety of related actinomycete species, this test cannot directly confirm the presence of *Mtb* (48). However, in high-prevalence areas, the presence of such high concentrations of acid-fast bacilli is considered highly suggestive of TB and sufficient to confirm diagnosis (35).

The sensitivity of sputum smears has been reported to range from 80% to as low as 20%, although the use of centrifugation or sedimentation of liquefied sputum to concentrate the sample or magnetic beads to separate out the tuberculosis bacilli has been shown to increase sensitivity (49-51). This low sensitivity is the primary drawback of this method, with a detection limit of between 5,000-10,000 bacilli/ml of sputum (31). Furthermore, this approach does not allow the identification of drug resistant strains of *Mtb* and also has reduced sensitivity for the HIV positive patient cohort (52). This reduced sensitivity is due to the reduced granuloma cavity formation and sputum production caused by the weak immune response to *Mtb* infection in HIV positive individuals (34).

The current gold standard for TB diagnostics remains the microbial culture test in which the sample is cultured on either specialist solid or liquid media optimized for mycobacterial growth e.g. Löwenstein–Jensen agar or Middlebrook D7H9 broth. It has the highest sensitivity of all current methods with a detection limit as low as 10 bacilli/ml of sputum and is relatively low cost (31). However, there are a number of factors that make this test problematic for TB management. *Mtb* is a slow-growing microbe and thus culture is time consuming, taking typically over one month for a confirmed diagnosis (31). While automated liquid culture systems such as the Bactec MGIT 960 can shorten the time to diagnosis to two weeks with improved sensitivity, it is still much slower than other direct detection methods such as NAATs and acid-fast staining (53,54). Another drawback is that culture cannot immediately determine species as a variety of non-tuberculous mycobacteria can grow in the same media. However, where liquid culture methods do stand out is as follow up tests for drug resistance in combination with the microscopic observation drug susceptibility assay, where mycobacterial growth and cording behaviour is examined under a microscope to rapidly determine drug susceptibility within a week (55,56). Due to their accuracy, such tests are still recommended over DNA based assays for the diagnosis of extensively drug resistant tuberculosis (XDR-TB) (1).

In recent years, nucleic acid amplification tests (NAATs) have been introduced into TB diagnostics and have been shown to be capable of almost equivalent sensitivity and specificity to sputum culture tests (57-60). Its primary disadvantage is its high costs, which make it unsuitable for use in developing countries (31). It also has high infrastructure requirements in terms of lab equipment and reagents. On the other hand, in first world countries, NAATs are routinely carried

out to diagnose TB infections due to their ability to accurately and rapidly (same-day) diagnose both standard and multi-drug resistant tuberculosis (MDR-TB) and is recommended for use alongside culture and acid fast staining (5,36). In particular, line probe assays, in which labelled amplified DNA is hybridized to DNA probes along a strip membrane, are fast and highly accurate (57,61). This has led to WHO recommending these assays for the identification of mycobacterial species and rifampicin and/or isoniazid resistance directly from sputum samples or cultures from smear-negative samples (62).

1.3 TB diagnostics in resource-poor settings

The various methods described above all have significant drawbacks: detection based on host response e.g. X-rays/TST/IGRA suffers from poor specificity, while acid fast staining is insensitive. Culture and NAATs are both sensitive but are slow or expensive respectively. Furthermore, all require significant infrastructural support e.g. electrical power, refrigeration as well as lab equipment e.g. microscopes, incubators, thermal cyclers, and trained medical personnel to carry out the tests and interpret the results. As a result, these tests while readily accessible to the wider public in first-world countries are often limited to the level of the national or regional reference lab in resource-poor third world countries (Fig. 1-1). Even acid-fast staining, which is considered to have the lowest requirements for resources, is not considered to be a true point-of-care test due to its need for trained microscopists and lab equipment and is estimated to be not readily available to up to 60% of the populace in such countries (31).

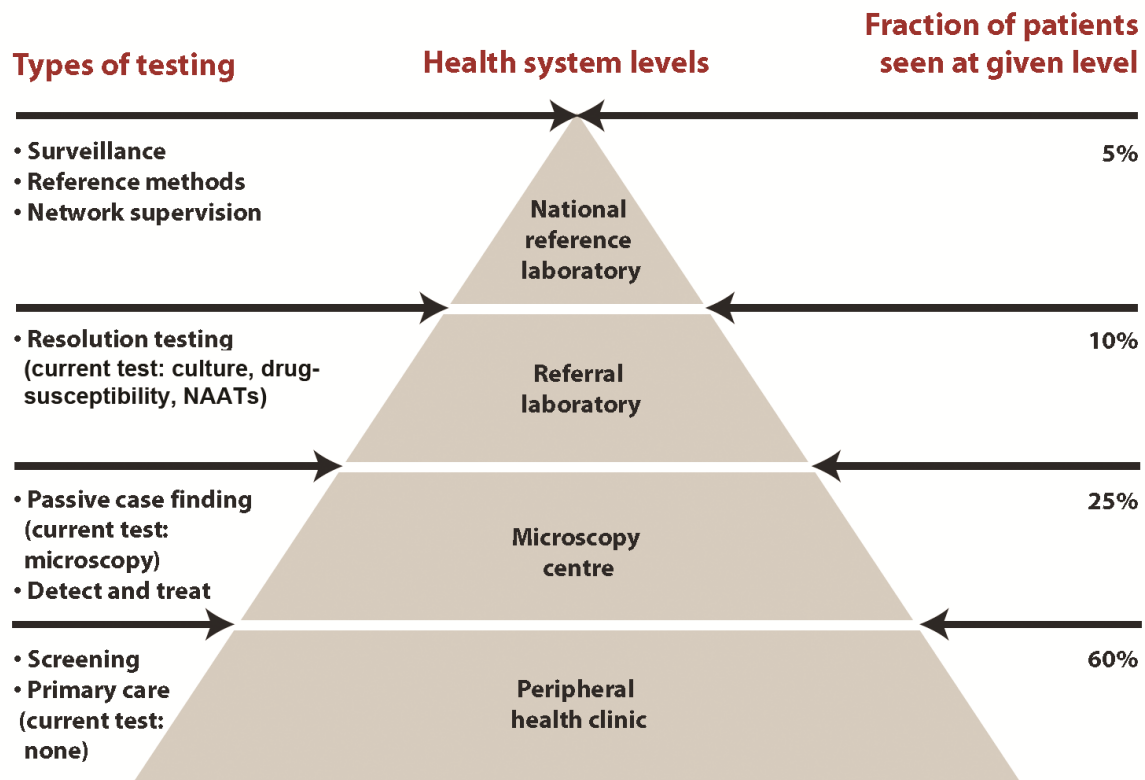


Figure 1-1: Location of the various current direct detection TB diagnostics in a typical health care system.

The ideal point-of-care test would be portable, have no infrastructure or electrical requirements, rapid and sensitive and require little training to operate. No existing test currently meets these requirements. (Adapted from WHO, 2006)

1.3.1 Improving current diagnostics for resource-poor countries

Despite the limitations of these diagnostics, efforts have been made to improve these methodologies for use in resource-poor settings. Recently, the WHO has introduced a global rollout of the Xpert *MTB*/RIF NAAT platform for simultaneous detection of TB infection along with rifampicin resistance for MDR-TB (1,63). It is a self-contained automated disposable cartridge system that combines sputum sample processing, PCR amplification and detection of *Mtb* and rifampicin resistance associated gene sequences. Hence, minimal sample handling and training is

required and this enables the deployment of the system into more rural areas in third world countries where highly trained personnel and sophisticated infrastructure is not available. It has virtually equivalent specificity and sensitivity to sputum culture while allowing for same-day diagnosis with performance better or equal to other commercially available NAATs (64-67). However, it has poorer performance for extra-pulmonary TB diagnosis with sensitivity as low as 25% for lung pleural fluid samples (68).

By recommending a world-wide introduction of a single platform, the Foundation for Innovative New Diagnostics was able to negotiate a reduced price for developing countries at approximately USD\$10 per test in contrast to a price of USD\$65 in the European Union, thus reducing the prime disadvantage of such tests which are high costs (63). Nonetheless, it has been estimated that implementation of this assay in high burden, low-income countries will still require additional funding in spite of the reduced prices given current spending rates on TB healthcare, as implementation of this test to diagnose all suspected TB cases would consume over 80% of the national TB budget of these countries alone (69). This could limit the use of this assay in these countries.

Similarly, efforts to improve the sensitivity of acid-fast staining have led to the development of portable battery powered light emitting diode (LED) fluorescent microscopes. WHO has advocated switching from light to fluorescent microscopy (using Auramine-O dye) as it offers an incremental increase in sensitivity (10%) and also reduces the assay time taken due to the reduction in number of visual fields required to be screened (70-72). This reduced assay turnaround time, in combination

with a recommendation to only test two rather than three samples (due to negligible reduction in sensitivity) has facilitated the introduction of same-day microscopy where diagnosis and initiation of therapy can be carried out in a single visit (73). This is an important factor in third world rural settings when patient access to medical care is limited and inconvenient. However, the increase in sensitivity is not comparable to that achievable by culture and NAATs, and also cannot provide species identification, while the requirements for trained microscopists remain. As such, even in its optimized format, acid-fast stain remains unsuitable as a point-of-care test.

1.3.2 Potential point-of care diagnostics for resource-poor countries

What is required is a point-of-care test that is rapid i.e. sample collection, processing and testing completed in a few hours and allow for same-day treatment, cheap, accurate (>95% specificity and >90% sensitivity) and have minimal infrastructure and training requirements for operation i.e. no need for refrigeration or additional instrumentation, portable and no need for specialized personnel (31). It has been estimated that such a test with 100% sensitivity on pulmonary samples would cut annual deaths by 625000 (or 36% of deaths globally), excluding deaths due to HIV co-infection, drug resistant TB and inadequate drug availability (7). Various diagnostic methodologies have been evaluated to determine if they can meet these requirements.

Serology, which relies on detection of the antibody response against the pathogen, is used for the detection of a variety of other diseases such as HIV and

Hepatitis B (74). Despite the large number of commercially available serological assays available, a recent meta-analysis of published data on their efficacy has reported no significant improvement over sputum smear microscopy (75). Due to the poor reproducibility of data and lack of improvement in sensitivity over sputum smear, WHO has issued a rare blanket recommendation not to use commercial serological assays for the diagnosis of TB (76).

In spite of this, various groups have continued to evaluate new antigens or new combinations of antigens to improve sensitivity and specificity. Recently, a group identified four TB lipolytic enzymes as potential serological markers, out of which one showed 93% and 87% sensitivity for smear-positive and smear-negative culture-positive patient serum samples respectively with over 95% specificity against the negative control population which included both BCG vaccinated and latent TB infected individuals (77). Another group showed that a combination of six novel antigens expressed in combination as fusion proteins could achieve 93% sensitivity (78). However, these studies did not include large numbers of HIV positive individuals, in which assay sensitivity might be lower due to a deficient immune response and thus this platform remains un-validated.

Another diagnostic technology platform that is widely used for other diseases, but has not been developed into a suitable TB diagnostic test is that of antibody-based assays (79). These have been developed in a variety of formats such as plate-based or membrane dot blot ELISAs, lateral flow dipstick tests, and more recently handheld enzymatic electroimmunosensor-type assays (8,80,81). Antibody-based assays are ideal for point of care testing due to their potential low cost, ease

of use, rapidity and low infrastructure requirements; provided sufficient sensitivity and specificity is achieved with the right antibody-detector and antigen-target pair. The range of TB antigen targets include specific single antigens such as lipoarabinomannan, ESAT-6, and MPT64 as well as antibodies raised against antigen mixtures such as culture filtrate protein precipitate, whole cell bacilli or a mix of known TB specific proteins (8,55,81-90) . However, while *Mtb* protein targets have been widely explored, lipid targets found in the bacterial cell envelope have not been as thoroughly investigated for their diagnostic potential in antibody-based assays; principally due to their insolubility in aqueous solution, as well as difficulty in obtaining specific high affinity antibodies. Some advantages of lipid targets include their resistance to extreme temperatures and pH which allows for sterilization of clinical samples in contrast to proteins which are prone to denaturation, and their general high abundance in comparison to individual protein targets, due to the thick glycolipid-based cell envelope of *Mtb*. These represent an interesting source of novel biomarkers for the diagnosis of TB provided suitable antibodies can be identified and developed.

In addition to application of the above methodologies which are widely used for other diagnostic applications, various novel techniques have been developed which may have potential for point-of-care diagnostics in resource-poor settings. One example is loop-mediated isothermal amplification (LAMP), which relies on DNA polymerases with high strand displacement activity and requires no melting step. This obviates the need for a thermal cycler as PCR can be carried out at a single temperature, while also allowing for easy visual readout via fluorescent double stranded DNA binding dyes, although manual sample preparation is still required

(91). Nonetheless, LAMP assays have been successfully carried out in resource-limited settings with minimally trained personnel and achieved sensitivities equivalent to in house PCR assays and better than sputum smears, though still poorer than sputum culture (91-93). Another option that is still in the early stage of technology demonstration and feasibility testing is the detection of volatile *Mtb* derived organic compounds released in breath (94).

1.4 Anti-lipid antibodies

1.4.1 Lipids as disease biomarkers

A number of lipids have been found to be associated with infectious and other diseases which can be detected in patient clinical samples and used as biomarkers. In oncology, elevated levels of plasma lysophospholipids have been associated with ovarian cancer, while oxidized low density lipoprotein and cholesterol in plasma have been associated with atherosclerosis and systemic lupus erythematosus respectively (95-97). In infectious disease, *Mtb* membrane lipids such as lipoarabinomannan (LAM) and mycolic acid have been reportedly found in patient urine and sputum samples respectively (12,13). Current methods for the analysis of lipids include mass spectrometry or high performance liquid/gas chromatography. While these methods are extremely sensitive, accurate and capable of generating detailed data on the various lipid species present, they are also expensive and require sophisticated equipment and data processing (98). As such, they are not ideal for point-of-care diagnostics especially in third world countries. However, they provide important lipidomic profiles which can be used to identify lipid biomarkers that may be exploited for the development of antibody based assays.

Antibodies are ideal diagnostic reagents due to their high affinity and specificity. However, the traditional method for producing antibodies, whether for production of polyclonal sera or monoclonal development relies on an efficient *in vivo* B cell immune response to the antigen to produce high affinity IgGs and requires the involvement of T helper cells to support affinity maturation and class switching in the germinal centre (99,100). This in turn requires presentation of peptide epitopes and as such is only efficacious for proteinaceous targets, which have been extensively exploited for the development of rapid antibody tests (100). For non-proteinaceous biomolecules e.g. carbohydrates, lipids, and small molecules such as drugs and steroids, conjugation to protein carriers can increase the immunogenicity (termed a hapten in these cases) as this enables B cells that bind and endocytose these haptens to concurrently engage T cell help via the protein carrier epitopes displayed on MHC class II molecules (9).

Antibodies have also been successfully generated against lipids through animal immunization when delivered as part of an intact bacterial cell or in the presence of an adjuvant such as lipid A. These are typically soluble glycolipids such as bacterial lipopolysaccharide or amphipathic membrane lipids such as phosphatidylinositol (101-105). Analysis of the epitopes targeted indicates that the generated antibodies primarily bind the phosphate or carbohydrate headgroup portion of these lipids, which indicate that the non-polar lipid tails are generally not immunodominant. Furthermore, the antibodies generated are usually of the IgM isotype and are generally low-affinity as they have not undergone significant affinity

maturation (101,106). As such, immunization has limited value for generating high quality antibodies for diagnostic use against lipid or glycolipid targets.

1.4.2 Recombinant phage display

In vitro antibody phage display technology, first developed by Winter et al, enabled antibody selection without the need for prior animal immunization (107). By engineering the display of a diverse antibody repertoire on the surface of filamentous bacteriophage with each individual phage carrying both the functional antibody and its particular DNA sequence packaged within, antibody specificity and genotype were coupled together and could now be selected in tandem. This was achieved by cloning variable domain antibody sequences, extracted from B cells via PCR, into a plasmid vector in-frame with the gene III phage coat protein to create a polyclonal library of antibody sequences. Transformation of the library into a suitable bacterial host along with the genome of the phage, typically M13 bacteriophage, resulted in expression of a polyclonal collection of antibodies displayed on phage. The genome of the phage could be delivered either as part of the library plasmid vector or separately through a helper phage. The second method is generally preferred as it results in a smaller library vector allowing for easier manipulation.

Non-immune, immune and synthetic antibody libraries (with randomized CDRs) have been created from both human and animal sources. They are displayed on both phage as well as alternative display platforms such as ribosome, yeast, bacteria and mammalian cells, all of which rely on the principle of coupling of phenotype and genotype and have been used to select antibodies against a wide

variety of targets (108-110). In particular, the ability to recover a diverse range of antibody sequences from human B cells through the use of degenerate primer sets or the construction of semi-synthetic libraries using germline human frameworks and CDRs comprised of randomized amino acids enabled the production of extremely diverse and unbiased fully human antibody libraries with the ability to target both foreign and self-antigens (11,111). A considerable advantage of *in vitro* antibody screening via phage libraries is the ability to bias selection for antibodies with specific properties such as binding at pH or temperature extremes, or for fast or slow on and off-rates respectively, or to incorporate negative selection to remove cross-reactive epitopes; all of which is not possible in an *in vivo* system as binding always occurs under physiological conditions (109). This lack of constraint on selection conditions has allowed phage display to be used for the selection of non-polar lipids that are insoluble in aqueous medium such as oxidized cholesterols, long chain fatty acids and prostaglandins (10,112,113).

1.4.3 Recombinant antibody expression

While recombinant antibody offers a comprehensive antibody selection methodology, the end result is typically just the genetic sequence of the variable heavy and light chains of identified antigen-specific antibodies encoded on the library vector. As such, the complete antibody molecule must be expressed using a separate methodology. This is in contrast to hybridomas in which the selected clone continues to secrete the whole antibody in culture (99). Expression of recombinant antibody has been carried out in a variety of hosts, including mammalian cell culture, yeast and bacteria. Expression in eukaryotic cells such as mammalian cell culture

has the advantage of being the original expression environment of the protein, as well as being able to provide post translation modification such as N-linked glycosylation of the N297 residue on the constant domain of IgG, which is required for Fc receptor (FcR) binding and complement fixation (114-116). The disadvantages of mammalian cell culture however are reduced speed due to slower growth in culture and increased costs (117,118). An alternative eukaryotic expression system that lacks both these disadvantages is yeast, which as a eukaryotic system has advanced protein folding machinery and secretory apparatus and has been used to produce full length soluble antibodies (119). However, unmodified strains of yeast produce highly mannosylated N-linked glycosylation, which target proteins for rapid clearance *in vivo* in mammals. Using glyco-engineering, proprietary strains of *Pichia pastoris* have been developed which produce more mammalian type glycosylation to overcome this limitation, though access to these strains is limited (120).

For antibodies where effector function is not required, such as those intended for diagnostic use, prokaryotic systems may be used to produce antibodies or antibody fragments, which offers significant reduction in speed of production and costs (117,118). While expression of full length monomeric IgM was achieved in the bacterial host *Escherichia coli* soon after the development of monoclonal hybridomas, it required refolding of the antibody from the insoluble protein fraction (121). Instrumental for the expression of soluble antibody fragments was the development of expression constructs with the ability to direct protein translation into the periplasm by addition of a heterologous signal peptide at the N-terminus of the protein coding sequence. Export into the periplasm enables proper formation of inter and intramolecular disulphide bonds due to its greater oxidizing environment

compared to the cytoplasm and hence allows for proper assembly of the antibody molecule (122).

E. coli is not ideal for the periplasmic expression of antibodies or antibody fragments due to the limited ability of the bacterial host to ensure proper polypeptide pairing, folding and disulphide bond formation of the antibody molecule, resulting in poor yields of soluble protein due to aggregation and/or degradation of improperly folded protein (123). As such, considerable effort has been made to optimize bacterial hosts for antibody and antibody fragment expression. Engineering of oxidizing cytoplasmic environments, co-expression of molecular chaperones, use of periplasmic protease deficient strain of *E. coli* and balancing of heavy and light chain expression have all enabled increased yield (123-126). More recently, various groups have used a combination of specially engineered protease-deficient *E. coli* strains and reduced rates of expression to produce full length aglycosylated antibodies to appreciable levels (110,125).

1.5 Lipid biomarkers for TB diagnostics

The development of recombinant antibody technology has made the development of high specificity and affinity diagnostic antibodies against lipid and carbohydrate targets viable. *Mtb* has a wide variety of lipid and glycolipid targets which are typically found in the cell wall of the microbe (Fig. 1-2). Insoluble lipids include sulfolipids, phthiocerol dimycocerosate (PDIM), mycolic acid- both free and covalently bound to the peptidoglycan layer of the cell wall and mycolic acid derivatives such as trehalose di- and monomycolate (127,128). Soluble glycolipids

are comprised of phosphatidylinositol mannosides, lipomannan and lipoarabinomannan (LAM) (127). Of particular interest as biomarkers are mycolic acid and LAM, due to their reported presence in sputum and urine clinical samples respectively (12,13).

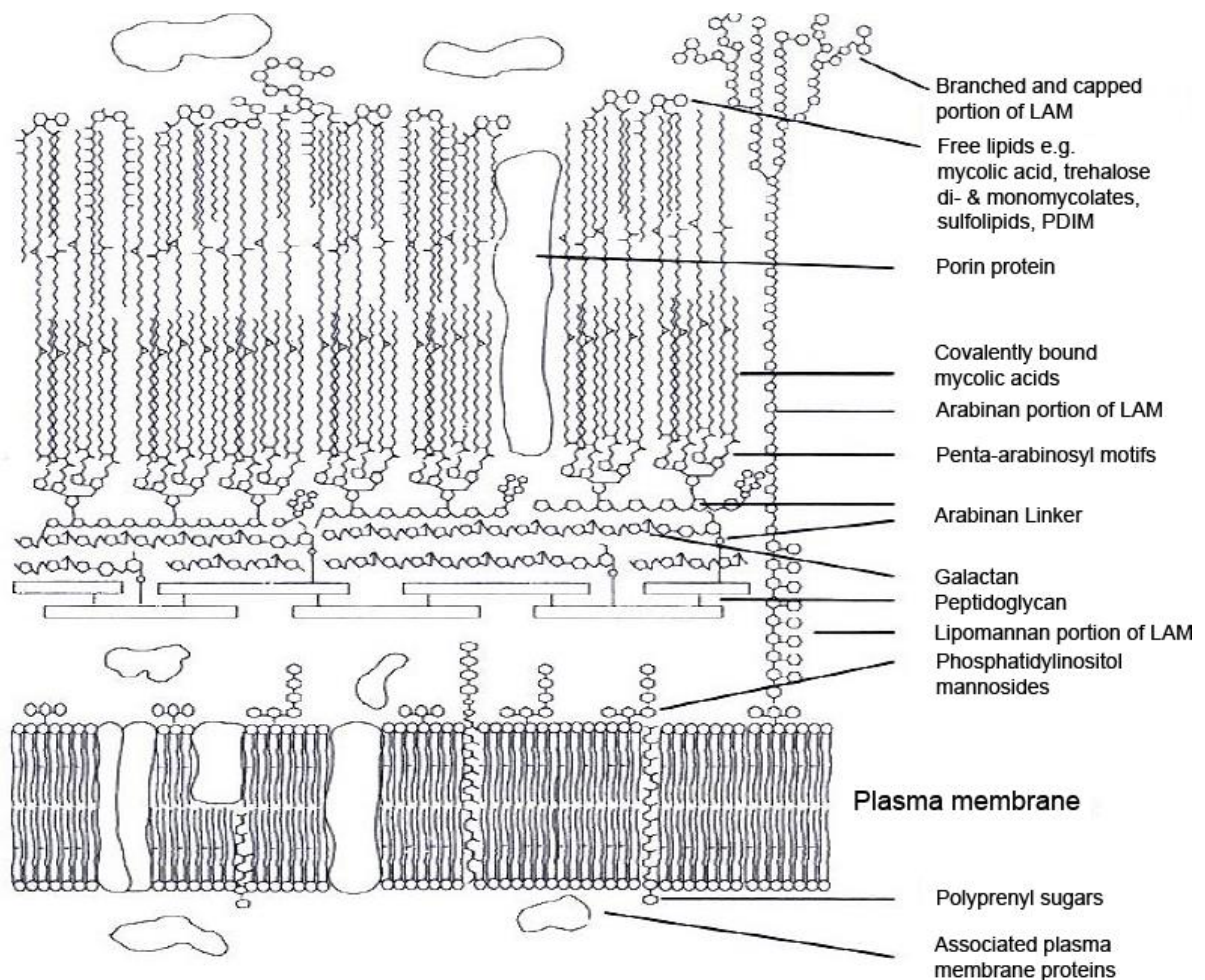


Figure 1-2: Structure of the mycobacterial cell wall

LAM and mycolic acids can be seen integrated into the cell wall. The majority of the mycolic acids are covalently attached to the arabinosyl residues of the peptidoglycan layer of the cell wall

1.5.1 Lipoarabinomannan

Lipoarabinomannan (LAM) has become a target of particular interest in TB for two principle reasons; first, unlike most lipids it is soluble and immunogenic and hence generating antibodies in animals is straightforward; and second, it has purportedly been found in the urine of TB patients, which is easier to sample / collect and less likely to be biohazardous compared to the collection of sputum (129). LAM has a core structure consisting of a mannosyl-phosphatidyl-*myo*-inositol lipid anchor attached to a highly branched polysaccharide with a repeating α 1-6 mannose backbone and α 1-5 arabinose branches which are decorated with secondary arabinose branches with α 1-3,5 and β 1-2 linkages (Fig. 1-3) (130). The core lipid anchor has up to four fatty acid chains which are thought to anchor the LAM in the plasma membrane of the bacterium. LAM can be extracted from a crude cell wall fraction using ethanol solvent or boiling with SDS, indicating that it is tightly integrated but not covalently bound to the cell wall (131). However, the ability of antibodies to bind LAM on the surface of intact mycobacteria and the role of LAM in mannose receptor driven phagocytosis suggests that a portion of it at least is exposed to the external environment.

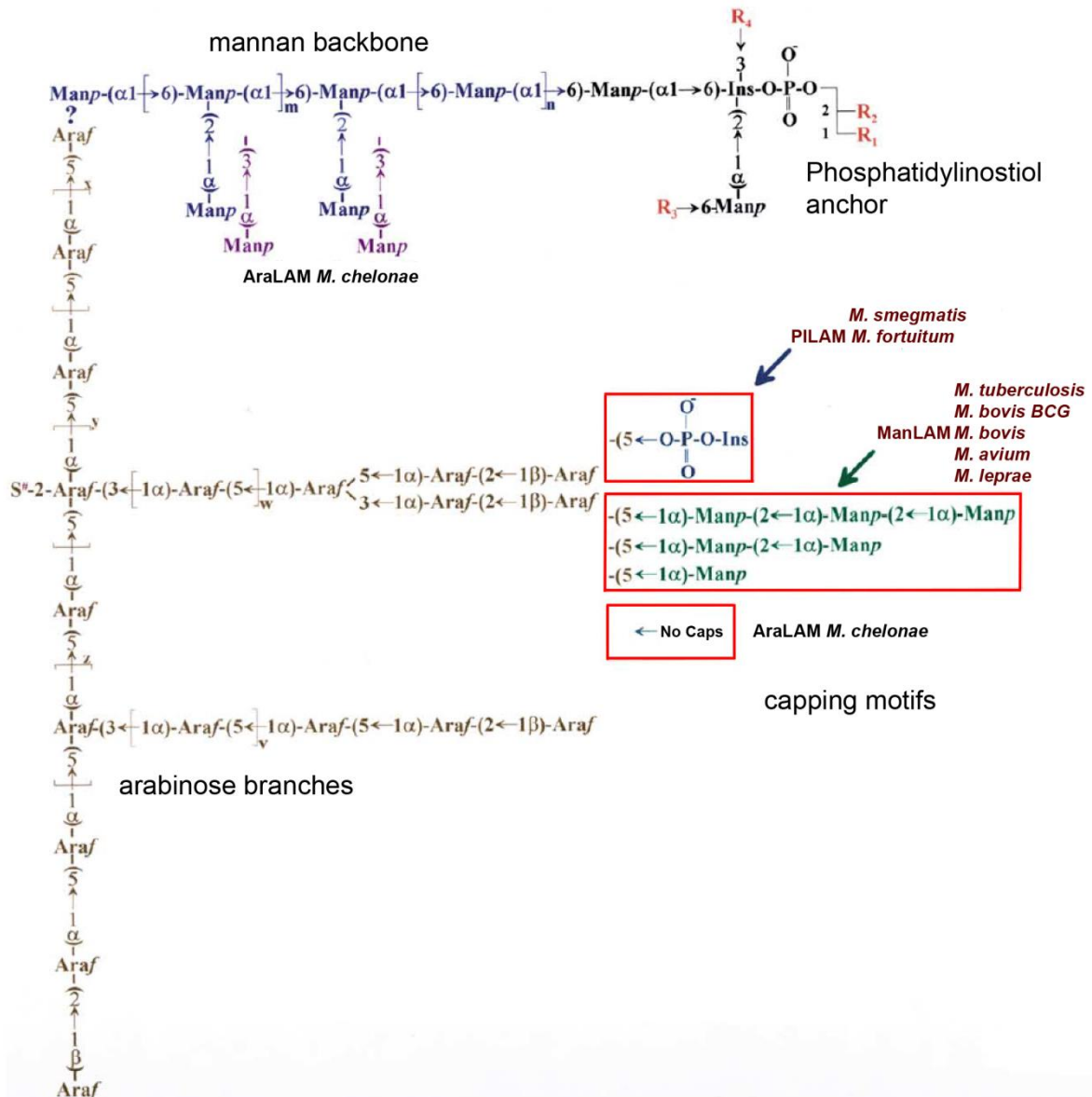


Figure 1-3: Structure of lipoarabinomannan

Red boxes highlight the three different capping motifs found on mycobacterial LAM. The core of the LAM structure is formed from α 1-6 mannose and α 1-5 arabinose residues (Adapted from Nigou et al, 2003).

Investigations into the cell wall components of mycobacteria have indicated that LAM is present in all mycobacterial species studied to date although the wide variety of mycobacterial species discovered has precluded an exhaustive search for LAM in all mycobacterial species. In addition, LAM has also been found in a variety

of actinomycete species of related genera such as *Amycolatopsis sulphurea*, *Corynebacterium diphtheriae*, *Rhodococcus ruber*, *Tsukamurella paurometabolum* and *Turicella otitidis*, although the majority of these lack the arabinose branches and instead have individual monosaccharide arabinose and mannose residues decorating the main oligomannose backbone (130,132-135). As such, there is a high chance that anti-LAM antibodies could cross react with these species. Interestingly, there is variation in the LAM structure across different mycobacterial species which occurs primarily at the capping motifs at the end of the secondary arabinose branches. These are thought to coincide with the phylogenetic organization of the various species and are believed to be responsible for much of the biological activity of this molecule. At least three different LAM variants with different capping motifs have been described (Fig. 1-3): PILAM – with a phosphoinositide cap in fast growing mycobacteria such as *M. fortuitum* and *M. smegmatis*; ManLAM – with a mannose cap with up to three α 1-2 linked mannose residues in slow-growing mycobacteria, which include all major pathogenic species such as *M. tuberculosis*, *M. bovis*, *M. leprae* and *M. avium*. Lastly, the fast growing mycobacterial species *M. chelonae* has been found to have no sugar caps on its secondary arabinose branches (AraLAM) (130). An antibody specific for these α 1-2 mannose motifs could therefore distinguish the pathogenic slow-growing mycobacteria from the non-pathogenic fast-growing mycobacteria.

α 1-2 mannose-capped LAM (ManLAM) has been found to be involved in the phagocytosis and entry of virulent *M. tuberculosis* into host macrophages and suppression of their immune response. A comparison of phagocytosis of beads coated with LAMs of different capping motifs has indicated a requirement for the

mannose caps for binding and uptake via the mannose-receptor (136,137). This receptor is a major point of entry for mycobacterial infection and ManLAM mediated entry via the mannose-receptor has been associated with the inhibition of fusion of the lysosome with the phagosome and enhanced survival of intracellular bacteria (136). Reduction in the availability of surface exposed mannose residues due to variation in the degree of mannose capping among different *M. tuberculosis* strains correlates with reduced uptake of mycobacteria and infectivity, thus confirming its key role in macrophage infection (138).

Mtb is known to interfere with phagocytosis progression by inhibiting phagosome-lysosome fusion, as well as blocking apoptosis of infected macrophages, thus ensuring its intracellular survival (139,140). While the effector mechanisms have not been completely elucidated, ManLAM has been shown to have inhibitory effects on phagocytosis-related signalling pathways such as blockage of cytosolic Ca^{2+} release via inhibition of sphingosine-1-kinase activity and insertion of the endosomal marker EEA1 into the phagosome (139,141). These effects may be mediated by the incorporation of free LAM into the cell membrane of the infected host cell (142). In addition, other immunosuppressive effects of ManLAM have been observed, including modulation of cytokine secretion from a stimulatory to inhibitory phenotype, inhibition of T cell activation and blockage of dendritic cell maturation (143-145). These effects have not been noted with LAMs carrying other capping motifs, indicating that these mannose caps on the termini of the LAM molecule are critical to its virulence.

More recently, evidence arguing against the mannose caps of LAM as virulence factors was reported. A mutant strain of BCG expressing a LAM lacking mannose caps was found to survive equally well in a mouse infection model and produce a similar cytokine profile as the non-mutant strain, although it had slightly reduced uptake and increased phagosome-lysosome fusion (146). The same mutation in *Mtb* similarly had no effect on its survival and cytokine induction in mice *in vivo* and well as in macrophage *in vitro* (147).

1.5.2 LAM diagnostics

The first LAM test was developed in 1990 as a sandwich ELISA using a monoclonal antibody detector and anti-BCG polyclonal antibodies to detect LAM from the centrifuged sputum pellet and showed intermediate sensitivity between sputum smear and culture (82). Another similar study was carried out using liquefied sputum supernatant, but tested primarily smear-positive patients and thus did not provide a representative patient cohort (84). A separate study on serum samples using cohaemagglutination of *S. aureus* Cowan strain incubated with anti-*Mtb* polyclonal indicated high specificity, but used a laborious method of processing serum requiring several rounds of ethanol precipitation to remove interfering serum proteins and antibodies (148). Subsequently, two groups explored urine as a potential clinical sample for testing of LAM. Both groups used a rabbit polyclonal raised against the crude *Mtb* cell wall fraction and affinity purified against LAM as opposed to previous groups which used unpurified polyclonals. Their data showed better sensitivity of around 80-93% (83,85,87).

The initial success of urinary LAM diagnostics led to the development of two commercial LAM ELISA kits (Clearview TB ELISA, Inverness Medical Technology & Determine TB LAM Ag Test, Alere) based on those studies' protocols, which was extensively tested in a variety of clinical studies but failed to show significant utility above sputum smear microscopy due to low sensitivity (6-51%) in urine samples (139,149-153). In sputum samples, sensitivity was better but this was further complicated by low specificity due to cross-reactivity with other microbacterial flora present in the patients' sputum such as *Nocardia* and *Tsukamurella* species (154). Sensitivity was also not enhanced by the use of induced sputum (155). This low sensitivity was confirmed by a recent meta-analysis combining all available clinical data on commercial LAM assays and has been attributed to either low levels of LAM in the urine or modification of LAM by the host leading to reduced binding and detection (13).

A recent paper suggested that low levels of excreted urinary LAM in immunocompetent individuals could be due to retention of LAM in the circulation caused by formation of immune complexes with anti-LAM antibodies; alternatively, high levels of LAM in immunodeficient individuals could be due to spread of infection to the urinary tract (156). However, more recently, Lawn et al has shown that a LAM lateral flow type urinary assay (Determine TB LAM Ag Test, Alere) which is both rapid and cheap, in combination with sputum smear microscopy, can achieve detection sensitivities approaching that of the Xpert *MTB*/RIF assay in HIV patients with low CD4 levels (157,158). As the test has increased sensitivity in patients with lower CD4 levels whom are more likely to progress rapidly towards severe disease and death, it has been suggested that urinary LAM assays could be used as a rule-in

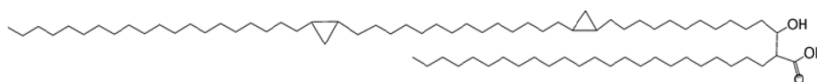
test to identify TB/HIV co-infected patients at high risk of fatal disease (159). Given that the main drawback for urinary LAM assays are their lack of sensitivity, use of more sensitive technologies or targeting alternative forms of clinical material from patients (such as serum) may potentially yield better outcomes.

1.5.3 Mycolic acid

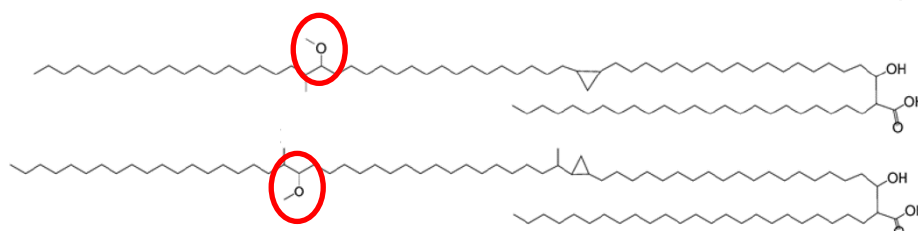
Unlike LAM, mycolic acid is extremely hydrophobic and insoluble in aqueous solution and therefore more difficult to manipulate in a diagnostic assay. However, it is highly abundant in the cell wall of *Mtb*, consisting of around 40% of the dry weight of the cell and therefore should be one of the most abundant targets for detection (47). The majority is covalently anchored to the arabinogalactan-peptidoglycan cell wall and can only be released by alkaline hydrolysis (Fig. 1-2). Free mycolic acids are also present interspersed between the anchored mycolic acids and can be extracted just with organic solvents (127). These are either unmodified or conjugated to carbohydrates to form dimycolates such as trehalose dimycolate (TDM, also known as cord factor) and phthiocerol dimycocerosate. To date, there is no method devised that allows for the detection of mycolic acid directly from clinical samples. Instead, analysis of mycolic acid must be carried out on lipid extracts of culture or sputum using a combination of organic solvent extraction and alkaline hydrolysis to liberate both free and covalently bound mycolic acid (12,160). Identification of mycolic acid can then be performed using high performance liquid chromatography, electrospray ionization mass spectrometry, thin layer chromatography or nuclear magnetic resonance (12,161-164).

The general structure of mycolic acid can be described as a β -hydroxyl fatty acid with an α -alkyl branch (Fig. 1-4) (48,165). The α -alkyl is the shorter branch and does not contain any functional groups while the longer fatty acid tail, referred to as the meromycolate branch can have unsaturated double bonds, cyclopropane and various other functional groups which enable mycolic acids to be classified as follows: alpha mycolic acids, which only has the aforementioned functional groups, as well as keto, methoxy, epoxy and wax ester mycolic acids which carry their named functional groups respectively.

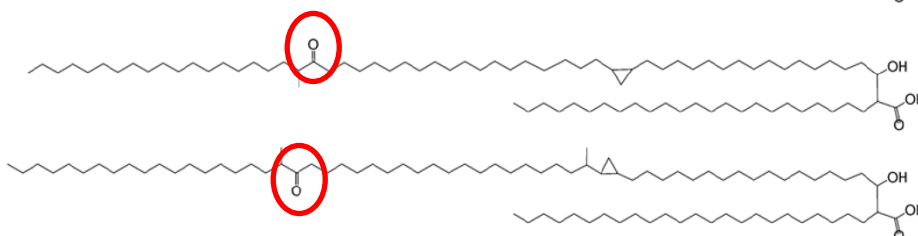
Alpha mycolic acid



Methoxy mycolic acid



Keto mycolic acid



W-shaped configuration of methoxy mycolic acid

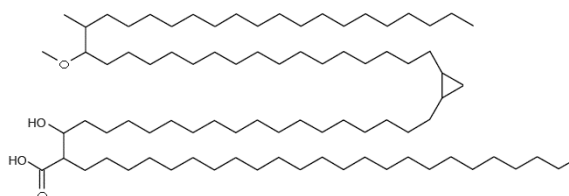


Figure 1-4: Structure of the three main classes of mycolic acid in *Mtb*.

The longer chain is the meromycolate chain with the functional methoxy and keto groups circled in red. The cyclopropane groups are represented by triangles. The folded W configuration of mycolic acid is shown with the functional groups exposed at the edges of the structure. (Adapted from Sekanka et al, 2007 & Barkan, 2009)

Mycolic acids can be found in all mycobacterial species and also in the related actinomycete genera *Corynebacterium*, *Gordona*, *Nocardia*, *Rhodococcus*, and *Tsukamurella* (48,166,167). Within these genera and among the individual species and strains, there are characteristic variations in the types of mycolic acid found and the length of the α -alkyl and meromycolate branches and the locations of the functional groups therein (165,168). These can be used as diagnostic indicators for identification of the mycobacterial species (160,161). There are also overall mycolic acid characteristics that can be attributed to particular genera; mycobacteria are notable for having mycolic acids with the longest carbon chains with a total of 60-90 carbons atoms and an α -alkyl of 20-26 carbon atoms followed by *Tsukamurella* mycolic acids with a total of 64-78 carbon atoms (48,167). *Corynebacterium* on the other hand has the smallest mycolic acids with a range of 22-40 carbon atoms (169,170). Similarly, individual mycobacterial species have different types of mycolic acid, with the methoxy mycolic acids being limited to the *Mtb* complex group of species (*M. tuberculosis*, *africanum*, *bovis*) and a few other pathogenic species including *M. gordonae* and *M. marinum* while alpha mycolic acids are found in all species (48). *Mtb* also contains keto mycolic acids but lack the wax ester and epoxy mycolic acids (164).

Mycolic acid plays a vital role in the virulence of *Mtb*. Structurally, mycolic acid plays a major role in maintaining the impermeability of the mycobacterial cell wall due to its hydrophobicity with its long alkyl chains and immobile nature in covalent attachment to the peptidoglycan layer, which serves to limit drug access to the core of the bacilli (128). Free mycolic acid has also been found in abundance in

extracellular *Mtb* biofilms, which are believed to enhance drug tolerance (171). It has also been found to have immunomodulatory properties; *Mtb* oxygenated mycolic acids were found to induce formation of foamy macrophages which act as nutrient reservoirs within which the intracellular mycobacteria can replicate (172,173). Loss of different cyclopropane functional groups within mycolic acid has various contradictory effects in mouse infection models with enhanced inflammation and cytokine production and either enhanced or attenuated virulence (57,174). Different classes of mycolic acids have also been shown to elicit differential immune responses when dosed intra-tracheally in mice: while alpha mycolic acids were relatively inert, *cis*-cyclopropane containing methoxy and keto mycolic acids elicited inflammatory responses. In contrast, *trans*-cyclopropane methoxy mycolic acid partially lost its inflammatory activity and keto mycolic acid exerted anti-inflammatory alternative activation of alveolar macrophages and counteracted effects of *cis*-cyclopropane mycolic acids. Thus, the various functional groups of mycolic acid may exert both anti-inflammatory and pro-inflammatory effects so as to modulate the immune response to maximise chances of survival, such as triggering granuloma formation but not macrophage apoptosis (175). Mycolic acid specific CD1b⁺ T cells were also found to be present in the immune response of TB patients but not in healthy BCG vaccinated controls, suggesting that they may also have a significant role in driving host response to infection (176). However, mycolic acids are also targets of several widely used anti-mycobacterial drugs such as isoniazid, ethionamide and ethambutol, which interfere with mycolic acid or cell wall synthesis (23,177).

While mycolic acids can be readily detected by chromatographical techniques, their hydrophobicity renders them difficult to target with antibodies. Nonetheless, it is known that anti-mycolic acid antibodies can be produced during infection in humans and detected using mycolic acid-containing liposomes as the target for a serological assay (178). However, high cross-reactivity with control serum samples was observed, which was proposed by Verschoor to be due to mycolic acids adopting a cholesterol-like structure when in a lipid membrane (179). Studies with purified mycolic acid monolayers on aqueous medium have supported this theory by indicating that mycolic acids form a W-shaped configuration with the functional groups at the corners of the W and the alkyl chains running folded and parallel to each other and perpendicular to the membrane surface (180). In particular, the keto mycolic acids were found to prefer this configuration as the greater hydrophilic nature of the keto groups encourages solvent exposure and discourages burying of these functional groups within the hydrophobic core of the molecule (181). This theory is supported by the isolation of anti-mycolic antibodies from a chicken scFv phage display library that also had cross-reactivity to cholesterol (182). Nonetheless, the surface exposure of distinguishing hydrophilic functional groups suggests that developing highly specific anti-mycolic acid antibodies is a possibility.

1.6 Aims of this project

In this study we address key challenges in TB diagnostics. We aim to develop antibodies targeting lipids and glycolipids enriched in the TB cell envelope and we will combine this with developing technology platforms that allow for the production of these antibodies at low cost in bacterial systems. Taken together, these will form

the basis for the development of a low cost diagnostic platform for TB that will be applicable in the developing world. Specifically, our aims are to:

1.6.1 Optimize expression of full length IgG in *E. coli*

Expression of IgG in bacterial culture is one way of reducing costs of antibody production. This may be important in ensuring that the costs of antibody-based assays are kept to a minimum. Current methods of bacterial IgG expression rely on specially optimized strains not available to general laboratories (125). Alternatively, studies have shown that balancing translation rates to ensure that the protein secretory machinery is not overloaded can improve yields of heterologous proteins (183). Using a generally available *E. coli* expression strain, we aim to optimize bacterial IgG expression using simple methods for reducing translation rates.

1.6.2 Develop antibodies targeting the *Mtb* lipids Lipoarabinomannan and mycolic acid

Previous studies on LAM based diagnostic assays have primarily relied on polyclonal antibodies, which may have batch to batch variation and have been shown to exhibit cross-reactivity to non-pathogenic mycobacteria and non-mycobacterial actinomycete species (154). By using antibody phage display selection on ManLAM coupled with negative selection with a non-mannose capped LAM to drive selection towards the α 1-2 mannose caps, we aim to isolate a ManLAM specific monoclonal antibody that would be selective for slow-growing pathogenic mycobacteria.

Similarly, while antibodies have been previously generated against purified mycolic acid, these are in the scFv format which may lose affinity when converted to full IgG and are also cross-reactive to cholesterol (184). We therefore aim to isolate a mycolic acid-specific Fab from the same antibody phage display library that can be readily converted to an IgG for use in a diagnostic assay.

1.6.3 Thoroughly characterize anti-LAM/anti-mycolic acid antibodies

Antibodies isolated from the library will be tested for their specificity for ManLAM and mycolic acid, limit of detection and cross-reactivity to other antigens in a variety of immunoassays. One advantage of recombinant antibody expression is the ability to switch constant regions; we will explore the use of different human and murine constant regions to improve the clinical utility of our antibodies.

1.6.4 Determine the diagnostic utility of the antibodies

We will employ clinical samples from healthy controls spiked with the target biomarkers as well as actual clinical samples (urine, sputum and serum) to determine the diagnostic utility of the antibody. We also aim to optimize the antibody and the assay protocols to maximize assay sensitivity and specificity.

Chapter 2: Materials and methods

2.1 Buffers and solutions

1xPBS & 1xPBS/T wash buffer

200ml of 10x PBS buffer (1st Base, Singapore, Cat.No. BUF-2040) was topped up to 2L with deionized water. Tween-20 detergent (Sigma-Aldrich, United States, Cat. No. P1379) was added at 1:2000 dilution for PBS/T (0.05% Tween). Filter sterilization was carried out with a 0.22µM bottle-top filter.

Bacterial periplasmic extraction buffer

Reagents were made up to the following final concentrations in Milli-Q water and filter sterilized with a 0.22µM bottle top filter: 100 mM Tris pH 8.0 (1st Base, Singapore, Cat.No. BUF-1415-1L-pH8.0), 150 mM NaCl, 1 mM EDTA (Duchefa, Netherlands, Cat. No. E0511), 0.5 M sucrose (Sigma-Aldrich, United States, Cat. No. S0389), 1 mM PMSF (Sigma-Aldrich, United States, Cat. No. P7626), 1 µg/ml pepstatin A (Sigma-Aldrich, United States, Cat. No. P5318), 10 mM iodoacetamide (Sigma-Aldrich, United States, Cat. No. I6125)

Bacterial Lysis buffer

Reagents were made up to the following final concentrations in Milli-Q water and filter sterilized with a 0.22µM bottle top filter: 20 mM sodium phosphate pH 7.4, 300 mM NaCl, 1 mM EDTA (Duchefa), 0.5 mM PMSF (Sigma-Aldrich), 1 µg/ml pepstatin A (Sigma-Aldrich), 10 mM iodoacetamide (Sigma-Aldrich) and Complete EDTA-free protease inhibitor (Roche, Switzerland, Cat. No. 05056489001, 1 tablet/50ml solution)

Protein L binding buffer

Reagents were made up to the following final concentrations in Milli-Q water and filter sterilized with a 0.22µM bottle top filter: 100 mM sodium phosphate buffer pH 7.2, 150 mM NaCl

IMAC (Immobilized metal affinity chromatography) wash buffer

Reagents were made up to the following final concentrations in Milli-Q water and filter sterilized with a 0.22µM bottle top filter: 50mM sodium phosphate buffer pH7.4, 500mM NaCl

IMAC elution buffer

Reagents were made up to the following final concentrations in Milli-Q water and filter sterilized with a 0.22µM bottle top filter: 50mM sodium phosphate buffer pH7.4, 500mM NaCl, 250mM imidazole (Sigma-Aldrich, United States, Cat. No. I01250)

5x Sodium dodecyl sulphate loading buffer

11.25ml of 1M Tris-HCl pH 6.8 (1st Base, Singapore, Cat. No. BUF-1415-1L-pH6.8), 2.5g of sodium dodecyl sulphate (SDS) (Bio-Rad, United States, Cat. No. 161-0302), 25ml glycerol, 25mg of bromophenol blue (Bio-Rad, United States, Cat. No. 161-0404) were mixed and made up to a final volume of 50ml with deionised water. Dithiothreitol (Sigma-Aldrich, United States, Cat No. D9163) was added to a final concentration of 250mM for reducing SDS-PAGE gels

1xTBS pH7.4

Reagents were made up to the following final concentrations in Milli-Q water and filter sterilized with a 0.22µM bottle top filter: 20mM Tris pH7.4 (1st Base, Singapore, Cat.No. BUF-1415-1L-pH7.4), 150m NaCl

PEG solution for phage precipitation

73.05g of NaCl and 100g of polyethylene glycol-6000 (Sigma-Aldrich, United States, Cat. No. 81260) was dissolved in deionized water to a final volume of 500ml (final concentration 2.5M NaCl, 20% w/v PEG) and autoclaved to sterilize. The hot autoclaved solution was cooled rapidly by shaking in a water bath to mix polyethylene glycol and aqueous layers which are immiscible at high temperatures.

Alkaline hydrolysis buffer

Solid potassium hydroxide (BDH, United Kingdom, 102104V) was dissolved in 100% methanol (VWR, United Kingdom, Cat. No. 20864-320) to give either 1 or 3M methanolic potassium hydroxide solution.

Concentrated hydrochloric acid

Concentrated hydrochloric acid (Fluka, United States, Cat. No. 84435) was added to distilled water to give a final solution of 4 or 8M hydrochloric acid.

TMB stop solution

97% concentrated sulphuric acid, approximately 18.3M, (Sigma-Aldrich, United States, Cat. No. 07208) was added to distilled water to give a final solution of 2M sulphuric acid.

2.2 Construction of antibody expression vectors

2.2.1 Construction of mammalian expression vectors

All mammalian expression vectors were constructed on the pTT5 vector (Fisher Scientific, United States, Cat. No. 50-148-474) backbone which contains an Epstein-Barr virus oriP origin of replication for episomal persistence in cell lines expressing the EBNA1 protein and an improved cytomegalovirus-based expression cassette (185). Separate expression vectors were created for the heavy and light chain. For both vectors, a mammalian signal peptide was inserted upstream of the cloning site to direct antibody expression into the secretory pathway for disulphide bond formation, glycosylation and convenient harvesting from the culture supernatant. Either an SfiI or ApaLI restriction site was introduced at the signal peptide C-terminus to allow the heavy or light chain antibody sequence to be cloned in-frame. For the heavy chain vector, the IgG constant region sequence with an N-terminal BsmBI restriction site (human G1, G3 or mouse G2a CH1-3 sequence for full length IgG; human G1 CH1 sequence up to the heavy-light chain disulphide bridge cysteine, followed by a myc and 6xHis-tag for Fab) was inserted downstream of the signal peptide. An XbaI site was added after the stop codon to allow for swapping of different constant region sequences. Heavy chain variable region sequences could then be sub-cloned directly in-frame from the phage library vector via the SfiI/BsmBI restriction sites. For the light chain expression vector, an Ascl site was added downstream of the signal peptide to enable the sub-cloning of the complete light chain sequence (both variable and constant, including the stop codon) into the light chain expression vector in-frame.

2.2.2 Construction of bacterial expression vectors

The backbone of the antibody expression plasmid for employment in *E. coli* was derived from pASK-IBA2 (IBA GmbH, Germany, Cat. No. 2-1301-000), which contains a tetracycline based promoter and an OmpA leader sequence for export into the periplasm. To introduce the antibody sequences, the bicistronic expression cassette consisting of the light chain sequence, the intercistronic ribosomal binding site, and the heavy chain variable region with the PelB leader sequence was cloned in as a complete construct from the phage display library vector via ApaLI and BsmBI cloning sites with the light chain in-frame with the plasmid OmpA leader sequence. The heavy chain constant region of human G1 was cloned in from the mammalian IgG expression vector to be in frame with the variable heavy region. During the course of plasmid construction, deletion of a backbone restriction enzyme site situated within the origin of replication had created a reduced copy number plasmid in addition to the normal high copy number plasmid. For cloning in of the chimeric 4G2 antibody, the whole light chain and the heavy variable chain was cloned in via ApaLI/Ascl and Mfe/Xho restriction sites respectively.

2.2.3 Construction of chimeric antibody constructs

Human G1 and G3 CH1 sequences and Mouse G2a CH2 and CH3 (Fc) sequences were amplified from previously constructed pTT5 expression vectors with primers designed to permit a second overlapping PCR of the human CH1 and mouse Fc sequences as follows, human G1 CH1: SEQ1B 5'-CGGATCTCTAGCGAATTCC-3' & HuG1MoG2aRev 5'-CCACCCAAGAG

GTTAGGTGCTGGGCACGGTGGGCATGTG-3'; human G3 CH1: SEQ1B and HuG3MoG2aRev 5'-CCACCCAAGAGGTTAGGTGCTGGGCACCGTGGGCATGGGGG-3'; Mouse G2a: HuG1MoG2aFor 5'-CACATGCCCCACCGTGCCCAGCACCTAACCTCTTGGGTGG-3' or HuG3MoG2aFor 5'-CCCCCATGCCCCACGGTGCCCAGCACCTAACCTCTTGGGTGG-3' with MoG2aRev 5'-ATCCAGCTTCTAGACTATTTACCCGGAGTCCGGGAGAAG-3'. The first round of PCR was carried out using Native Pfu polymerase (Stratagene, United States, Cat. No. 600135) with an initial melt at 95°C for 5min, followed by 30 cycles at a melting temperature of 95°C for 30s, an annealing temperature of 56°C for 30s and extension at 72°C for 1min for CH1 sequences and an annealing at 62°C for 30s and extension at 72°C for 2min for Fc sequences, followed by a final extension step at 72°C for 15min. PCR products were run on 1% agarose gel and the appropriate bands excised and DNA extracted (QiaQuick, Qiagen, Germany, Cat. No. 28704). 1µl of each purified PCR products were then combined in a second PCR using the same polymerase enzyme to overlap the human G1 or G3 CH1 and mouse G2a Fc sequences. Overlap extension PCR was carried for the first five cycles without primers with an initial melt at 95°C for 5min, followed by cycling at a melting temperature of 95°C for 30s at an annealing temperature of 62°C for 30s and extension at 72°C for 2min. 1µl of each primer SEQ1B and MoG2aRev (at 10µM stock concentration) were then added and a further 25 cycles carried out at an annealing temperature of 56°C for 30s to amplify the final chimeric sequence before final extension at 72°C for 15min. The chimeric constant region PCR product were then purified on 1% agarose gel as above and cloned into the heavy chain mammalian expression vectors via the BsmBI and XbaI restriction sites.

To create the chimeric light chain with a mouse light constant region for moG2afull, a reverse primer (LC-Rev) was designed that could anneal to the C-terminal region of the variable light chain and also contained a short sequence of the N-terminal region of the mouse constant light chain (either kappa or lambda to match the isotype of the human variable light chain). This reverse primer together with SEQ01B primer was used to amplify the human variable light chain sequence from the pTT5 mammalian expression vector using the first round PCR protocol above with an annealing temperature of 56°C. A mouse kappa or lambda constant light chain sequence was also amplified using the same PCR protocol from a pTT5 expression vector carrying a complete mouse light chain. The reverse primer SEQ03 (5-‘CCTTTATTAGCCAGAGGTCG-3’) was used along with a forward primer that is the reverse complement of LC-Rev, which anneals to the N-terminal region of the constant light chain. PCR products were purified on 1% agarose gel as above and 1µl of each PCR product used for overlap extension PCR to join the human variable and mouse constant region. Overlap extension PCR was carried for the first five cycles without primers with an initial melt at 95°C for 5min, followed by cycling at a melting temperature of 95°C for 30s at an annealing temperature of 56°C for 30s and extension at 72°C for 2min. 1µl of each primer SEQ1B and SEQ03 (at 10µM stock concentration) were then added and a further 25 cycles carried out to amplify the final chimeric sequence before final extension at 72°C for 15min. The PCR product was purified on 1% agarose gel and sub-cloned back into the pTT5 light chain expression vector via the ApaLI/Ascl restriction sites.

2.2.4 Sub-cloning of antibody heavy and light chains by restriction digest and ligation

Individual heavy chain variable region or complete light chain sequences were digested from selected monoclonal plasmid minipreps of the phage library vector (see section 2.8.4) using the pairs of restriction enzymes SfiI/BsmBI or ApaLI/AsclI respectively (New England Biolabs, United States: SfiI – Cat. No. R0123, BsmBI - Cat. No. R0580, ApaLI – Cat. No. R0507, AsclI – Cat. No. R0558) at the recommended digestion temperature and buffer. Cut DNA fragments were isolated by running on 1% agarose gel and the appropriate DNA band excised and gel extracted (QiaQuick, Qiagen). Vectors were cut similarly with the exception of the light chain vector where BsmBI was used to generate an ApaLI overhang due to the presence of multiple ApaLI sites in the vector. Cut insert and vector were ligated together with T4 DNA ligase (New England Biolabs, United States, Cat. No. M0202) and transformed into chemically competent XL1 blue *E. coli* (Stratagene, United States, Cat. No. 200249). Clones containing the inserted sequences were identified by restriction digest with of the same pairs of enzyme and grown up in 400ml of LB broth (BD, United States, Cat. No. 244610) with 100µg/ml carbenicillin (Novagen, United States, Cat. No. 69101-3) in a shaking incubator at 37°C and DNA extracted using a Endo-free Maxiprep kit (Macherey Nagel, Germany, Cat. No. 740426.50) for transfection into mammalian cell culture.

2.3 Expression and purification of bacterial IgG

2.3.1 Initial periplasmic expression in BL21 or HB2151

The low copy number 4G2 expression plasmid was transformed into either HB2151 or BL21(DE3) *E. coli* (Stratagene, United States, Cat. No. 200131) and grown up in 2YT (BD, United States, Cat. No. 244020) broth with 100 µg/ml carbenicillin (Novagen). Induction was carried out at OD₆₀₀ 1.0 with 1/10 normal inducer concentration (final concentration of 20ng/ml). Periplasmic extraction was carried out by resuspending the pellet in 1/40 volume chilled periplasmic extraction buffer, sonicating briefly on ice and then gently rotated at 10 rpm for 1 hr at 4 °C. Cells were collected at 40000 g for 30min at 4 °C and the supernatant was retained.

2.3.2 Small scale optimization of bacterial IgG expression conditions

Expression plasmids were transformed into *E. coli* strain HB2151 and grown up as a starter culture. 50 ml of 2YT (BD) broth with 100 µg/ml carbenicillin (Novagen) was inoculated with 1/50 volume of starter culture and grown at 30 °C at 220 rpm. Induction was carried out as indicated and cultures transferred to room temperature and grown overnight at 120 rpm. The bacterial pellet was weighed and resuspended in chilled lysis buffer at a ratio of 1 ml per 200 mg wet cell mass and sonicated on ice. Lysates were clarified by centrifugation at 16000 g for 30 min at 4°C. All cultures were grown up in non-baffled shake flasks and cytoplasmic extraction carried out as described above for all subsequent experiments.

2.3.3 Large-scale expression and purification of bacterial IgG

Expression was carried out in 2x 800 mL of 2YT broth (BD) with 100 µg/ml carbenicillin (Novagen) in 2L non-baffled shake flasks as described above with the

following optimized conditions: high expression construct was used and induction was carried out at OD₆₀₀ 1.0 using 20ng/ml or 50ng/ml final inducer concentration. The cell pellet was weighed and resuspended in lysis buffer at the same volume to wet cell mass ratio as above, sonicated and clarified by centrifugation at 20000g for 30min at 4°C. The cell lysate was passed through a 0.22µm filter before purification on a 1 ml recombinant Protein A FF column (GE Healthcare, United Kingdom, Cat. No. 17-5079-01) fitted to a AKTApriime Plus or Explorer FPLC system (GE Healthcare, United Kingdom). Lysate was passed through the column at a flow rate of 0.5 ml/min, then the column washed with 30 ml 1x PBS before elution in 0.5 ml fractions with IgG elution buffer (Pierce Thermo Scientific, United States, Cat. No. 21004). Fractions were neutralized with 1/10 volume 1 M Tris pH 8.0. Peak fractions were pooled and buffer exchanged into 2 ml Protein L binding buffer with an Amicon 30000 MWCO concentrator (Merck Millipore, United States, Cat. No. UFC903024) and then bound to 400µl Protein L agarose bead 50% slurry (Pierce Thermo Scientific, United States, Cat. No. 20512) overnight at 4°C. The beads were washed with ten column volumes of 1x PBS in column and antibody eluted with IgG elution buffer (Pierce, United States) and neutralized as above. Eluate was buffer exchanged into 1x PBS/20 % glycerol and concentrated down to 150 µl volume.

2.4 Expression and purification of mammalian IgG and Fab

Paired antibody heavy and light chain plasmids were transfected into HEK293-6E cells (ATCC, United States,) which stably expresses the EBNA1 protein using branched polyethyleneimine (Sigma-Aldrich, United States, Cat. No. 408727) as a transfection reagent. Cells were cultured in suspension at a density of 10⁶ cells/ml in

complete serum-free F17 medium (20 ml GlutaMAX-I - Invitrogen Gibco, United States, Cat. No. 35050-061; 0.5 ml 50mg/ml Geneticin - Invitrogen Gibco, United States, Cat. No. 10131-027; 9 ml Pluronic F68 – Invitrogen Gibco, United States, Cat. No. 24040-032; 1 L F17 medium - Invitrogen Gibco, United States, Cat. No. A13835-01). 10 μ g (equal amounts of heavy and light chain plasmids by mass) of total DNA and 30 μ g of PEI were mixed in 1ml of filter sterilized 150mM NaCl solution (per 10ml of cell culture) and incubated for 15min before addition to the cell culture. Cells were incubated in a shaking incubator at 37°C in 5% CO₂, 125rpm and tryptone-N1 (Organotechnie, France, Cat. No. 19553) added to a final concentration of 0.5% the following day. The cell culture was maintained for one week before harvesting the supernatant to recover the antibody.

One week old cell culture was centrifuged at 8000g for 20min and the supernatant passed through a 0.22 μ M filter before affinity purification on a 1ml recombinant Protein A FF column (GE Healthcare, United Kingdom, Cat. No. 17-5079-01) fitted to a AKTAprime Plus or Explorer FPLC system (GE Healthcare, United Kingdom) at a flow rate of 1ml/min. The column was washed with filter sterilized 1xPBS and bound antibody was eluted in 1ml fractions with IgG elution buffer (Pierce Thermo Scientific) and neutralized with 1/10 volume 1 M Tris pH 8.0. Peak fractions were pooled and buffer exchanged into 1xPBS with an Amicon 30000 MWCO concentrator (Merck Millipore) and stored at -80°C after flash freezing with liquid nitrogen. For Fab, supernatant was passed through a 1ml IMAC column (GE Healthcare, United Kingdom, Cat. No. 17-0920-03) charged with 0.1M cobalt chloride and rinsed with deionized water. The column was then washed with IMAC wash buffer and then eluted in 1ml fractions with IMAC elution buffer. Peak elute

fractions were buffer exchanged into 1xPBS and stored at -80°C as above for purified IgG.

2.5 Polyacrylamide gels and western blot

SDS-PAGE gels were cast from 40% 37.5:1 acrylamide-bisacrylamide solution (Bio-Rad, United States, Cat No. 161-0148) polymerised with 10% APS and TEMED. Samples taken during extraction and purification of bacterial or mammalian antibodies were resolved on 8 or 10% SDS-PAGE gels. Samples were heated in SDS loading buffer with or without addition of the reducing agent dithiothreitol for 5min at 95°C and chilled on ice before running. For western blot, gels were transblotted to a Hybond-C nitrocellulose membrane (GE Healthcare, United Kingdom, Cat. No. RPN137E). IgG was detected using anti-Human Fc-HRP conjugated polyclonal secondary antibody (Pierce Thermo Scientific, United States, Cat. No. 31413) alone or in combination with anti-human Kappa-HRP conjugated polyclonal secondary antibody (Invitrogen, United States, Cat. No. AH11804) diluted 1:2500 or 1:5000 respectively in 5 % skim milk (Sigma-Aldrich, United States, Cat. No. 70166) in 1xPBS/T. Blots were washed four times with 1x PBS/T and once with 1x PBS for five minutes each wash and then signal developed with SuperSignal West Pico Substrate (Pierce Thermo Scientific, United States, Cat. No. 34080).

2.6 Measurement of protein concentration

To measure protein concentration, purified antibody was measured by the Bradford method. 300µl of Coomassie Plus reagent (Pierce Thermo Scientific,

United States, Cat. No. 23236) was added to 10µl of sample or protein standards in a flat-bottom 96-well plate and incubated for 10min at room temperature before reading absorbance at 595nm. Protein standards were used to generate a standard curve plotted on a log-log axis to determine sample concentration.

2.7 Bacterial strains and culture

Mycobacterium smegmatis was a kind contribution from Dr Ayi Teck Choon, DSO National Laboratories and *Mycobacterium bovis* Bacille Calmette-Guérin (BCG) was a kind contribution from Dr Sylvie Alonso, National University of Singapore. All other mycobacterial species were provided by Dr Seah Geok Teng, National University of Singapore. *Nocardia cyriacigeorgica* (ATCC BAA-1517) and *Tsukamurella paurometabolum* (ATCC 8368) was purchased from American Type Culture Collection, United States. Live mycobacterial culture was grown up to log-phase growth in Middlebrook 7H9 media (BD, United States, Cat. No. 271310) at 37°C in shake flasks with the exception of *M. bovis* (BCG) which was cultured in 100ml of Middlebrook 7H9 broth at 37°C with 5% CO₂ in T175 cell culture flasks for two weeks. *Nocardia cyriacigeorgica* and *Tsukamurella paurometabolum* were cultured in Brain-Heart Infusion Broth (BD, United States, Cat. No. 237500) while *Escherichia coli* strain XL1 blue was cultured in LB broth (BD), at 37°C in flasks in a shaking incubator. Heat killed inactivated *Mtb* (H37Rv strain) was kindly provided by Dr Sylvie Alonso and carried out by heating bacterial suspension at 90°C for 30min.

To standardize mycobacterial cultures by colony-forming units (CFU) for subsequent experiments, bacteria were pelleted by centrifugation at 4000g for 15min

in a 50ml Falcon, weighed and re-suspended in PBS containing 50% (v/v) glycerol to OD₆₀₀ of 1.0 and then serially diluted 1:10 six times. 100µl of each dilution was plated onto Middlebrook 7H11 (BD, United States, Cat. No. 283810) agar plates supplemented with 10% OADC enrichment (BD, United States, Cat. No. 212351) and incubated at 37°C (with 5% CO₂ for BCG) for 3 and 21 days for *M. smegmatis* and BCG respectively before the colonies were enumerated. The procedure was performed in duplicate and the average CFU per unit OD₆₀₀ was calculated to determine the appropriate dilutions for subsequent experiments.

2.8 Phage display

2.8.1 Negative selection panning against ManLAM

A non-immune human Fab-antibody phage display library (Humanyx Pte Ltd, Singapore) constructed by the method of Hans de Haard et al was screened for anti-LAM antibodies after multiple rounds of selection on Mannose capped lipoarabinomannan (ManLAM) from *Mycobacterium tuberculosis* Ayoma-B strain (Nacalai Tesque, Japan, Cat.No. 02449-61) coupled with negative depletion on Phosphoinositide capped lipoarabinomannan (PILAM) from *M. smegmatis* (Invivogen, United States, Cat. Code TLRL-LAMS) (11). Cross-reactive LAM antibodies were first depleted from the library by pre-absorption to 100µg PILAM coated onto a Maxisorp immunotube for 1½ hr at room temperature (Nalgene Nunc, United States, Cat. No. 470319). Remaining cross-reactive antibodies were blocked in solution by the addition of 100µg of soluble PILAM. The phage library was then applied to an immunotube coated with 100µg of ManLAM to pull out anti-ManLAM antibodies by binding for 1½-2hrs at room temperature. Coated tubes had been

washed twice with 1xPBS after coating and pre-blocked with 4% skim milk in 1xPBS for 2hrs at room temperature prior to application of the library. Unbound phage were removed by repeated washing with 2% skim milk block in 1x PBS/T, followed by 1xPBS/T and 1xPBS washes. Three skim milk washes, three PBS/T washes and two PBS washes were carried out for the first pan and for subsequent pans the number of skim milk and PBS/T washes was increased to seven. Solid surface pre-absorption with PILAM on an immunotube was carried out only for the first two rounds of selection and a total of four rounds of selection were carried out. Phage was then recovered after each round of selection on immunotube to produce an enriched polyclonal library as described below in section 2.8.3.

2.8.2 Lipid panning against mycolic acid

The same non-immune human phage Fab antibody phage display library (Humanyx Pte Ltd, Singapore) used for generating anti-LAM antibodies was panned against mycolic acid based on a previously developed protocol for generating anti-lipid antibodies (10). Briefly, the Maxisorp immunotube (Nalgene Nunc) was coated by evaporating 200µg of *Mtb*-derived mycolic acid (Sigma-Aldrich, United States, Cat. No. M4537) dissolved in 0.5ml n-hexane overnight at 4°C, washed twice with 1xPBS and then blocked with 4% skim milk in 1xPBS for 2hrs at room temperature. The phage library was then panned against the lipid coated immunotube as described above in section 2.8.1 without any negative depletion and a modified washing protocol. After the library was allowed to bind, the immunotube was washed four times with 2% skim milk in 1xPBS and eight times with 1xPBS for the 1st pan. The number of washes was doubled for subsequent pans. Phage was then

recovered after each round of selection on immunotube to produce an enriched polyclonal library as described below in section 2.8.3.

2.8.3 Phage recovery after each round of panning

Bound phage was recovered by enzymatic elution with 500µl of 2mg/ml trypsin (Sigma-Aldrich, United States, T9935) in 1xTBS with 2mM CaCl₂ at 37°C for 30min and re-infected into 5ml of freshly cultured TG1 *E. coli* at OD₆₀₀ 0.5 for the library recovery. After the second round of selection, a 1.2ml portion was set aside, spun down and resuspended in 2YT/50% glycerol and stored at -80°C for subsequent isolation of monoclonal phage. Phage infected TG1 was further infected with M13KO7 helper phage (New England Biolabs, US, Cat. No. N0315S) at an MOI of 1:20 and grown overnight at 30°C on 2YT (BD) with 100µg/ml of ampicillin and 25µg/ml of kanamycin (2YTAK) agar plates to produce polyclonal phage. Expressed phage was recovered the next day by scrapping the bacterial lawn with 5ml of Tris-buffered saline (1xTBS, pH7.4) per plate and centrifuging the bacterial suspension at 4000g for 20min. Phage in the recovered supernatant was precipitated by adding a 1/5 volume of PEG solution (2.5M NaCl/20% polyethylene glycol 6000), incubating on ice for 1hr and then centrifuging for 15min at 10000g. Precipitated phage was resuspended in 2ml of 1xPBS, clarified by centrifugation at 16000g for 2min to remove any insoluble particles and then precipitated with PEG solution as above and pelleted with centrifugation at 16000g for 5min. The purified phage pellet was finally resuspended in a final volume of 1.5ml in 1xPBS and centrifuged one last time at 16000 for 1min to remove any remaining insoluble debris or phage. 100µl of this enriched polyclonal library was then mixed with 900µl of 4% skim milk in PBS and

blocked for 1hr before binding to a freshly coated immunotube for the next round of selection. Recovered polyclonal phage was also used in phage polyclonal ELISA to test for enrichment against the target antigen.

2.8.4 Screening of phage libraries

Phage libraries were screened by producing monoclonal phage culture as follows: infected TG1 glycerol stock (from an appropriately enriched pan as determined by polyclonal phage ELISA) was diluted 1:10 from 10^{-3} to 10^{-6} in 2YT broth and the dilutions plated out on 2YT with 100µg/ml of ampicillin and 2% glucose (Sigma-Aldrich, United States, Cat. No. G8270)-2YTAG agar plates to obtain single colonies. Approximately 400 individual colonies were picked and each inoculated into 300µl of 2YTAG media in a 2ml deep well plate (Nalgene Nunc, United States, Cat. No. 278752) and grown overnight at 37°C shaking at 700rpm for starter culture. 10µl of starter culture was inoculated the next day into 200 µl of fresh 2YTAG media in a new deep well plate and grown up by shaking at 37°C at 700rpm until a culture density of OD_{600} 0.5 was reached. M13KO7 helper phage (New England Biolabs) was then added at an MOI of 1:20 and the culture incubated for a further 1hr. The culture was pelleted by centrifugation at 4000g for 10min and supernatant discarded. The pellets were resuspended in 300µl of fresh 2YTAK media and then grown at 30°C overnight at 700rpm for monoclonal phage production. Monoclonal phage secreted into the culture supernatant was tested by ELISA as described below in section 2.13.2 to identify target-specific clones.

Subsequently, positive clones were screened for unique clones by BstN1 digestion of the amplified heavy and light chain coding region. Clones with different sequences would have different digestion patterns. The antibody coding region was amplified by colony PCR using HotStarTaq PCR Master Mix (Qiagen, Germany, Cat. No. 203443) according to manufacturers' protocol from 1µl of bacterial culture in a 20µl reaction volume with 1µl each of the following primers at 10µM concentration: HX01-F (5'-AGCGGATAACAATTTACACAGG-3')/HX01-R (5'-TGATTGCAGACCTTTCTGCTGTTT-3') The PCR reaction was run as follows: 95°C initial melt for 15min, then 30 cycles of melting for 45s at 95°C, annealing for 45s at 52°C and extension for 1min 40s at 72°C, followed by a final extension step at 72°C for 10min. 10µl of the PCR mix was digested with 1µl of BstN1 (New England Biolabs, United States, Cat. No. R0168) for 3hrs at 60°C and run on a 3% agarose gel. Confirmation of unique sequences was done by Sanger sequencing using BigDye v3.1 (Applied Biosystems, United States, Cat. No. 4337455) of the Fab heavy and light chain sequences with the same primers used for colony PCR along with two additional primers that anneal in the intercistronic region (pCES-LR – 5'-ATGCCGTCGGCGACCTAACA-3'/pCES-HF – 5'-GGCGCGCCAATTCTATTTCAAG-3') to provide overlapping coverage of the heavy and light sequences. Identified unique positive clones were grown up in 4ml of 2YT broth (BD) with 100µg/ml carbenicillin (Novagen) and 2% glucose at 37°C in a shaking incubator for recovery of the monoclonal plasmid DNA (prepared using plasmid miniprep kit, Qiagen Germany, Cat. No. 27104) for subsequent cloning into expression vectors.

2.9 Carbohydrate microarrays

Carbohydrate microarrays were fabricated as described previously (186). Gamma Amino Propyl Silane (GAPS) II slides (Corning, United States, Cat. No. 40003/4) were submerged in dimethylformamide containing 2% diisopropylethylamine and 0.5 mg/mL maleimido-*N*-hydroxysuccinimide hexanoic acid for 14hrs at room temperature. Functionalized slides were washed three times with methanol, dried and stored under an argon atmosphere. The functionalized oligosaccharides were synthesized as described previously (187). The oligosaccharide compounds with 1M equivalent tris(2-carboxyethyl)phosphine to reduce disulphides were dissolved to the desired concentration in PBS. Per spot, 1nl of the solution was printed onto the maleimide functionalized slides using an automated printing robot in replicates of ten at four different concentrations (2 mM, 0.4 mM, 80 μ M and 16 μ M). Slides were incubated in a humid chamber to complete reaction for 24hr and stored in a dessicator until usage. Printed carbohydrate microarray slides were washed three times with water and quenched in 0.1 % (v/v) β -mercaptoethanol in PBS for 1 h at room temperature. Afterwards, slides were washed three times with water and two times with ethanol. Slides were blocked by a solution of 2.5% BSA in Tris buffer with calcium (20mM Tris, 150 mM NaCl, 1 mM CaCl_2 , pH 7.4 for 1 h at room temperature, washed three times with Tris buffer with calcium and centrifuged. The antibody (50 μ g/mL) was incubated on the slides in in 20mM HEPES, 150 mM NaCl, 1 mM CaCl_2 , pH 7.4, washed three times with the same buffer and centrifuged. For inhibition, mannan, PILAM or ManLAM (each at a final concentration of 30 μ g/mL) was added to the incubation solution. A fluorescence-labelled anti-human antibody (10 μ g/mL in 20mM HEPES, 150mM

NaCl, 1mM CaCl₂, pH 7.4; Invitrogen, United States) was incubated on the slide in a similar fashion. Afterwards, slides were scanned using a fluorescence microarray scanner (GenePix 4300A, Molecular Devices).

2.10 Immunofluorescence and acid fast-staining

Cover slips were rinsed with deionized water and 100% ethanol and then dried on a heating block at 60°C. Bacterial cultures were grown up as described above in section 2.7 and 20µl of bacteria re-suspended in filter sterilized deionized water to a density of OD₆₀₀ 0.1 (approximately 10⁶ CFU) was pipetted onto the cover slip and allowed to dry onto the cover slip on the heating block at 60°C. The cover slips were then transferred to a 24-well plate and fixed with 500µl of 1:1 mix of methanol-acetone for 30min at -20°C for immunofluorescence or 5% phenol-70% ethanol solution for 15min at room temperature for acid fast staining respectively. Cover slips were then taken out of the fixative and allowed to dry. For immunofluorescence, fixed cover slips were washed once with 1xPBS and then blocked with 2% foetal calf serum in 1xPBS, washed again with 1xPBS and then incubated with primary antibody, either 5µg/ml my2F12 chimeric antibody or 1:200 rabbit anti-LAM polyclonal (Acris Antibodies, Germany, Cat. No. PAB14007) in blocking solution. Cover slips were then washed with two 5-min incubations in 1xPBS/T and rinsed in 1xPBS before incubation with secondary antibody, either anti-rabbit or anti-mouse polyclonal (Invitrogen, United States, Cat. No. A-21207 and A-11001) conjugated to Alexa Fluor 594 and 488 respectively, at 1:100 dilutions in blocking solution. The cover slips were washed again as above, rinsed in deionized water before mounting with Mowoil on glass slides. All washes were done in 24-well

plates and incubations done on parafilm with 50µl of reagent for 30min at room temperature. Mounted slides were viewed using a Confocal Laser Microscope system (Leica SP5, Germany). For acid fast staining, fixed slides were stained with TB Quickstain (BD, United States, Cat. No. 212315) according to manufacturer's instructions in 24-well plates. The slides were stained with carbolfushin for 5min, rinsed liberally with deionized water then flooded with TB Quickstain Methylene Blue to counterstain for 3min and then rinsed again with deionized water. Cover slips were allowed to dry and then fixed to glass slides and viewed under a light microscope (Leica, Germany).

Common throat bacterial smears on glass slides were provided heat fixed and formalin activated by Dr Timothy Barkham, National University of Singapore. These were incubated with 5µg/ml my2F12 chimeric antibody in blocking buffer (5%BSA in 1x PBS) for 1hr, washed and probed with Alexa Fluor 488 anti-mouse polyclonal (Invitrogen) and washed again as above. After washing, DAPI mounting medium (Invitrogen, United States, Cat. No. P-36931) was added and the smear covered with a glass slip and visualized at 100x power using a fluorescence microscope (Olympus BX51, United States) under UV and 488nm illumination for detection of DAPI and secondary antibody respectively.

2.11 Collection and processing of bacterial cultures for ELISA

2.11.1 Bacterial supernatants and whole cell suspension for LAM ELISA

To harvest the supernatant, fresh mycobacterial cultures at stationary phase growth were spun down at 4000g for 20min and the supernatant harvested and

sterilized by passing through a 0.22 μ M syringe filter. To adjust for differences in culture density, the OD₆₀₀ of each culture was measured prior to harvesting and the supernatant diluted with fresh Middlebrook 7H9 broth media (BD) at a ratio equivalent to produce a culture density of OD₆₀₀ 1.0. For testing whole bacteria suspensions, the pellet was re-suspended in filter sterilized 1xPBS and adjusted to OD₆₀₀ 0.5.

2.11.2 Lipid extraction from bacterial cultures for mycolic acid ELISA

1ml of OD0.1 *M. smegmatis* (5.8×10^7 CFU/ml) were centrifuged from pure culture at 16000g for 15min in 2ml Eppendorf tubes and the pellet was re-suspended in 1mL of n-hexane (Sigma-Aldrich, United States, Cat.No. 27050-4). The mixture was vortexed for 15 minutes, incubated on a rotator at room temperature overnight, then centrifuged and the organic layer was recovered. To enhance the effectiveness of solvent extraction, a second methodology was tried where the sample was heated for two hours at 70°C before vortexing. To lyse the bacteria to improve extraction, a third protocol was carried out where the same amount of mycobacteria was re-suspended in 1mL of Milli-Q water and incubated at 99°C for 30 minutes using a Thermomixer heating block (Eppendorf, United States, Cat.No. 5355-000.011). 1mL of n-hexane was then added and processed as above without heating. A fourth protocol was also done where the bacteria was pelleted after incubation in boiling water and then re-suspended in 1ml of n-hexane as above.

For the fifth method of alkaline hydrolysis, the pellet was re-suspended in 500 μ L of 1M potassium hydroxide (KOH) in methanol at 80°C for 1 hour, then

neutralized with 100 μ L of 4M hydrochloric acid (HCl). 500 μ L of n-hexane was added to each sample, which was then vortexed for 15 minutes, centrifuged, and the upper organic layer was recovered for experimentation and made up to 1ml in n-hexane. 100 μ l of extract was used for monoclonal IgG ELISA.

For determination of CFU limit of detection and species specificity, fresh overnight bacterial cultures were adjusted to the appropriate concentration (10^6 to 10^9 CFU/ml for limit of detection, OD0.1 for species specificity) by pelleting at 16000g for 15min and resuspension in the appropriate volume of filter sterilized 1xPBS. 1ml of this bacterial suspension was pelleted again as above and treated by the alkaline hydrolysis method described above and the recovered lipid extract standardized to 1ml with n-hexane. 100 μ l of extract was used for monoclonal IgG ELISA.

2.12 Collection of clinical samples for ELISA

2.12.1 Spiked whole blood and serum samples for LAM ELISA

Venous blood was drawn from healthy Singaporean adult volunteers with informed consent (DSRB No. 08-171) using a 10ml Vacutainer-red cap serum tube (BD, United States, Cat.No. 366430) and ManLAM (Nacalai Tesque) was added to whole blood at indicated concentrations prior to coagulation and then the blood was allowed to clot at room temperature. Serum was harvested by centrifugation at 2000g for 15min of a portion of the spiked whole blood. Spiked serum or clotted whole blood was treated with Proteinase K (20mg/ml dissolved in 1xPBS, Sigma-Aldrich, United States, Cat.No. P2308) at a final concentration of 1mg/ml for 1hr or

1.5hr respectively at 56°C on a Thermomixer heating block (Eppendorf) to digest serum proteins and antibodies. A final heating step for sterilization and inactivation of Proteinase K and any remaining active antibodies was carried out by incubation at 95°C for 30min and then the sample was centrifuged at 2000g for 15min to pellet precipitate. Untreated serum underwent standard heat inactivation for 30min at 56°C.

2.12.2 TB patient selection criteria and sample collection procedure

Adult volunteers were recruited from patients presenting with symptoms suggestive of pulmonary TB infection (persistent fever, night sweats, cough of more than 2 weeks duration, haemoptysis, chest pain, loss of weight and/or appetite, and generalized fatigue) at the National Centre of Tuberculosis and Lung Diseases, Tbilisi, Georgia according to the following inclusion criteria: >18 years of age, HIV negative, no recent illness or hospitalization within the last two weeks, not a re-treatment case. After informed consent was given, sputum, serum and urine samples were collected and stored. A duplicate sputum sample was taken for standard clinical diagnosis via light microscopy acid-fast sputum smear and culture. Patients were then classified into four groups as follows based on the diagnostic results: non-TB (smear and culture-negative), TB smear-negative (smear-negative but culture positive), TB smear grade 1+ only and TB smear grade 2+ and above. 15 samples were collected for each group.

2.12.3 Clinical patient serum samples for LAM ELISA

Venous blood was drawn using a 4ml Vacutainer-red cap serum tube (BD, United States, Cat.No. 367812) and allowed to clot at room temperature. Serum was recovered by centrifugation at 2000g for 15min, heat inactivated by incubation at 56°C for 30min and then stored at -80°C until further processing in 1.5 ml Eppendorf tubes. Serum was digested by addition of Proteinase K (Sigma-Aldrich) to a final concentration of 1mg/ml and incubation at 56°C in a drying oven for 2hrs followed by the final inactivation and sterilization step at 95°C for 30min. Processed samples were then allowed to cool at room temperature and stored at -20°C before testing by ELISA.

2.12.4 Clinical patient urine samples for LAM ELISA

Approximately 5ml of mid-stream urine was collected and incubated in a plastic sample container at 95°C for 30min in a drying oven. Samples were then allowed to cool at room temperature and stored at -20°C before testing by ELISA

2.12.5 Clinical patient sputum samples for LAM ELISA

Approximately 6ml of purulent sputum was collected in a 50ml Falcon tube and liquefied by addition of 10% N-acetyl L-cysteine (Sigma-Aldrich, United States, Cat.No. A7250) dissolved in 1xPBS, to a final concentration of 0.25%, and incubation at 37°C for 2hrs in a drying oven. 2ml of liquefied sputum was transferred into a 15ml Falcon tube and Proteinase K (Sigma-Aldrich) added to a final

concentration of 2mg/ml and incubated for a further 2hrs at 56°C in a drying oven before sterilization at 95°C for 30min. Samples were then allowed to cool at room temperature, centrifuged at 4000g for 10min to pellet debris and stored at -20°C before testing by ELISA.

2.12.6 Clinical patient sputum samples for mycolic acid ELISA

2ml of sputum liquefied by addition of N-acetyl L-cysteine (Sigma-Aldrich) as described above in section 2.12.5 was transferred to a second 15ml Falcon tube. Alkaline hydrolysis for the release of mycolic acids was carried out by addition of 1ml of 3M potassium hydroxide (KOH) in methanol and incubation at 80°C for 2hrs in a drying oven. Samples were cooled to room temperature and then 300µl of 8M hydrochloric acid was then added to neutralize the alkali. 1ml n-hexane (Sigma-Aldrich) was added and mixed by repeatedly inverting the Falcon tube. The mixture was allowed to stand for separation of the lower aqueous and upper organic layers and the lower aqueous layer removed carefully with a micropipette. 1ml of 10x PBS (1st Base) was added and mixed to neutralize any remaining acid. The upper organic layer was recovered by centrifugation at 1000g for 10min and 300µl of extract was used for monoclonal IgG ELISA.

2.13 ELISAs

2.13.1 Comparison of functional IgG levels in bacterial lysate and determination of purified bacterial IgG affinity curves by indirect ELISA

For ELISAs, 96-well Maxisorp ELISA plates (Nalgene Nunc, United States, Cat. No. 442404) were coated with 20µg/ml of protein antigen or 5µg/ml ManLAM (Nacalai Tesque) in 1x PBS overnight at 4°C, washed twice with 1xPBS and blocked with 380µl/well of 4% skim milk in 1xPBS for 2hrs at room temperature and then washed twice with 1xPBS/T prior to addition of antibody. For ELISAs with the anti-dengue antibody 4G2, 50µl of live dengue-2 virus (strain ST) virus was captured with incubation for 1hr at room temperature in wells coated with 5µg/ml mouse 4G2 and blocked and washed as above. Wells were subsequently washed twice with 1xPBS/T to remove unbound virus. For comparison of functional IgG levels, clarified cell lysate was used while either purified bacterial or mammalian expressed IgG was used to plot their respective affinity binding curves. Clarified cell lysate (at dilutions from 1:2 to 1:64) or 100µl of purified antibody (diluted at a 1:2 ratio from 5µg/ml to 0.076µg/ml) diluted in 4% skim milk block in 1xPBS was added. Binding of IgG was detected using 1:5000 anti-Human Fc HRP conjugated polyclonal secondary antibody (Pierce Thermo Scientific, United States, Cat. No. 31413) diluted in 2% skim milk block in 1xPBS. All steps except the blocking step were carried out in 100µl volumes and for 1hr at room temperature except for ELISAs involving dengue virus which were done at 50 µl volumes. ELISA plates were washed four times with 1x PBS/T between after primary antibody incubation and three times with 1xPBS/T and once with 1xPBS after secondary antibody incubation prior to addition of TMB (Pierce Thermo Scientific, United States, Cat. No. 34021). Reaction of TMB was stopped with 2M sulphuric acid. For ELISAs with 4G2 only two 1x PBS/T washes were carried out except for the last prior to addition of TMB where an additional 1x PBS wash was done and for ELISAs with my2F12 1xPBS was used in place of 1xPBS/T.

2.13.2 Indirect phage polyclonal and monoclonal ELISAs

For phage polyclonal and monoclonal indirect ELISAs, 96-well Maxisorp ELISA plates (Nalgene Nunc) were coated with 10µg/ml of LAM antigen (ManLAM, Nacalai Tesque; PILAM, Invivogen) in 1xPBS or 25 µg/ml of *Mtb*-derived mycolic acid (Sigma-Aldrich) or cholesterol/phosphocholine in a 1:2 w/w ratio (Avanti Polar Lipids, United States, Cat Nos. 700000 and 850345) in n-hexane (Sigma-Aldrich) and incubated overnight at 4°C to bind or evaporate respectively. ELISA plates were then washed twice with 1xPBS and blocked with 380µl per well of block at room temperature for 2hrs. For ELISAs involving LAM, Casein in PBS block (Pierce Thermo Scientific, United States, Cat. No. 37528) was used while for ELISAs involving mycolic acids and other lipids 4% skim milk in 1xPBS was used as a blocking agent. The plates were washed and then polyclonal phage at 1:10 dilution or monoclonal phage at 1:2 dilution in block was added. Plates were washed and then bound phage detected with HRP-conjugated anti-M13 polyclonal antibody (GE Healthcare, United States, Cat. No. 27-9420-01) diluted 1:5000 in block. Plates were washed again before colour development with TMB (Pierce Thermo Scientific) for 10min. All incubations and reactions were carried out for 1hr at room temperature with 100µl volume per well and washes between incubations were done four times with 1xPBS (for LAM ELISAs) and 1xPBS/T (for lipid and mycolic acid ELISAs) unless indicated. The last wash for lipid ELISAs prior to incubation of TMB is with 1xPBS in order to reduce bubble formation from the Tween-20 detergent.

2.13.3 Indirect monoclonal IgG ELISA against LAM or lipids

LAM (ManLAM, Nacalai Tesque; PILAM, Invivogen) and lipids were coated and blocked as described for indirect ELISAs in Section 2.13.2 on 96-well Maxisorp ELISA plates (Nalgene Nunc). Commercial synthetic lipids or purified lipid extracts for determination of antibody specificity were purchased from Sigma-Aldrich, United States (*Mtb*-derived mycolic acid, Cat. No. M4537; *M. bovis*-derived trehalose dimycolate, Cat. No. T3034, β -hydroxylmyristic acid, Cat. No. H4148) or from Avanti Polar Lipids, United States (cholesterol, Cat. No. 700000; 7-ketocholesterol, Cat. No. 700015; 15-ketocholestene, Cat. No. 700008; 15-ketocholestene, Cat. No. 700009; 15-hydroxycholestene, Cat. No. 7000010; 15-hydroxycholestane, Cat. No. 700013; dimyristoyl phosphatidic acid, Cat. No. 830845 ; dimyristoylphosphosphocholine, Cat. No. 770345; C-80 alpha mycolic acid, Cat. No. 791280; keto mycolic acid, Cat. No. 791281; methoxy mycolic acid, Cat. No. 791281). Lipids extracts of various bacterial species or from mycobacteria at different concentrations were processed as described above in section 2.11.2.

Detector antibody in the appropriate block (Casein for anti-LAM antibodies, 4% skim milk for anti-mycolic acid antibodies) was added at 1 μ g/ml. The plates were washed and binding detected with anti-human Fc HRP conjugated polyclonal secondary antibody (Pierce Thermo Scientific) at 1:5000 dilution in the appropriate block). The plates were washed for a final time and colour developed with TMB (Pierce Thermo Scientific) and stopped with 2M sulphuric acid. All incubations and reactions were carried out for 1hr at room temperature with 100ul volume per well and washes between incubations were done four times with 1xPBS (for LAM

ELISAs) or 1xPBS/T (for lipid and mycolic acid ELISAs) unless indicated. The last wash for lipid ELISAs prior to incubation of TMB is with 1xPBS in order to reduce bubble formation from the Tween-20 detergent.

2.13.4 Determination of chimeric antibody affinity binding curves

96-well Maxisorp ELISA plates were coated with ManLAM (Nacalai Tesque) at 10µg/ml in 1xPBS or 25µg/ml *Mtb*-derived mycolic acid (Sigma-Aldrich), washed and blocked with either Casein or 4% skim milk in PBS as described for indirect ELISA in section 2.13.2 and then washed again. Each of the six antibody variants, serially diluted to various standardized molar concentrations (taking into account their molecular weight) in the appropriate block was added, 100µl per well, and incubated for 1hr at 37°C. The plates were then washed and 100µl of a mix of anti-human Fc and anti-mouse Fc HRP-conjugated secondary polyclonal antibodies (Pierce Thermo Scientific) each at 1:5000 dilutions in the appropriate block was added to each well and incubated 1hr at 37°C. The plates were washed for a final time and colour developed with TMB (Pierce Thermo Scientific), incubated for 15min at 37°C and stopped with 2M sulphuric acid. Incubation at 37°C was done to ensure the antibody binding and TMB substrate reactions had reached equilibrium. Washes between incubations were done four times with 1xPBS (for LAM ELISAs) and 1xPBS/T (for lipid and mycolic acid ELISAs) unless indicated. The last wash for lipid ELISAs prior to incubation of TMB is with 1xPBS in order to reduce bubble formation from the Tween-20 detergent. Raw absorbance values were converted to percentage of maximum signal and plotted on a XY graph for subsequent data analysis (section 2.15)

2.13.5 Determination of limit of sensitivity for anti-mycolic acid antibodies

Purified mycolic acid extract (Sigma-Aldrich) or synthesized mycolic acid alpha, keto and methoxy subclasses (Avanti Polar Lipids) was serially diluted in n-hexane (Sigma-Aldrich) to indicated concentrations and evaporated overnight onto 96-well Maxisorp ELISA plates (Nalgene Nunc) at 4°C. The next day, plates were washed, blocked with 4% skim milk in 1xPBS and washed again as described in section 2.13.2 for indirect ELISA. 100µl of each anti-mycolic acid antibody at 1µg/ml concentration in 4% skim milk block was added to each well and the remainder of the ELISA was carried out as described in section 2.13.3 for indirect IgG ELISA with lipids.

2.13.6 Indirect sandwich ELISA on purified LAM, bacterial suspensions and culture supernatants

For sandwich ELISA, 96-well ELISA plates (Nalgene Nunc) were coated with 5µg/ml capture antibody (either Fab or HuG1) in 1xPBS overnight at 4°C, washed twice in 1xPBS, blocked with 380µl per well of Casein in PBS block (Pierce Thermo Scientific) for 2hrs at room temperature and washed twice again with 1x PBS before adding antigen. Bacterial suspensions, culture supernatants and spiked serum samples were prepared as described above in section 2.11.1 and 2.12.1 respectively while purified PILAM or ManLAM or H37Rv LAM (a gift from Dr. Patrick Brennan, Colorado State University) was spiked into 1xPBS at indicated concentrations. After antigen binding, the plate was washed and detector antibody (either HuG1 or hG3mG2a) added at 1µg/ml in casein block. The plates were washed again and the

appropriate HRP-conjugated anti-human or anti-mouse Fc (Pierce Thermo Scientific, United States, Cat. Nos. 31413 and 31439 respectively) secondary polyclonal antibody (depending on the detector antibody used) added at 1:5000 dilution in Casein block. After incubation, plates were washed and signal was developed using TMB and stopped with 2M sulphuric acid. ELISA with polyclonal anti-LAM was carried out using pre-coated plates and HRP-conjugated antibody from Clearview commercial LAM ELISA kit (Inverness Medical Innovations, UK) used according to manufacturer's instructions as follows: 100µl of sample was added to ELISA plates already pre-coated with polyclonal anti-LAM and pre-blocked for 1hr at room temperature. Plates were washed four times with the manufacturer's buffer solution (PBS/T) and the detector antibody (same as capture, rabbit polyclonal anti-LAM pre-conjugated with HRP) added at 100µl per well and incubated for 1hr at room temperature. Plates were washed again four times and colour developed with manufacturers' TMB solution and stopped with 2M sulphuric acid. ELISA with live bacterial suspensions was carried out in a Biological Safety Cabinet and washes done with a multichannel pipette dispenser vacuum aspirator. All incubations and reactions were carried out for 1hr at room temperature with 100µl volume per well and washes between incubations were done four times with 1xPBS unless indicated.

2.13.7 Determination of anti-LAM antibody titres in healthy serum samples

ManLAM (Nacalai Tesque) and PILAM (Invivogen) was coated at 10µg/ml onto 96-well Maxisorp ELISA plates (Nalgene Nunc), washed, blocked and washed again as described in section 2.13.2 for indirect ELISA. Serum samples serially diluted in Casein block (Pierce Thermo Scientific) as indicated were added at 100µl

per well and incubated for 1hr at room temperature. Plates were then washed four times with 1xPBS and then the binding of human serum IgG detected with anti-human Fc HRP-conjugated polyclonal secondary antibody as described in section 2.13.3 for monoclonal IgG ELISA against LAM. This protocol was also used to confirm loss of binding of endogenous anti-LAM serum IgG after heat and proteinase K inactivation.

2.13.8 Indirect sandwich ELISA on spiked or patient clinical samples

Indirect sandwich ELISA was carried out as described in section 2.13.6 on patient samples processed as described in section 2.12, with capture and detector antibody concentrations varied as indicated. Spiked or patient clinical samples were added at either 100µl or 300µl per well as indicated and antibody and TMB volumes used as 100µl or 200µl per well respectively. 100µl of 2M sulphuric acid was used to stop all reactions after the indicated incubation time. For calibration and as a positive control, ManLAM (Nacalai Tesque) in 1x PBS at indicated concentrations was added at the same volume per well as the sample.

2.13.9 Indirect ELISA on patient lipid extracts

Indirect ELISA was carried out on 300µl of sputum lipid extracts (extracted as described in section 2.12. evaporated onto 96-well Maxisorp ELISA plates (Nalgene Nunc).

2.14 Mass spectrometric profiling and quantification of mycolic acids.

Mycolic acid profiles were determined by means of high-resolution tandem mass spectrometry. Lipid extract from *M. smegmatis* prepared by alkaline hydrolysis as described in section 2.11.2 were diluted to 2:1 (v/v) with isopropanol: methanol: chloroform 4:2:1 containing 2mM ammonium acetate. 10 μ l samples were infused into a LTQ Orbitrap XL mass spectrometer (Thermo Scientific, United States) using nanomate interface (Advion, United States). The nanospray voltage was -1.35kV (negative ionisation) and mass spectra were acquired in duplicate at a resolution of 30,000 and 100,000. α -alkyl chains were identified by product ion scans, using collision energies between 35 and 45eV. Once the mycolic acid profile of the samples was determined, individual mycolic acid molecular species were quantified by multiple reaction monitoring (MRM) analysis. A comprehensive set of MRM transitions was set-up, including all mycolic acid species and α -alkyl chains identified by HR-MS/MS. A total of 90 mycolic acid species were analysed. 5 μ l of lipid extract were diluted to 50 μ L in chloroform:methanol 1:1 containing two internal standards (I.S., keto- and methoxy- mycolic acids, m/z 1266 and 1254, final concentration: 0.5 μ g/ml each, Avanti Polar Lipids) and injected into a 4000QTrap mass spectrometer (ABSciex, United States). These two mycolic acids were not detected in the samples during HR-MS/MS analysis and could then be used safely as internal standards. The carrier solvent was chloroform:methanol 1:1 containing 10mM piperidine, flowing at 250 μ l/min. Each sample was injected in duplicate (injection volume: 20 μ l). The MS parameters were as follows: negative ESI, capillary voltage -4.5kV, source temperature 250 $^{\circ}$ C, DP -120, EP -10, CE -90, CXP -5. For

quantification, the signal intensity of each MRM transition value was normalised to the internal standard transition intensity.

2.15 Data analysis and statistics

Tests for significant difference were carried out using 1 or 2-way ANOVA with Bonferroni corrections for multiple T-test comparisons for discrete and grouped data sets respectively while affinity binding curves were plotted using non-linear regression with a single-binding site specific binding model, using Prism 5.0 software (GraphPad Software, United States). ROC analysis was carried out using the same software. Test for significant differences between percentages of positive patient samples was carried out using multiple Z-test for independent groups (<http://www.mccallum-layton.co.uk/stats/ZTestTwoTailSampleSize.aspx>).

Chapter 3: Optimization of IgG expression in bacteria

3.1 Introduction

The bacterial host *Escherichia coli* has been widely used for the production of heterologous proteins with over several thousand eukaryotic proteins successfully expressed and purified, along with thousands more bacterial and viral proteins (188). This is typically achieved using T7 or *lac* promoter driven expression systems carried on a plasmid vector and induced with an exogenously delivered chemical signal such as isopropyl- β -D-thiogalactoside. This has enabled the expression of proteins including complex multimeric polypeptides such as IgG at high yield but at low cost, in contrast to expression in mammalian cell culture which is expensive (118). Published work on soluble IgG expression has so far relied on methodologies that are technically challenging, such as refolding of denatured antibodies from inclusion bodies, modification of promoter regions to balance light and heavy chain expression; or using reagents and equipment that may not be readily available such as optimized bacterial expression strains and large scale fermenters (121,125,183,189). A methodology that can be easily replicated using commercially available vectors and strains would be very useful for the low-cost production of diagnostic antibodies for research and clinical use.

Previous work on expression of antibody fragments and antibodies has demonstrated the importance of an oxidizing environment for the proper formation of disulphide bonds (190). We have therefore modified a commercial tetracycline (*tet*) promoter-based vector (pASK-IBA2, IBA GmbH) previously used for the expression of soluble Fab in the periplasm, for the expression of soluble full length IgG. (Fig. 3-1). Studies had also previously shown that expression of heterologous secretory (i.e.

periplasmic) proteins in *E. coli* could be enhanced by reducing translational rates, which is thought to reduce the demand on the limited protein chaperone, folding and secretion machinery (183). We therefore sought a promoter system that allows for homogenous modulation of translation rates. The *tet* promoter/inducer system does not rely on repressor/operator elements endogenous to the host and functions independently of host-strain background and metabolism as the *tet* repressor gene is encoded on the plasmid vector backbone itself (190). This allows for tight and regulated control of protein expression levels independent of host growth or protein expression rates and as such is ideal for this purpose (191,192).

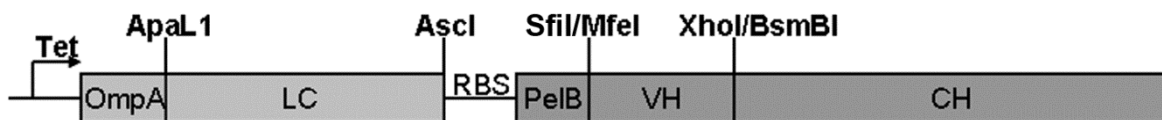


Figure 3-1: Design of the bacterial IgG expression vector

The backbone of the vector was derived from pASK-IBA2 plasmid using a *tet* promoter. The appropriate restriction sites for cloning in of the light and variable heavy chains, leader sequences (OmpA, PeIB) and the constant heavy chain sequence (CH) were added. Light (LC) and variable chains (VH) were cloned in as a complete construct together with the intercistronic ribosomal binding site (RBS) from the phage display vector or as separate constructs from the 4G2 mammalian IgG expression vector.

3.2 Preliminary expression in two common *E. coli* bacterial strains

We initially decided to try expression in two different *E. coli* strains commonly used for protein expression: BL21(DE3), which is deficient in the cellular proteases Lon and OmpT, to reduce any potential protein degradation; and *HB2151*, an *E. coli* strain commonly used for periplasmic expression of antibody fragments, to determine which is more suitable for antibody production. Rather than whole cell

lysis, we tried extraction of only the periplasm so as to limit the release of unassembled heavy and light chain. Analysis of the periplasmic extract after overnight expression of a control antibody: chimeric 4G2, an anti-dengue E protein antibody, showed fully assembled IgG with both HB2151 and BL21(DE3) along with significant amounts of partially assembled IgG (Fig. 3-2A). Surprisingly, reduction of the extracts to allow resolution of the heavy and light chains revealed the presence of increased degradation of the heavy chain with the protease deficient BL21(DE3) compared to HB2151, suggesting that proteolysis of the heavy chain is not due to Lon or OmpT proteases and that HB2151 is more suitable for IgG expression as compared to BL21 (Fig. 3-2B). Despite the reduced degradation, purification of 4G2 on protein A did not give any measurable level of purified protein as measured by Bradford assay.

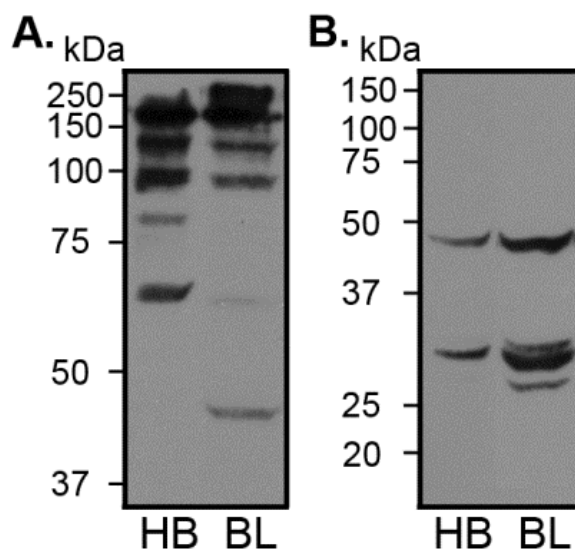


Figure 3-2: Periplasmic extract of bacterial IgG expressed in two different *E. coli* strains

Non-reducing (**A**) and reducing (**B**) western blot of periplasmic extract from overnight expression of 4G2 in HB2151 (**HB**) and BL21(DE3) (**BL**) *E. coli* strains, respectively. All blots were probed with anti-Human Fc HRP conjugated secondary antibody.

3.3 Optimization of expression in small scale culture

We subsequently explored various methods for reducing translation rates as this had been known to improve yields for secretory proteins (183). Previous experiments using the *tet* system had shown that below 50ng/ml, the concentration of inducer becomes limiting although the relationship between expression yield and inducer is not completely linear (191,192). We therefore carried out induction at the manufacturer's recommended concentration of 200ng/ml, and at 50ng/ml and 20ng/ml. Other methods which can reduce translation rates include induction of expression when the bacteria are approaching late exponential growth phase and was used in a method by Mazor et al for the production of full-length IgG (110). Accordingly, apart from induction at the standard time point, when the culture optical density at 600nm reaches 0.6 (OD_{600} 0.6), we also tested using induction at OD_{600} 1.0. Use of low copy number plasmids has also been shown to decrease translation rate (191). In the course of constructing our expression vector, we also generated both a low copy and high copy version of our expression plasmid, by addition of a single base pair mutation in the origin of replication. The difference in copy number between the high and low copy plasmids, based on miniprep DNA yields, is estimated to be approximately eight- to ten- fold and the low-copy variant is expected to significantly reduce production of mRNA and hence translation rates.

In order to ensure that the results would be generally applicable to all antibodies, we expressed PA38 and PA64, two antibodies against the Protective Antigen component of anthrax toxin; ET21 and ET149, two antibodies against epsilon toxin of *Clostridium perfringens* along with chimeric 4G2 (184). With the

exception of 4G2, all other antibodies were isolated from panning with the Humanyx phage display library. Expression of these five antibodies were carried out first in small scale shake cultures with various combinations of different concentrations of inducer, induction at different OD₆₀₀ and using either high or low copy expression vector, as indicated. Standard induction conditions (200ng/ml inducer, high copy plasmid & induction at OD₆₀₀ 0.6) were also used as a comparison. Levels of fully assembled and functional IgG in the clarified cell lysate were then determined by Western blot and indirect ELISA respectively (Fig. 3-4). In order to prevent leakage of expressed antibody into the culture media, which commonly occurs during periplasmic expression in the HB2151 *E. coli* strain, protein expression was carried out in non-baffled flasks at a slower shaking speed of 120rpm to reduce agitation. Extraction was carried out by whole cell lysis as described by Mazor et al for bacterial IgG expression (110).

Initial experiments indicated that variation of inducer concentration resulted in significant differences in wet cell mass yields (Fig. 3-3), which could have a significant influence on overall yield. Therefore, in order to distinguish whether improved yield is due to an increase in wet cell mass or an increase in levels of fully assembled IgG per cell (unit yield), pellets were weighed after harvesting and resuspended in a volume of lysis buffer adjusted for wet cell mass thus ensuring that subsequently derived lysate samples are equivalent. There was little variation in wet cell mass when the low copy plasmid was used, regardless of inducer concentration or induction OD₆₀₀ although the mass obtained was higher compared to standard induction concentrations. However, when the high copy plasmid was used, there was a significant increase in wet cell mass when the lowest inducer concentration

(20ng/ml) was used as compared with the two other concentrations with up to approximately two-fold increase over the standard induction concentrations. This pattern was consistent for all five antibodies tested.

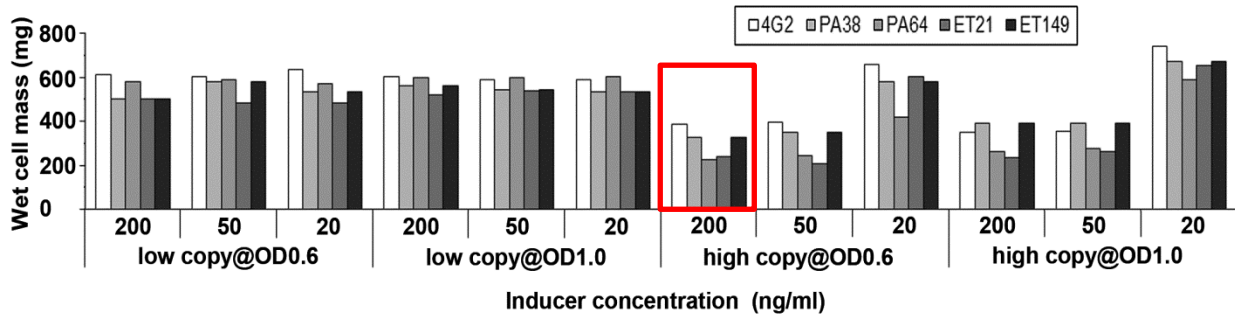


Figure 3-3: Variations in wet cell mass under different inductions conditions

Wet cell mass of the pellet was weighed after overnight induction at indicated inducer concentrations, plasmid copy number and induction OD_{600} . Red box represents standard conditions

The levels of fully assembled and functional IgG as measured by immunoblot and indirect ELISA respectively appear to correlate well for all antibodies expressed, as the intensity of the full sized IgG bands (≈ 200 kDa, black arrow) on the immunoblot approximately corresponded to the signals by ELISA (Fig. 3-4A-E). However, the highest unit yields were not always given by the same induction conditions for each antibody. When low copy plasmid was used, unit yields were generally higher or similar to that obtained under standard conditions with the exception of ET149. They also appeared not to be influenced by varying inducer levels or induction OD_{600} , a pattern similar to that observed earlier for wet cell mass. However, they did not give the best unit yields, which were obtained using high copy number plasmids.

On the other hand, when high copy number plasmid was used, there was significant variation with inducer concentration. Three different patterns were observed. Firstly, with antibody PA38, no significant changes were observed with inducer concentrations, although induction at the later time point of OD₆₀₀ 1.0 increased yield (Fig. 3-4A). A second pattern was observed in which unit yield increased with a reduction in inducer concentration, which was observed in antibodies 4G2 and PA64 (Fig. 3-4B-C). For PA64, induction at OD₆₀₀ 1.0 also increased yields. The third pattern observed with ET21 and ET149 was increased yield with increased inducer concentration (Fig. 3-4D-E). Induction at different OD₆₀₀ did not appear to significantly affect the pattern of yield and in fact for ET149 the best unit yield was at standard conditions of 200ng/ml inducer, induction at OD₆₀₀ 0.6 with high copy plasmid.

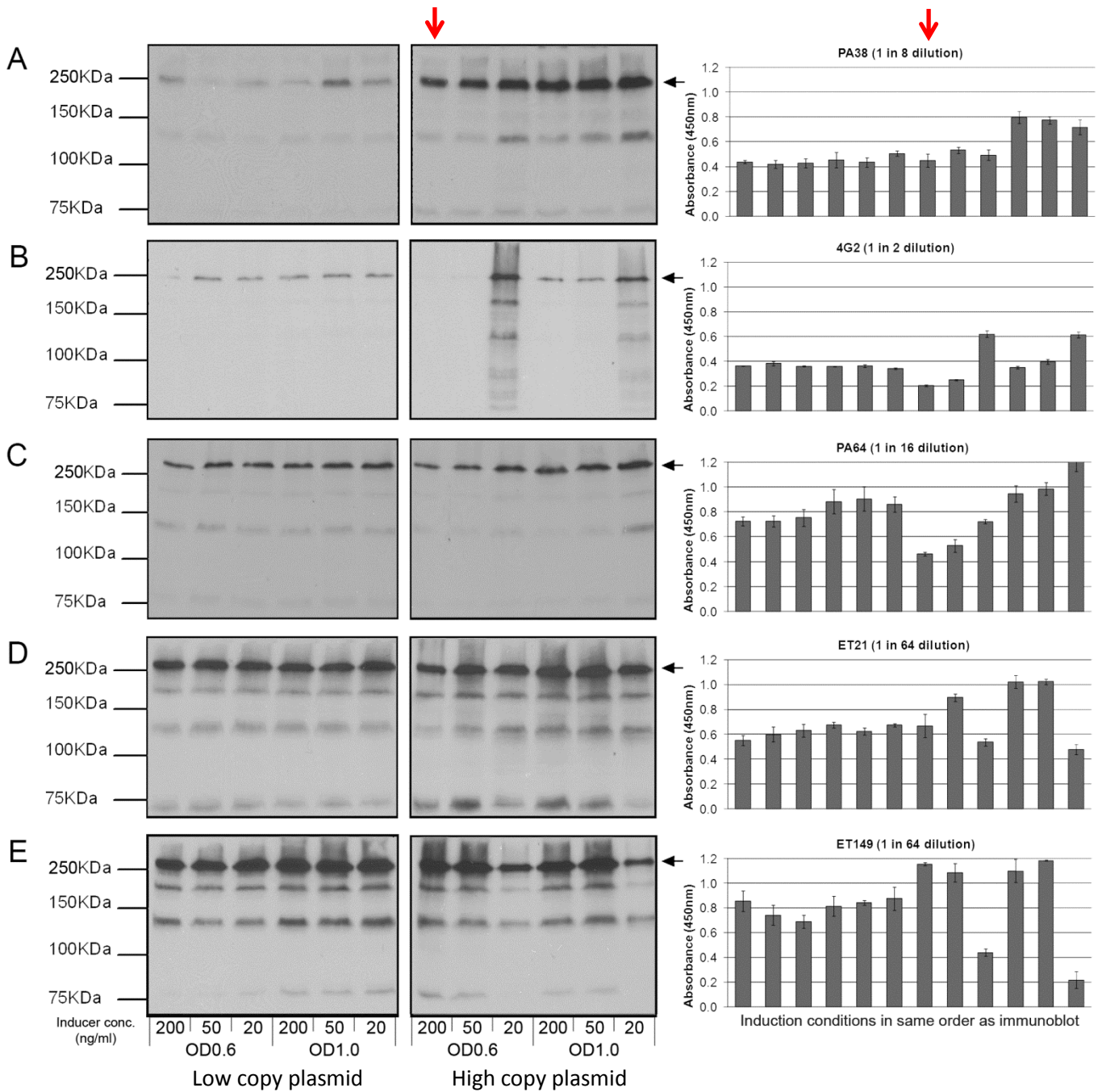


Figure 3-4: Levels of fully assembled or functional bacterial IgG obtained under different induction conditions

Left and middle panels: Non-reducing western blot of 7.5µl clarified cell lysate from small scale overnight expression of bacterial IgG in shaking culture. All blots were probed with anti-Human Fc-HRP and adjusted to ensure equal intensity. **Right panel:** Indirect ELISA indicating levels of functional IgG. Background binding signal was negligible for all cell lysate samples at the indicated dilution or neat. Expressed antibodies were PA38 (A), 4G2 (B), PA38 (C), ET21 (D), ET149 (E). Red arrows indicate original standard induction conditions while black arrows indicate size of fully assembled IgG.

3.4 Comparison of yield by large scale expression

We then sought to determine the potential yield of bacterial IgG from a large scale production. Based on the small scale expression, the best unit yields for PA38, PA64 and 4G2 would be given by using high copy plasmid, 20ng/ml inducer concentration and induction at OD₆₀₀ 1.0. The yield would also be enhanced further by the greater wet cell mass obtained under this condition. For ET21 and ET149, 50ng/ml inducer concentration appears to be best in comparison to 20ng/ml (with high copy plasmid and induction at OD₆₀₀ 1.0) for giving the best unit yield, but overall yield would be affected by the reduction in wet cell mass. To determine likely overall yields, we therefore carried out large scale expression in 1.6 litres of culture on one antibody of each group, 4G2 and ET149 respectively. All were induced at OD₆₀₀ 1.0 with high copy plasmid and at inducer concentrations of 20 and 50ng/ml respectively.

Purification was carried out on a 1ml Protein A HPLC column and elution of IgG was tracked using absorbance at 280nm. Analysis of the individual peak fractions indicated successful expression of full length IgG (2H2L) for both 4G2 and ET149 (Fig. 3-5A & B). Protein bands of other sizes were also observed in the elute peak fractions. Analysis of selected 4G2 and ET149 fractions by western blot (Fig. 3-5B) indicated that some of these protein bands were not antibody heavy or light chains as they were not detected with anti-human Fc or Kappa polyclonal antibody and hence are probably bacterial proteins that co-purify with the bacterial expressed IgG. This non-specific elution of bacterial proteins was unexpected, as previous papers had reported clean elution of bacterially expressed full-length IgG from

Protein A (110,125). Some degradation of the heavy chain was also observed as bands larger than the full sized light chain but smaller than the full sized heavy chain was observed on the reducing western blot (Fig. 3-5B).

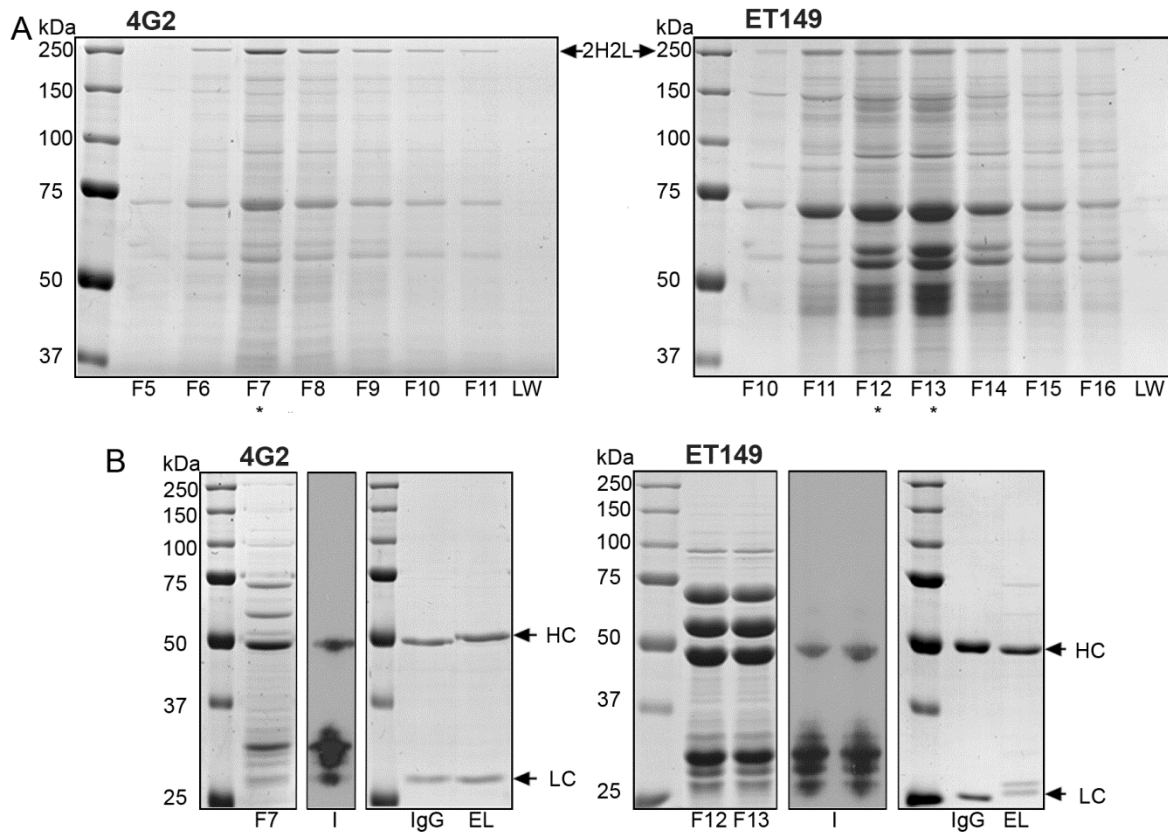


Figure 3-5: Purification of bacterial IgG on Protein A and Protein L

(A) Non-reducing Coomassie gel of peak fractions from Protein A HPLC purification of cell lysate of 4G2 and ET149. A wash sample (LW) was run and shows no contaminants present indicating the column was washed sufficiently to remove non-binding proteins. 2H2L indicates fully assembled IgG. **(B)** Reducing Coomassie gels and adjacent western blots (I) showing representative fractions from each Protein A elution (indicated with * on panel A). Blots were probed with both anti-IgG Fc and anti-Kappa chain polyclonals showing that majority of protein bands in the fraction are neither IgG heavy chain nor light chain. A separate reducing Coomassie gel shows 2 μ g of pooled elute (EL) after Protein L purification showing successful removal of the contaminating proteins and degraded heavy chain fragments. The equivalent amount of mammalian cell culture-derived IgG (IgG) was loaded for comparison. Individual heavy (HC) and light (LC) chains are indicated although the light chain for ET149 appears as two separate species. 30 μ l sample was loaded for Coomassie and 3.75 μ l for western blot.

Due to the impurity of the Protein A eluate, it was decided to carry out an additional purification step using Protein L, which binds the antibody light chain. Sequential purification on first Protein A and then Protein L should enable isolation of only antibody that contain both heavy and light chain, thus eliminating any unpaired heavy or light chain along with degraded fragments and contaminating bacterial proteins. Indeed, the higher molecular weight contaminants as well as the heavy chain degradation products were removed by Protein L purification of 4G2 and ET149 (Fig. 3-5B). Final yields of antibody were 12.6 μ g and 6.3 μ g for these antibodies respectively.

3.5 Comparison of bacterial and mammalian expressed IgG

Following removal of the bacterial contaminant proteins and heavy chain degradation products through protein L purification we next decided to check for the presence of fully assembled tetrameric IgG. Analysis of the protein L eluate on non-reducing SDS-PAGE indicated that a large proportion of the purified chimeric 4G2 and ET149 IgG was present as fully assembled IgG (2H-2L, Fig. 3-6). However partially assembled IgG representing 2H-1L and 1H-1L was also evident. The increase of partially assembled IgG seen with expression in *E. coli* could be due to inefficient disulphide bond formation during assembly within the bacterial periplasm.

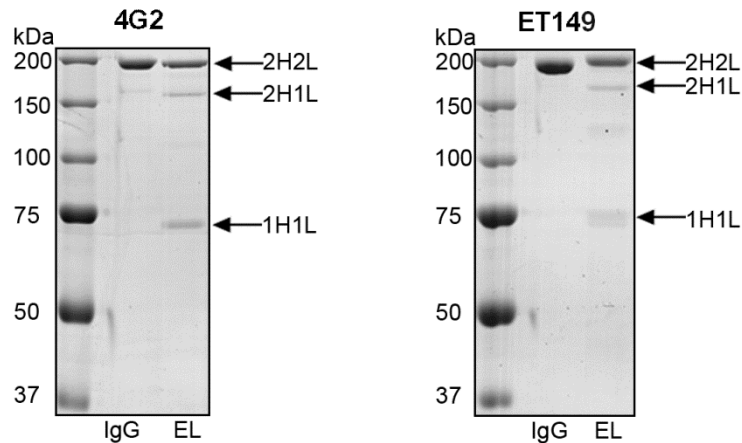


Figure 3-6: Coomassie gel of purified bacterial IgG

Non-reducing SDS-PAGE of 2 μ g of pooled bacterial IgG eluate after protein L purification (EL) and mammalian cell culture-derived IgG (IgG) indicates that the majority of purified IgG was fully assembled IgG (2H2L) although partially assembled IgG (2H1L, 1H1L) are also present

To determine whether the bacterially expressed IgG retained the same binding avidity as those expressed in mammalian cell culture, an indirect ELISA of serially diluted purified IgG expressed from both bacterial and mammalian cell cultures was carried out against Dengue-2 and epsilon toxin using 4G2 and ET149 respectively. A slight decrease in avidity was observed for both 4G2 and ET149 bacterially expressed IgG in comparison to mammalian cell culture derived IgG (Fig. 3-7). This could be due to an increased percentage of partially assembled IgG in the bacterially expressed antibodies as observed in the SDS-PAGE gels (Fig. 3-6). These partially assembled IgGs would have reduced avidity due to the presence of only one antigen binding site.

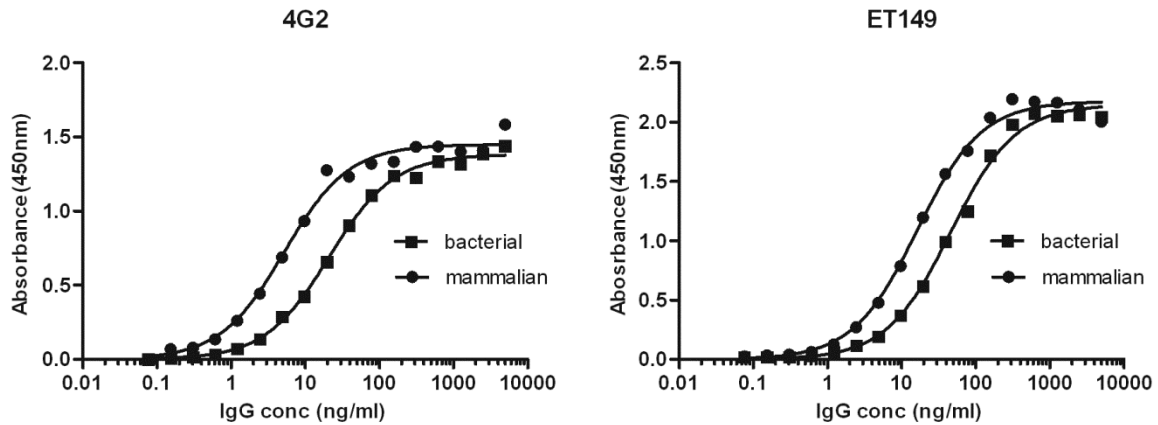


Figure 3-7: Comparison of mammalian and bacterial culture expressed IgG affinity

Indirect ELISA of serially diluted bacterial (-■-) and mammalian cell culture (-●-) derived IgG against Dengue serotype-2 virus and epsilon toxin showing similar binding curves. Binding was detected with anti-human Fc-HRP secondary antibody.

3.6 Discussion

From our initial experiments, it was clear that IgG expression in *E. coli* laboratory strains using general expression protocols gave poor yields and highly degraded product and the use of the protease-deficient BL21 strain was unable to reduce degradation (Fig. 3-2). Previous studies suggested that overload of the protein secretory and folding system was responsible for the poor yield and we therefore undertook optimization of expression conditions to minimize load via reduction of translational levels. We have demonstrated on the basis of expression of three different antibodies (PA38, PA64 and 4G2) against two separate antigens that reduction of translational levels can improve unit yields of full-length IgG (Fig. 3-4). This was achieved by using either low copy plasmid, reducing inducer concentrations or induction at a later time point. However, the effects of these changes is antibody dependent and may negatively impact unit yields for certain

antibodies as seen in the effect of reducing inducer concentrations for antibodies ET21 and ET149. This could be because they are more efficiently processed by the *E. coli* secretory and folding machinery and thus can be translated at high rates without any significant impact on final yields. Lowering translation rates hence decreases yields instead. This is supported by our observation that two antibodies appear to have the best unit yields overall, as they have the most intense band on western blot and also require a greater dilution, 1:64 compared to 1:16, 1:8 or 1:2, to obtain an equivalent signal by ELISA (Fig. 3-4).

The effect of varying inducer concentration and induction OD_{600} on wet cell mass and unit yields was minimal when low copy plasmids were used. It may be that the low copy number results in a low baseline translation level which cannot be further reduced by delayed induction or inducer concentration. This low baseline translational level could also enable the *E. coli* host to redirect more of its metabolism into replication rather than protein expression, which explains the uniform increase in wet cell mass obtained (Fig. 3-3). This redirection of energy towards growth may also be the reason for the increase in wet cell mass observed at the lowest inducer concentration. Hence, wet cell mass yield is either unaffected or improved by reducing translational levels and as such antibodies which can have their unit yields improved by reducing translational levels, such as 4G2, PA38 and PA64, also benefit from a simultaneous increase in wet cell mass yield.

Purification of the cell lysate with Protein A was insufficient to give pure full-length IgG with bacterial proteins and heavy chain fragments co-purifying in the eluate and as a result subsequent Protein L purification was required (Fig. 3-5). The

inability of Protein A purification alone to give purified antibody, in contrast to previously reported findings, could be due to the extremely low yield of IgG resulting in non-specific binding of bacterial proteins to unoccupied Protein A binding sites. This could also be due to the binding of chaperone and heat shock proteins to the hydrophobic surfaces of unfolded expressed antibody (193). However, due to the large volume of lysate required to be processed for reasonable antibody yields, a sufficiently large Protein A column must be used for efficient antibody capture and hence having empty binding sites is an unavoidable consequence of the low yield of fully assembled IgG.

The ability of our bacterial IgGs to bind both Protein A and Protein L indicates that the binding sites on the antibody are presented on the surface and suggests that the IgG is properly folded. Crucially, the purified 4G2 and ET149 antibodies were able to bind their respective antigens albeit with slightly reduced avidity as compared to mammalian cell expressed antibody and indicates that bacterially expressed IgG could substitute for mammalian derived IgG (Fig. 3-7). *E. coli* expressed IgG1 has been found to bind the neonatal Fc receptor (FcRn) and have the same pharmacokinetic parameters in the circulatory system as mammalian cell expressed IgG2 and IgG4b, but was unable to bind complement (C1q) or FcγRI (125). This suggests that *E. coli* derived antibodies lack effector functions as expected for aglycosylated antibodies. The inability of aglycosylated antibodies to bind Fcγ receptors has also been demonstrated in mammalian derived aglycosylated antibodies (194). However, this function is not required for diagnostic antibodies and hence should not hinder the use of bacterially expressed antibodies for this purpose.

We have therefore evaluated the effect of reducing translational rates using simple mechanisms such as delayed induction or reducing induction concentrations to improve yields. Use of a combination of both methods clearly improved yields for several antibodies (4G2, PA38, PA64) due to both increased unit yield and increased wet cell mass. This is reflected in the levels of recoverable full length IgG which in 4G2 was improved to 7.87 μ g/L of culture while previously no full length antibody could be purified or even detected on western blot (at standard conditions, Fig. 3-4).

Previous studies on improvement of yields have often focused only on unit yields (as comparisons were based on percentage of total protein) or on overall yields per volume of culture (125,183) . Here we show that reducing translational rates can improve yields, but this occurs due to two separate processes. We also show that for certain antibodies, unit yield can occasionally be increased at the expense of wet cell mass yield and therefore both have to be taken into account during optimization. We use only commercially available plasmid vectors, inducer and *E. coli* strains and do not rely on extensive molecular biology reengineering of the promoter or coding regions, or expression of additional chaperones. Our methodology should therefore be readily applicable in the majority of laboratories to produce bacterial IgG that have virtual identical performance to their mammalian cell culture expressed counterparts in terms of avidity.

Chapter 4: Generation of anti-ManLAM antibodies by phage display

4.1 Introduction

Lipoarabinomannan (LAM) is a *Mtb* membrane glycolipid that is currently the subject of significant research for the purpose of TB diagnostics due to its reported presence in patient urine, an easily sampled clinical specimen (13). However, although initial studies were promising, with sensitivity and specificity above 80%, subsequent studies showed poor performance due to low sensitivity which ranged from 13% to 59%, although sensitivity remained high at above 83% (13,83,85,87,151,153,154,195). Sensitivity has been shown to be improved in HIV positive patients and especially in the cohort with low CD4 counts and has been attributed to spread of *Mtb* infection to the urinary tract resulting in higher levels of LAM excretion, or alternatively, formation of immune complexes in the blood due to anti-LAM antibodies resulting in reduced excretion in the urine in immunocompetent individuals (156,157). The paucity of LAM in the urine has led to studies on the possibility of LAM detection in other clinical material such as sputum or serum. However, a study on detection of LAM in sputum using a commercial polyclonal antibody had improved sensitivity (86%) but very poor specificity (15%) (154). Low specificity was shown to be due cross-reactivity to non-mycobacterial species that reside in the oral cavity such as *Nocardia* and *Tsukamurella* species.

LAM is present in all mycobacterial species as three different structural variants (ManLAM, AraLAM and PILAM), as well as in other actinomycete species including those mentioned above (130,132-135,196). It is therefore highly likely that polyclonal anti-LAM antibodies, which bind multiple epitopes on the LAM molecule, would recognize non-mycobacterial LAM along with all mycobacterial species. In

addition, monoclonal anti-LAM antibodies may also not be able to distinguish between mycobacterial LAM variants. This has been shown to be the case for well characterized anti-LAM monoclonals, as they recognize mycobacteria from both the fast-growing group such as *M. smegmatis* and *M. fortuitum* that carry PILAM as well as slow-growers such as *Mtb*, or been shown to bind the core LAM oligosaccharide (84,197). An antibody that is capable of recognizing only the α 1-2 mannose caps of ManLAM would have high specificity for the slow-growing highly pathogenic group of mycobacteria which includes *Mtb*. This would potentially improve the specificity of LAM based diagnostic assays and allow for testing of clinical samples that may have high concentrations of LAM (such as sputum) but are also contaminated with other microbiota that express related glycolipids without the specific mannose caps.

4.2 Panning of the Humanyx phage library

Phage display allows for the application of antibody selection techniques not possible with traditional animal immunization. As the mannose caps comprise only a small proportion of the entire LAM molecule, we considered it unlikely that a straightforward selection against LAM would produce antibodies against the mannose caps. We therefore developed a novel method of phage display screening that used a related antigen, PILAM, to deplete antibodies against epitopes common to all LAM species (negative selection) from a non-immune human antibody phage display library (Humanyx) in order to drive antibody selection towards the targeted unique region of the desired antigen, the α 1-2 mannose caps of ManLAM (Fig. 4-1A). Depletion was achieved by binding the phage library to PILAM prior to binding against ManLAM. Using this method, we were able to demonstrate ManLAM-specific

enrichment of the polyclonal phage library preparations from Pan 1 to Pan 4 as measured by indirect phage ELISA (Fig. 4-1B). No increase in binding for PILAM was observed from Pan 1 to Pan 4, indicating that there was no enrichment of antibodies against the common backbone of LAM. While Pan 4 had the highest polyclonal signal, Pan 3 only had a slightly lower signal, indicating that the proportion of ManLAM-specific phage were probably only slightly reduced in Pan 3 versus Pan 4. Since repeated panning can result in loss of antibody diversity due to competition for limited antigen, Pan 3 was expanded into monoclonals for screening so as to capture as wide a diversity of ManLAM specific antibodies as possible.

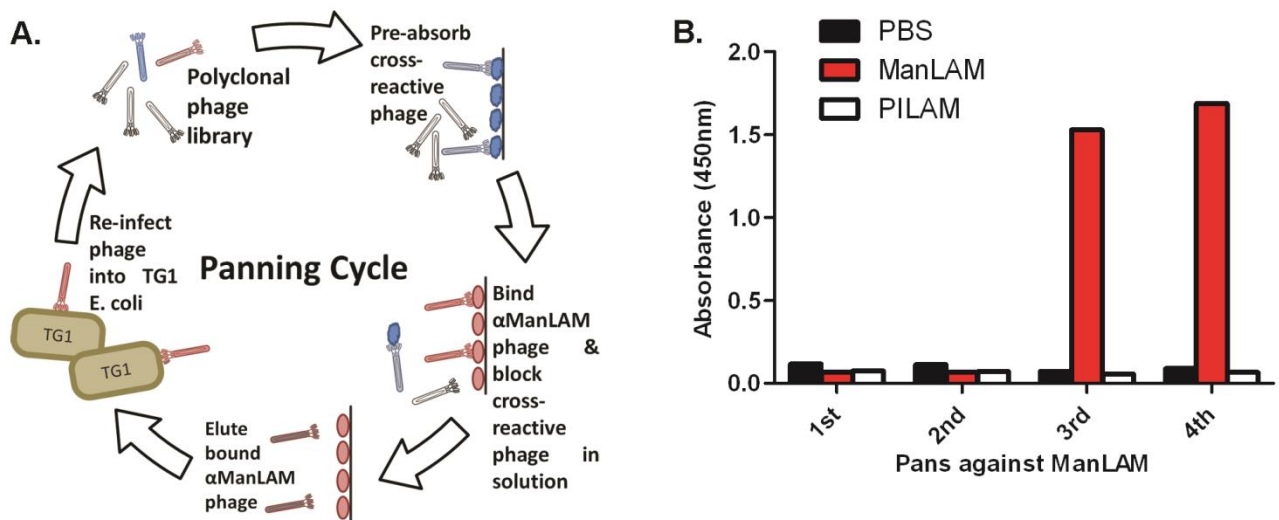


Figure 4-1: Panning of Humanyx antibody phage library against ManLAM

(A) Procedure for phage panning with negative selection. **(B)** Selective enrichment of Humanyx library for ManLAM-specific binders as indicated by indirect polyclonal phage ELISA.

4.3 Monoclonal screening and identification of my2F12

Three hundred and eighty (380) monoclonals from Pan 3 were screened for ManLAM specificity by indirect phage ELISA by testing against PILAM as the negative control. There were a significantly greater percentage of strong and moderate specific binders (ManLAM signal vs. PILAM signal > 5, 66.6%) as compared to weak and negative binders (ManLAM signal vs. PILAM signal < 5, 33.3%), indicating that there was efficient selection for strong binders (Table 4-1). 96 clones with highest specific signal against ManLAM were selected and their antibody sequence amplified via colony PCR. BstN1 digests were carried out on the PCR products and the digestion pattern compared. All 96 selected clones had identical digestion patterns suggesting that only one unique clone was present (Fig. 4-2). Six clones were sequenced which confirmed that only one unique clone (my2F12) present, the CDR sequence and germline variable gene source is given in Table 4-2. This was cloned into our mammalian expression vector carrying the huG1 constant region (198), and transiently expressed in HEK 293 cells as full length human IgG1. This recombinant antibody was specific for ManLAM of two different *Mtb* strains but did not shown any binding to PILAM from *M. smegmatis* thus verifying its specificity for ManLAM (Fig. 4-3). In contrast, a commercial rabbit polyclonal sandwich ELISA bound both the two ManLAMs and PILAM tested positive for all variants.

Signal-to-noise ratio (ManLAM vs PILAM signal)	No. of clones	Percentage of Total (%)
Negative (SNR < 2)	81	24.47
Weak (SNR 2-5)	46	12.11
Moderate (SNR 5-10)	160	42.11
Strong (SNR > 10)	93	24.47

Table 4-1: Binding characteristics of monoclonals from 3rd Pan

Proportion of negative, weak, moderate and strong binding clones isolated from the 3rd Pan as determined by monoclonal phage ELISA.

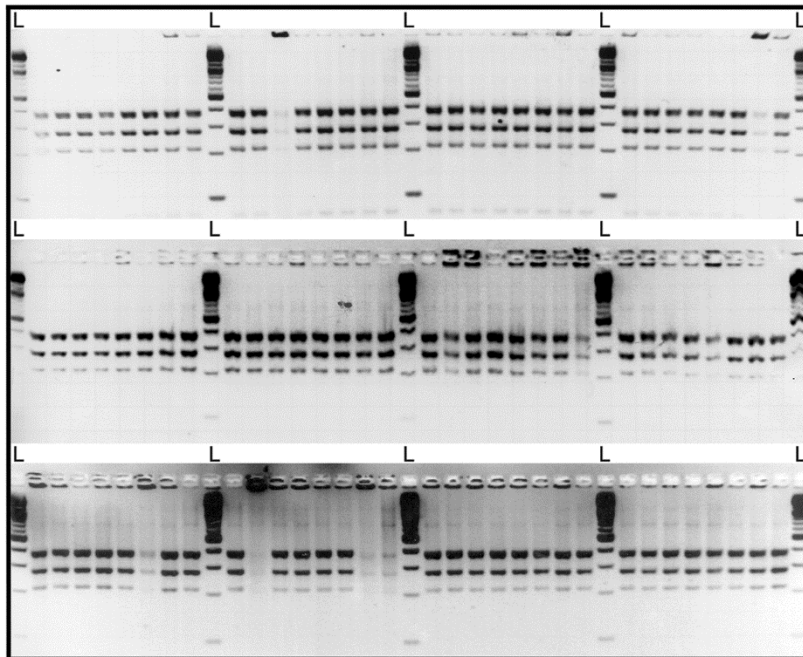


Figure 4-2: Diversity of monoclonals from the enriched 3rd Pan

BstN1 digest of 96 selected highest binding clones. All clones had the same digestion pattern. DNA Ladder (L) is loaded alongside digested samples for reference.

Chain	CDR1	CDR2	CDR3	Germline
Heavy	NYAMS	TIGTTDGGDIHYADSVKG	RFGEHFDYWGGQTL	HV3-23*04 HD3-10*01 HJ4*02
Light	RSSQSLVHSDGNTYLS	KISNRFS	MQATQFPWTFGQGTK	KV2-24*01 KJ1*01

Table 4-2: CDR sequences of isolated monoclonal my2F12

Amino acid sequences of the heavy and light CDR regions and germline genes used in my2F12. Basic amino acids are in bold.

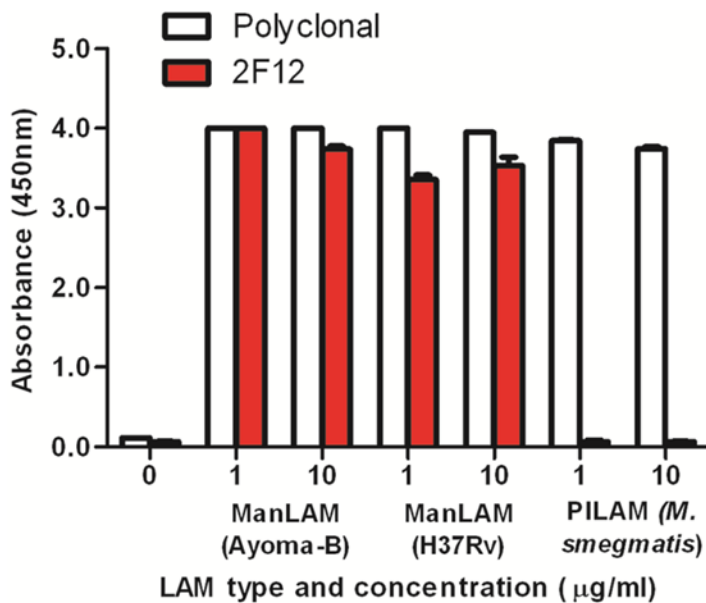
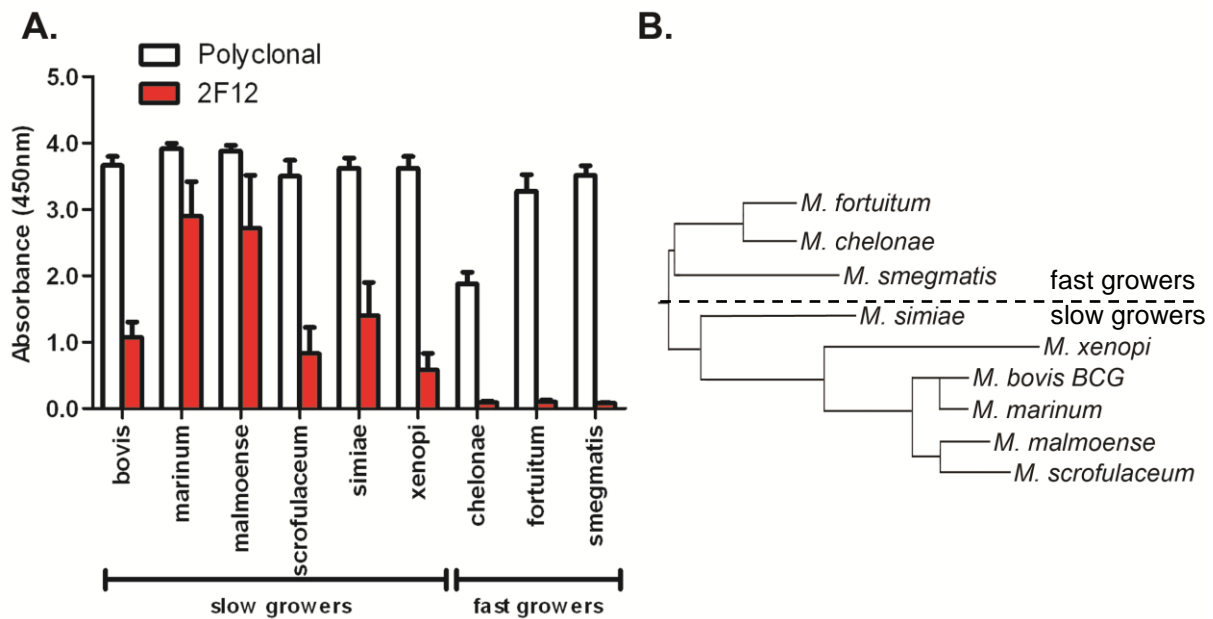


Figure 4-3: ManLAM-specificity of isolated monoclonal my2F12

Sandwich ELISA using my2F12 Fab fragment as capture and my2F12 HuG1 as detector or with Clearview commercial diagnostic assay using rabbit anti-LAM polyclonal on ManLAM and PILAM in PBS. Results are the average of three independent experiments with error bars showing standard error of mean.

4.4 Characterization of my2F12 specificity

To verify that specificity for the α 1-2 mannose caps conferred the ability to distinguish LAM derived from fast growing mycobacteria from slow growing mycobacteria as predicted, we then tested our antibody via sandwich ELISA on secreted LAM-containing culture supernatants from various mycobacterial species grown in Middlebrook 7H9 broth. As predicted, antibody binding was only observed for the culture supernatants of slow-growing species (Fig. 4-4A, a phylogenetic tree of the mycobacterial species is given in Fig. 4-4B). In contrast, a commercial rabbit anti-LAM polyclonal was observed to bind all LAM variants and supernatants of all mycobacterial species. However, variability in signal for my2F12 binding was observed between the various slow-growing species. This is probably due to



variation in levels of secreted LAM because of differences in length of time in culture and rate of growth.

Figure 4-4: Mycobacterial specificity of ManLAM specific antibody my2F12

(A) Sandwich ELISA using my2F12 Fab fragment as capture and my2F12 HuG1 as detector or with commercial kit using rabbit anti-LAM polyclonal on LAM secreted by slow-growing versus fast-growing mycobacteria in culture supernatant my2F12 is only specific for ManLAM and LAM secreted by slow-growers while the rabbit polyclonal binds all LAM variants. Results are the average of three independent experiments and error bars show standard error

of mean **(B)** Phylogenetic tree of tested species based on 16s ribosomal RNA sequences. Adapted from Shinnick & Good, 1994

To definitively identify the types of carbohydrates recognized by my2F12 we tested for antibody binding to various synthetic carbohydrates printed onto microarray slides (Fig. 4-5). The antibody was shown to bind only oligomannose carbohydrates containing α 1-2 mannose linkages and did not bind those with only α 1-4 or α 1-6 mannose linkages such as PIM₄ (phosphatidylinositol tetramannoside) hexamannan or trimannose. Binding was possible even with one α 1-2 mannose linkage present (PIM₅), which suggests that this is the minimal binding footprint of the antibody. No binding was observed to other saccharides consisting of other hexose or pentose monomers, such as maltotriose, fucose, rhamnose, lactose, galactose, and di- & hexa-arabinan (Fig. 4-6). This specificity of my2F12 for α 1-2 linked mannans, the only type of linkage found in the cap of ManLAM, thus clarifies and confirms our earlier results showing specificity for the mannose-caps of ManLAM.

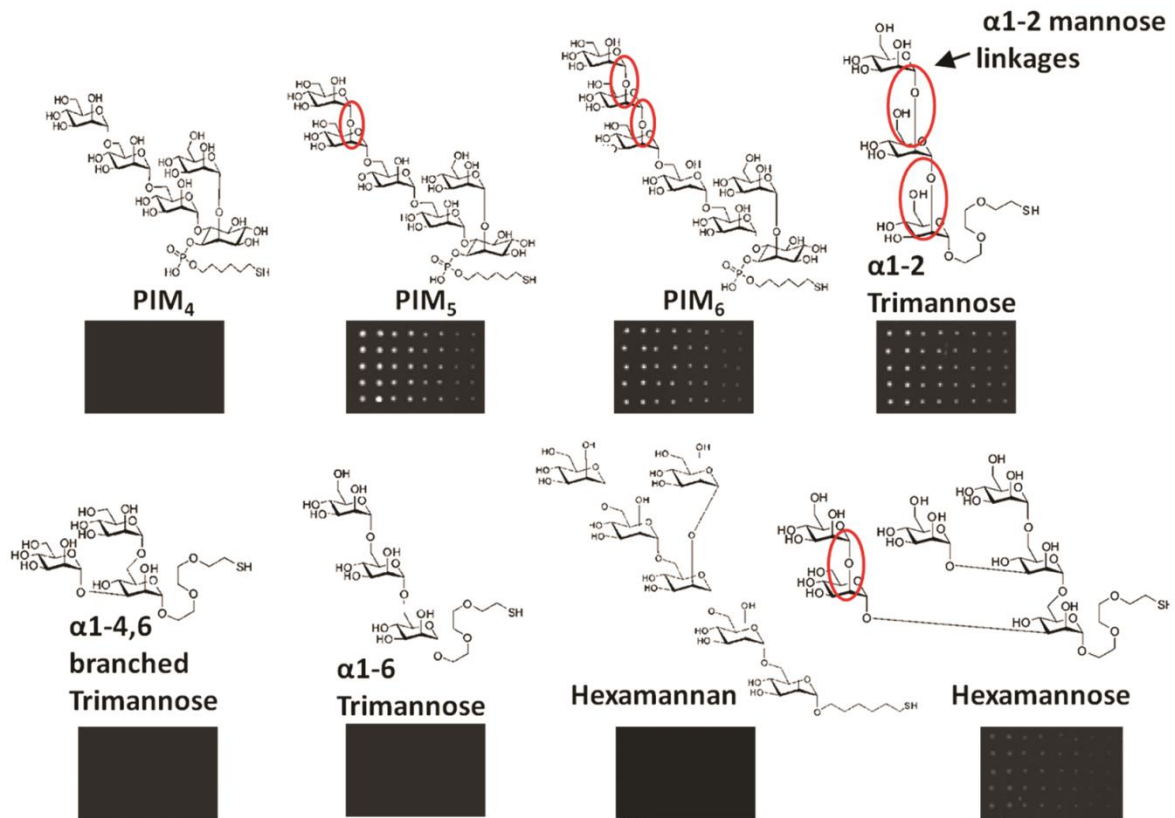


Figure 4-5: my2F12 specificity for α 1-2 mannose linkages

Carbohydrate microarray with oligomannose carbohydrates with α 1-2 (red circles), as well as α 1-4 and α 1-6 linkages. my2F12 was only found to bind oligomannose carbohydrates with at least one α 1-2 mannose linkage.

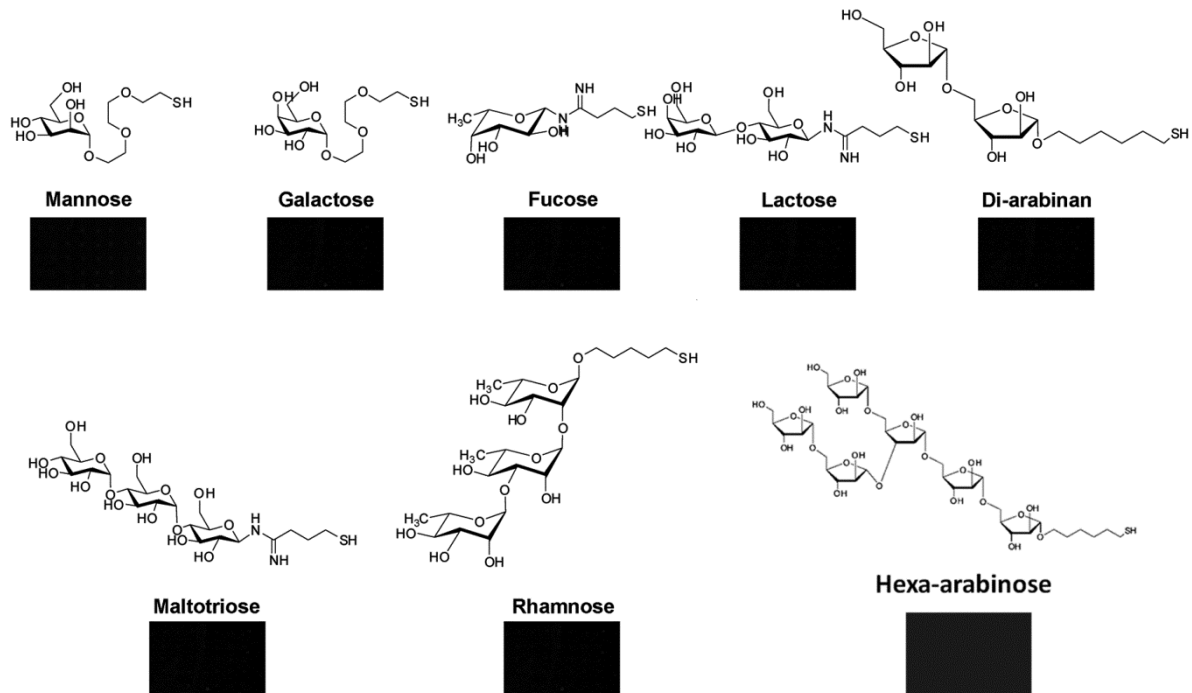


Figure 4-6: Lack of my2F12 binding to other oligosaccharides

Other mono, di- and oligosaccharides were bound on microarray and tested for affinity to my2F12. No binding was observed

4.5 Expression of my2F12 in bacteria

In the previous chapter, we sought to determine if we could express full length IgG in a bacterial host. We were able to express limited quantities of full length IgG using simple methods to boost yields such as reducing inducer concentrations and induction at a later time point to reduce translation rates. The expressed bacterially IgG had virtually identical binding avidity compared to that of mammalian IgG and could potentially be used for as a diagnostic reagent. We therefore attempted to express my2F12 using this same methodology. We had previously shown that the optimal inducer concentration and induction OD needs to be determined for each individual antibody. We also showed that a generally high but not optimum yield can

be obtained just by using low-copy plasmid. We therefore applied the same optimizations carried out in the previous chapter to my2F12 to determine whether this antibody could be successfully expressed in bacteria.

my2F12 had a similar pattern of wet cell mass yield as compared to the other antibodies tested, with the highest yields given by the low copy number plasmid, which were not affected by other induction conditions, while the yields with high copy plasmid varied with inducer concentration as before with higher yields obtained with lower inducer concentrations (Fig. 4-7).

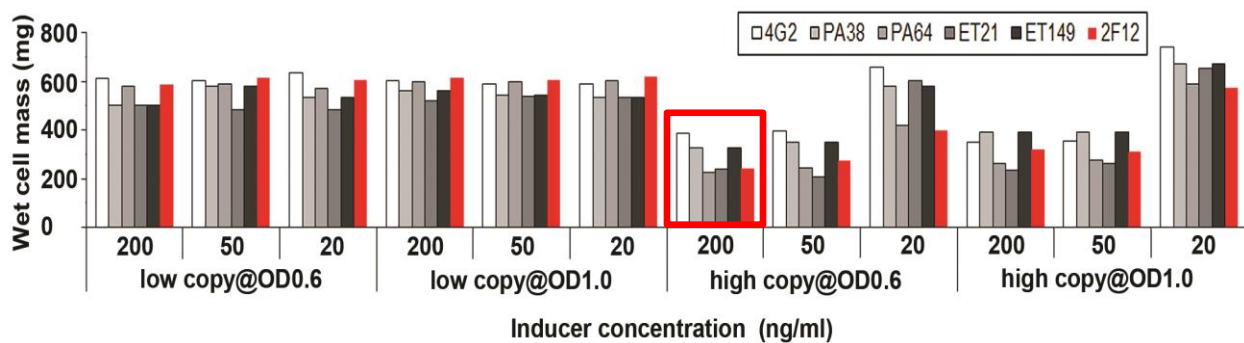


Figure 4-7: Wet cell mass obtained during expression of my2F12 bacterial IgG

Variation in wet cell mass for my2F12 (red bar) in comparison to the previously expressed five antibodies under different induction conditions. Red box represents yield under standard induction conditions

Like the other antibodies, levels of fully assembled antibody approximately correlated with the levels of functional antibody, as indicated by western blot and ELISA respectively, over the various conditions tested (Fig. 4-8). Unit yields of antibody under low copy plasmid conditions remained relatively unchanged when inducer concentrations and induction time point was varied, consistent with the pattern observed with other antibodies. When high copy number plasmid was used,

reducing inducer concentration improved unit yields at induction at OD₆₀₀ 0.6 but decreased yields at OD₆₀₀ 1.0. This pattern had not been observed previously. The best unit yield was given by expression with high copy plasmid at OD₆₀₀ 1.0 with 200ng/ml of inducer.

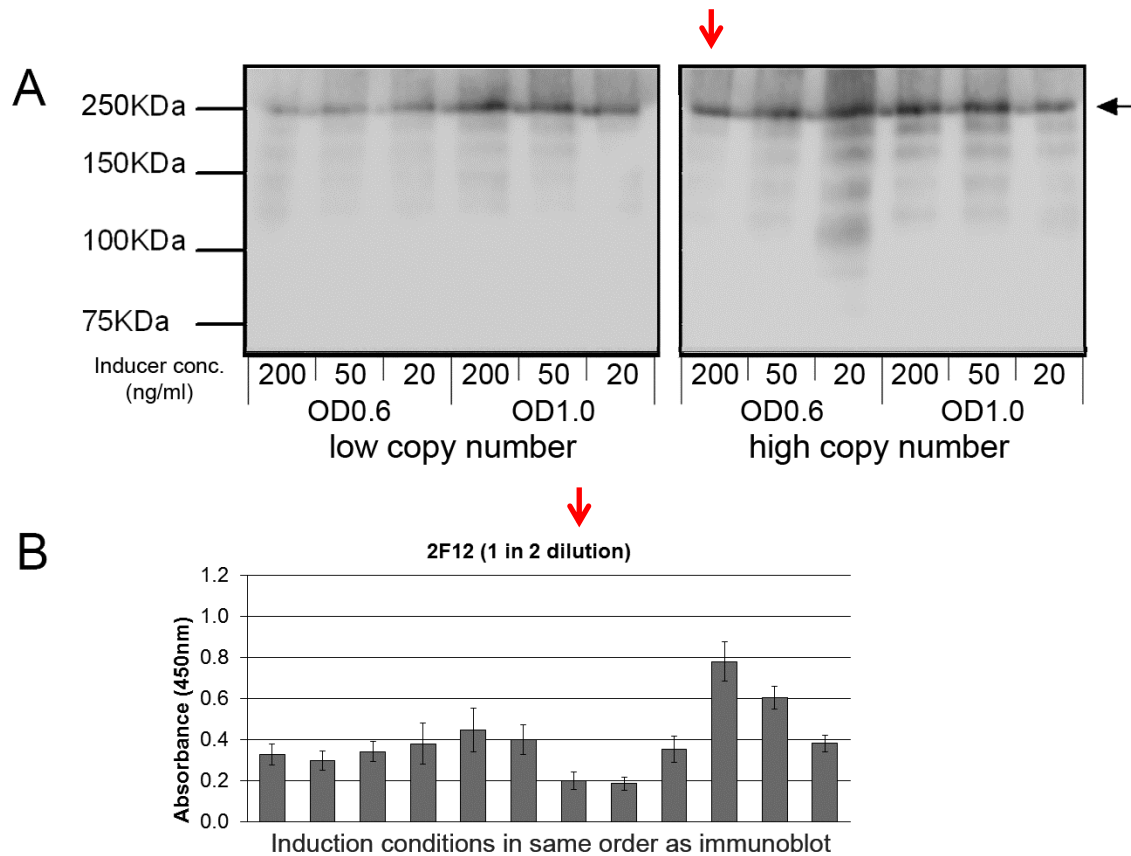


Figure 4-8: Levels of fully assembled or functional my2F12 bacterial IgG obtained under different induction conditions

(A) Left and right panels: Non-reducing western blot of 7.5µl clarified cell lysate from small scale overnight expression of my2F12 in shaking culture. All blots were probed with anti-Human Fc-HRPO and adjusted to ensure equal intensity. **(B):** Indirect ELISA indicating levels of functional IgG. Background binding signal was negligible for all cell lysate samples at the indicated dilution or neat. Red arrows indicate original standard induction conditions while black arrows indicate size of fully assembled IgG.

Having determined the optimal conditions for highest unit yields, we then proceeded to determine potential yield from a large-scale purification. This was carried out in the same manner as in the previous chapter using sequential Protein A and Protein L purification. No protein band representing fully assembled IgG was detected on the Coomassie gel of the Protein A elute fractions or in the pooled eluate (Fig. 4-9). Consistent with the lack of full length IgG expression, purification on protein L on the pooled Protein A eluate of my2F12 eliminated all protein bands and the eluate had negligible amounts of protein (<1 µg) as measured by Bradford assay. This was unexpected given our success at achieving recoverable yields previously and the detection of fully assembled, functional IgG by Western blot and ELISA.

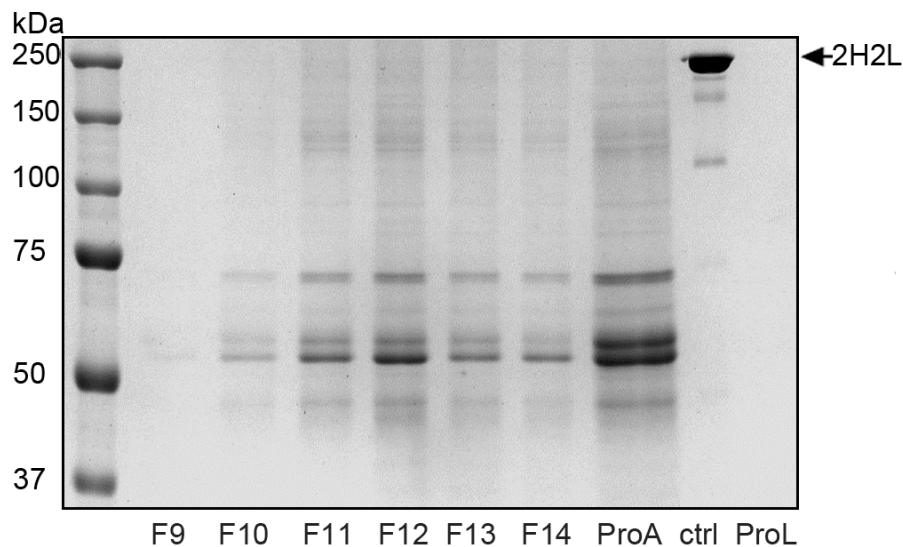


Figure 4-9: Large scale expression and purification of my2F12 bacterial IgG

Non-reducing Coomassie gel of peak fractions from Protein A HPLC purification of cell lysate of my2F12. 30µl of each fraction or pooled Protein L eluate (ProL) or 2µg of pooled Protein A eluate (ProA) was run. 2µg of mammalian culture expressed full length my2F12 was added as a control (ctrl) which is indicated by the arrow 2H2L. No protein bands were observed at that size for all peak fractions and pooled eluate indicating very low protein expression of full length IgG

4.6 Discussion

A ManLAM-specific antibody could be of great benefit to LAM-based TB diagnostics by improving the specificity of such assays for various types of clinical samples. Using a subtractive phage display technique, we have developed an antibody that can distinguish the mannose-capped LAM produced by slow growing mycobacteria from other forms of LAM produced by fast-growing mycobacteria. We have proven its specificity based on differential binding to both purified LAM as well as LAM secreted into culture supernatant from both groups of mycobacteria (Fig. 4-2 & 4-3) As the major pathogenic species of mycobacteria such as *M. tuberculosis*, *avium*, *bovis* and *leprae* all fall within this group of slow-growers, our antibody is likely to be extremely useful for detecting infections arising from such pathogens.

We also show using carbohydrate microarrays that our antibody's specificity for ManLAM is its ability to only recognize the α 1-2 mannose linkage while having no binding for other mannose linkages such as α 1-4 and α 1-6, or to other mono-, di-, and oligosaccharides, some with identical linkages. X-ray crystallography of another anti-LAM antibody (CS-35) specific for the secondary arabinose branches of LAM shows that the binding pocket of that antibody forms a surface that can uniquely recognize arabinofuranose residues in that branched configuration (199). Therefore it is not surprising that our antibody is capable of having such exquisite specificity for mannose residues in that particular linkage.

While phage display libraries have previously been used to generate anti-carbohydrate antibodies, this is the first time a subtractive depletion technique has

been applied to focus antibody specificity to a particular antigenic region on the carbohydrate molecule (200). As the utility of diagnostic antibodies depends highly on their specificity, this methodology for generating highly specific, high-affinity anti-carbohydrate antibodies could prove to be highly useful. Typically, panning of phage libraries produces multiple antibodies specific for the target antigen (200,201). Interestingly however, all isolated antibodies from our enriched library were clones of one unique high-affinity antibody, indicating that there are an extremely limited set of ManLAM-specific antibodies within our library, or that competition for limited antigen resulted in only one high-affinity antibody displacing all other weaker binding clones in the process of enrichment. Either possibility suggests that such a high affinity ManLAM-specific is extremely rare and may not be easily obtained through standard phage library panning or hybridoma techniques.

Given the diagnostic purpose of our antibody, functions such as complement and Fc receptor binding are not required and hence we sought to use the bacterial IgG optimization and expression methodology developed in the earlier chapter to determine if my2F12 can be expressed in bacteria in useful quantities. This would significantly reduce the cost of diagnostic assay production. However, although the small scale optimization experiments indicated that some functional, fully assembled antibody was successfully expressed and that reduction of translational rates by using induction at a later time point did enhance unit yields (Fig. 4-8), large scale expression and purification with those optimized conditions failed to recover a quantity of antibody sufficient for characterization and testing on additional diagnostic samples (Fig. 4-9). It must be noted that even at optimized unit yields, antibody expression levels were low as in order to obtain moderate levels of ELISA signal, a

high 1:2 dilution of the lysate was required (Fig. 4-8). Furthermore, conditions that gave the best optimized unit yields significantly decreased wet cell mass yields, a pattern noted with some of the antibodies tested earlier (ET21 and ET149) and which would impact on overall yield. It may also be that my2F12 may just be prone to degradation in *E. coli*, as evidenced by multiple bands on the Western blot smaller than the full sized antibody. We therefore switched to mammalian expression of IgG for the subsequent further characterization and testing of this antibody.

Based on our data, my2F12 has exquisite specificity for ManLAM and presents a unique opportunity to develop highly specific point-of-care TB diagnostics. Subsequent characterization on a variety of assay formats and clinical material will be done in order to determine the diagnostic utility of this antibody.

**Chapter 5: Optimization of my2F12 antibody and sample
processing for diagnostic use**

5.1 Introduction

In the previous chapter, we described the isolation of a ManLAM specific antibody using a novel negative selection method on the Humanyx phage display antibody library. The antibody was shown to bind directly to α 1-2 mannose linkages on synthetic oligosaccharides and recognized only the LAM secreted by the slow-growing group of mycobacterial species such as *Mtb* as predicted based on its mannose linkage specificity. This is the first anti-LAM antibody characterized with such specificity and we therefore sought to determine its utility on a variety of antibody-assays that are applicable to TB diagnostics.

A common type of antibody assay used in diagnostics is the sandwich ELISA (enzyme-linked immunosorbent assay), in which antigen is captured from solution by surface adsorbed antibodies coated onto an ELISA plate. The bound antigen is then subsequently detected by a second antibody added after the capture phase. This mode of ELISA is particularly useful for detecting antigen in a complex matrix without the need for prior purification or concentration, is capable of very high sensitivity and thus is ideal for the detection of LAM from clinical samples such as sputum, urine or serum (79). While sandwich ELISAs typically require a pair of antibodies that bind different epitopes so as to prevent competitive binding for a single epitope, the multiplicity of α 1-2 mannose caps on a single LAM molecule (7-10 depending on species) allows for the same antibody to be used both as a capture and detector antibody without interference to the binding of either antibody, as seen in functionality of our monoclonal sandwich ELISA in the previous chapter (196,202).

However, in order to use the same antibody, it must be modified such that the binding of the detector antibody can be distinguished from the capture antibody which is already present on the ELISA plate. This can be accomplished either by direct labelling of the detector antibody with the signal generating enzyme (typically horseradish peroxidase), or modifying the detector antibody with a tag e.g. biotin that can be recognized by a secondary antibody (79,202). Detection with secondary antibody is generally preferred for diagnostics due to a generally lower background and higher amplification of signal (Michel, G., personal communication). Use of recombinant antibodies offers a third option in the ability to express chimeric antibodies with the same variable domain but with switched constant regions (203). Thus, an antibody with the same specificity can be expressed as a human or mouse isotype, which can be detected separately with an appropriate species-specific secondary antibody. This avoids having to chemically label the detector antibody. The use of anti-mouse secondary rather than an anti-human secondary also has the advantage of reduced cross-reactivity to endogenous antibodies found in clinical samples such as serum.

A second type of antibody assay is the immunofluorescence (IF) or Immunohistochemistry (IHC) assay, in which a sample on a slide is probed with fluorescently labelled or enzyme conjugated pathogen-specific antibodies. For IHC, antibody binding is followed by a development step where the slide is incubated with a dye that precipitates onto the slide in the presence of the enzyme conjugate, thus identifying the location of the antigen (204). Such techniques are particularly useful for the detection of extrapulmonary TB, where traditional methods such as culture, acid-fast staining and NAATs have shown low sensitivity while relying on cell

histology alone is non-specific (205,206). IF can be also easily applied to sputum smear fluorescent microscopy, which can be now carried out in resource poor settings due to the development of battery powered portable light-emitting diode based fluorescent microscopes (71). This would enable slow-growing mycobacteria to be rapidly distinguished from other acid-fast bacilli and be useful in areas of low TB incidence. A chimeric antibody would also be of value in this assay for the same reasons described above. We therefore constructed chimeric variants of my2F12 and verified that they retained similar avidity as the parent antibody. We also explored their potential utility in the two types of diagnostic assays described above by determining their specificity with regards to a wide range of mycobacterial and other bacterial species.

5.2 Design and expression of my2F12 chimeric antibodies

A traditional chimeric antibody consisting of a human light chain and heavy variable region and mouse constant regions would be suitable for diagnostic use as it minimizes the structural similarity of the domains not involved in direct antigen binding. However, making a chimeric antibody often results in significantly reduced affinity relative to the parental antibody (huG1full) as modification of constant regions and antibody isotype is known to affect avidity even if the equivalent murine homologs (in this case mouse G2a and kappa light chain) are used (207). We reasoned that a chimeric my2F12 consisting of the first heavy chain constant domain (CH1) and hinge of human IgG3 followed by the Fc of mouse IgG2a (hG3mG2a) would have near parental avidity, as the increased length and flexibility of the G3 hinge would minimize the influence of the switch in Fc on the structure of the antigen

binding fragment (Fab) (208). In addition a set of constructs was engineered to highlight the regions of the antibody that were important for retention of parental avidity; hG1mG2a contained the CH1 and hinge of human IgG1 coupled to the Fc of mouse IgG2a; and 2 more traditional chimeric antibodies which had the complete human heavy chain constant region replaced with that of mouse IgG2a, with a fully human or chimeric light chain, moG2a and moG2afull respectively. A fully human IgG3 version (huG3full) of my2F12 was also produced. The structural layout of these variants is shown in Figure 5-1A.

Purified antibody was run on both reducing and non-reducing SDS-PAGE gels to verify that the antibodies were of the right size and properly assembled. On the reducing gel, the light chain, human G1/mouse G2a and human G3 heavy chains ran at the appropriate sizes of 25kDa, 50kDa and 60kDa respectively and the intensities of the heavy and light chain bands were balanced indicating equivalent amounts of both polypeptide chains as expected (Fig. 5-1B). All six antibodies ran as a single main band greater than 150kDa on the non-reducing gel although some minor bands were observed, indicating that the majority of the antibody molecules were fully assembled although small amounts of incompletely assembled antibody were also present (Fig. 5-1C). A western blot of the six variants with anti-human Fc secondary was also carried out to confirm that the chimeric variants did indeed carry mouse Fc and as expected only the huG1full and huG3full isotypes showed up on western while the mouse chimerics did not (Fig. 5-1D).

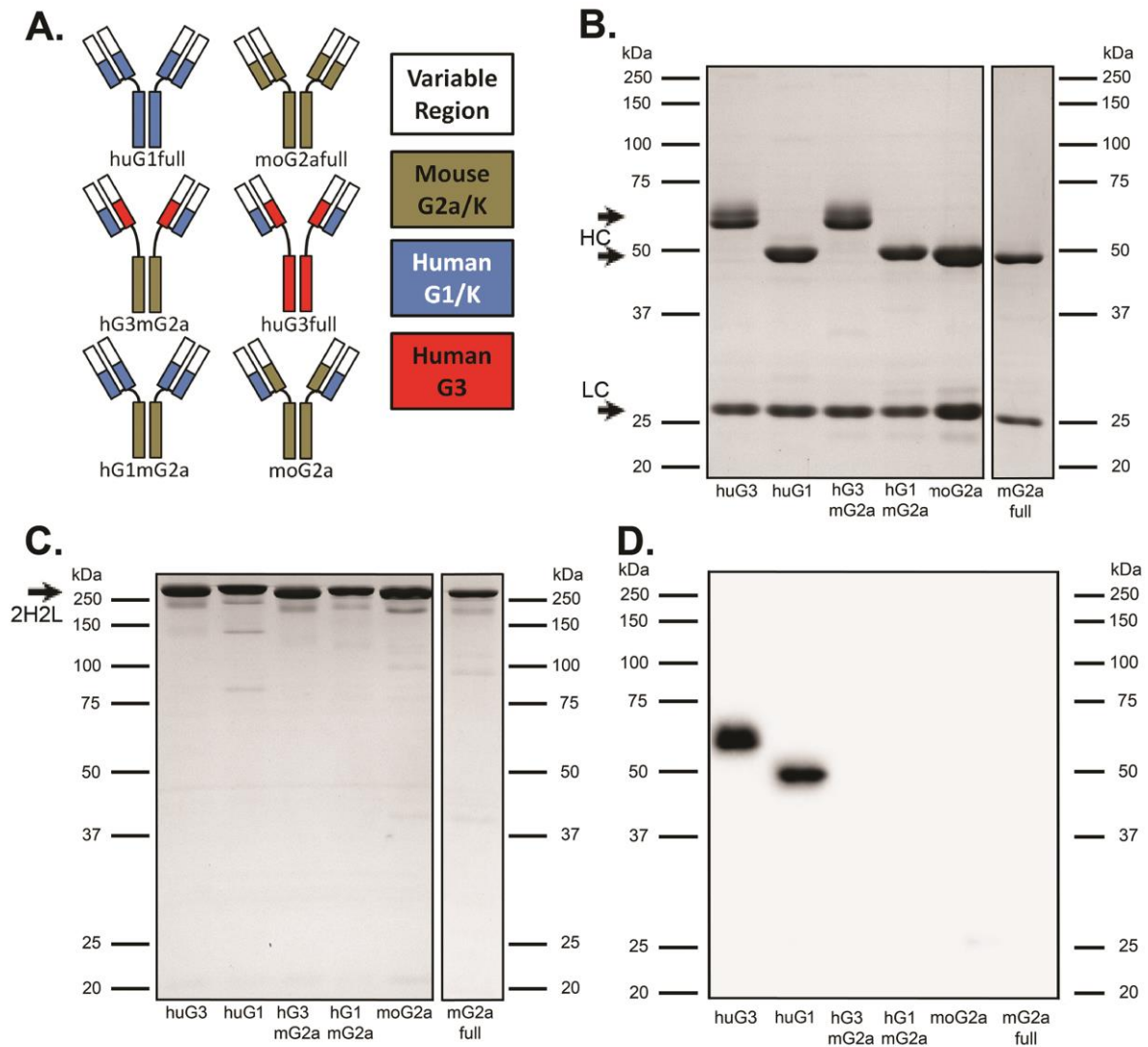


Figure 5-1: Design and expression of my212 chimeric variants

(A) Structural diagram of the six my2F12 antibody variants including the original huG1 my2F12 showing the human/mouse origins and isotypes of the various constant domains. **(B)** Reducing and **(C)** Non-reducing Coomassie of the six variants. 2 μ g of each antibody was run on 10% SDS-PAGE gel showing individual heavy and light chains (HC/LC) or fully assembled antibody (2H2L) **(D)** Western blot of the six variants with 1:5000 anti-Human Fc-HRP on 0.5 μ g of each antibody run on a reducing SDS-PAGE and transblotted to a nitrocellulose membrane showing detection of only the fully human G3 and G1 antibodies

5.3 Characterization of my2F12 chimeric antibody avidity

The relative avidities of these antibodies were analysed by binding of serially diluted antibody to a fixed concentration of ManLAM by indirect ELISA and plotting the logarithmic dilution curves (Fig. 5-2A). Expectedly, both of the more traditional chimeric antibodies moG2a and moG2afull displayed significant reductions in avidity with a greater than one-log shift in the dilution curve relative to huG1full. As was hypothesized, hG3mG2a retained near parental avidity, as the dilution curve of avidity was largely similar to huG1full. The suggestion that retention of avidity is due to the presence of the IgG3 hinge is supported by observation that there is a half log reduction in the avidity of hG1mG2a which only differs in this region and that huG3full has higher than parental avidity. Interestingly, the loss of avidity between the antibody pairs huG1full and hG1mG2a, along with huG3full and hG3mG2a, was similar, suggesting that the effects of switching hinge and Fc on avidity are additive and that despite increased flexibility of the hinge, it cannot completely isolate the Fab region from changes in the Fc structure. Having determined that huG3full has higher avidity than huG1full, we also evaluated its suitability as a capture antibody compared to huG1full at equimolar coating concentrations in an indirect sandwich ELISA using ManLAM at low concentrations (1-10ng/ml) (Fig. 5-2B). It performed significantly worse than huG1full giving poorer signal to noise ratios at all concentrations tested and so huG1full was used as the capture antibody in subsequent sandwich ELISAs.

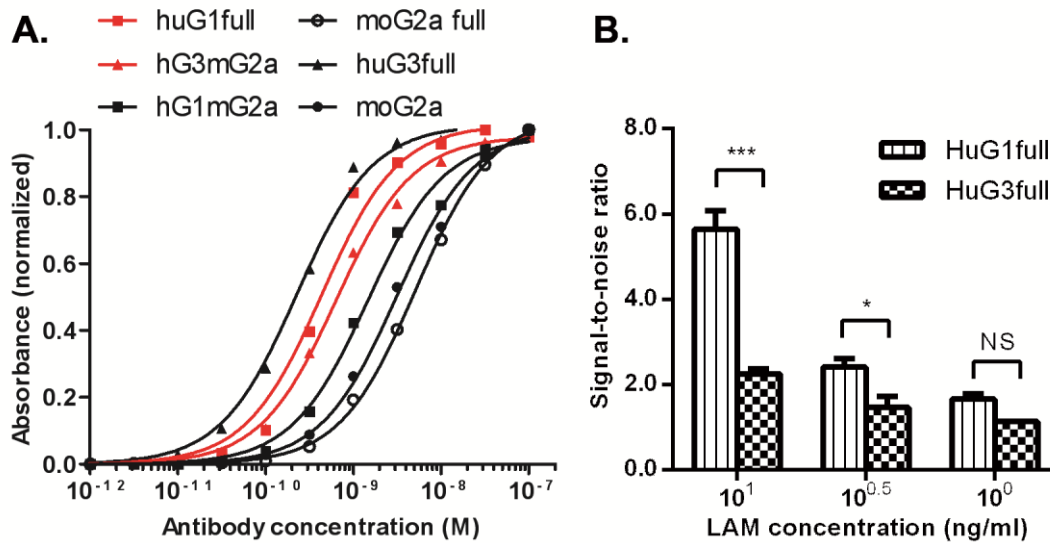


Figure 5-2: Variation in binding affinity of different my2F12 chimeric antibodies

(A) Serial dilution of IgG against ManLAM on indirect monoclonal IgG ELISA showing relative affinities of different chimeric constructs. Red lines indicate parental antibody (huG1full) and engineered diagnostic (hG3mG2a) **(B)** Relative binding efficiencies of HuG1 and HuG3 represented by signal-to-noise ratio when used as capture antibody at 5.0 $\mu\text{g/ml}$ and 5.4 $\mu\text{g/ml}$ (equimolar concentrations) with hG3mG2a at 1 $\mu\text{g/ml}$ as detector at various low concentrations of ManLAM. ***: $p < 0.001$, *: $P < 0.05$, NS: not significant. Results are the average of three independent experiments and error bars show standard error of mean.

5.4 Identification of pathogenic mycobacteria with chimeric my2F12 by immunofluorescence microscopy

In order for the chimeric antibody to be diagnostically useful, we have to verify that it retained the same specificity as the parent human my2F12. We therefore evaluated the specificity of my2F12 for various mycobacterial and actinomycete species on slides of fixed bacterial culture via confocal IF microscopy using the chimeric mouse antibody (moG2a) and an anti-mouse fluorescently labelled

secondary antibody to detect binding. For comparison, a commercial rabbit polyclonal α LAM IF and the traditional Ziehl–Neelsen acid-fast stain was also carried out on duplicates of these slides. We also included two additional non-mycobacterial actinomycete species that had previously been isolated from clinical sputum samples and cross-reacted with polyclonal anti-LAM antibodies and hence could potentially give false positives; *Nocardia cyriacigeorgica* and *Tsukamurella paurometabolum* (154). The Gram negative bacterium *Escherichia coli* was also included as a negative control. A classification of the species used, their pathogenicity and IF and acid-fast stain results is given in Fig. 5-3

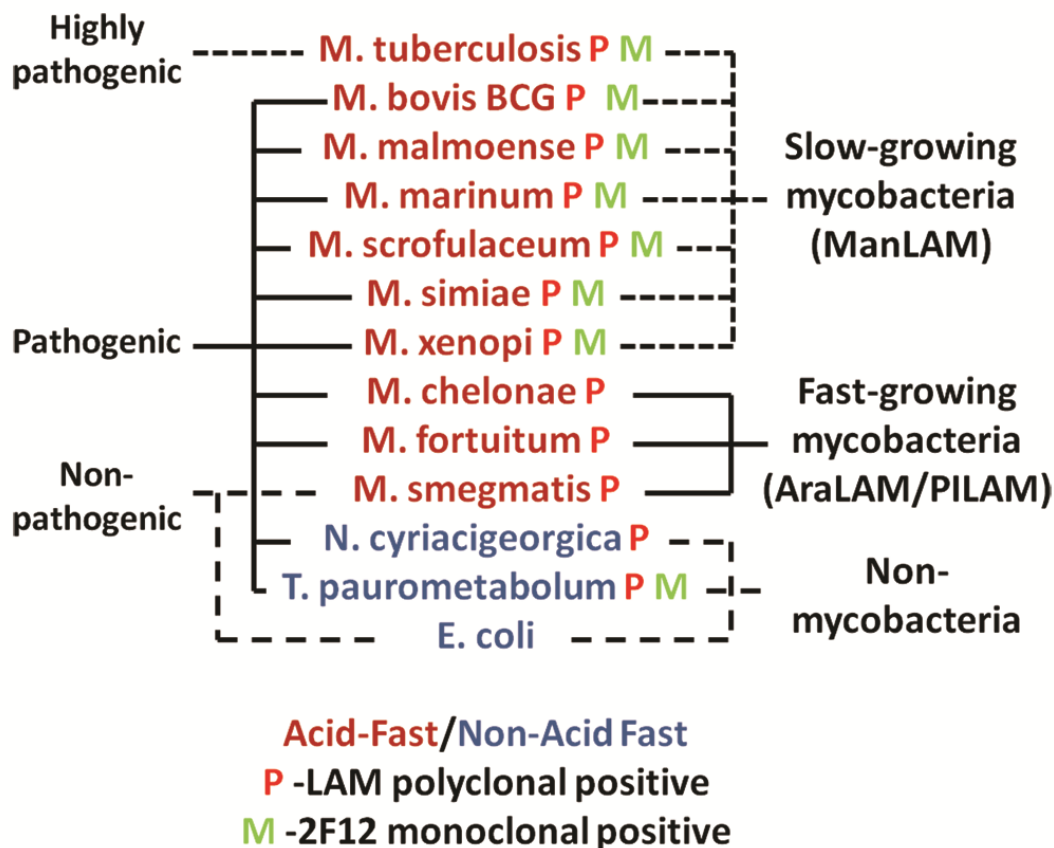


Figure 5-3: Phylogenetic distribution and diagnostic characteristics of various mycobacterial species

Tree diagram showing classification of mycobacterial and non-mycobacterial species into fast and slower growers, their pathogenicity, antibody specificity and acid-fast staining.

Confocal IF microscopy with my2F12 gave clear fluorescence for *Mtb* bacilli previously heat killed and subsequently fixed by methanol–acetone onto slides (Fig. 5-4A). This indicates that our antibody can probably be used for detection of TB infection via IF sputum smears. The *Mtb* bacilli were also positive on IF with the commercial rabbit polyclonal α LAM and also were stained strongly red (positive) by the acid-fast stain, as expected for a slow-growing mycobacteria species. Other slow-growing mycobacterial species were similarly positive for both my2F12 and polyclonal α LAM IF as well as the acid-fast stain (Fig. 5-4B).

On the other hand, all fast-growing mycobacterial species such as *M. smegmatis* could not be detected by my2F12 IF but were uniformly positive for polyclonal α LAM IF as well as the acid-fast stain (Fig. 5-5A). For the non-mycobacterial actinomycete species, all were negative for the acid-fast stain and my2F12 but positive for polyclonal α LAM IF with the exception of *T. paurometabolum* which bound both the my2F12 and polyclonal antibodies (Fig. 5-5B). To further determine the likelihood of additional cross-reactivity on sputum samples, we subsequently tested our antibody against common throat bacteria species such as *Streptococcus*, *Staphylococcus* and *Pseudomonas aeruginosa* using the same IF methodology, but no binding was observed (Fig. 5-6).

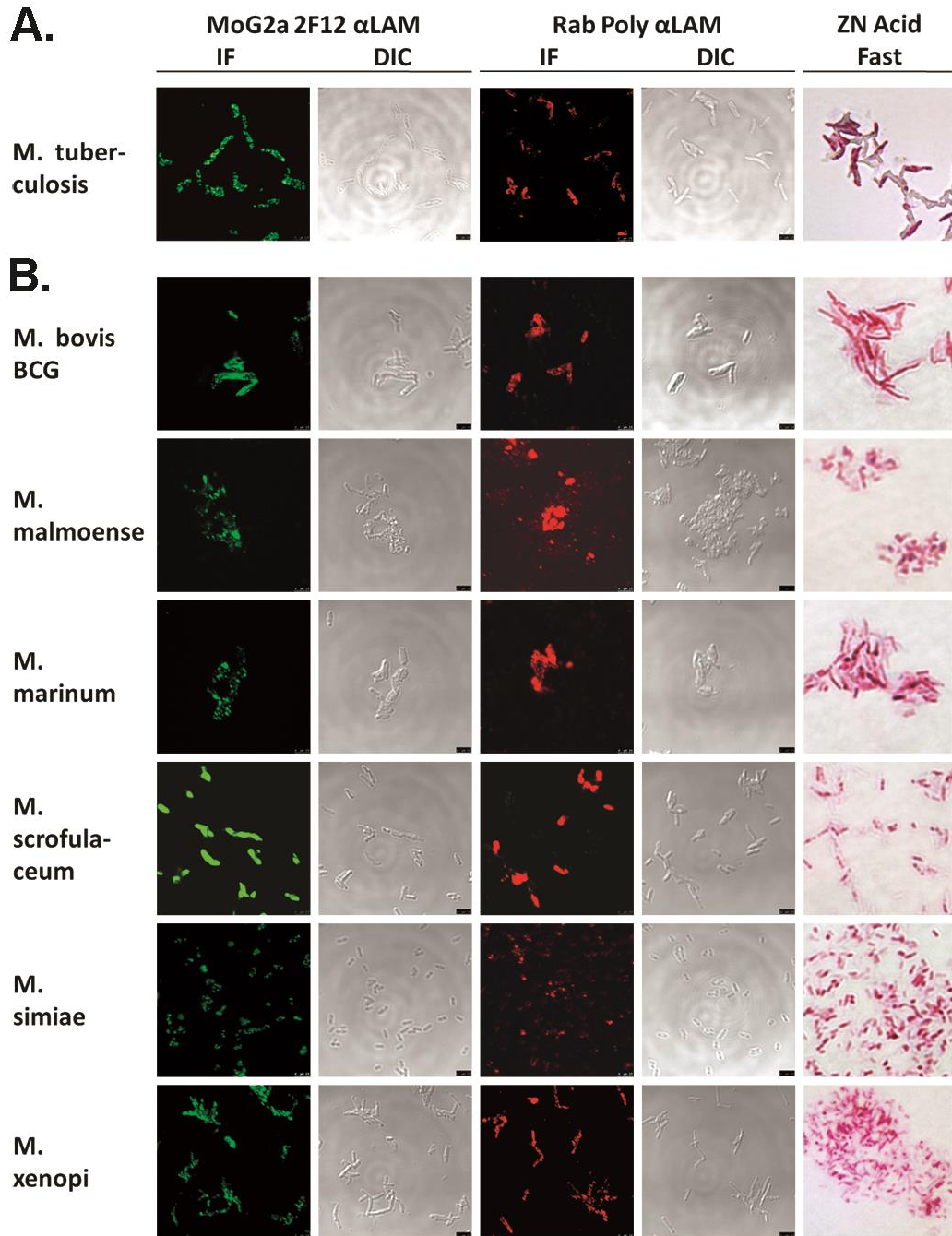


Figure 5-4: my2F12 immunofluorescent staining for slow-growing mycobacteria

my2F12 chimeric staining for slow growing mycobacteria by confocal IF microscopy for fixed heat-killed *Mtb* (A) and fixed live cultures of other slow growing species (B) Staining was carried out with my2F12 or rabbit polyclonal α LAM with corresponding differential interference contrast (DIC) microscopy images and a separate Ziehl-Neelsen acid-fast stain

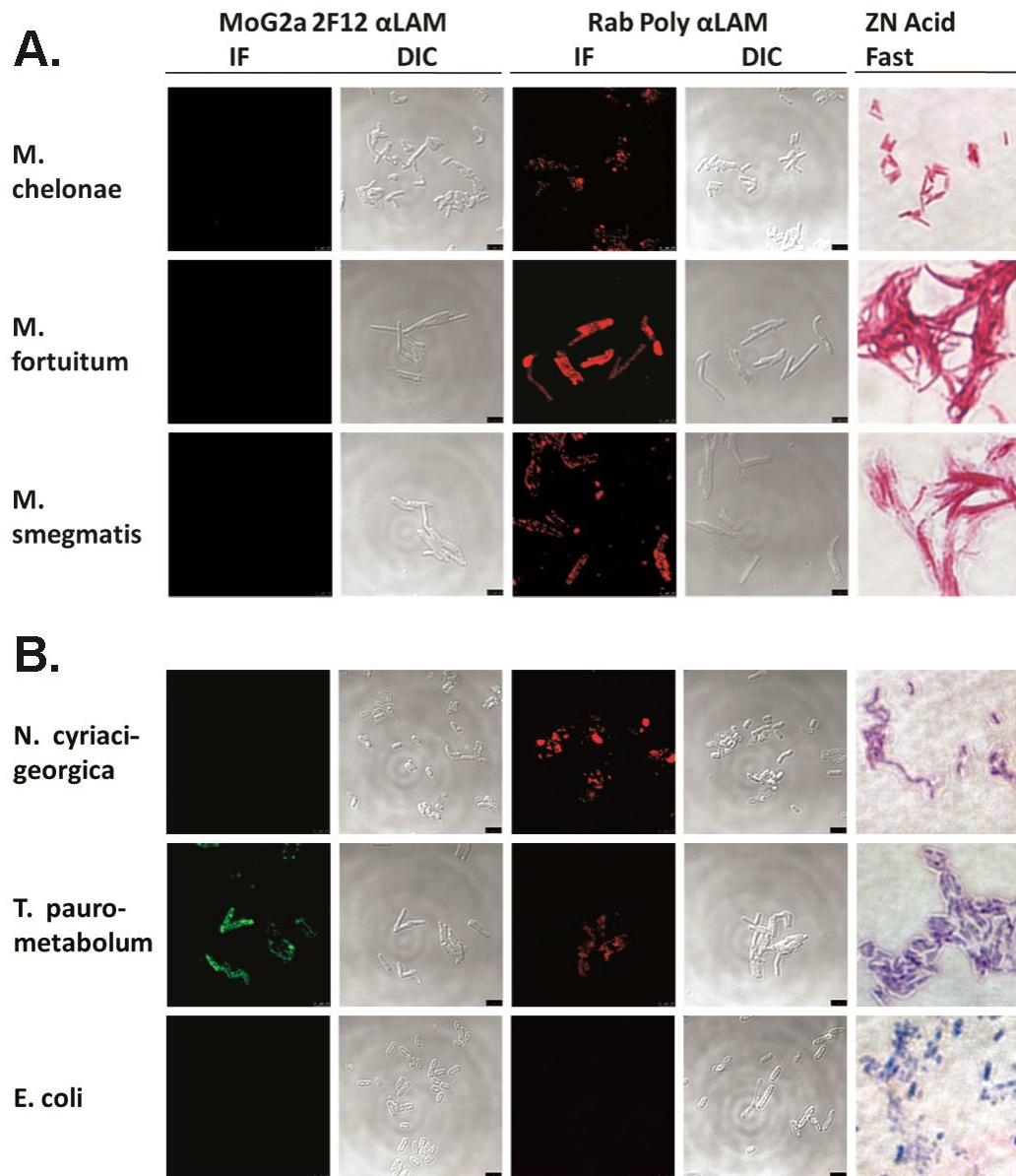


Figure 5-5: Lack of my2F12 immunofluorescent staining for fast-growing mycobacteria or non-mycobacterial species

Lack of binding of my2F12 chimeric antibody to fast growing mycobacterial species **(A)** or non-mycobacterial species **(B)** with the exception of *T. paurometabolum* by confocal IF microscopy. Staining was carried out with my2F12 or rabbit polyclonal αLAM with corresponding differential interference contrast (DIC) microscopy images and a separate Ziehl-Neelsen acid-fast stain

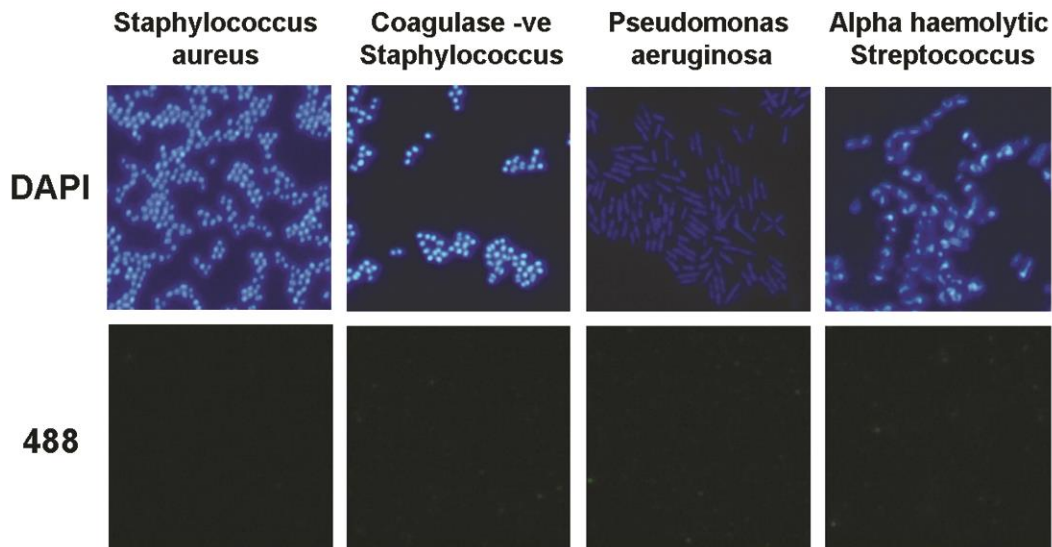


Figure 5-6: Lack of my2F12 immunofluorescent staining for common throat bacteria

Lack of binding of my2F12 chimeric antibody to *Staphylococcal*, *Streptococcal* and *Pseudomonas* bacteria as shown by double staining with DAPI and my2F12 coupled with an anti-mouse Alexa Fluor-488 secondary antibody (488) under confocal IF microscopy.

5.5 Identification of pathogenic mycobacteria with chimeric my2F12 by sandwich ELISA

Sandwich ELISA is another potential TB diagnostic assay and one that has been previously used assay for LAM in urine (87). We therefore tested our chimeric antibody alongside the Clearview polyclonal anti-LAM based commercial sandwich assay in a sandwich ELISA using intact whole bacteria re-suspended in PBS as the test antigen instead of the filtered culture supernatant used in the previous chapter to reduce variability in LAM amounts as length of time grown in culture is no longer a factor. For this assay, the antibody showed identical specificity to that observed on confocal IF microscopy, binding only the slow-growing mycobacteria and *T. paurometabolum* but not the fast-growing mycobacteria as well as *E. coli* and *N.*

cyriacigeorgica (Fig. 5-7). In contrast, the polyclonal anti-LAM antibody bound all mycobacterial and actinomycete species, which is consistent with the earlier studies and our IF microscopy results. Critically, *Mtb* gave a clear signal on my2F12 ELISA, again indicating the suitability of this antibody as a TB diagnostic reagent. However, the signal was lower than that of other slow-growing mycobacterial species, possibly due to the heat-killing treatment required for safe manipulation of the bacteria. The heat-treatment is likely to have disrupted some of the cell wall and leached a portion of the ManLAM, potentially reducing levels of ManLAM in intact bacilli. The higher signal of polyclonal α LAM is probably due to multiplicity of binding sites on the complex LAM molecule for the various antibodies present in a polyclonal preparation.

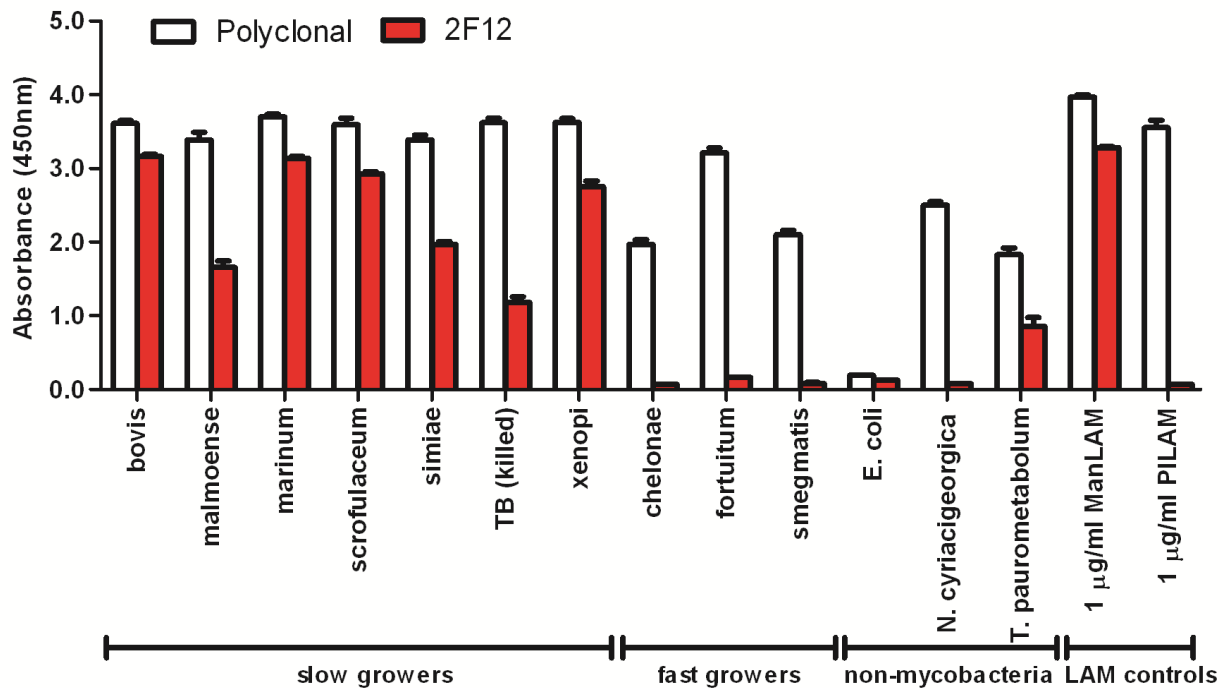


Figure 5-7 Specificity of chimeric my2F12 for various mycobacterial species

Sandwich ELISA with my2F12 chimeric antibody as detector and my2F12 HuG1 as capture or with commercial kit using rabbit anti-LAM polyclonal against whole bacteria at OD₆₀₀ 0.5. my2F12 is specific only for mycobacterial slow-growers and a unique actinomycete *T. paurometabolum* while rabbit polyclonal binds all mycobacterial and actinomycete species tested. Data are the average of three independent experiments and error bars show standard error of mean

5.6 Enhancing the sensitivity of my2F12 ELISA on spiked serum samples

Due to the potential for cross-reactivity in sputum due to the presence of other actinomycete species that express α 1-2 mannose capped LAM, we decided to investigate alternative clinical sample types where the burden of environmental bacteria is likely to be much less, i.e. serum. We therefore tested serum samples to determine the sensitivity of serum ELISAs and whether serum anti-LAM antibodies could interfere with detection, which had been observed previously (209). Serum was obtained from three previously BCG vaccinated and one unvaccinated

volunteers and analysed for antibodies against ManLAM and PILAM by indirect ELISA. While all serum samples were found to have both anti-ManLAM and anti-PILAM antibodies, as expected, the non-vaccinated serum had the lowest titre (Fig. 5-8A). The other BCG vaccinated serum had varying higher levels of anti-LAM antibodies and were classified into high, medium and low titre serum respectively. Interestingly, both the anti-ManLAM and anti-PILAM antibody titres were roughly equivalent in each serum sample, which is probably due to the majority of endogenous anti-LAM antibodies being cross-reactive and binding both types of LAM equally well. Therefore, we expected that the endogenous antibodies in serum would not be able to interfere with our antibody binding to the mannose-cap epitope. However, on testing LAM spiked serum on the same sandwich ELISA used previously, we found that sensitivity correlated with the level of endogenous anti-LAM antibodies in the serum and that the limit of detection (defined as signal-to-noise ratio of 2) in the highest titre serum was almost twenty-five-fold less than in non-vaccinated serum (100ng/ml vs. 4ng/ml, Fig. 5-8B) and one hundred-fold less than in LAM spiked into PBS (100ng/ml vs. 1ng/ml, Fig. 5-8B). This suggested that endogenous anti-LAM antibodies in serum interfered with detection of LAM.

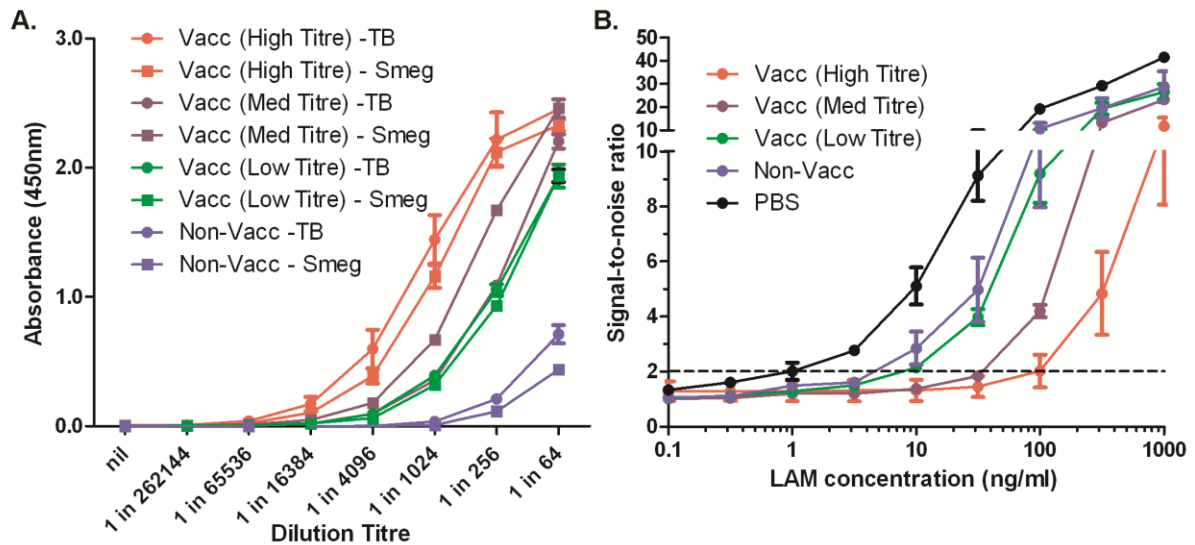


Figure 5-8: Influence of serum anti-LAM antibodies on my2F12 assay sensitivity

(A) Serial dilution of serum from BCG vaccinated and non-vaccinated volunteers showing range of titres of endogenous anti-LAM antibodies (non-specific signal as determined by binding against PBS has already been subtracted). (B) Detection of spiked ManLAM in serum by sandwich ELISA showing increasing interference and reduced sensitivity with increasing levels of endogenous anti-LAM antibodies in serum as indicated by signal-to-noise ratio. A limit of detection is set at a ratio of 2 and noise is defined as the signal obtained with no LAM added. Figure data are the average of three independent experiments and error bars show standard error of mean

As a result, we investigated simple methodologies to remove endogenous antibodies. We developed a hybrid method that first used proteinase K to digest serum antibody and proteins, followed by a heating at 95°C to inactivate proteinase K and any remaining antibodies as well as to sterilize the sample. This was done for both the high titre serum and unvaccinated serum after spiking with LAM and the treated serum was subsequently tested by the above sandwich ELISA in comparison with the untreated LAM spiked serum to determine if sensitivity was improved. In addition, both were also tested by indirect ELISA against PILAM and ManLAM to confirm that endogenous antibodies had been denatured. Comparison of the serum

antibody binding activity showed a significant drop in levels of IgG antibody binding against both ManLAM and PILAM to almost close to that of background for the high titre serum (Fig. 5-9A). A drop in the non-vaccinated serum was also observed but this was not significant as the levels of anti-LAM antibody were extremely low even before treatment. Treatment of both the high-titre serum and unvaccinated serum resulted in improvements in the limit of detection, from 3ng/ml to 0.5ng/ml in unvaccinated serum and from 50ng/ml to 2ng/ml in high-titre serum (Fig. 5-9B). As expected the improvement was much greater in the high-titre serum. In both cases, sensitivity in the treated serum was similar to that of LAM spiked into PBS (limit of detection at 3ng/ml). Specificity of the antibody was retained as the signal obtained with 1µg/ml of PILAM spiked into either treated or untreated serum ranged from 97.5% to 112% that of the background noise signal (no LAM added). In addition, we also tested the same treatment process on whole blood to whether the coagulation step to obtain serum could be omitted. To ensure full digestion, incubation with Proteinase K was extended for 30min. However, the limit of detection was about 6ng/ml for both high-titre and unvaccinated serum, which was an improvement for the high-titre sample but a decrease for the unvaccinated serum and compares poorly with both the PBS standard and treated serum (Fig. 5-9C).

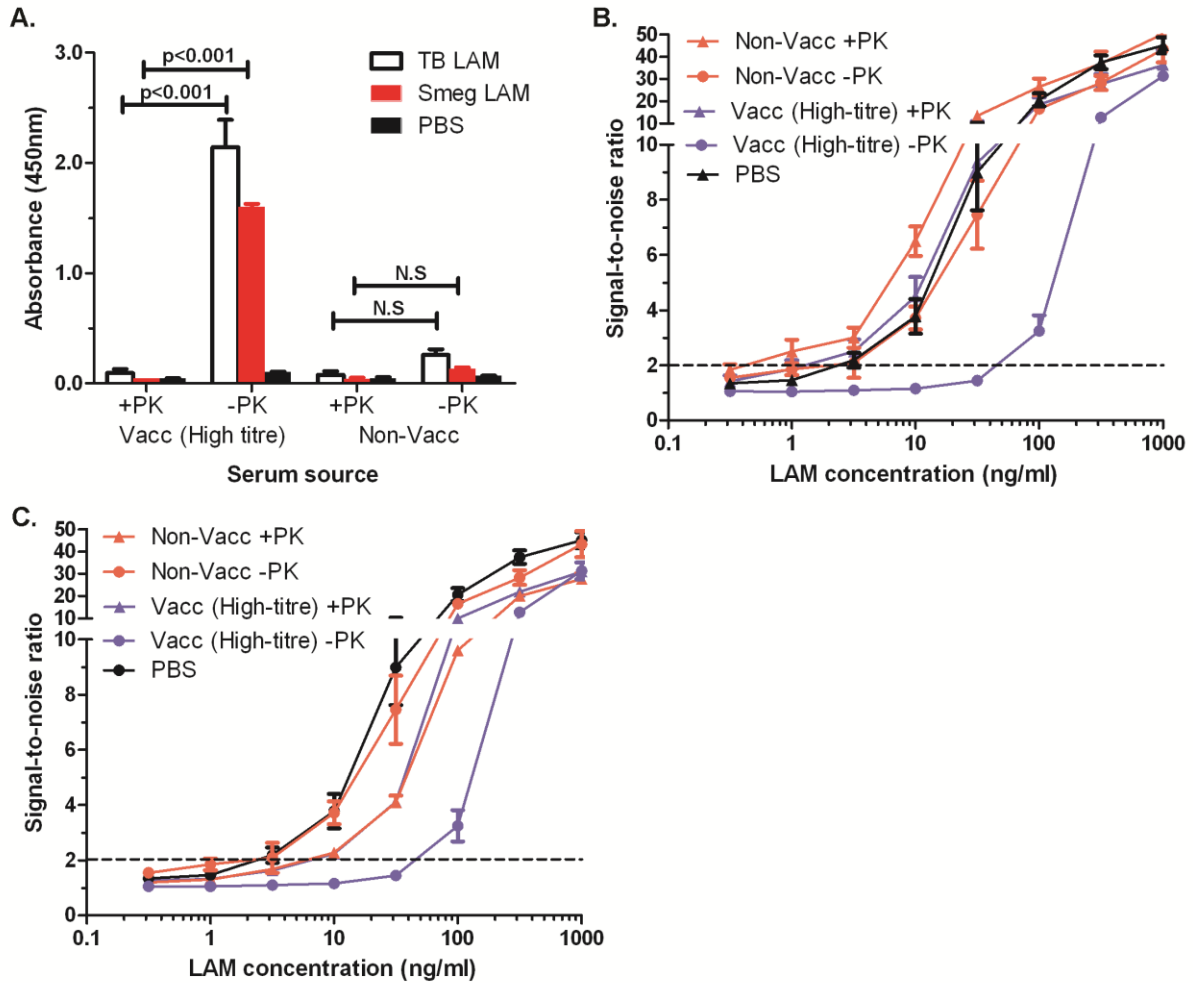


Figure 5-9: Improvement in assay sensitivity by heat and proteinase K denaturation of serum anti-LAM antibodies

(A) Significant reduction of levels of endogenous anti-LAM antibodies in serum (at 1:512 dilution) by simple Proteinase K and heat treatment. Changes in sensitivity of sandwich ELISA as indicated by signal-to-noise ratio after denaturation of endogenous anti-LAM antibodies in spiked serum (B) or whole blood samples (C) with proteinase K and heat treatment (+PK) as compared to untreated spiked (-PK) samples and PBS standards. Concentrations of ManLAM are that in whole blood spiked before coagulation. Treatment of serum improves sensitivity for both samples while treatment of whole blood only improves sensitivity in the high-titre sample. Figure data are the average of three independent experiments and error bars show standard error of mean. Concentrations of ManLAM are that in whole blood spiked before coagulation.

5.7 Discussion

The clinical utility of our antibody is dependent on whether it can be used in clinical diagnostic techniques such as immunofluorescence microscopy or ELISA to distinguish the relevant pathogens. Previous studies have shown that other monoclonal and polyclonal anti-LAM antibodies cannot distinguish between pathogenic and non-pathogenic mycobacterial species or even cross-react to other LAM producing actinomycete species such as *Nocardia* despite their high-affinity for the LAM molecule itself and thus have limited clinical value (154,210). On the other hand, our antibody, both the parental and chimeric versions, do not cross-react to fast growing mycobacterial species such as *M. smegmatis*, *chelonae* and *fortuitum* but was able to detect all slow-growing mycobacterial species tested using both immunofluorescence confocal microscopy and ELISA (Fig. 5-4, 5-7).

The division of mycobacterial species into these two taxonomical groups was first based on the phenotypic difference of growth-rates, but was later supported by phylogenetic analysis of 16s ribosomal RNA (18). While the vast majority of slow growers are pathogenic in humans or animals, the majority of fast growers are environmental non-pathogenic bacteria with only a few exceptions that cause typically mild disease (18,211). Slow-growing mycobacteria include species such as *M. malmonese*, *marinum*, *scrofulaceum*, *simiae* and *xenopi*, which have not had their LAM structure and capping motifs characterized to date. Our study is the first to screen for α 1-2 mannose capping motifs over such a wide variety of mycobacterial species. The observation that ManLAM capping motifs were present in all slow growing species tested but none of the fast-growing species that we tested makes it

highly probable that these motifs are exclusive to the slow growers and could be considered one of the defining characteristics of their group. It is therefore likely that our antibody will be able to detect all slow-growing mycobacterial species and represents an improvement over other anti-LAM antibodies available for diagnostic purposes.

The cross-specificity of my2F12 will also enable clinicians to detect other non-tuberculous mycobacterial infections, but distinguishing these from TB may then depend on clinical presentation of the patient or other diagnostic tests. Testing of our antibody on clinical samples from TB positive and negative patients will therefore be required to confirm its utility and determine its predictive value in TB diagnosis. Our antibody was also shown to have affinity for a related actinomycete, *T. paurometabolum*. This is not surprising as this organism has been found to produce LAM with terminal α 1-2 mannose linkages (135). Although this may lead to false positives as this species has been previously been found in sputum clinical isolates, such mannose linkages are thought to be a pathogenic determinant as they enable host cell invasion via the mannose receptor and suppression of immune cell responses through DC-SIGN in the case of mycobacterial infection (136,143,154). This antibody could hence potentially be used to determine if any particular mycobacterial or actinomycete strain carries such carbohydrate motifs and have pathogenic potential.

To adapt our antibody for diagnostic purposes, we have successfully engineered our antibody to a format with a murine Fc but retained avidity by switching to a human G3 hinge, thus enabling us to use an anti-mouse secondary

instead of an anti-human and avoid undesirable cross-reactivity. The fact that there is minimal background on our ELISA with unspiked human serum samples validates this approach. While changes in affinity have been reported due to switch in antibody isotype or species origin (212), no general observation for an increase by switching to G3 from G1 has been made. Our findings nonetheless suggest a simple but effective method for improving avidity of diagnostic antibodies by switching to a G3 isotype. We have also shown that our chimeric antibodies, both the moG2a and hG3mG2a variants, retain their specificity for slow-growing mycobacteria and thus by inference the α 1-2 mannose linkage, as tested on IF and sandwich ELISA respectively. Interestingly, the huG3full was less sensitive compared to huG1full when used as capture antibody even though both were coated at equimolar concentrations. However, the efficiency of the capture antibody is also dependent on how it binds when it is immobilized onto the ELISA plate, which can be affected by the protein stability and structure. Binding in the wrong orientation may result in occlusion of the binding surface or structural alteration and loss of affinity (213). It may be that the increased flexibility or size of the huG3full antibody renders it less ideal as a capture antibody compared to huG1full.

Finally, by engineering a chimeric antibody (hG3mG2a) with near equivalent avidity to the parent human antibody, we are now able to test samples that have high concentrations of endogenous human antibodies but have low burden of environmental bacteria such as serum. A previous study showed that that heat and urea denaturation of serum improved sensitivity, but did not directly demonstrate the presence of anti-LAM antibodies in serum (209). Here, we extend their observations by showing that the higher levels of anti-LAM antibodies correlate with decreased

sensitivity of the LAM sandwich ELISA and that denaturation of these antibodies by heat and proteinase K treatment restores sensitivity. While the previous study used urea for denaturation, which would not only denature endogenous serum antibodies but also potentially denature the assay antibodies, we used proteinase K which was subsequently inactivated by heat and thus unlikely to affect our assay. This is also one of the advantages of a lipid biomarker in its resistance to heat. This could explain why we were able to achieve a significant improvement in sensitivity (25-fold improvement in high-titre serum (Fig. 5-9B), compared to the previous study which only showed several-fold increase in signal.

Our final limit of detection was approximately 0.5-2ng/ml in serum, which compares favourably with published data on the sensitivities of both polyclonal and monoclonal based anti-LAM sandwich ELISAs (0.8ng/ml, Boehme et al; 0.5ng/ml; Sakar et al, 1ng/ml, Hamasur et al) (83,85,209). As such, this antibody in the sandwich ELISA format, along with the procedure for heat treatment of serum, is a good candidate for a useful point-of-care test for TB diagnosis. Furthermore, while use of sputum as a clinical sample may have a higher risk for false positives, the exact rate needs to be defined by clinical testing. Our antibody's higher specificity when used in IF microscopy compared to acid-fast dyes and the general higher sensitivity and rapidity of fluorescent microscopy over basic light microscopy indicates that it might be of use in areas where acid-fast staining alone is insufficient for confirmation of TB due to the presence of fast-growing mycobacteria. Use of this antibody would thus remove the need to conduct additional speciation tests such as line probe assays and enhance the utility of the battery powered light-emitting diode fluorescent microscopes now being introduced by WHO.

**Chapter 6: Generation of anti-mycolic acid antibodies by phage
display**

6.1 Introduction

Mycolic acid is an attractive lipid biomarker for TB diagnosis due to its attested presence at high concentrations (>1µg/ml total average) in the sputum samples of TB patients and its abundance in the mycobacterial cell wall (40% of dry mass) (12,47). In contrast to lipoarabinomannan, no anti-mycolic acid antibody has yet been generated using traditional methodologies of animal immunization due to its insolubility in solution and lack of immunogenicity. However, using a semi-synthetic chicken scFv (single chain fragment variable) antibody phage display library, Beukes et al were able to successfully generate several antibodies against mycolic acid, although some showed cross-reactivity to cholesterol (182). They and others have shown that generating antibodies against highly hydrophobic lipids is feasible by panning phage libraries against pure lipid evaporated onto a solid surface, thus avoiding the need for *in vivo* immunization (10,112). The isolated anti-lipid antibodies have been shown to be able to recognize not just the purified target but also the same lipid when present in organic solvent extracts from biological materials and evaporated in the same manner. This raises the possibility that such antibodies could be used to detect the presence of lipid biomarkers in extracts from clinical samples such as sputum and hence enable cost-effective, rapid and easy detection that is amenable to point-of-care use.

We have therefore used the same Humanyx Fab phage library used to generate the my2F12 antibody against ManLAM to screen for mycolic acid-specific antibodies. Fab libraries have an advantage over semi-synthetic scFv libraries in the ability of their antibodies to retain binding affinity when converted to IgG (184). We

have applied a modified version of the panning strategy, leaving out the negative selection and panning against evaporated *Mtb*-derived mycolic acid instead of LAM which was coated by adsorption in solution. In order to determine the feasibility of anti-mycolic acid antibodies as a TB diagnostic, we also explored the ability of these antibodies to recognize mycolic acid in organic solvent extracts of mycobacteria and distinguish these from other mycolic acids species present in extracts from related actinomycete species, as well as means for rapid extraction of mycolic acid from bacterial samples.

6.2 Isolation of mycolic acid-specific antibodies

Purified *Mtb*-derived mycolic acid was coated onto solid polystyrene surface by evaporation from hexane, allowing the Humanyx Fab phage library to be panned against it. This was done for four successive rounds and the subsequent polyclonal ELISA indicated successful enrichment for binders to mycolic acid as shown by the increase in specific absorbance (Fig. 6-1). To verify that enrichment for high affinity Fab-phage clones occurs and to identify suitable high affinity monoclonal antibodies, 376 individual clones from the fourth pan (the pan with the highest signal) were screened for binding activity by indirect phage monoclonal ELISA against mycolic acid and a 2:1 w/w mix of phosphocholine/cholesterol coated in the same manner as a negative control. The ELISA signals were classified by signal-to-noise ratio (SNR) as follows: negative binders (SNR<2), weak binders (SNR 2-5), moderate binders (SNR 5-10) and strong binders (SNR >10). The distribution of the various types of binders is given in Table 6-1. The strong binders formed the largest group with 51%

of all sampled clones while the negative binders formed only 4% of all tested clones indicated clear preference for strong binders.

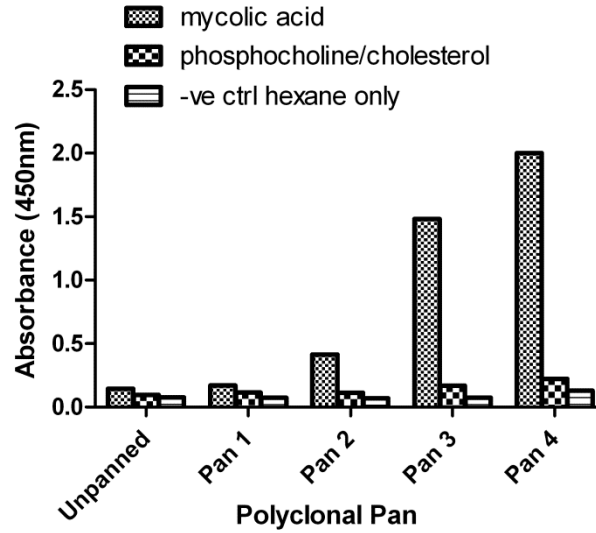


Figure 6-1: Panning of Humanyx antibody phage library against mycolic acid

Polyclonal phage ELISA showing enrichment of successive phage pans. Each ELISA plate was coated with either mycolic acid or phosphocholine/cholesterol in a 2:1 w/w ratio as a negative control at a final concentration of 25µg/ml. Hexane was added as a negative vehicle control.

Signal-to-noise ratio (mycolic acid vs PC/chol. signal)	No. of clones	Percentage of Total (%)
Negative (SNR < 2)	15	3.99
Weak (SNR 2-5)	36	9.57
Moderate (SNR 5-10)	132	35.11
Strong (SNR > 10)	193	51.33

Table 6-1: Binding characteristics of monoclonals from 4th Pan

Proportion of negative, weak, moderate and strong binding clones isolated from the 4th Pan as determined by monoclonal phage ELISA.

The top 48 binders were sequenced to identify unique clones and the four best unique binders mc3, mc6, mc26 and mc47 were cloned into a mammalian expression vector, expressed as full length human IgG1 and purified from culture supernatant (Fig. 6-2). The heavy and light chain amino acid CDR sequences and germline genes are given in Table 6-2A and 6-2B respectively. Purified IgG was also run on four antibodies were retested for binding activity and all retained specificity to mycolic acid (Fig. 6-3).

A.

Clone	CDR1	CDR2	CDR3	Germline
mc3	RASQSISKYLA	DASTRAT	QQRSDWPPTWT	IGKV3-11*01, IGKJ1*01
mc6	RSSQSLLYRSRYNYLD	LGSNRAS	MQALQTPYT	IGKV2D-28*01, IGKJ2*01
mc26	RSSQSLHHRKGYNYLN	LGSNRAS	MQATHWPLT	IGKV2D-28*01, IGKJ4*01
mc47	RASQRLSFRSVA	AASRRAA	QQYGSSPQT	IGKV3-20*01, IGKJ2*02

B.

Clone	CDR1	CDR2	CDR3	Germline
mc3	GYYS	EINHSGSTNYNPSLKS	GRRYGRVPAARR DNWFDP	IGHV4-34*01, IGHD2- 2*03, IGJ5*02
mc6	GYYS	EINHSGSTNYNPSLKS	GPRRLRFLERQOS EYFQH	IGHV4-34*01, IGHD3- 3*01, IGJ1*01
mc26	SYAIS	RIIPILGIANYAQKFQG	DSSWRRRWLQF PAY	IGHV1-69*09, IGHD5- 24*01, IGJ1*01
mc47	NHLIH	WVNTGTANTKYSEFLG	SNRIVGATRRSFY GMDV	IGHV1-3*01, IGHD1- 26*01, IGJ6*02

Table 6-2: CDR sequences of isolated anti-mycolic antibodies

Light (**A**) and heavy (**B**) chain CDR sequences and germline genes of the four anti-mycolic acid antibodies.

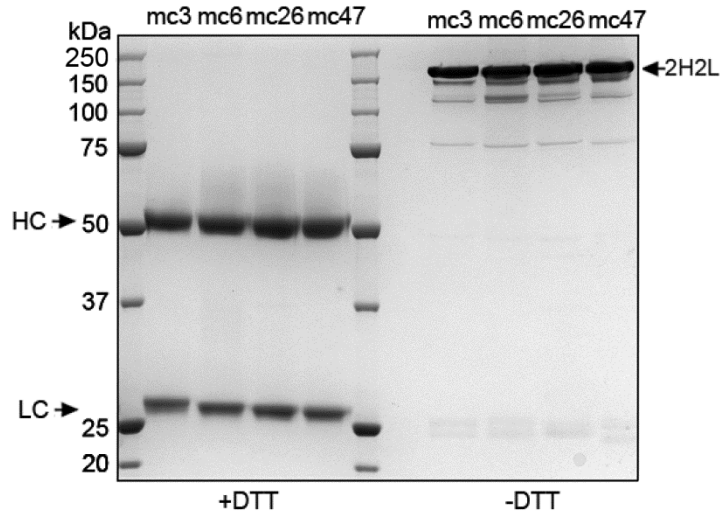


Figure 6-2: Expression of four unique antibodies from the 4th Pan

Reducing (+DTT) and non-reducing (-DTT) 8% SDS-PAGE Coomassie gel of the four antibodies showing the individual chains (HC/LC) or the intact IgG1 molecule (2H2L). 2µg of antibody was loaded.

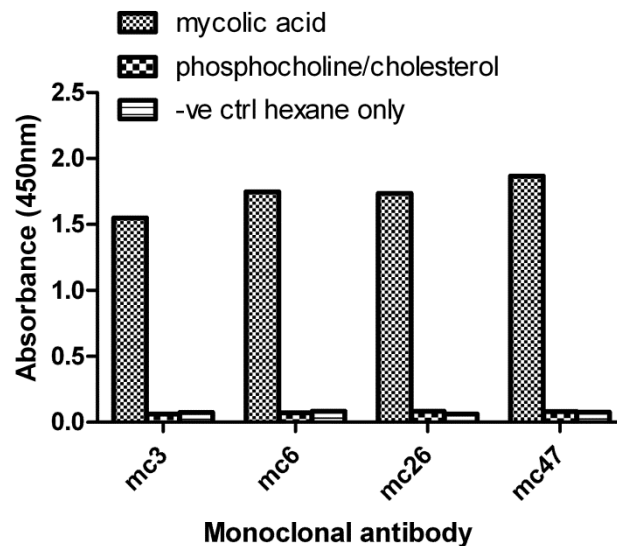


Figure 6-3: Confirmation of mycolic acid specificity of four isolated monoclonal IgGs

Antibodies were tested by indirect ELISA. ELISA plate was coated with either mycolic acid or phosphocholine/cholesterol in a 2:1 w/w ratio as a negative control at a final concentration of 25µg/ml. Hexane was added as a negative vehicle control.

6.3 Characterization of mycolic acid antibody specificity and sensitivity

All four antibodies were subsequently tested against a panel of synthetic and purified lipids. Earlier studies had indicated that mycolic acid might have a similar 3D structure to cholesterol and evidence of cross-reactivity to cholesterol was observed in anti-mycolic acid antibodies previously isolated from a chicken phage display library (22, 23). We therefore tested all four antibodies against purified cholesterol and oxidized cholesterol derivatives. We also tested for cross-reactivity to common membrane lipids such as dimyristoyl phosphocholine (DMPC) and dimyristoyl phosphatidic acid (DMPA), as well as the structurally related β -hydroxyl lipids sphingosine and β -hydroxyl myristic acid. Finally, to determine the exact specificity of our antibodies, we tested for binding against synthesized subclasses of mycolic acid in *Mtb*, namely alpha, keto and methoxy mycolic acid, as well as purified extracts of trehalose dimycolate (TDM) and mannose-capped lipoarabinomannan (ManLAM) which are present in *Mtb* and the phosphoinositol-capped LAM (PILAM) found in *M. smegmatis*.

No binding was observed to any other cholesterol lipid, membrane lipid, β -hydroxyl lipid or mycobacterial lipid, even TDM which is comprised of two mycolic acid molecules attached to a trehalose sugar (Fig. 6-4A). All antibodies bound the original purified *Mtb*-derived mycolic acid as well as the synthesized methoxy mycolic acid strongly, but bound alpha mycolic acid weakly and not to keto mycolic acid at all. To ensure that negative signals were not due to lack of effective antigen coating, the ELISA wells were imaged under phase contrast light microscopy to visualize the adsorbed insoluble lipids prior to the blocking step. All wells except the

hexane control clearly contained evaporated lipid droplets (Fig. 6-4B). ManLAM and PILAM could not be visualized as they are coated in aqueous solution and are not evaporated onto the well surface as droplets. Adherence of these glycolipids to the ELISA plates used had been previously verified using a rabbit anti-LAM polyclonal in the previous chapter.

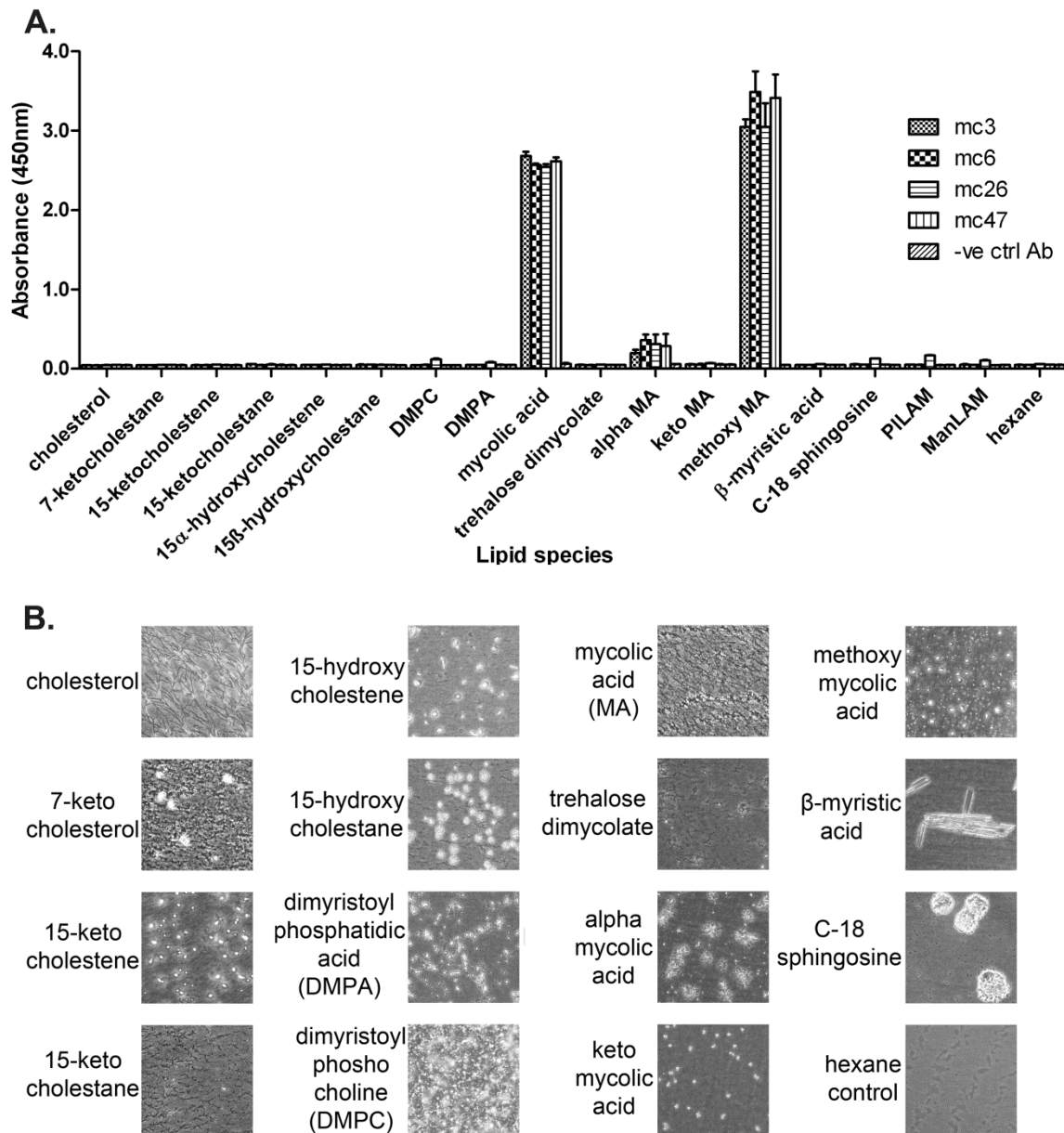


Figure 6-4: Lipid specificity of four anti-mycolic acid antibodies

(A) Indirect monoclonal ELISA showing specificity of isolated recombinant monoclonal IgGs mc3,6,26 and 47 for mycolic acid extract and methoxy mycolic acid in contrast to other synthetic cholesterol derivatives, membrane lipids, β -hydroxyl lipids and mycobacterial lipids. All antibodies including the control antibody (anti-dengue E protein antibody 14C10) were at 1 μ g/ml concentration and the lipids were coated at 25 μ g/ml **(B)** Phase contrast light microscopy images of ELISA well bottoms indicating adherence of evaporated lipid onto the ELISA plate. Images are at 100x magnification. Results are the average of three independent experiments and the error bars show the standard error of mean.

To determine the sensitivity of the antibodies, all four antibodies were tested against serially diluted concentrations of purified *Mtb*-derived mycolic acid and synthetic mycolic acid subclasses. All four antibodies had similar binding curves although mc3 and mc6 had the highest affinity as defined by signal-to-noise ratio. The limit of detection (defined by a signal-to-noise ratio of 2) for mycolic acid extract and methoxy mycolic acid was similar at about 45ng/ml for mc6 while the rest had a slightly poorer sensitivity of about 80-100ng/ml (Fig. 6-5A & 6-5D). The limit of detection range for alpha mycolic acid was 200ng/ml for the mc6 to 800ng/ml for mc26 and mc47 (Fig. 6-5B). Keto mycolic acid could only be detected weakly by mc26 but not the other antibodies at concentrations above 4µg/ml (Fig. 6-5C).

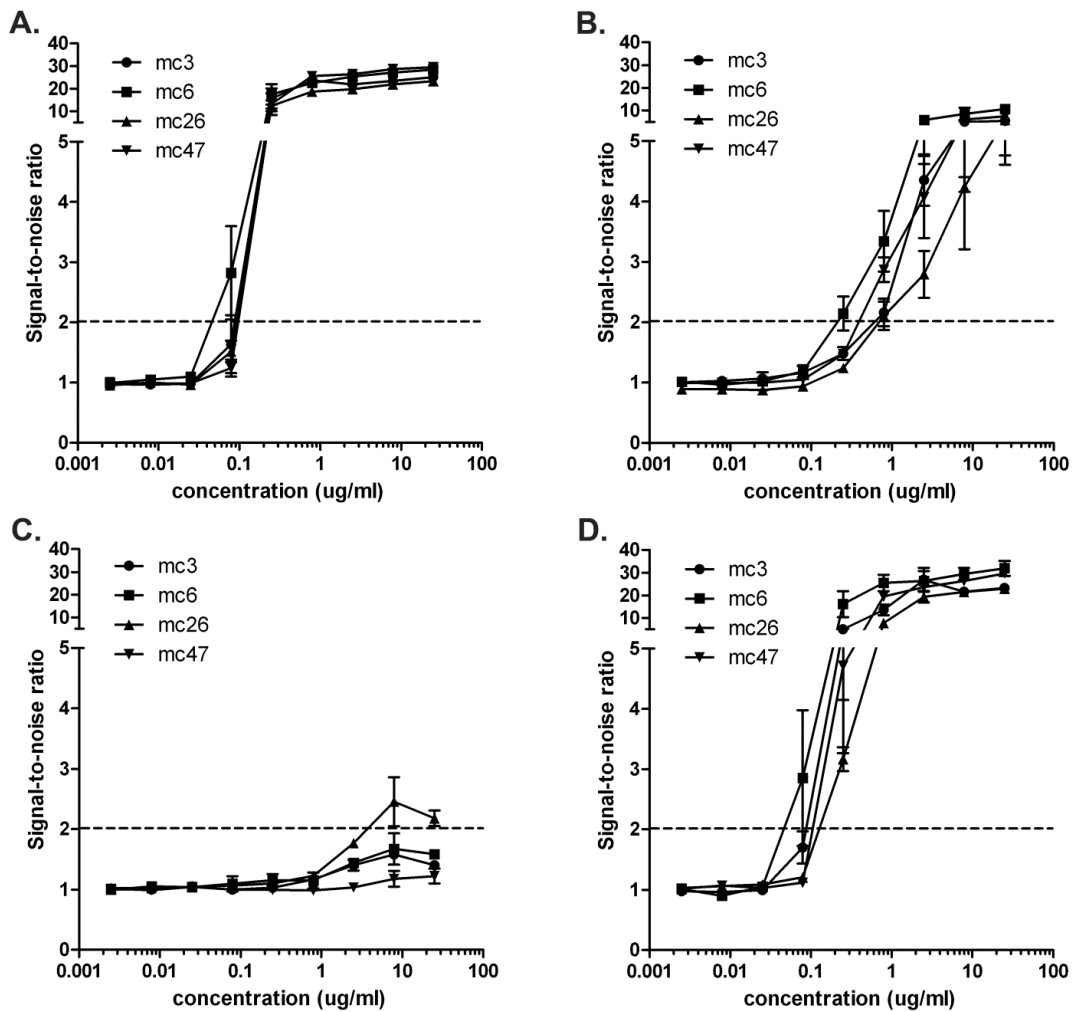


Figure 6-5: Limit of detection for various classes of mycolic acids

Limit of detection curves for *Mtb*- derived mycolic acid (**A**), and synthetic alpha (**B**), keto (**C**) and methoxy (**D**) mycolic acids as determined by indirect ELISA. Antibodies were used at a concentration of $1\mu\text{g/ml}$ and lipids were coated in hexane at the indicated concentrations, both with a volume of $100\mu\text{l/well}$. Results are given as signal-to-noise ratio and the limit of detection of a signal-to noise ratio of 2 is shown by the dashed line. Results are the average of three independent experiments and the error bars show the standard error of mean.

6.4 Optimization of mycolic acid extraction protocol

In order for the antibodies to be useful for diagnostics, a simple method for extraction of mycolic acid from the mycobacteria in clinical samples is required. We therefore optimized the sensitivity and efficiency of the assay by introducing various heating and alkaline hydrolysis steps to the basic lipid extraction protocol of vortexing in hexane described by Minnikin et al (214). To ensure that enhancement of signal could be observed, we carried out this extraction at a low concentration of *M. smegmatis* bacteria (1ml of OD₆₀₀ 0.1, 5.8x10⁷ CFU/ml). We tested incubation with or without prior heating in hexane to improve lipid extraction or boiling in water to lyse the bacteria. An additional alkaline hydrolysis protocol was also tested as the majority of mycolic acid is known to be covalently bound to the peptidoglycan cell which can be liberated by treatment with alkali (12,215). Lipid extraction via these various methods was carried out independently in triplicate and evaporated onto ELISA plates and tested with mc3 and mc6, the two antibodies with the best limit of detection.

At this low concentration of bacteria, simple vortexing did not give a significant signal over background (hexane only). However, lipid extracted by alkaline hydrolysis gave a strong signal compared to all other methods by a large and statistically significant margin. Extraction by heating in hexane also gave significantly higher signal for mc3 only over vortexing and background although the increase was slight (Fig. 6-6). Other methods showed no significant increase in signal over vortexing in hexane or background. Given that alkaline hydrolysis only requires several hours to complete as compared to the other methods which require overnight

incubation in hexane, this is the method we selected to determine the limit of detection on standardized CFU amounts of mycobacteria.

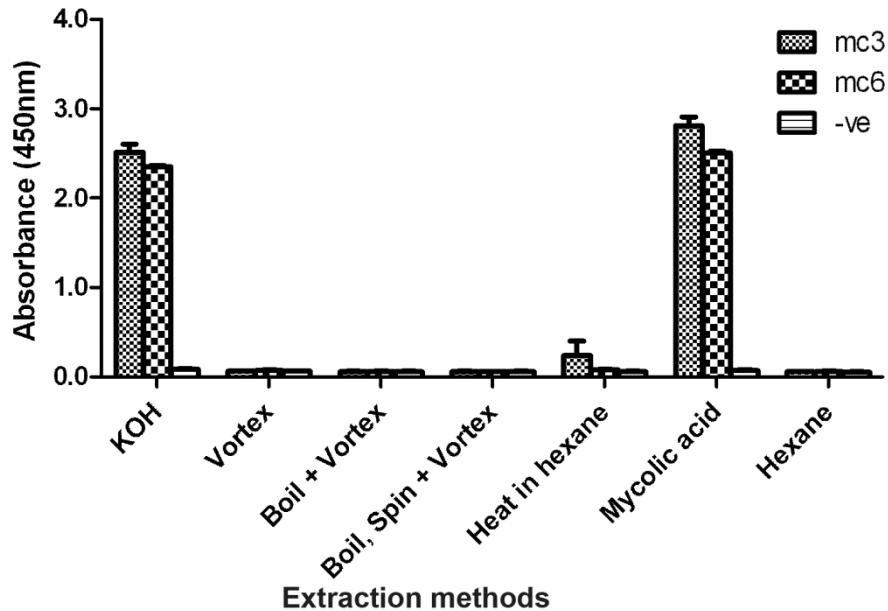


Figure 6-6: Determination of optimal lipid extraction method

Various methods of extraction were tested using the two most sensitive IgGs mc3 & 6 and 1ml of OD₆₀₀ 0.1 (5.8×10^7 CFU) *M. smegmatis* as a test sample. Mycolic acid was extracted by either overnight incubation at room temperature with hexane after vigorous vortexing only (Vortex) or with additional prior heating (Heat in hexane). Two more methods using a lysis step with boiling water where hexane was added directly to the water after heating (Boil + Hexane) or sequentially following an intermediate centrifugation to pellet the bacteria (Boil, spin + Hexane) were also carried out. A fifth protocol involving rapid alkaline hydrolysis (KOH) to release covalently bound mycolic acid was also done. *** $p < 0.001$, alkaline hydrolysis vs. all other methods * $p < 0.05$ for heat in hexane vs. all other methods.

To confirm that the alkaline hydrolysis procedure released mycolic acid from the bacteria and that our antibodies were indeed detecting mycolic acid, triplicate alkaline hydrolysis extracts were first analysed by high-resolution tandem mass spectrometry (HR-MS/MS). Identification was based on accurate mass measurement and product ion scans (Fig. 6-7A). Mycolic acids were ionised as $[M-H]^-$ ions and observed m/z were within 2ppm of expected values. Product ion analysis allowed for the identification of α -alkyl chains (the most abundant being C24:0, Fig. 6-7B). Identified mycolic acids were then quantified in the same triplicate extracts by multiple reaction monitoring (MRM) analysis, using Q1/Q3 transitions previously identified in mycolic extracts of mycobacterial species and adjusted based on an internal synthetic mycolic acid standard (8). Identified unique mycolic acid transitions were ranked by concentration and analysis of the top ten mycolic acids identified indicated that the majority of these were alpha mycolic acids and their total concentration was approximately 3.4 μ g/ml (Fig. 6-7C). The levels of methoxy mycolic acids were insignificant compared to alpha mycolic acid which was expected for the particular species of mycobacteria tested (*M. smegmatis*). Nonetheless, the concentration of alpha mycolic acid alone is well within the detection limit of our antibodies indicated earlier and can account for the high signal detected.

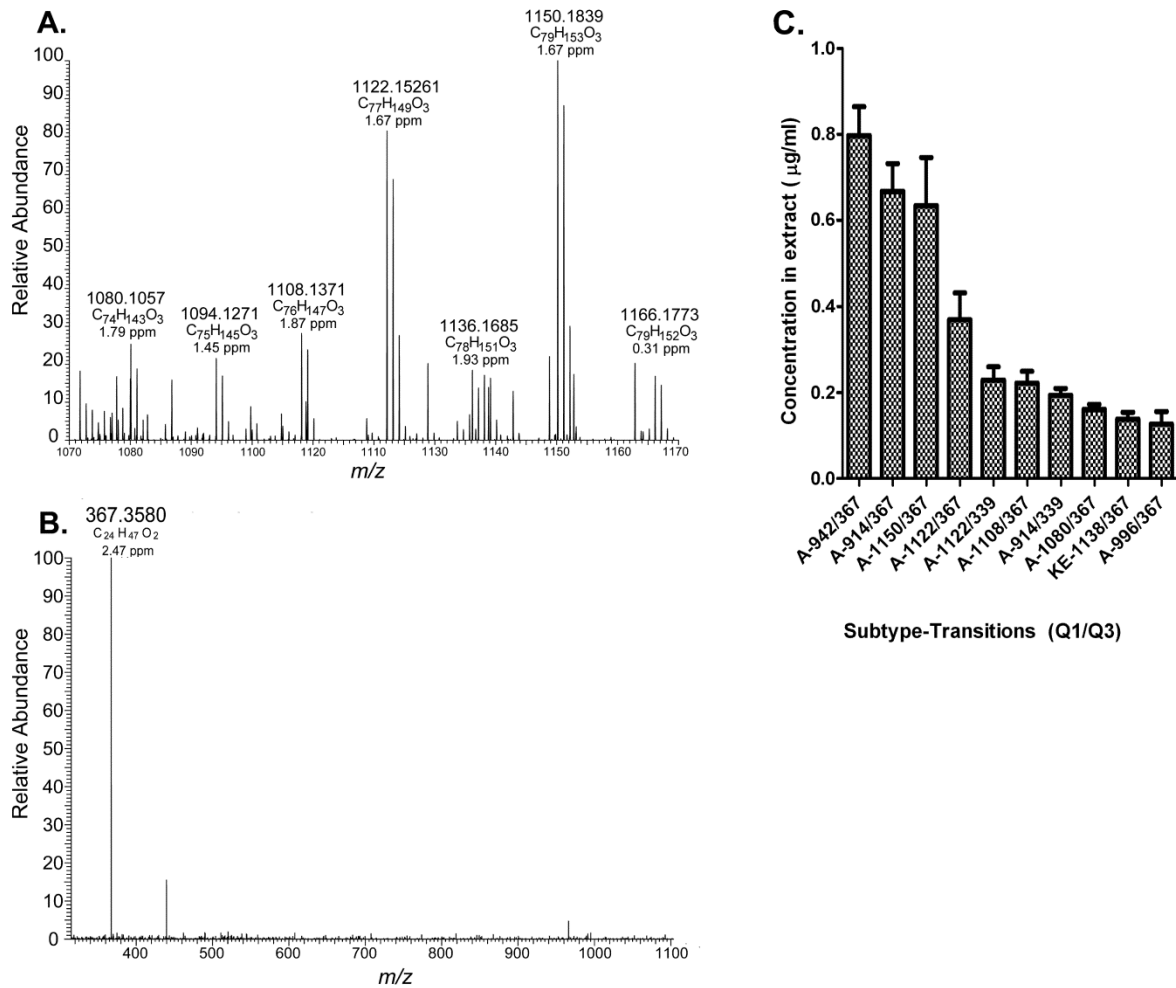


Figure 6-7: Identification of mycolic acids in lipid extract by mass spectrometry

Representative high-resolution mass spectrum of alkaline hydrolysis lipid extracts, showing measured m/z of mycolic acids, elemental formulae and mass accuracy (in ppm). **(B)** Product ion spectrum of mycolic acid at m/z 1150.2, showing a main fragment at m/z 367.3580 ($C_{24}H_{47}O_2$, fatty acyl 24:0) **(C)** Detection of individual species of mycolic acid in *M. smegmatis* KOH extract by mass spectrometry in MRM mode, the concentrations of the top ten mycolic acids, identified by Q1/Q3 transitions, are indicated along with the subtype (A or KE for Alpha and Keto/Epoxy respectively). No methoxy mycolic acid was detected. Results are the average of three independent experiments and the error bars show the standard error of mean.

6.5 Determination of species specificity

Having optimized a methodology for mycolic acid extraction, we then proceeded to apply this method to two other actinomycete species found previously in sputum samples, *Nocardia cyriacigeorgica* and *Tsukamurella paurometabolum* as these actinomycete species are also known to contain mycolic acids (48,154). As a comparison, we also tested the unrelated gram negative bacteria *Escherichia coli*. Extracts from 1ml of OD₆₀₀ 0.1 were tested by indirect ELISA in the same manner as above. mc3 was specific for only *M. smegmatis* extract while mc6 was strongly cross reactive for *T. paurometabolum* but not *N. cyriacigeorgica* extract. No binding to *E. coli* was observed for either antibody, which is to be expected as it does not contain any mycolic acid.

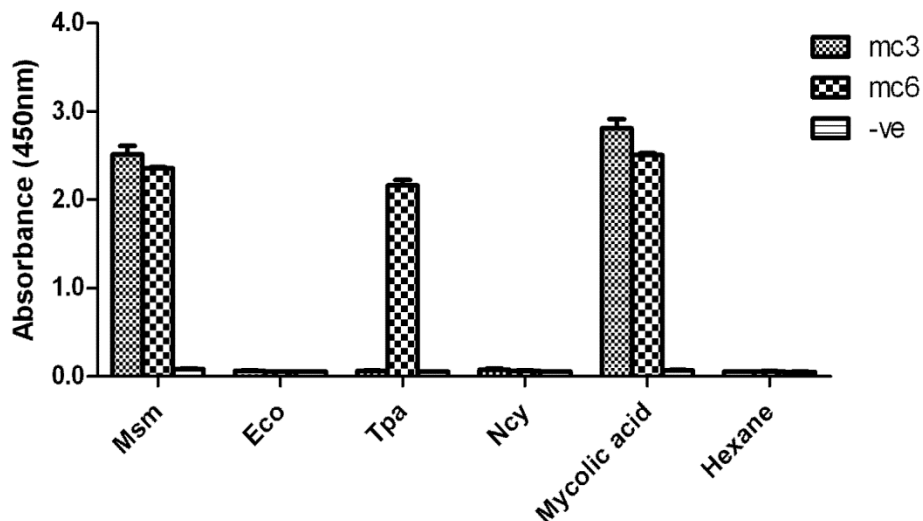


Figure 6-8: Bacterial species specificity of anti-mycolic acid antibodies

Indirect monoclonal IgG ELISA showing specificity of IgGs mc3 and mc6 for *M. smegmatis* lipid extract (*Msm*) compared to lipid extract from other actinomycete genera (*N. cyriacigeorgica*-*Ncy*, *T. paurometabolum*-*Tpa*) and *E. coli* (*Eco*) and hexane as negative controls. Mycolic acid at 6.25µg/ml was added as a positive control. Results are the average of three independent experiments and the error bars show the standard error of mean.

6.6 Determination of CFU limit of detection

Various standard amounts of bacteria from 10^9 to 10^6 CFU/ml were treated using the alkaline hydrolysis method to extract lipids into 1ml of n-hexane and 100 μ l of lipid extract was evaporated onto ELISA plates and tested with mc3 and mc6. We tested both the non-pathogenic mycobacterium *M. smegmatis* as well as a less pathogenic (BSL2) close relative of *Mtb- M. bovis* BCG. Both antibodies were able to bind the lipid extract of both mycobacterial species (Fig. 6-9). As before, mc6 had superior sensitivity compared to mc3, giving higher signal at the same bacterial concentration. Based on the limit of detection of signal-to-noise ratio of 2, the range of detection for both antibodies was roughly similar at between 10^6 to 10^7 CFU of *M. smegmatis* and one order of magnitude better for BCG at 10^5 to 10^6 CFU. Given that the volume of lipid extract evaporated was 100 μ l, this translates into a lower concentration limit of 10^7 to 10^8 CFU/ml for *M. smegmatis* and 10^6 to 10^7 CFU/ml for BCG.

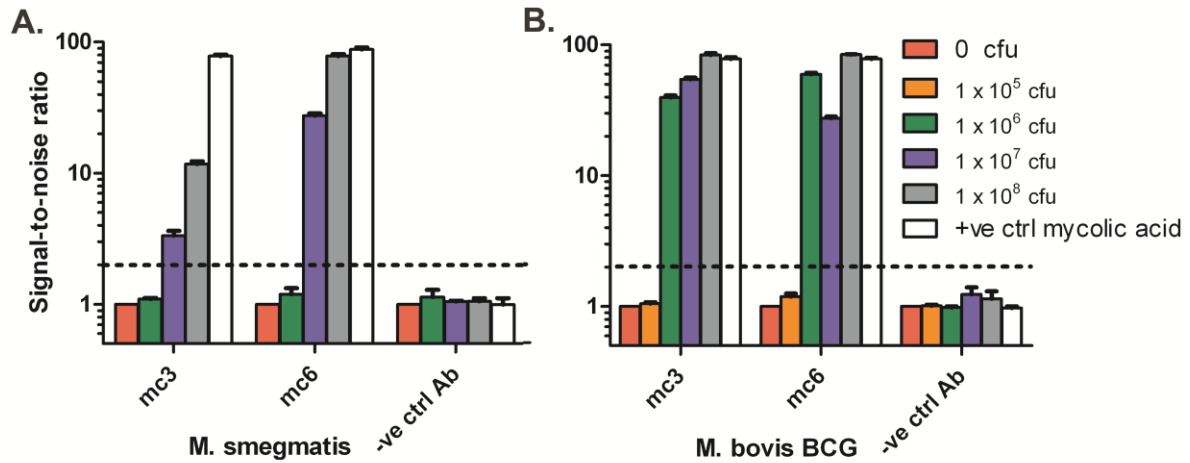


Figure 6-9: Sensitivity of anti-mycolic acid antibodies for whole mycobacteria

Limit of detection of the two most sensitive IgGs mc3 and mc6 using the rapid alkaline hydrolysis extraction method for various CFU amounts of *M. smegmatis* (A) and *M. bovis BCG* (B) based on a signal-to-noise ratio of 2 (indicated by dashed line). Both antibodies mc3 and mc6 can detect between 10⁶ to 10⁷ CFU of *M. smegmatis* and 10⁵ to 10⁶ CFU of *M. bovis BCG* in a 100µl volume. All results are the average of three independent experiments and the error bars show the standard error of mean.

6.7 Discussion

Our isolated antibodies had specificity primarily for the methoxy subclass of mycolic acid, with weak binding to alpha mycolic acid and no binding to keto mycolic acid or any other lipid tested (Fig. 6-4A). This is despite the fact that *Mtb* contains mycolic acid species of all three subclasses. While keto and methoxy mycolic acids have a W-shaped configuration that exposes the charged functional groups that allow for interactions with antibodies via electrostatic and hydrogen bonds in an aqueous environment, keto mycolic acid has the greatest tendency to fold in this manner and it is therefore unexpected that the antibodies all bound methoxy well but not keto at all (180,181). Alternatively, it may be possible that keto has weaker adherence to the ELISA plate and lost during the washing process. This could be determined by re-dissolving the dried lipid with hexane after completion of the assay and measuring the levels of recovered lipid via mass spectrometry in the same manner as done for the lipid extract.

However, serological studies have shown that anti-TDM antibodies produced in the course of TB infection in humans are generally methoxy mycolic acid specific (216). It may thus be that the human antibody repertoire is predisposed towards recognition of this particular subclass and may explain the tendency of our human-derived non-immune library to produce methoxy mycolic acid antibodies. The ability of our antibodies to distinguish between similar lipids with only small changes in molecular structure has been shown previously for antibodies raised in the same manner against oxy-sterols and indicates the ability of antibodies to provide fine specificity for lipid detection (10).

As some related bacterial genera such as *Nocardia* and *Tsukamurella* contain mycolic acid in their cell walls as well, we wanted to determine whether our antibodies could specifically recognize mycobacterial mycolic acid so as to reduce the potential for false negatives. We showed that our two best antibodies mc3 and mc6 strongly bound *M. smegmatis* lipid extract only and not extract from other non-mycobacterial species with the exception of mc6 to *T. paurometabolum* lipid extract (Fig. 6-8). This could be because its mycolic acids in terms of fine structure such as total number of carbon atoms and fatty acid chain length more closely resemble mycobacterial mycolic acids as compared to some other genera such as *Nocardia* and *Corynebacteria* which have fewer carbon atoms and shorter chain length (9). A previous study had indicated that a phage display-derived antibody against methyl palmitate, a non-polar lipid, could distinguish between this lipid and others with similar structure but longer carbon aliphatic tail (112). Therefore, while it is generally assumed that antibodies principally target and recognize polar epitopes even on lipids, it is possible that our antibodies can differentiate apolar portions of the mycolic acid molecule as well, such as the fatty acid tail. This ability to discriminate mycobacterial mycolic acids is important for diagnostic purposes as the abovementioned species of actinomycetes have been identified in sputum samples from TB patients (154).

Our most sensitive antibody, mc6, was able to detect 4.5ng of total mycolic acid or methoxy mycolic acid by indirect ELISA (Fig. 6-5A & 6-5D). While this is the first time the sensitivity of an anti-mycolic acid antibody has been determined, this is not too dissimilar to other antibody-based TB diagnostic assays such as the urinary

lipoarabinomannan test, which also detect in the low-to sub nanogram level at similar signal-to-noise ratios (83,85). In order to determine whether such sensitivity is sufficient for clinical use, we sought to establish a limit of detection based on bacterial count (CFU). However, to ensure that our assay was as sensitive as possible while remaining suitable for use as a point-of-care test in a resource poor setting, we first had to optimize the protocol for maximum efficiency of lipid extraction from the sample while minimizing time, reagents and equipment required.

While the initial method of vortexing in hexane was the simplest and did not require heating or neutralization, it did not give the highest signal and presumably had very low lipid yield. The procedure is also lengthy and required an overnight incubation. A shorter two hour hexane incubation with heating improved the signal, but was still clearly inferior to alkaline hydrolysis (Fig. 6-6). The efficiency of the latter method is probably due to its ability to also release covalently bound mycolic acid (12,215). It is also the shortest method requiring only one hour and thus is ideal for a rapid point-of-care test although it will require additional reagents. A variant of this method, which utilized a more complex protocol requiring overnight incubation with organic solvent to inactivate and delipidate cells, had also been applied previously in combination with mass spectrometry to give a limit of detection of 10^4 CFU *Mtb* in spiked sputum and was also used to extract detectable levels of mycolic acid from patient samples, thus indicating its suitability for clinical use (12). We therefore chose the alkaline hydrolysis method to determine the CFU limit of detection for the two most sensitive antibodies mc3 and mc6 and verified its ability to extract mycolic acids through HR-MS/MS and MRM analyses of the lipid extract which confirmed the presence of mycolic acid.

To determine the equivalent CFU detection limit, we used both *M. smegmatis* as well as *M. bovis* BCG mycobacterial species. The choice of *M. bovis* BCG was due to the fact that while these two mycobacterial species along with *Mtb* have alpha mycolic acids, both *M. bovis* BCG and *Mtb* but not *M. smegmatis* produce methoxy mycolic acids (48). Thus, they have a greater similarity in the subclasses of mycolic acids detected by our antibodies although the levels of methoxy mycolic acid in BCG have reported to be low (48,164). Our results indicate that mc3 and mc6 recognize *M. bovis* BCG at a limit of between 10^5 to 10^6 CFU (Fig. 6-9) and are less sensitive to *M. smegmatis* by an order of magnitude, which is not surprising given the partial dissimilarity in mycolic acid composition and the higher sensitivity of our antibodies to methoxy mycolic acid over alpha mycolic acid. This higher sensitivity would be an advantage if the antibodies are to be used for diagnostic purposes as there are only a very limited number of mycobacterial species other than the *Mtb* complex group of species (*Mtb*, *M. bovis*, *M. africanum*, *M. microti*) that contain methoxy mycolic acids (48).

As this is a lipid antigen insoluble in aqueous solution, using a capture antibody in a sandwich ELISA to improve sensitivity is not possible. It is also unlikely that mc3 and mc6 can be used concurrently to bind separate epitopes as given the small size of the molecule and their similar specificity and affinity; they are likely to bind the same epitope. This could be confirmed by completion ELISA. While our assay is currently less sensitive than mass spectrometry which detects 10^4 CFU, this is not surprising given that mass spectrometry is generally far more sensitive than immunological assays and can detect as low as 1pg of pure lipid (12). Nevertheless,

based on CFU alone, this result is still less sensitive as compared to current diagnostic methods such as sputum culture, which can detect levels as low as 10 CFU/ml of mycobacteria and even sputum smear which requires 10^4 CFU/ml for reliable detection (217). However, both these methods require intact bacteria and in case of culture, live bacteria for successful detection. As our technique relies on antigen detection instead, it can also detect mycolic acids in sputum released by dead bacterial fragments and thus may be more sensitive than indicated based on CFU counts alone. Furthermore, the higher affinity of our antibodies for methoxy mycolic acid over other subclasses (45ng/ml limit vs. 200ng/ml) probably results in an artificially poor CFU limit of detection as our test species *M. smegmatis* and *M. bovis BCG* have no or low levels of methoxy mycolic acid respectively as compared to alpha mycolic acids as indicated by our own mass spectrometry data and previous publications (48). On the other hand, nuclear magnetic resonance analysis has indicated that the proportion of methoxy to alpha mycolic acid is at least 50% or above in various *Mtb* strains (164). Mass spectrometry data has also indicated that the most common species of methoxy and alpha mycolic acids are present in TB patient sputum at an average concentration of over 100ng/ml, although detection was extremely poor in the smear-negative cohort which suggests lower levels of mycolic acid (although exact amounts in this cohort were not described in the paper) (12). This is well within the detection limits of mc3 and mc6 and samples can be further concentrated by evaporation of organic carrier solvent thus allowing for enhanced sensitivity when mycolic acid concentrations are low.

We have therefore isolated and produced the first full length IgG anti-mycolic acid antibodies with preferential specificity for the methoxy subclass present in only a

subset of slow-growing mycobacteria. Crucially, these antibodies also do not cross-react with cholesterol, a previously reported observation with anti-mycolic acid antibodies. We also show that one antibody mc3 can distinguish mycolic acids from related actinomycete genera. Its detection limit for methoxy mycolic acid is around 80ng/ml, a concentration that is below the average in TB patient sputum. It therefore has high potential for TB diagnosis but needs verification on patient samples. More generally, we have shown that the combination of anti-lipid antibodies obtained via phage display and a rapid and simple lipid extraction method can enable the rapid and cost effective detection of a set of novel lipid biomarkers in a point-of-care setting, which were previously accessible only via expensive and sophisticated techniques such as mass spectrometry or chromatography.

Chapter 7: Validation of antibodies on clinical samples

7.1 Introduction

Having optimized our my2F12 antibody and sample processing procedure for use on tuberculosis clinical samples, we then proceeded to test our antibody on three different types of clinical samples: sputum, urine and serum. All three types of clinical samples have been evaluated previously for use in LAM detection assays with urine been the focus of multiple studies. The primary assay used has been the Clearview sandwich ELISA kit, which was reported to have poor sensitivity in the HIV negative cohort when tested on urine samples, ranging from 6% to 21%, although specificity was acceptable, ranging from 83% to 100% (151-154,195). It was found to have better sensitivity (67%) in HIV patients with CD4 T cell counts less than 50 per ml and it was suggested that it could be used as a rule-in assay to provide rapid results during severe TB infection for quick initiation of treatment (157,218).

We and others have shown that polyclonal anti-LAM antibodies, such as those used in the Clearview ELISA, cross-reacts with multiple non-tuberculous mycobacterial species as well as other related non-mycobacterial species (85). This has resulted in extremely high cross-reactivity and poor specificity when sputum samples were used (154). We therefore sought to ascertain if our monoclonal ManLAM antibody can provide improved specificity for this sample group. We also tested our antibody on matched urine and serum samples. These are likely to have a lower bacterial burden and hence reduced potential for cross-reactivity, which is a concern as our antibody is not absolutely specific for *Mtb*, but also binds other slow growing mycobacteria and a related actinomycete species.

Adult volunteers were recruited from patients admitted to the National Centre for Tuberculosis and Lung Disease in Tbilisi, Republic of Georgia with suspicion of tuberculosis infection. As urinary LAM levels have been reported to be higher in HIV positive individuals, we excluded these from our study to ensure that our assay will be functional in HIV negative individuals, which comprise the majority of TB patients. Recruited patients were classed into four groups: firstly, TB-negative, which were confirmed microbiologically negative by sputum smear microscopy and culture and without any clinical suspicion of TB; and three TB-positive groups: smear-negative, which were not detected by acid-fast staining but positive by culture; patients with grade 1+ smears (>10 acid-fast bacilli/100 microscopy fields) and patients with grade 2+ smears and above (>100 acid-fast bacilli/100 microscopy fields). Patients diagnosed only on the basis of clinical presentation without any microbiological confirmation of TB were excluded from this study. Fifteen individuals were recruited into each group. The purpose of segregating the TB positive patients into three groups was firstly for comparison with sputum culture, currently the gold standard assay in resource-limited countries (31). Detection of smear-negative, culture-positive individuals by our assay would suggest that it is a potential substitute for culture, which cannot deliver a diagnosis on the same day. The grade 1+ group enables comparison with sputum smear microscopy, the current rapid test in resource-limited countries (31). Finally, given the low levels of LAM in urine and serum, we may not be able to detect LAM in individuals with low grade infection (209,219). Therefore, the grade 2+ group, which are likely to have the most severe infections, can serve as a positive control to confirm that the antibody is functional in actual clinical samples. Clinical sensitivity could subsequently be improved by using diagnostic technologies that can provide a lower limit of detection.

We also evaluated the potential of the anti-mycolic acid antibody mc3 on lipid extracts of sputum using the same chimeric antibody constructs developed for my2F12. For initial validation, we chose to focus on sputum as its presence in this sample type is known and method for extraction well characterized, although this does not preclude the possibility that other sample types may also contain mycolic acid (12). Out of the four monoclonals initially characterized, we decided to focus on the antibody mc3 due to its high avidity and reduced cross-reactivity to non-mycobacterial mycolic acids in contrast to mc6. Although we are testing lipid extract which should contain minimal amounts of protein, we also sought to produce a chimeric variant of mc3 for diagnostic use and thus expressed mc3 using the various chimeric constructs developed earlier for my2F12 and tested them for avidity and specificity compared to the original antibody.

7.2 Optimization of assay antibody concentration

Due to the reported low levels of LAM in urine and serum, we first sought to further optimize the assay by determining the appropriate concentrations of capture (HuG1full) and detector (hG3mG2a) antibodies for maximal signal at such concentrations. We coated ELISA plates at 2, 5 and 10 μ g/ml of HuGfull1 and detected ManLAM in spiked serum with 1, 2.5 or 5 μ g/ml of hG3mG2a, while the secondary antibody concentration was kept the same. All possible combinations of the above antibody concentrations were tested and the signal-to-noise ratios (SNR) and specific absorbance determined (Fig. 7-1A). The pattern for both SNR and specific absorbance was the same with an increase from 1 to 5 μ g/ml of detector antibody, which was statistically significant. SNR and specific absorbance also

increased with higher antibody concentration, although this was not statistically significant. We tested the best combination (10 μ g/ml capture with 5 μ g/ml detector) on ManLAM serially diluted into 1xPBS to obtain a general sensitivity estimate and the limit of detection with SNR of 2 was 0.5ng/ml, an improvement from 2ng/ml in the previous chapter using 5 μ g/ml capture with 1 μ g/ml detector (Fig. 7-1B). This concentration was used in all subsequent clinical assays

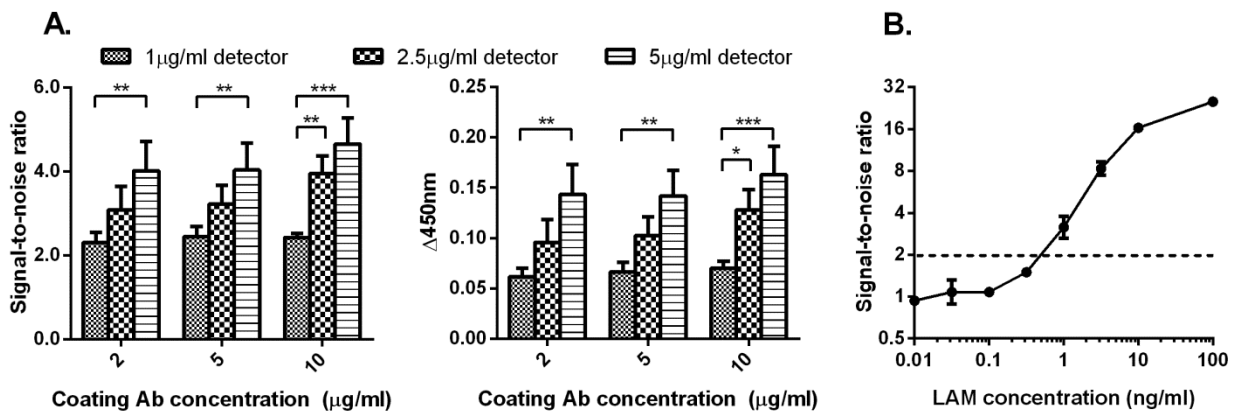


Figure 7-1: Optimization of capture and detector antibody concentration

(A) Significant enhancement of signal-to-noise ratio (left panel) and specific absorbance above background (right panel) at different antibody concentrations in sandwich ELISA, using spiked serum with a low concentration of ManLAM (2ng/ml) **(B)** Limit of detection of 0.5ng/ml (at signal-to-noise ratio of 2) at optimal antibody concentrations of 10 μ g/ml capture and 5 μ g/ml detector antibody with a 100 μ l sample of ManLAM spiked into PBS. All results are the average of three independent experiments and the error bars show standard error of mean. *: $p < 0.05$, **: $p < 0.01$, ***: $p < 0.001$

7.3 Testing of clinical samples for ManLAM

Using the optimized antibody concentrations, we then proceeded to test processed clinical samples for the presence of ManLAM. The strength of the sandwich ELISA signal (absorbance) can be influenced by the amount of sample

used and the length of time of TMB substrate incubation for colour development, which can potentially give in improved sensitivity but also higher background and reduced specificity i.e. higher false positive rates. We therefore tested sample volumes of 100 μ l and 300 μ l with incubation times of 15min and 30min in different combinations. Initial results were assessed by comparison of the TB negative set with the three groups of TB positive individuals combined as a single set.

Receiver-operating characteristic (ROC) analysis was carried out on these two groups to determine the optimal absorbance cut-off value to demarcate positive from negative test results due to overlap in the test absorbance values of each populations. ROC analysis plots sensitivity against false positive rates as the absorbance cut-off value is varied. Sensitivity is defined as the number of true positive samples (positives that test positive) divided by the total number of positive samples. Specificity is defined as the number of true negative (negatives that test negative) divided by the total number of negative samples (false positive rate = 1-specificity). Decreasing the cut-off reduces both false positive rates and sensitivity but at different rates. The plot enables identification of the cut-off value which minimises false positive rates without incurring too great a loss of sensitivity. For diagnosing TB, priority is set on keeping false positive rates low to minimise unnecessary treatment of non-infected individuals. Therefore we have placed emphasis during ROC analysis on minimising false positive rates even though the trade-off is reduced sensitivity. Sensitivity and false positive percentages were then tested for significant differences using Z-test for proportion at the 95% confidence level.

Sputum samples were tested at 100µl sample volume for 15min and 30min incubation and 300µl at 30min. Samples were liquified prior to testing to ensure unimpeded capture of target antigen in the assay. Both results obtained at 30min incubation gave high background with the mean absorbance of the TB-negative group being higher than that of the TB-positive group (Fig. 7-2B & C). As a result, no ROC analysis could be done and suitable cut off value determined. This indicated that enhancing the signal through increased sample volume or longer incubation time was not necessary. When 100µl sample was incubated for 15min, a high specificity of 93.3% but low sensitivity of 22.2% was obtained (Fig. 7-2A). However, this sensitivity was not significantly different from the false positive rate.

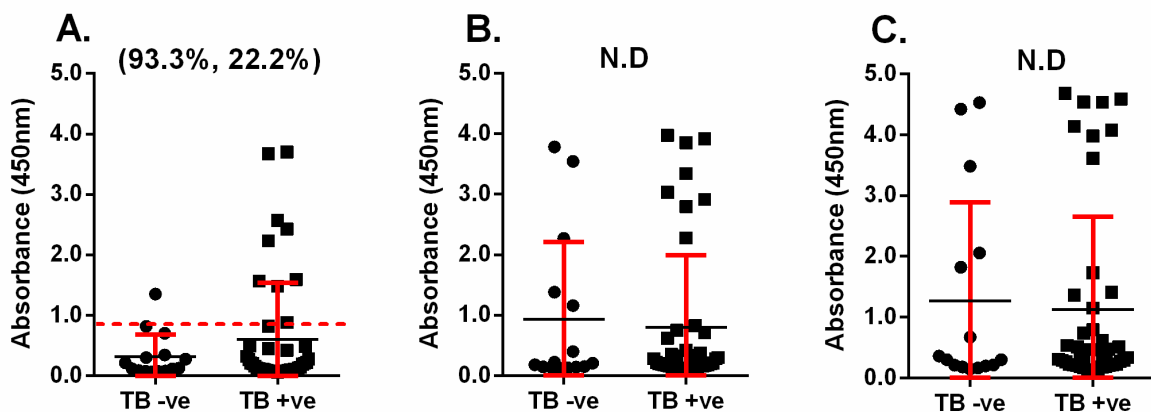


Figure 7-2: Detection of ManLAM in TB patient sputum samples

Absorbance values from the optimized my2F12 indirect sandwich ELISA on TB patients (TB +ve, n=45) and healthy controls (TB -ve, n=15) using **(A)** 100µl sample with 15min TMB incubation **(B)** 100µl sample with 30min TMB incubation **(C)** 300µl sample with 30min TMB incubation. Specificity and sensitivity (L/R) percentages indicated above (A) based on optimal cut-off (red line) as determined by ROC analysis. ROC analysis was not carried out for (B) and (C) as the mean value for the TB +ve cohort was below that of the TB-ve. Error bars show standard deviation of the sample.

Serum samples, which were anticipated to have very low LAM levels, were tested at both sample volumes for 30min and the mean absorbance of the TB-positive group was higher than the TB-negative under both conditions. ROC analysis provided an absorbance cut-off with 93.3% specificity for both groups but only 26.7% and 35.6% sensitivity for sample volume of 100 μ l and 300 μ l respectively (Fig. 7-3). Both sensitivity percentages were significantly different from the false positive rate. In contrast with the sputum sample results, increased sample volume improved sensitivity without degrading specificity.

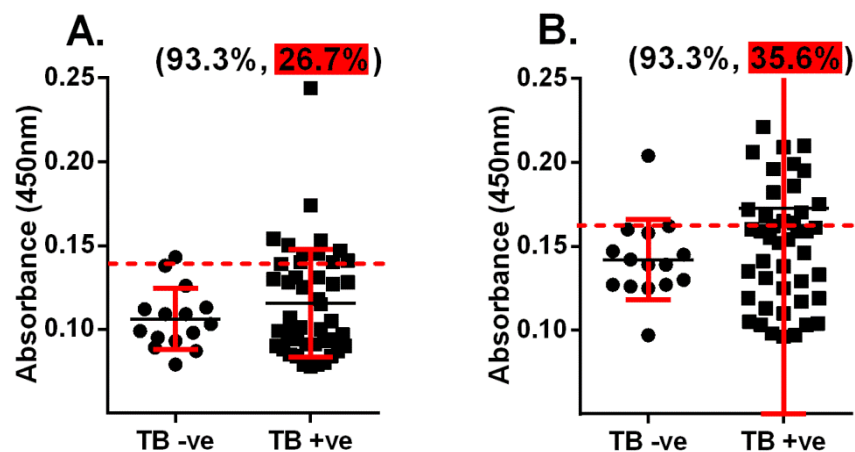


Figure 7-3: Detection of ManLAM in TB patient serum samples

Absorbance values from the optimized my2F12 indirect sandwich ELISA on TB patients (TB +ve, n=45) and healthy controls (TB -ve, n=15) using **(A)** 100 μ l sample with 30min TMB incubation **(B)** 300 μ l sample with 30min TMB incubation (one outlier at OD1.162 not shown). Specificity and sensitivity (L/R) percentages are indicated above each chart based on optimal cut-off (red line) as determined by ROC analysis. Red highlight indicates test sensitivity rate has significant difference from false positive rate in TB -ve group at 95% confidence level. Error bars show standard deviation of the sample.

Urine samples were tested in all four possible sample volume and incubation time combinations and the mean absorbance for the TB-positive group was higher in all cases. ROC analysis gave a specificity of 92.3% for all four testing conditions but

the best sensitivity (37.8%) was obtained by using 100µl sample with 15min incubation time (Fig. 7-4). Only this level of sensitivity was significantly different from the false positive rate. Similar to the sputum results, enhancing signal did not improve sensitivity as the increased signals from the TB-negative cohort required raising the cut-off value to maintain suitable specificity and hence reduced sensitivity instead.

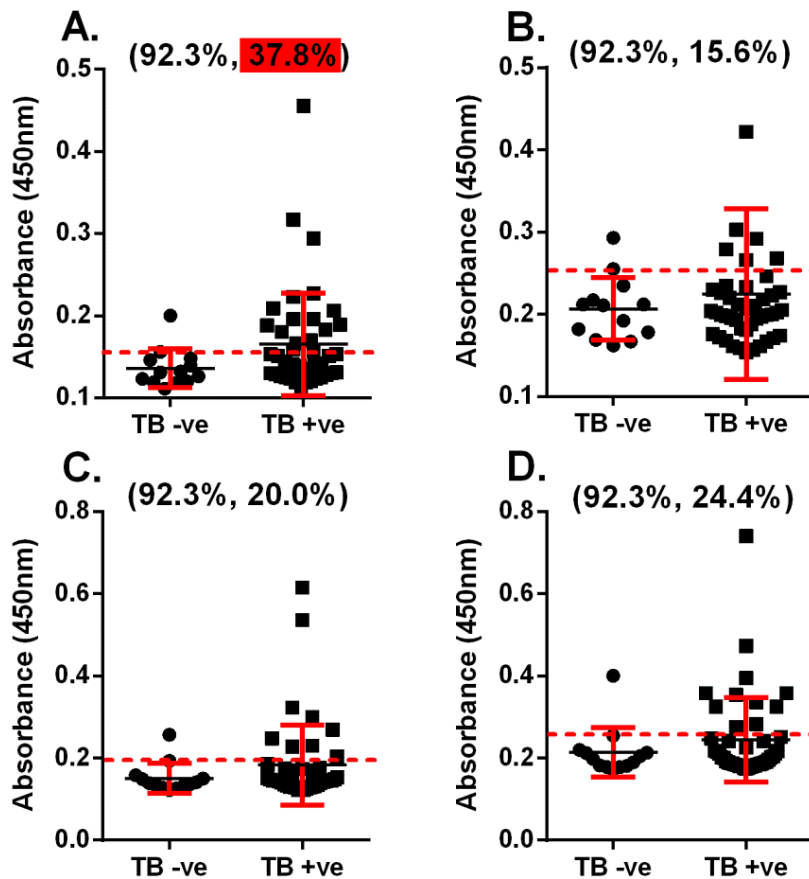


Figure 7-4: Detection of ManLAM in TB patient urine samples

Absorbance values from the optimized my2F12 indirect sandwich ELISA on TB patients (TB +ve, n=45) and healthy controls (TB -ve, n=13) using **(A)** 100µl sample with 15min TMB incubation **(B)** 300µl sample with 15min TMB incubation (one outlier at OD0.826 not shown) **(C)** 100µl sample with 30min TMB incubation **(D)** 300µl sample with 30min TMB incubation. Specificity and sensitivity (L/R) percentages are indicated above each chart based on optimal cut-off (red line) as determined by ROC analysis. Red highlight indicates test sensitivity rate has significant difference from false positive rate in TB -ve group at 95% confidence level. Error bars show standard deviation of the sample.

7.4 Analysis of results by individual patient groups

The data obtained from the most suitable experimental conditions i.e. gave best overall specificity and sensitivity rates for each sample type, was then analysed according to the individual patient groups. Based on the previously determined cut-off values, sensitivities for each of the three TB-positive groups were determined, along with the false positive rate for the TB-negative group. The ROC curve used to determine the cut-off value is also shown (Fig. 7-5). The sensitivities obtained for each group were also tested for significant difference using the Z-test for multiple independent proportions.

While sputum and serum had the highest sensitivities in the smear 2+ and above group, this rate was not statistically different from the false positive rate for sputum (Fig 7-5A). Serum had very high sensitivity in this group (53%) and this rate was significantly different from both the false positive rate as well as the sensitivity rate of the smear 1+ group (Fig 7-5B). Urine had high sensitivity (40-47%) in both the smear 1+ and 2+ or greater groups although the difference between the two was not statistically significant (Fig 7-5C). Both rates were significantly different from the false positive rate.

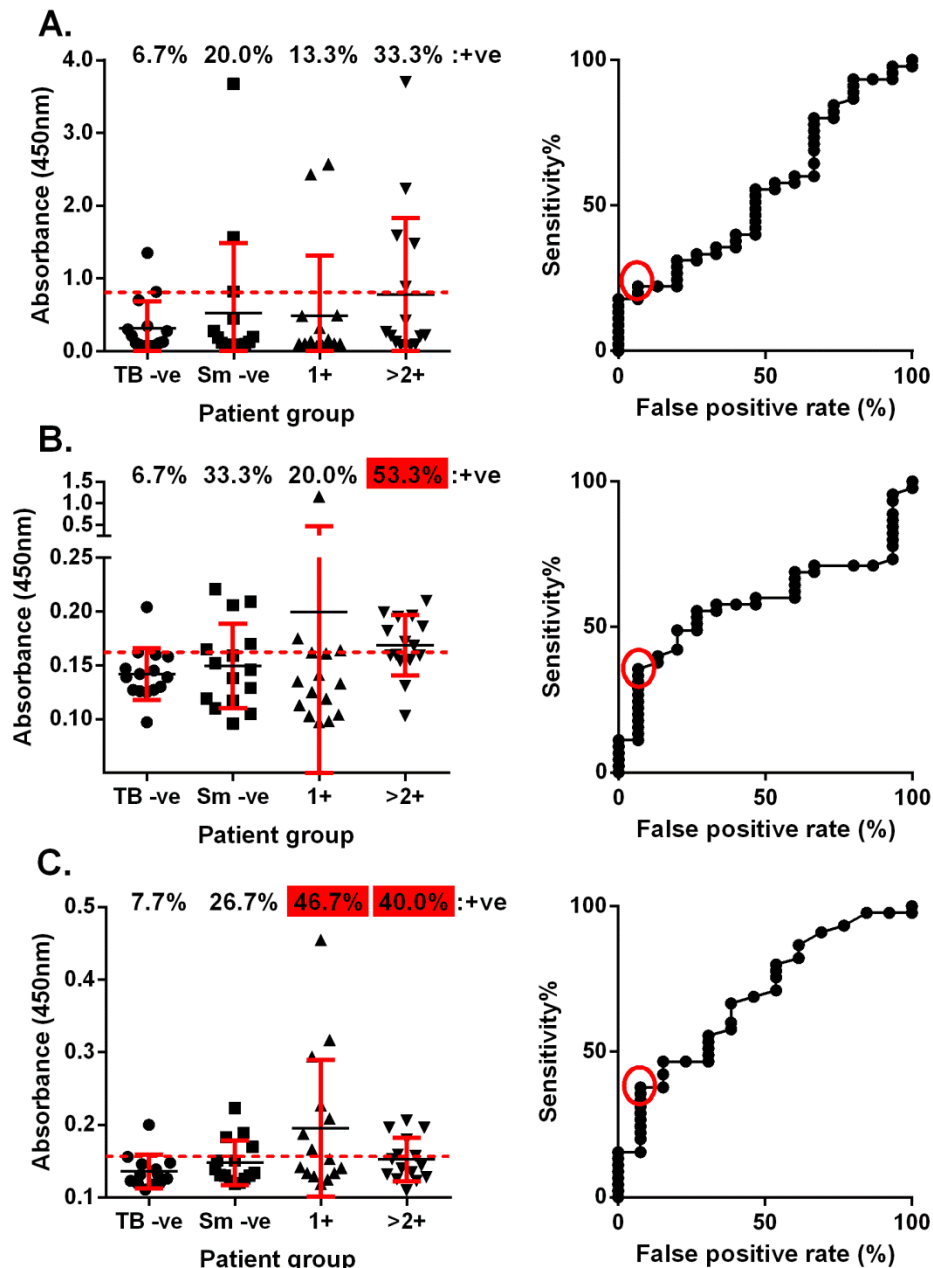


Figure 7-5: Sensitivity of optimized my2F12 sandwich assay for individual patient groups

Left panel: Absorbance values of (A) 100 μ l sputum at 15min TMB incubation, (B) 300 μ l serum at 30min incubation and (C) 100 μ l urine at 15min TMB incubation by individual patient groups (TB –ve: healthy patients, Sm –ve: smear-negative, culture positive, 1+: Smear-positive grade 1+, <2+: Smear-positive grade 2+ and above) Percentage positive values are indicated based on the optimal cut-off values (red line), red highlight indicates significant difference from TB –ve group at 95% confidence level). **Right panel:** ROC chart indicating variation of false positive rate with sensitivity at increasing absorbance cut-off values. Red circle indicates optimal point for greatest sensitivity with minimum false positive rates to obtain maximum accuracy. Error bars show standard deviation of the sample.

7.5 Analysis of combined data

As tests on different sample types were most sensitive for different patients groups, we looked to determine if combinations of test results or combination of absorbance values of different tests could give better test sensitivity and specificity. For combination of test results, a positive test result (as defined by the cut-offs established earlier) in any sample type was considered positive while a negative result required tests on all three samples to be negative. The combined results these could then be used to determine test specificity and sensitivity.

Sample Combination	Specificity %	Sensitivity %			
		Sm -ve	1+	>2+	Overall
Serum OR Urine OR Sputum	76.92	60.00	53.33	73.33	62.22
Serum OR Urine	84.62	53.33	53.33	60.00	55.56
Urine OR Sputum	84.62	40.00	46.67	53.33	46.67
Serum OR Sputum	84.62	53.33	53.33	60.00	55.56

Table 7-1: Specificity and sensitivity from combination of assay results on different clinical sample types.

Samples were considered positive if they were positive for any one of the sample types based on the cut-off values defined earlier. Number of test positives/negatives was then used to calculate specificity and sensitivity values. N=15 for each TB positive group and N=13 for the TB-negative group. TB -ve: healthy patients, Sm -ve: smear-negative, culture positive, 1+: Smear-positive grade 1+, <2+: Smear-positive grade 2+ and above. Test sensitivity percentages in bold indicates significant difference from the false positive rate in the TB-negative group (at 95% confidence level)

Combinations of any two tests showed improved sensitivity up to 55.56% but concurrently drop in specificity to 84.6%. A combination of all three tests gave further reduced specificity but a higher sensitivity of 62.2% (Table 7-1). This is better than that given by the individual tests at that level of specificity; which is 46.62%, 31.1% and 48.9% *sensitivity* for the optimized urine, sputum and serum individual assays respectively based on the ROC plots. The overall sensitivity rates for all test combinations were significantly different from the false positive rate.

Individual group sensitivity was the highest in the smear 2+ cohort for all combinations and was significantly different from the false positive rate. However, in the combination of all three tests, the sensitivity rate for the smear 1+ was not significantly different from the false positive rate. In contrast, using the serum test results in combination with either urine or sputum gave sensitivity rates for all three groups that were significantly different from the false positive rate. The worse result was given by the combination of urine and sputum tests which had the lowest rates that mostly did not reach statistical significance (2 out of 3)

Alternatively, absorbance values from individual tests can be summed, a new ROC analysis conducted and cut-off values determined. Absorbance summations from all three tests or a combination of any two tests were analysed and new sensitivity and specificity rates determined for each. While specificity remained high at 92.4%, the best sensitivity, given by an absorbance combination of the urine and serum tests, was no better than that given by the individual urine test at 37.8% (Fig. 7-6). Only this sensitivity rate was significantly different from the false positive rate.

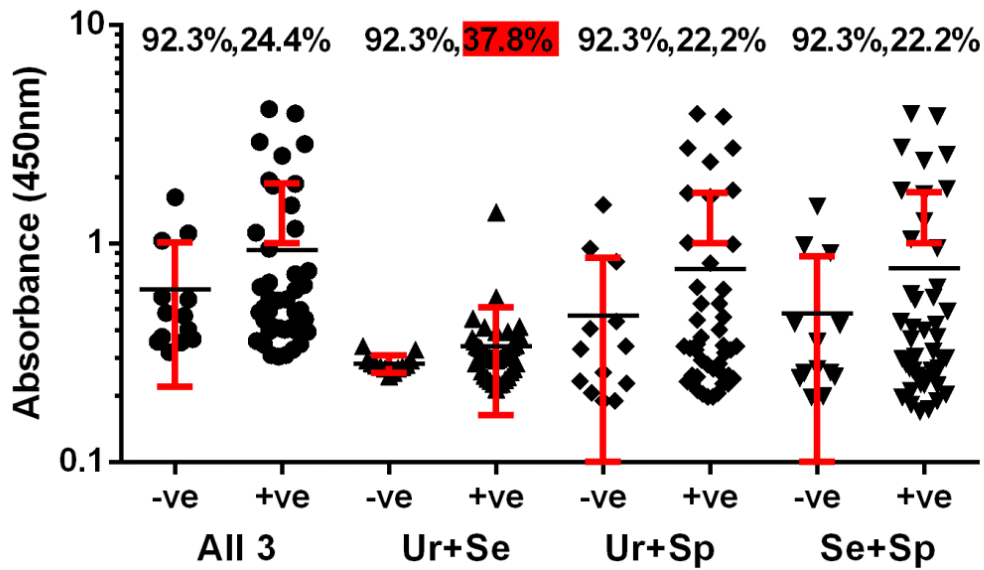


Figure 7-6: Sensitivity and specificity rates obtained using combination of absorbance values (OD) from different clinical sample types

ROC analysis was carried out on different combinations of absorbance values (All 3: serum + urine + sputum, Ur+Se: urine + serum, Ur+Sp: urine + sputum, Se+Sp: serum + sputum) to determine if any combination offered improvement in specificity and/or sensitivity. Specificity and sensitivity rates (L/R) based on individually calculated cut-off values for each combination are shown above. Red highlight indicates test sensitivity has significant difference from false positive rate of that particular combination at 95% confidence level. Error bars show standard deviation of the sample.

Based on the above results, using a combination of optimal test results appeared to at best improve sensitivity at the cost of specificity. An alternative however is to combine absorbance values from non-optimal tests that individually had poorer sensitivity rates. One suitable set of results is the absorbance values of serum tested using 100µl sample volumes, which had only slightly lower sensitivity compared to the optimal serum test which used 300µl sample volumes. A combination of absorbance values from this test and the optimal urine test gave an overall sensitivity of 60.0% (which was statistically significant) while maintaining high specificity (Fig. 7-7). Sensitivity was also maintained or improved for each TB

positive patient group up to 46.7% for smear-negative patients and 66.7% for smear-positive patients. All sensitivity rates were significantly different from the false positive rate but were not significantly different from each other.

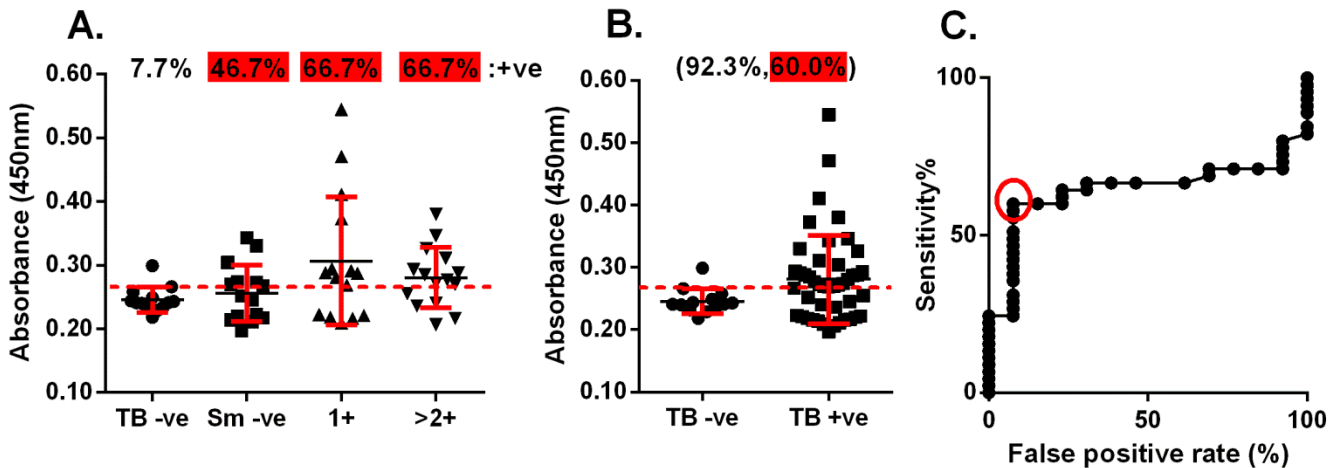


Figure 7-7: Sensitivity and specificity rates obtained from combination of absorbance from urine (100 μ l sample at 15min TMB) and serum (100 μ l sample at 30min TMB)

Combined absorbance values according to: **(A)** individual patient groups (TB –ve: healthy patients, Sm –ve: smear-negative, culture positive, 1+: Smear-positive grade 1+, <2+: Smear-positive grade 2+ and above) **(B)** With all three positive groups combined (TB +ve). Overall specificity and sensitivity rates (L/R) are indicated above. Percentage positive values are indicated based on the optimal cut-off values (red line). Red highlight indicates significant difference from false positive rate in TB –ve group at 95% confidence level **(C)** ROC chart indicating variation of false positive rate with sensitivity at increasing absorbance cut-off values. Red circle indicates optimal point for greatest sensitivity with minimum false positive rates to obtain maximum accuracy. Error bars show standard deviation of the sample.

7.6 Conversion of mc3 to chimeric antibody for diagnostic use

To avoid potential cross-reactivity to endogenous human antibodies in clinical samples, the same constructs developed for my2F12 were used to produce chimeric variants of mc3. The antibodies expressed were properly assembled as indicated in the reducing and non-reducing Coomassie gels, with a balanced level of heavy and light chain on the reducing gel and the majority of the antibody running as fully assembled IgG (greater than 150kDa) on the non-reducing gel (Fig. 7-7B & C). Western blot probed with anti-human Fc also confirmed the species identity of the fully human and chimeric antibodies by highlighting only huG1full and huG3full heavy chains (Fig. 7-7D)

The antibodies were tested for their binding avidity using serially diluted antibody against *Mtb* mycolic acid extract and a pattern similar to that observed for the my2F12 antibody variants was observed (Fig. 7-8A). HuG1full and huG3full had the highest binding avidity although huG3full binding curve was only marginally higher than that of huG1full. hG3mG2a had lower binding avidity than HuG1 full while hG1mG2a, moG2a and moG2afull had virtually identical binding curves with the lowest binding affinity. hG3mG2, as the chimeric with the highest binding avidity and suitable for use as a diagnostic antibody for reduced cross-reactivity, was subsequently compared against the original huG1 for specificity with a subset of lipids tested earlier, including all the mycolic acid subtypes. 5µg/ml of each antibody was used as the earlier binding curves had indicated that maximal absorbance was obtained for both antibodies at that concentration. Specificity was identical although

the absorbance signal is weaker which is probably due to the different secondary antibodies used (Fig. 7-8B).

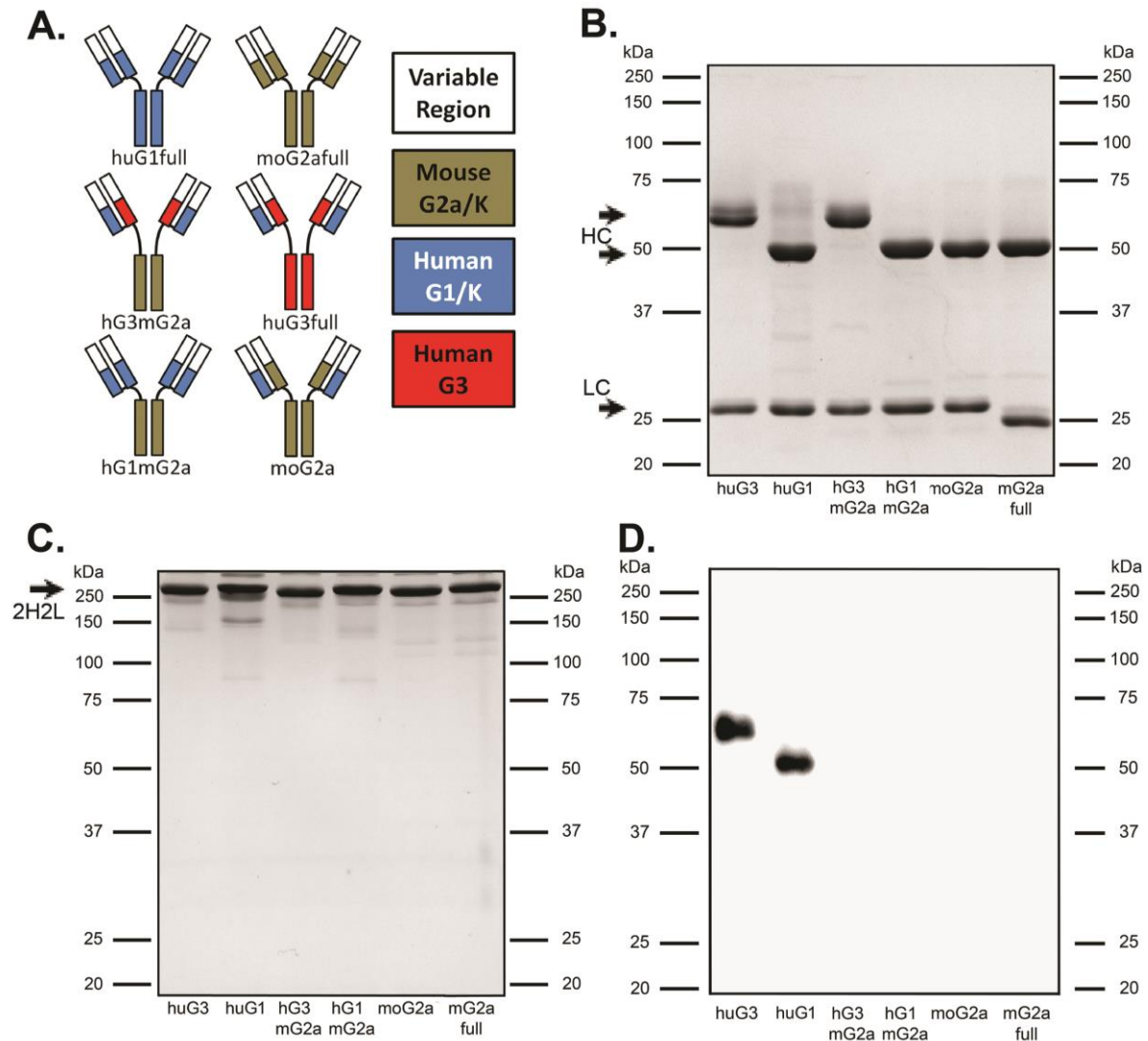


Figure 7-8: Design and expression of mc3 chimeric variants

(A) Structural diagram of the six mc3 antibody variants including the original huG1 mc3 showing the human/mouse origins and isotypes of the various constant domains. **(B)** Reducing and **(C)** Non-reducing Coomassie of the six variants. 2 μ g of each antibody was run on 10% SDS-PAGE gel showing individual heavy and light chains (HC/LC) or fully assembled antibody (2H2L) **(D)** Western blot of the six variants with 1:5000 anti-Human Fc-HRP on 0.5 μ g of each antibody run on a reducing SDS-PAGE and transblotted to a nitrocellulose membrane showing detection of only the fully human G3 and G1 antibodies

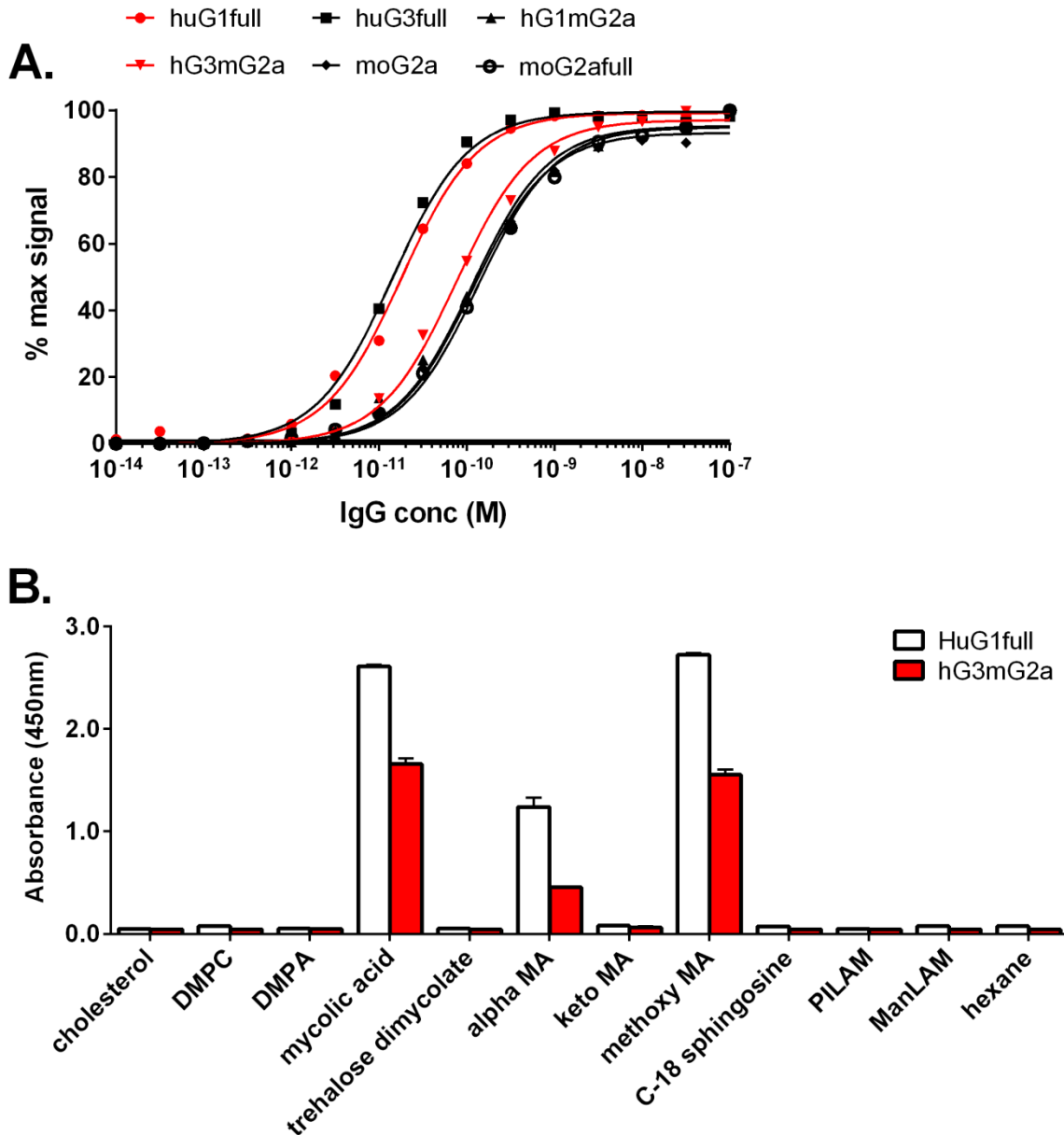


Figure 7-9: Avidity and specificity of engineered chimeric mc3

(A) Serial dilution of IgG against mycolic acid on indirect monoclonal ELISA showing relative affinities of different chimeric constructs. Red lines indicate parental antibody (huG1full) and engineered diagnostic (hG3mG2a). **(B)** Indirect monoclonal ELISA showing specificity of huG1full and the chimeric variant hG3mG2a for mycolic acid extract and methoxy mycolic acid in contrast to cholesterol, membrane lipids, β -hydroxyl lipids and mycobacterial lipids. All antibodies were at $5\mu\text{g/ml}$ concentration and the lipids were coated at $25\mu\text{g/ml}$

7.7 Testing of clinical patient samples for mycolic acid

We then proceeded to test sputum lipid extracts in hexane using the hG3mG2a antibody at the optimized concentration of 5µg/ml to give maximal signal. 100µl and 300µl of lipid extracts were evaporated onto the ELISA in the same manner as that used for testing the purified lipids and bacterial lipid extracts. Although high signals were observed for some of the TB positive samples, these were also obtained for the TB negative samples, despite the use of a short TMB incubation time of 5min (Fig. 7-10). Due to the high background, to obtain high specificity, the resultant cut-off had virtually zero sensitivity of 2.2% based on ROC analysis for the 100µl sample with no significant difference from the false positive rate. No ROC analysis could be carried out for the 300µl sample as the mean of the TB negative was higher than that of the TB positive population.

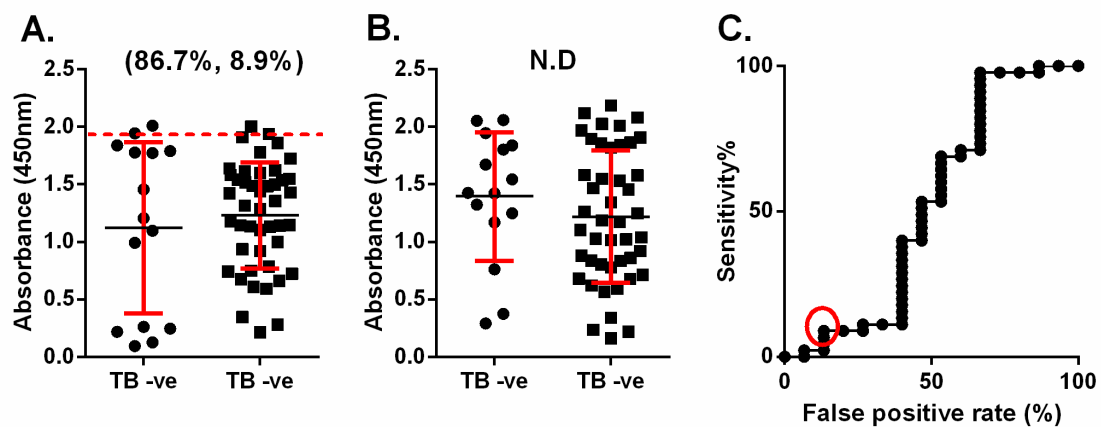


Figure 7-10: Detection of mycolic acid in TB patient sputum

Absorbance values from the optimized mc3 indirect ELISA on TB patients (TB +ve, n=45) and healthy controls (TB -ve, n=15) using **(A)** 100µl sample with 5min TMB incubation **(B)** 300µl sample with 5min TMB incubation. Specificity and sensitivity (L/R) percentages are indicated for chart (A) based on optimal cut-off (red line) as determined by ROC analysis **(C)**. Red circle indicates optimal point for greatest sensitivity with minimum false positive rates to obtain maximum accuracy. Error bars show standard deviation of the sample.

7.8 Discussion

Despite multiple studies, the utility of LAM in urine as a tuberculosis biomarker remains unproven especially in HIV negative cohorts. Limited studies have been carried out on both serum and sputum, but the data available suggest that the challenges are low sensitivity in the former and low specificity in the latter (154,209). Our results on sputum samples also indicate that high background is a potential problem, with significant signals observed in the TB negative cohort when too much sample was used or when the TMB was incubated for too long. This signal was high enough to render the TB negative cohort indistinguishable from the TB positive cohort. However, if a lesser amount of sample was used (100µl) and incubated for only 15min, the strong signal from the TB positive samples was maintained while that from the TB negative cohort was reduced with maximal absorbance values of around 1.35 (Fig. 7-2). This could be due to the specificity of the my2F12 for ManLAM. In contrast, the polyclonal anti-LAM antibodies used in the Clearview test have been shown to generate high absorbance values in TB negative samples greater than 2.0 due to high cross-reactivity for other actinomycetes such as *Nocardia* spp. (154). Thus, our results suggest that my2F12 outperforms the antibody used in that commercial assay.

Our antibody is not specific only for *Mtb*-it can bind LAMs produced by other mycobacterial and actinomycete species provided they have α 1-2 mannose capping motifs and this may be the cause of the high absorbance values observed. This resulted in a high-cut off and a lowered sensitivity rate, which was unable to reach statistical significance when evaluated both as individual patient groups and when

the TB-positive groups were combined. Thus, in spite of the superior specificity of our antibody, sputum may still not be a suitable sample type for LAM biomarker detection by ELISA due to the potential for false positives. Further investigation into the source of the false positive signals observed in our assay e.g. determining the bacterial species responsible or the type of LAM present, would be useful in ascertaining whether sputum is a suitable clinical sample for this assay.

In contrast, in urine and serum, high false positive signals were not observed. This was expected based on previous studies and the lower bacterial burden in these sample types. Serum is a particularly attractive sample type as the likelihood of bacterial contamination is very low and thus has a very low risk of false positives. This allowed for a larger sample volume and long incubation time which served to enhance overall sensitivity to a maximum of 36% while retaining good specificity at 93%, which was statistically significant in contrast to sputum (Fig. 7-3). This result is inferior to an earlier study that used polyclonal antibodies in a coagglutination reaction and a more recent study that used a bispecific detector antibody that bound both LAM and HRP, with 57% and 60% sensitivity respectively and 100% specificity (209,220). However, both studies did not distinguish patients by HIV status. Meta-analysis of studies on urinary LAM diagnostics have indicated that there is a positive correlation between the sensitivity performance of the assay and the percentage of HIV positive individuals in the study cohort, due to the higher levels of LAM secreted in these individuals (13). This may also be the case for detection of LAM in serum and may account for the poorer performance in our study.

In urine, our maximal overall sensitivity attained is 38% with a specificity of 92% which was statistically significant (Fig. 7-4). While this lies within the range of overall assay sensitivities reported previously, meta-analysis of the data suggests that the overall sensitivity of previous urinary LAM assays in the HIV negative cohort is 14% (13). As such, our antibody assay clearly outperforms the commercial polyclonal anti-LAM ELISAs thus far used in these studies. To boost the sensitivity of these assays, more sensitive detection technologies could be applied which may decrease the lower limit of detection for LAM by several orders of magnitude compared to the current sandwich ELISAs in use (221,222). However, with polyclonal antibodies, their broad specificity for all LAM variants could also result in higher false positive rates. This is evidenced by a recent study that sought to improve sensitivity in the polyclonal LAM assay by concentrating urine and hence boosting LAM levels (219). While sensitivity was indeed improved, significant increases in absorbance values in the TB negative cohort was also observed, which could be due to the concentration of contaminating environmental LAM. As our antibody is ManLAM specific, it is thus likely to prove superior to polyclonal antibodies where extremely sensitivity assay technologies are used.

As our TB positive cohort is not a representative sample of the TB positive population but actually a combination of three separate groups, our calculated overall sensitivity is not an exact determination of the assay performance in the field. Nevertheless, it provides a general estimate of the performance of the assay and helped the establishment of optimal assay parameters as one-third smear-negative is similar to that of a typical HIV negative population (52). However, a more detailed analysis of the individual groups within the TB positive cohort will give a more

accurate comparison provided that comparison studies are suitably stratified. It also allows us to determine if this assay can offer improvement over smear microscopy and substitute for culture. While this cannot be carried out for our sputum and serum assays as the data was not stratified, three separate studies on urinary LAM have shown that sensitivity in the smear-negative HIV negative cohort in non-concentrated urine is 0% for all three studies and 8-23.5% in the smear-positive cohort (154,195,219). These results were clearly inferior to smear microscopy. With our antibody, the best sensitivity obtained from an individual assay for smear-negative samples is 33% from testing serum. In a like for like comparison, our urine assay offers a sensitivity of 27% (Fig. 7-5). Although our study was insufficiently powered to statistically differentiate these results from our observed false positive rate, these are significantly different from the 0% rate reported in other studies assuming the same TB-negative sample size.

The advantage of having matched samples is the ability to combine results from various sample types. We have evaluated combinations of either raw absorbance values, or individual test results and the best performance is provided either by combining results from all three sample types or combination of absorbance values of the tests using 100µl serum at 30min incubation and 100µl urine sample at 15min incubation. For comparison of individual TB positive patient groups, the sensitivity in the smear-negative group is 60% or 47% for combination of test results or absorbance values respectively (Table 7-1 and Fig. 7-7). Performance in the smear-positive group is higher at 66-63%. These values are statistically significant and clearly superior to that of the previously published polyclonal ELISA assays on urinary LAM. Higher sensitivity rates in the smear-positive group were

also observed in individual assays, although the difference was not statistically significant for all evaluated results with the exception of the smear 2+ cohort in the serum individual assay which was extremely high at 53.3%. However, this result is expected as smear-positive patients, especially grade 2+ and above, have higher mycobacterial load and as such is likely to carry more LAM in their clinical samples.

The objectives of this study were to determine the utility of my212 sandwich ELISA assay on three different sample types in comparison to previous LAM assays and current TB diagnostics. While it appears to reduce false positive signals in sputum compared to polyclonal LAM antibodies, high background was still observed and further investigation into the cause is required to determine whether this sample type has any diagnostic utility. In serum, our assay appears to be less sensitivity than others previously reported, but the small sample size in earlier studies and the lack of stratification by smear and HIV status prevented an exact comparison. However, as an individual assay, it offers better sensitivity in the smear-negative cohort as compared to previous polyclonal ELISAs targeting urinary LAM. This is also the case if we use a combination of tests including urine. While no combination of test offers us 100% sensitivity in the smear-positive group, we surpass the previously reported sensitivity of polyclonal LAM ELISAs for both smear-negative and positive groups in the HIV negative cohort. As a significant proportion of smear-positive cases remain undetected, our assay in its current format is unsuitable as a direct replacement for smear microscopy. However, it can detect a significant proportion of smear-negative cases, which previous LAM assays could not, and as such could be useful in combination with smear microscopy as a rapid test in place of culture.

In contrast to my2F12, sputum tested with the anti-mycolic acid antibody mc3 showed no difference between TB-positive and TB-negative samples due to the high background/noise of the assay. This is despite the use of a chimeric antibody and an anti-mouse secondary antibody to avoid cross-reactivity with any endogenous antibodies. Although our extraction method was optimized and is similar to that used in previous studies, this was carried out only on bacterial culture and not sputum. Further optimization on sputum will be required in order to produce a cleaner lipid extract that could be used in this assay.

Chapter 8: Discussion & Conclusion

The aim of this thesis was to identify and characterize novel anti-*Mtb* lipid antibodies that could provide superior point-of-care detection of TB infection in resource-limited settings as compared to other methods currently in use or in testing such as smear microscopy or polyclonal anti-LAM ELISA respectively. In comparison to proteins, lipids have not been as extensively explored for their potential as disease biomarkers. On the other hand, multiple studies on a number of TB protein targets have failed to conclusively demonstrate their efficacy in TB diagnosis (8). The rationales behind targeting *Mtb* lipids, in this case LAM and mycolic acid, are their stability to heat and other denaturing agents, as well as their presence in multiple clinical sample types or high abundance in clinical samples respectively. We also aimed to develop a straightforward means of optimizing antibody expression in bacteria to enable low-cost production.

Targeting these lipids using traditional animal immunization methodologies has generally not been successful. In the case of LAM, such methods have not been able to isolate an antibody that is capable of distinguishing ManLAM, the form of LAM produced by *Mtb* and other slow-growing mycobacteria, from LAM produced by other mycobacteria and actinomycetes. This is primarily due to the conservation of the vast majority of the LAM molecule structure between the different variants and all currently described polyclonal and monoclonal anti-LAM molecules appear to bind this conserved structure (83-85,199). This cross-reactivity is the probable cause of the significant false positive rate observed when sample types with high bacterial load e.g. sputum or concentrated samples were used (154,219). We therefore sought to determine if recombinant antibody technology based on antibody phage

display libraries could be used to select ManLAM specific antibodies by driving selection *in vitro* towards the unique α 1-2 mannose caps on this molecule.

In contrast to LAM, mycolic acid is highly insoluble and hard to immunize with *in vivo*. Thus far only a limited number of anti-mycolic acid antibodies have been generated, all using recombinant antibody technology (182). These antibodies are cross-reactive to cholesterol and are of the semi-synthetic scFv format, which may be difficult to express as more stable full length IgG antibodies (184). We had previously optimized a methodology for the isolation of antibodies against insoluble lipids from a Fab phage display library and therefore we aimed to repeat this selection on mycolic acid to identify specific antibodies and test them as full length IgG (10). Our choice of recombinant antibody technology was therefore dictated by the constraints imposed by the nature of the target but also relies on the advantages of phage display selection, which are the independence from the requirement for a strong *in vivo* immune response and the freedom to apply *in vitro* selection techniques not possible in animals.

In order to obtain a ManLAM specific antibody, we modified the basic phage library panning technique to incorporate a negative selection step by first binding to PILAM. This depletes antibody phage that binds the conserved LAM structure but retains those against the α 1-2 mannose structure, which are then positively selected on ManLAM. We showed that this resulted in enrichment of only ManLAM-specific phage and isolated the antibody my2F12 from an enriched pan, it being the only specific sequence present. The rarity of ManLAM specific antibodies in the library suggests that the negative selection was critical to discovery of this antibody and that

in the absence of this step cross-reactive antibodies would have predominated selection. It would be interesting to evaluate whether this method can be replicated for other targets to focus specificity on a small region where there are many other competing epitopes.

Based on the ManLAM cap structure, we expected that α 1-2 mannose would be the principle determinant of the my2F12 epitope. We confirmed this with synthetic carbohydrate arrays, where binding was observed only to oligosaccharides with terminal α 1-2 mannose. We also demonstrated that this specificity is retained on conversion to chimeric antibody via sandwich ELISA and immunofluorescence microscopy. However, this binding specificity does not restrict recognition to only *Mtb* but to the slow-growing group of mycobacteria and also a unique actinomycete species *T. paurometabolum*. Consequently, our antibody is potentially less specific than antibodies and assays that target *Mtb* unique proteins such as ESAT-6, CFP-10 and MPT-64 (44,90). However, it is still more specific than currently described anti-LAM antibodies. Our next step was therefore to determine this antibody would have lower false positive absorbance values in clinical sputum samples.

Despite improved specificity, high signals were still observed in the sputum samples of the TB-negative cohort despite assay optimization to improve signal-to-noise ratio by adjusting assay concentrations, removing cross-reactivity to endogenous antibodies through use of chimeric antibodies and minimising background by optimizing sample volumes and incubation times. This resulted in reduced sensitivity due to elevated absorbance cut offs. Although these absorbance values were lower than that reported using polyclonal anti-LAM antibodies, it is

unclear whether this can be attributed to the better specificity of this antibody or due to differences in assay protocol. Follow up comparisons with the Clearview kit and determination of the source of the high signal (by identification of the bacterial species or LAM variant) in our TB-negative samples will be required to determine if the improved specificity of our antibody confers any diagnostic advantage.

Both the my2F12 human and chimeric variants have very high avidity and can detect LAM down to 0.5ng/ml in PBS or serum in a sandwich ELISA assay, which is comparable to other diagnostic assays for LAM that lack the fine specificity for pathogenic mycobacteria (85,87,209). This superior specificity might be useful for testing urine and sputum, which have low levels of LAM and where extremely low background would be advantageous (209,219). These sample types also have reduced bacterial contamination as compared to sputum and are hence likely to not suffer from high false positive values. In serum, sensitivity was speculated to be affected by endogenous anti-LAM antibodies that inhibit binding of the assay antibodies. A previous study has shown that detection is better in denatured serum but did not prove that anti-LAM antibodies were directly involved (209). In this study, we have shown that the level of anti-LAM antibodies correlates with reduced sensitivity of the assay and that denaturation of anti-LAM antibodies and loss of binding was associated with restored sensitivity.

In urine and denatured serum, high specificity was achieved but sensitivity was limited at up to 38% for the overall TB positive cohort. Significantly however, there was detection of a significant proportion of the smear-negative culture-positive cases (20-33%) and combination of all three assay types or the absorbance values

of serum and urine gave further improvement in sensitivity in this group to 60% or 47% respectively. This indicates that our antibody could complement smear microscopy and potentially substitute for culture by enabling detection of some smear-negative cases, although with the limited sensitivity in the smear-positive cohort it cannot replace microscopy in its current assay format. Although not as sensitive as culture (which is the gold standard to identify smear-negative cases), it can detect a significant proportion of these cases using just serum and urine samples, for which processing and testing is fairly straightforward and can be completed within one day in contrast to culture which requires a minimum of two weeks and can take up to one and a half months (31). This would enable initiation of treatment within one visit and accelerate provision of medical care especially in resource-limited countries where access to even basic facilities is limited.

It might be possible to improve sensitivity further through engineering of higher affinity mutants of my2F12 with the same specificity to enhance signal thus allowing for better discrimination of positive samples and also permit less sample to be used thus reducing non-specific background. Affinity enhancement has been carried out for other diagnostic antibodies against both protein (tumour necrosis factor, *Fusarium graminearum* cell wall protein) and lipid targets (estradiol). This is typically achieved by use of error prone PCR or degenerate primers to introduce random mutations into the antibody variable gene sequence to produce a library of mutated constructs which can then be screened for higher affinity mutants (224-226). *Mtb* is also unique in that it reportedly carried an additional molecule, 5-methylthiopentose at the tip of its ManLAM caps (196). This offers the opportunity to create a *Mtb* specific antibody by targeting the complete ManLAM-pentose motif,

using the same negative depletion technique described earlier but using ManLAM sourced from another slow-growing mycobacterial species, which lacks this molecule, as the depleting antigen. This could be carried out if further testing on clinical samples indicates that cross-reactivity to other slow-growing mycobacterial species, resulting in high false positive rates, is a significant issue.

Previous studies on clinical urine samples with the polyclonal anti-LAM indicated that they were unable to detect any smear-negative cases type in the HIV negative cohort and had inferior sensitivity in the smear-positive cohort (154,195,219). As such, our anti-LAM antibody appears to have superior performance as compared to current urinary LAM assays. It remains unclear as to whether this can be attributed solely to high avidity or whether ManLAM specificity had a role to play by giving very low background values. Again, comparison with the Clearview diagnostic kit would be useful in determining this. As LAM excretion in urine appears to be elevated in the HIV positive cohort, a trial of our assay might demonstrate even superior sensitivity to the current tests available. While HIV patients do not comprise the majority of TB patients, they are a significant minority at 13% globally and would benefit greatly from improved diagnostics (1).

We have also isolated four mycolic acid-specific antibodies using a panning strategy for isolation of antibodies against insoluble lipids. These antibodies all preferentially detect methoxy mycolic acid and one (mc3) was found to be specific for mycobacterial mycolic acid with no binding to *T. paurometabolum* and *N. cyriacigeorgica* mycolic extract in contrast to my2F12. Given the earlier high background observed with my2F12, this specificity might be critical in ensuring

accurate diagnosis with sputum samples. Its preferential avidity for methoxy mycolic acid is also likely to give it better specificity in comparison to my2F12 which detects all slow-growing mycobacteria, as only a limited number of slow-growing mycobacterial species, including *Mtb*, express this mycolic acid subtype (48). In contrast to its high specificity when tested on bacterial lipid extracts, extremely high absorbance signal was observed in the TB-negative cohort. This was despite use of the chimeric variant of mc3 to eliminate the risk of background from endogenous antibodies. This could be due to the presence of mycolic acid from a non-tuberculous source, especially alpha mycolic acid which is ubiquitous among mycobacteria, but is unlikely given that the sputum samples were all mycobacterial culture and smear negative, which have limits of detection of 10 and 5000 bacilli/ml respectively. Alternatively, there could be cross-reactivity to another antigen present in the sample that was not tested for in the earlier characterization. Mass spectrometry might be able to identify what these are and help determine a strategy for separation of these from the mycolic acid biomarker. If there is indeed alpha mycolic acid or another lipid present that causes cross-reactivity, re-panning of the library could be carried out to produce an antibody with no cross-reactivity to these above lipids. This could be accomplished either using negative depletion as described for the anti-ManLAM antibody selection and/or selection using synthetic methoxy mycolic acid alone instead of purified *Mtb* mycolic acid.

In the course of optimizing our antibody, we have developed various chimeric constructs to switch the Fc constant region from human to mouse. Comparison of the binding avidity of the various constructs for both my2F12 and mc3 have indicated a pattern of higher affinity when the human G1 hinge was replaced with the G3 hinge

and a reduction in affinity when the human constant regions were replaced with murine constant regions. Importantly, no change in specificity was observed for either antibody in the course of conversion, as previous studies had indicated that alterations of the constant region can influence specificity (212). It would therefore be interesting to evaluate if an avidity increase without a change in specificity could be obtained by using our hG3mG2a construct on a variety of antigens such as proteins along with lipids. This is deserving of further investigation as recombinant antibody technology is likely to make the isolation of human antibodies increasingly common; conversion of these antibodies to a chimeric format would be required for diagnostic use and ideally with minimal loss of specificity and avidity. Thus far, conversion of murine antibodies to chimeric antibodies with different human isotypes indicated that the substitution with the G1 isotype gave higher affinity as compared to the G3 isotype (207). However, this result may not be comparable as it involved the substitution of murine constant regions with human ones, while in this study the opposite was carried out. Interestingly, we also showed that G3 was less efficient as compared to G1 at capturing antigen. This effect has been observed previously with a human anti-HIV gp120 and could be another general characteristic of this isotype (223).

We have also identified various straightforward solutions for improving antibody expression yields in *E. coli*, namely through reducing translational levels via reducing inducer concentrations and delayed induction. We have characterized the effects of these modifications and our findings suggest that the improvement in overall yield is due to two separate mechanisms, increase in wet cell mass and unit yield. Despite these improvements, antibody yields especially with our target

antibody my2F12 were too low for the method to be practicable. As such, we had to rely on mammalian cell culture to produce the required antibodies. However, based on optimized assay concentrations, we will not require more than 0.5µg/well of detector antibody and 1µg/well of capture antibody if 100µl sample volumes are used, therefore 1mg of antibody can be used for 1000 tests and should not be prohibitively costly even if produced by mammalian cell culture.

In summary, during the course of this study, we have generated and characterized two highly-specific, high avidity recombinant antibodies against LAM and mycolic acid, my2F12 and mc3 respectively. Isolation of these antibodies required the use of techniques only possible *in vitro* and it is highly likely that such antibodies would be difficult to obtain using traditional immunization techniques. While promising, mc3 gave extremely high background on TB-negative sputum samples and further optimization of the assay will be required. Crucially, my2F12 is able to identify TB patients in the HIV negative, smear-negative cohort. These could previously only be identified through NAATs or culture, both of which have significant drawbacks in resource-limited settings. To confirm its suitability for TB diagnosis and further delineate its sensitivity rates in various patient groups, a follow up clinical trial should be carried out with a larger patient cohort and with side-by-side comparison to current state of the art polyclonal LAM ELISAs, sputum microscopy and culture.

Bibliography

1. WHO. *Global Tuberculosis Report 2012*. Geneva. 2012.
2. Lawn SD, Zumla AI. Tuberculosis. *Lancet*. Jul 2 2011;378(9785):57-72.
3. Paige C, Bishai WR. Penitentiary or penthouse condo: the tuberculous granuloma from the microbe's point of view. *Cellular microbiology*. Mar 2010;12(3):301-309.
4. Zumla A, Raviglione M, Hafner R, von Reyn CF. Tuberculosis. *The New England journal of medicine*. Feb 21 2013;368(8):745-755.
5. Parrish NM, Carroll KC. Role of the clinical mycobacteriology laboratory in diagnosis and management of tuberculosis in low-prevalence settings. *Journal of clinical microbiology*. Mar 2011;49(3):772-776.
6. Taylor Z, Nolan CM, Blumberg HM. Controlling tuberculosis in the United States. Recommendations from the American Thoracic Society, CDC, and the Infectious Diseases Society of America. *MMWR. Recommendations and reports : Morbidity and mortality weekly report. Recommendations and reports / Centers for Disease Control*. Nov 4 2005;54(RR-12):1-81.
7. Keeler E, Perkins MD, Small P, Hanson C, Reed S, Cunningham J, Aledort JE, Hillborne L, Rafael ME, Girosi F, Dye C. Reducing the global burden of tuberculosis: the contribution of improved diagnostics. *Nature*. Nov 23 2006;444 Suppl 1:49-57.
8. Flores LL, Steingart KR, Dendukuri N, Schiller I, Minion J, Pai M, Ramsay A, Henry M, Laal S. Systematic review and meta-analysis of antigen detection tests for the diagnosis of tuberculosis. *Clinical and vaccine immunology : CVI*. Oct 2011;18(10):1616-1627.
9. Singh KV, Kaur J, Varshney GC, Raje M, Suri CR. Synthesis and characterization of hapten-protein conjugates for antibody production against small molecules. *Bioconjug Chem*. Jan-Feb 2004;15(1):168-173.
10. Islam MO, Lim YT, Chan CE, Cazenave-Gassiot A, Croxford JL, Wenk MR, Macary PA, Hanson BJ. Generation and characterization of a novel

- recombinant antibody against 15-ketocholestane isolated by phage-display. *Int J Mol Sci.* 2012;13(4):4937-4948.
11. de Haard HJ, van Neer N, Reurs A, Hufton SE, Roovers RC, Henderikx P, de Bruine AP, Arends JW, Hoogenboom HR. A large non-immunized human Fab fragment phage library that permits rapid isolation and kinetic analysis of high affinity antibodies. *The Journal of biological chemistry.* Jun 25 1999;274(26):18218-18230.
 12. Shui G, Bendt AK, Jappara IA, Lim HM, Laneelle M, Herve M, Via LE, Chua GH, Bratschi MW, Zainul Rahim SZ, Michelle AL, Hwang SH, Lee JS, Eum SY, Kwak HK, Daffe M, Dartois V, Michel G, Barry CE, 3rd, Wenk MR. Mycolic acids as diagnostic markers for tuberculosis case detection in humans and drug efficacy in mice. *EMBO molecular medicine.* Jan 2012;4(1):27-37.
 13. Minion J, Leung E, Talbot E, Dheda K, Pai M, Menzies D. Diagnosing tuberculosis with urine lipoarabinomannan: systematic review and meta-analysis. *The European respiratory journal : official journal of the European Society for Clinical Respiratory Physiology.* Dec 2011;38(6):1398-1405.
 14. Daniel TM. The history of tuberculosis. *Respiratory medicine.* Nov 2006;100(11):1862-1870.
 15. Jarzembowski JA, Young MB. Nontuberculous mycobacterial infections. *Archives of pathology & laboratory medicine.* Aug 2008;132(8):1333-1341.
 16. Johnson MM, Waller EA, Leventhal JP. Nontuberculous mycobacterial pulmonary disease. *Current opinion in pulmonary medicine.* May 2008;14(3):203-210.
 17. Sasaki S, Takeshita F, Okuda K, Ishii N. Mycobacterium leprae and leprosy: a compendium. *Microbiology and immunology.* 2001;45(11):729-736.
 18. Shinnick TM, Good RC. Mycobacterial taxonomy. *European journal of clinical microbiology & infectious diseases : official publication of the European Society of Clinical Microbiology.* Nov 1994;13(11):884-901.

19. Pieters J. Mycobacterium tuberculosis and the macrophage: maintaining a balance. *Cell host & microbe*. Jun 12 2008;3(6):399-407.
20. Ramakrishnan L. Revisiting the role of the granuloma in tuberculosis. *Nature reviews. Immunology*. May 2012;12(5):352-366.
21. Andrews JR, Noubary F, Walensky RP, Cerda R, Losina E, Horsburgh CR. Risk of progression to active tuberculosis following reinfection with Mycobacterium tuberculosis. *Clinical infectious diseases : an official publication of the Infectious Diseases Society of America*. Mar 2012;54(6):784-791.
22. Ernst JD. The immunological life cycle of tuberculosis. *Nature reviews. Immunology*. Aug 2012;12(8):581-591.
23. Mitchison D, Davies G. The chemotherapy of tuberculosis: past, present and future. *The international journal of tuberculosis and lung disease : the official journal of the International Union against Tuberculosis and Lung Disease*. Jun 2012;16(6):724-732.
24. Caminero JA, Sotgiu G, Zumla A, Migliori GB. Best drug treatment for multidrug-resistant and extensively drug-resistant tuberculosis. *The Lancet infectious diseases*. Sep 2010;10(9):621-629.
25. Jassal M, Bishai WR. Extensively drug-resistant tuberculosis. *The Lancet infectious diseases*. Jan 2009;9(1):19-30.
26. Kaufmann SH. Fact and fiction in tuberculosis vaccine research: 10 years later. *The Lancet infectious diseases*. Aug 2011;11(8):633-640.
27. Trunz BB, Fine P, Dye C. Effect of BCG vaccination on childhood tuberculous meningitis and miliary tuberculosis worldwide: a meta-analysis and assessment of cost-effectiveness. *Lancet*. Apr 8 2006;367(9517):1173-1180.
28. Colditz GA, Brewer TF, Berkey CS, Wilson ME, Burdick E, Fineberg HV, Mosteller F. Efficacy of BCG vaccine in the prevention of tuberculosis. Meta-analysis of the published literature. *JAMA : the journal of the American Medical Association*. Mar 2 1994;271(9):698-702.

29. Brandt L, Feino Cunha J, Weinreich Olsen A, Chilima B, Hirsch P, Appelberg R, Andersen P. Failure of the *Mycobacterium bovis* BCG vaccine: some species of environmental mycobacteria block multiplication of BCG and induction of protective immunity to tuberculosis. *Infection and immunity*. Feb 2002;70(2):672-678.
30. Black GF, Weir RE, Floyd S, Bliss L, Warndorff DK, Crampin AC, Ngwira B, Sichali L, Nazareth B, Blackwell JM, Branson K, Chaguluka SD, Donovan L, Jarman E, King E, Fine PE, Dockrell HM. BCG-induced increase in interferon-gamma response to mycobacterial antigens and efficacy of BCG vaccination in Malawi and the UK: two randomised controlled studies. *Lancet*. Apr 20 2002;359(9315):1393-1401.
31. WHO. Diagnostics for Tuberculosis: Global demand and market potential: WHO 2006.
32. Tiemersma EW, van der Werf MJ, Borgdorff MW, Williams BG, Nagelkerke NJ. Natural history of tuberculosis: duration and fatality of untreated pulmonary tuberculosis in HIV negative patients: a systematic review. *PloS one*. 2011;6(4):e17601.
33. Bassili A, Al-Hammadi A, Al-Absi A, Glaziou P, Seita A, Abubakar I, Bierrenbach AL, van Hest NA. Estimating the tuberculosis burden in resource-limited countries: a capture-recapture study in Yemen. *The international journal of tuberculosis and lung disease : the official journal of the International Union against Tuberculosis and Lung Disease*. Apr 2013;17(4):456-461.
34. Reid MJ, Shah NS. Approaches to tuberculosis screening and diagnosis in people with HIV in resource-limited settings. *The Lancet infectious diseases*. Mar 2009;9(3):173-184.
35. Hopewell PC, Pai M, Maher D, Uplekar M, Raviglione MC. International standards for tuberculosis care. *The Lancet infectious diseases*. Nov 2006;6(11):710-725.

36. American Thoracic Society/Centers for Disease Control and Prevention/Infectious Diseases Society of America. Controlling tuberculosis in the United States. *American journal of respiratory and critical care medicine*. Nov 1 2005;172(9):1169-1227.
37. National Institute for Health and Clinical Excellence. *Tuberculosis: Clinical Diagnosis and Management of Tuberculosis, and Measures for Its Prevention and Control*. London: National Institute for Health and Clinical Excellence; 2011.
38. WHO. Use of tuberculosis interferon-gamma release assays (IGRAs) in low- and middle-income countries. Policy Statement. 2011.
39. Toman K, Frieden, T., Toman, K., & World Health Organization. *Toman's tuberculosis: Case detection, treatment, and monitoring : questions and answers*. Geneva: World Health Organization; 2004.
40. Nagpaul DR NN, Prakash M. Diagnostic photofluorography and sputum microscopy in tuberculosis case findings. *Proceedings of the 9th Eastern Region Tuberculosis Conference and 29th National Conference on Tuberculosis and Chest Diseases*. Delhi, India: Tuberculosis Association of India; 1974.
41. Trajman A, Steffen RE, Menzies D. Interferon-Gamma Release Assays versus Tuberculin Skin Testing for the Diagnosis of Latent Tuberculosis Infection: An Overview of the Evidence. *Pulmonary medicine*. 2013;2013:601737.
42. Trebucq A, Enarson DA, Chiang CY, Van Deun A, Harries AD, Boillot F, Detjen A, Fujiwara PI, Graham SM, Monedero I, Rusen ID, Rieder HL. Xpert(R) MTB/RIF for national tuberculosis programmes in low-income countries: when, where and how? *The international journal of tuberculosis and lung disease : the official journal of the International Union against Tuberculosis and Lung Disease*. Dec 2011;15(12):1567-1572.
43. Markowitz N, Hansen NI, Wilcosky TC, Hopewell PC, Glassroth J, Kvale PA, Mangura BT, Osmond D, Wallace JM, Rosen MJ, Reichman LB. Tuberculin

- and anergy testing in HIV-seropositive and HIV-seronegative persons. Pulmonary Complications of HIV Infection Study Group. *Annals of internal medicine*. Aug 1 1993;119(3):185-193.
44. Achkar JM, Lawn SD, Moosa MY, Wright CA, Kasprovicz VO. Adjunctive tests for diagnosis of tuberculosis: serology, ELISPOT for site-specific lymphocytes, urinary lipoarabinomannan, string test, and fine needle aspiration. *The Journal of infectious diseases*. Nov 15 2011;204 Suppl 4:S1130-1141.
45. Pai M, Zwerling A, Menzies D. Systematic review: T-cell-based assays for the diagnosis of latent tuberculosis infection: an update. *Annals of internal medicine*. Aug 5 2008;149(3):177-184.
46. Santha T, Garg R, Subramani R, Chandrasekaran V, Selvakumar N, Sisodia RS, Perumal M, Sinha SK, Singh RJ, Chavan R, Ali F, Sarma SK, Sharma KM, Jagtap RD, Frieden TR, Fabio L, Narayanan PR. Comparison of cough of 2 and 3 weeks to improve detection of smear-positive tuberculosis cases among out-patients in India. *The international journal of tuberculosis and lung disease : the official journal of the International Union against Tuberculosis and Lung Disease*. Jan 2005;9(1):61-68.
47. Rastogi N, Legrand E, Sola C. The mycobacteria: an introduction to nomenclature and pathogenesis. *Rev Sci Tech*. Apr 2001;20(1):21-54.
48. Barry CE, 3rd, Lee RE, Mdluli K, Sampson AE, Schroeder BG, Slayden RA, Yuan Y. Mycolic acids: structure, biosynthesis and physiological functions. *Progress in lipid research*. Jul-Aug 1998;37(2-3):143-179.
49. Liu J, Sun ZQ, Pei H, Zhang SL, Wilson S, De Smet K, Cerullakandiyil N, Thayyullathil T, Al-Suwaidi Z, Song YZ. Increased case finding of tuberculosis from sputum and sputum deposits after magnetic bead concentration of mycobacteria. *Journal of microbiological methods*. Mar 15 2013;93(2):144-147.
50. Wilson S, Lane A, Rosedale R, Stanley C. Concentration of Mycobacterium tuberculosis from sputum using ligand-coated magnetic beads. *The*

- international journal of tuberculosis and lung disease : the official journal of the International Union against Tuberculosis and Lung Disease*. Sep 2010;14(9):1164-1168.
51. Steingart KR, Ng V, Henry M, Hopewell PC, Ramsay A, Cunningham J, Urbanczik R, Perkins MD, Aziz MA, Pai M. Sputum processing methods to improve the sensitivity of smear microscopy for tuberculosis: a systematic review. *The Lancet infectious diseases*. Oct 2006;6(10):664-674.
 52. Elliott AM, Namaambo K, Allen BW, Luo N, Hayes RJ, Pobee JO, McAdam KP. Negative sputum smear results in HIV-positive patients with pulmonary tuberculosis in Lusaka, Zambia. *Tuber Lung Dis*. Jun 1993;74(3):191-194.
 53. Idigoras P, Beristain X, Iturzaeta A, Vicente D, Perez-Trallero E. Comparison of the automated nonradiometric Bactec MGIT 960 system with Lowenstein-Jensen, Coletsos, and Middlebrook 7H11 solid media for recovery of mycobacteria. *European journal of clinical microbiology & infectious diseases : official publication of the European Society of Clinical Microbiology*. May 2000;19(5):350-354.
 54. Lee JJ, Suo J, Lin CB, Wang JD, Lin TY, Tsai YC. Comparative evaluation of the BACTEC MGIT 960 system with solid medium for isolation of mycobacteria. *The international journal of tuberculosis and lung disease : the official journal of the International Union against Tuberculosis and Lung Disease*. Jun 2003;7(6):569-574.
 55. Shah NS, Moodley P, Babaria P, Moodley S, Ramtahal M, Richardson J, Heysell S, Li X, Moll A, Friedland G, Sturm AW, Gandhi NR. Rapid diagnosis of tuberculosis and multidrug resistance by the microscopic-observation drug-susceptibility assay. *American journal of respiratory and critical care medicine*. May 15 2011;183(10):1427-1433.
 56. Oberhelman RA, Soto-Castellares G, Gilman RH, Caviedes L, Castillo ME, Kolevic L, Del Pino T, Saito M, Salazar-Lindo E, Negron E, Montenegro S, Laguna-Torres VA, Moore DA, Evans CA. Diagnostic approaches for paediatric tuberculosis by use of different specimen types, culture methods,

- and PCR: a prospective case-control study. *The Lancet infectious diseases*. Sep 2010;10(9):612-620.
57. Traore H, van Deun A, Shamputa IC, Rigouts L, Portaels F. Direct detection of Mycobacterium tuberculosis complex DNA and rifampin resistance in clinical specimens from tuberculosis patients by line probe assay. *Journal of clinical microbiology*. Dec 2006;44(12):4384-4388.
 58. Teo J, Jureen R, Chiang D, Chan D, Lin R. Comparison of two nucleic acid amplification assays, the Xpert MTB/RIF assay and the amplified Mycobacterium Tuberculosis Direct assay, for detection of Mycobacterium tuberculosis in respiratory and nonrespiratory specimens. *Journal of clinical microbiology*. Oct 2011;49(10):3659-3662.
 59. Kambashi B, Mbulo G, McNerney R, Tembwe R, Kambashi A, Tihon V, Godfrey-Faussett P. Utility of nucleic acid amplification techniques for the diagnosis of pulmonary tuberculosis in sub-Saharan Africa. *The international journal of tuberculosis and lung disease : the official journal of the International Union against Tuberculosis and Lung Disease*. Apr 2001;5(4):364-369.
 60. Soo PC, Horng YT, Hsueh PR, Shen BJ, Wang JY, Tu HH, Wei JR, Hsieh SC, Huang CC, Lai HC. Direct and simultaneous identification of Mycobacterium tuberculosis complex (MTBC) and Mycobacterium tuberculosis (MTB) by rapid multiplex nested PCR-ICT assay. *Journal of microbiological methods*. Sep 2006;66(3):440-448.
 61. O'Grady J, Maeurer M, Mwaba P, Kapata N, Bates M, Hoelscher M, Zumla A. New and improved diagnostics for detection of drug-resistant pulmonary tuberculosis. *Current opinion in pulmonary medicine*. May 2011;17(3):134-141.
 62. WHO. Molecular Line Probe Assays for rapid screening of patients at risk of Multi-Drug Resistant Tuberculosis (MDR-TB). Policy Statement. 2008.
 63. Lawn SD, Mwaba P, Bates M, Piatek A, Alexander H, Marais BJ, Cuevas LE, McHugh TD, Zijenah L, Kapata N, Abubakar I, McNerney R, Hoelscher M,

- Memish ZA, Migliori GB, Kim P, Maeurer M, Schito M, Zumla A. Advances in tuberculosis diagnostics: the Xpert MTB/RIF assay and future prospects for a point-of-care test. *The Lancet infectious diseases*. Apr 2013;13(4):349-361.
64. Boehme CC, Nicol MP, Nabeta P, Michael JS, Gotuzzo E, Tahirli R, Gler MT, Blakemore R, Worodria W, Gray C, Huang L, Caceres T, Mehdiyev R, Raymond L, Whitelaw A, Sagadevan K, Alexander H, Albert H, Cobelens F, Cox H, Alland D, Perkins MD. Feasibility, diagnostic accuracy, and effectiveness of decentralised use of the Xpert MTB/RIF test for diagnosis of tuberculosis and multidrug resistance: a multicentre implementation study. *Lancet*. Apr 30 2011;377(9776):1495-1505.
65. Helb D, Jones M, Story E, Boehme C, Wallace E, Ho K, Kop J, Owens MR, Rodgers R, Banada P, Safi H, Blakemore R, Lan NT, Jones-Lopez EC, Levi M, Burday M, Ayakaka I, Mugerwa RD, McMillan B, Winn-Deen E, Christel L, Dailey P, Perkins MD, Persing DH, Alland D. Rapid detection of *Mycobacterium tuberculosis* and rifampin resistance by use of on-demand, near-patient technology. *Journal of clinical microbiology*. Jan 2010;48(1):229-237.
66. Barnard M, Gey van Pittius NC, van Helden PD, Bosman M, Coetzee G, Warren RM. The diagnostic performance of the GenoType MTBDRplus version 2 line probe assay is equivalent to that of the Xpert MTB/RIF assay. *Journal of clinical microbiology*. Nov 2012;50(11):3712-3716.
67. Scott LE, McCarthy K, Gous N, Nduna M, Van Rie A, Sanne I, Venter WF, Duse A, Stevens W. Comparison of Xpert MTB/RIF with other nucleic acid technologies for diagnosing pulmonary tuberculosis in a high HIV prevalence setting: a prospective study. *PLoS medicine*. Jul 2011;8(7):e1001061.
68. Lawn SD, Zumla AI. Diagnosis of extrapulmonary tuberculosis using the Xpert((R)) MTB/RIF assay. *Expert review of anti-infective therapy*. Jun 2012;10(6):631-635.
69. Pantoja A, Fitzpatrick C, Vassall A, Weyer K, Floyd K. Xpert MTB/RIF for diagnosis of TB and drug-resistant TB: a cost and affordability analysis. *The*

European respiratory journal : official journal of the European Society for Clinical Respiratory Physiology. Dec 20 2012.

70. Hooja S, Pal N, Malhotra B, Goyal S, Kumar V, Vyas L. Comparison of Ziehl Neelsen & Auramine O staining methods on direct and concentrated smears in clinical specimens. *The Indian journal of tuberculosis.* Apr 2011;58(2):72-76.
71. Habtamu M, van den Boogaard J, Ndarro A, Buretta R, Irongo CF, Lega DA, Nyombi BM, Kibiki GS. Light-emitting diode with various sputum smear preparation techniques to diagnose tuberculosis. *The international journal of tuberculosis and lung disease : the official journal of the International Union against Tuberculosis and Lung Disease.* 2012;16(3):402-407.
72. Cattamanchi A, Huang L, Worodria W, den Boon S, Kalema N, Katagira W, Byanyima P, Yoo S, Matovu J, Hopewell PC, Davis JL. Integrated strategies to optimize sputum smear microscopy: a prospective observational study. *American journal of respiratory and critical care medicine.* Feb 15 2011;183(4):547-551.
73. Davis JL, Cattamanchi A, Cuevas LE, Hopewell PC, Steingart KR. Diagnostic accuracy of same-day microscopy versus standard microscopy for pulmonary tuberculosis: a systematic review and meta-analysis. *The Lancet infectious diseases.* Feb 2013;13(2):147-154.
74. Peterson EM. ELISA: a tool for the clinical microbiologist. *The American journal of medical technology.* Nov 1981;47(11):905-908.
75. Steingart KR, Henry M, Laal S, Hopewell PC, Ramsay A, Menzies D, Cunningham J, Weldingh K, Pai M. Commercial serological antibody detection tests for the diagnosis of pulmonary tuberculosis: a systematic review. *PLoS medicine.* Jun 2007;4(6):e202.
76. WHO. Commercial Serodiagnostic Tests for Diagnosis of Tuberculosis. Policy Statement. 2011.

77. Brust B, Lecoufle M, Tuailon E, Dedieu L, Canaan S, Valverde V, Kremer L. Mycobacterium tuberculosis lipolytic enzymes as potential biomarkers for the diagnosis of active tuberculosis. *PloS one*. 2011;6(9):e25078.
78. Ireton GC, Greenwald R, Liang H, Esfandiari J, Lyashchenko KP, Reed SG. Identification of Mycobacterium tuberculosis antigens of high serodiagnostic value. *Clinical and vaccine immunology : CVI*. Oct 2010;17(10):1539-1547.
79. Jordan WJ. Enzyme-Linked Immunosorbent Assay. In: J. M. Walker RR, ed. *Medical Biomethods Handbook*. Totowa, NJ, USA: Humana Press, Inc. ; 2005:419-427.
80. Diaz-Gonzalez M, Gonzalez-Garcia MB, Costa-Garcia A. Immunosensor for Mycobacterium tuberculosis on screen-printed carbon electrodes. *Biosensors & bioelectronics*. Apr 15 2005;20(10):2035-2043.
81. Purohit MR, Mustafa T, Wiker HG, Sviland L. Rapid diagnosis of tuberculosis in aspirate, effusions, and cerebrospinal fluid by immunocytochemical detection of Mycobacterium tuberculosis complex specific antigen MPT64. *Diagn Cytopathol*. Sep 2012;40(9):782-791.
82. Cho SN, Shin JS, Kim JD, Chong Y. Production of monoclonal antibodies to lipoarabinomannan-B and use in the detection of mycobacterial antigens in sputum. *Yonsei Med J*. Dec 1990;31(4):333-338.
83. Tessema TA, Hamasur B, Bjun G, Svenson S, Bjorvatn B. Diagnostic evaluation of urinary lipoarabinomannan at an Ethiopian tuberculosis centre. *Scand J Infect Dis*. 2001;33(4):279-284.
84. Pereira Arias-Bouda LM, Nguyen LN, Ho LM, Kuijper S, Jansen HM, Kolk AH. Development of antigen detection assay for diagnosis of tuberculosis using sputum samples. *Journal of clinical microbiology*. Jun 2000;38(6):2278-2283.
85. Boehme C, Molokova E, Minja F, Geis S, Loscher T, Maboko L, Koulchin V, Hoelscher M. Detection of mycobacterial lipoarabinomannan with an antigen-capture ELISA in unprocessed urine of Tanzanian patients with suspected tuberculosis. *Trans R Soc Trop Med Hyg*. Dec 2005;99(12):893-900.

86. Araj GF, Fahmawi BH, Chugh TD, Abu-Salim M. Improved detection of mycobacterial antigens in clinical specimens by combined enzyme-linked immunosorbent assay. *Diagn Microbiol Infect Dis*. Aug-Sep 1993;17(2):119-127.
87. Hamasur B, Bruchfeld J, Haile M, Pawlowski A, Bjorvatn B, Kallenius G, Svenson SB. Rapid diagnosis of tuberculosis by detection of mycobacterial lipoarabinomannan in urine. *Journal of microbiological methods*. May 2001;45(1):41-52.
88. Ben-Selma W, Harizi H, Boukadida J. Immunochromatographic IgG/IgM test for rapid diagnosis of active tuberculosis. *Clinical and vaccine immunology : CVI*. Dec 2011;18(12):2090-2094.
89. Chowdhury IH, Sen A, Bahar B, Hazra A, Chakraborty U, Choudhuri S, Goswami A, Pal NK, Bhattacharya B. A molecular approach to identification and profiling of first-line-drug-resistant mycobacteria from sputum of pulmonary tuberculosis patients. *Journal of clinical microbiology*. Jun 2012;50(6):2082-2084.
90. Liu Z, Zhu C, Yang H, Hu H, Feng Y, Qin L, Cui Z, Bi A, Zheng R, Jin R, Fan L, Hu Z. Clinical value of ELISA-MPT64 for the diagnosis of tuberculous pleurisy. *Current microbiology*. Sep 2012;65(3):313-318.
91. Boehme CC, Nabeta P, Henostroza G, Raqib R, Rahim Z, Gerhardt M, Sanga E, Hoelscher M, Notomi T, Hase T, Perkins MD. Operational feasibility of using loop-mediated isothermal amplification for diagnosis of pulmonary tuberculosis in microscopy centers of developing countries. *Journal of clinical microbiology*. Jun 2007;45(6):1936-1940.
92. Aryan E, Makvandi M, Farajzadeh A, Huygen K, Alvandi AH, Gouya MM, Sadrizadeh A, Romano M. Clinical value of IS6110-based loop-mediated isothermal amplification for detection of Mycobacterium tuberculosis complex in respiratory specimens. *The Journal of infection*. Mar 4 2013.
93. Geojith G, Dhanasekaran S, Chandran SP, Kenneth J. Efficacy of loop mediated isothermal amplification (LAMP) assay for the laboratory

- identification of Mycobacterium tuberculosis isolates in a resource limited setting. *Journal of microbiological methods*. Jan 2011;84(1):71-73.
94. Bruins M, Rahim Z, Bos A, van de Sande WW, Endtz HP, van Belkum A. Diagnosis of active tuberculosis by e-nose analysis of exhaled air. *Tuberculosis (Edinburgh, Scotland)*. Mar 2013;93(2):232-238.
 95. Matsuura E, Hughes GR, Khamashta MA. Oxidation of LDL and its clinical implication. *Autoimmun Rev*. Jul 2008;7(7):558-566.
 96. Pyragius CE, Fuller M, Ricciardelli C, Oehler MK. Aberrant lipid metabolism: an emerging diagnostic and therapeutic target in ovarian cancer. *Int J Mol Sci*. 2013;14(4):7742-7756.
 97. Jovanovic V, Abdul Aziz N, Lim YT, Ng Ai Poh A, Jin Hui Chan S, Ho Xin Pei E, Lew FC, Shui G, Jenner AM, Bowen L, McKinney EF, Lyons PA, Kemeny MD, Smith KG, Wenk MR, Macary PA. Lipid anti-lipid antibody responses correlate with disease activity in systemic lupus erythematosus. *PloS one*. 2013;8(2):e55639.
 98. Wenk MR. The emerging field of lipidomics. *Nat Rev Drug Discov*. Jul 2005;4(7):594-610.
 99. Kohler G, Milstein C. Continuous cultures of fused cells secreting antibody of predefined specificity. *Nature*. Aug 7 1975;256(5517):495-497.
 100. Ramiscal RR, Vinuesa CG. T-cell subsets in the germinal center. *Immunological reviews*. Mar 2013;252(1):146-155.
 101. Wassef NM, Roerdink F, Swartz GM, Jr., Lyon JA, Berson BJ, Alving CR. Phosphate-binding specificities of monoclonal antibodies against phosphoinositides in liposomes. *Molecular immunology*. Oct 1984;21(10):863-868.
 102. Schuster BG, Neidig M, Alving BM, Alving CR. Production of antibodies against phosphocholine, phosphatidylcholine, sphingomyelin, and lipid A by injection of liposomes containing lipid A. *J Immunol*. Mar 1979;122(3):900-905.

103. Richards RL, Aronson J, Schoenbechler M, Diggs CL, Alving CR. Antibodies reactive with liposomal phospholipids are produced during experimental *Trypanosoma rhodesiense* infections in rabbits. *J Immunol.* Mar 1983;130(3):1390-1394.
104. Muller-Loennies S, Brade L, Brade H. Neutralizing and cross-reactive antibodies against enterobacterial lipopolysaccharide. *Int J Med Microbiol.* Sep 2007;297(5):321-340.
105. Kuhn HM. Cross-reactivity of monoclonal antibodies and sera directed against lipid A and lipopolysaccharides. *Infection.* May-Jun 1993;21(3):179-186.
106. Swartz GM, Jr., Gentry MK, Amende LM, Blanchette-Mackie EJ, Alving CR. Antibodies to cholesterol. *Proceedings of the National Academy of Sciences of the United States of America.* Mar 1988;85(6):1902-1906.
107. McCafferty J, Griffiths AD, Winter G, Chiswell DJ. Phage antibodies: filamentous phage displaying antibody variable domains. *Nature.* Dec 6 1990;348(6301):552-554.
108. Ho M, Nagata S, Pastan I. Isolation of anti-CD22 Fv with high affinity by Fv display on human cells. *Proceedings of the National Academy of Sciences of the United States of America.* Jun 20 2006;103(25):9637-9642.
109. Hoogenboom HR. Selecting and screening recombinant antibody libraries. *Nat Biotechnol.* Sep 2005;23(9):1105-1116.
110. Mazor Y, Van Blarcom T, Mabry R, Iverson BL, Georgiou G. Isolation of engineered, full-length antibodies from libraries expressed in *Escherichia coli*. *Nat Biotechnol.* May 2007;25(5):563-565.
111. Knappik A, Ge L, Honegger A, Pack P, Fischer M, Wellnhofer G, Hoess A, Wolle J, Pluckthun A, Virnekas B. Fully synthetic human combinatorial antibody libraries (HuCAL) based on modular consensus frameworks and CDRs randomized with trinucleotides. *Journal of molecular biology.* Feb 11 2000;296(1):57-86.

112. Gargir A, Ofek I, Meron-Sudai S, Tanamy MG, Kabouridis PS, Nissim A. Single chain antibodies specific for fatty acids derived from a semi-synthetic phage display library. *Biochim Biophys Acta*. Jan 15 2002;1569(1-3):167-173.
113. Tsuruta LR, Tomioka Y, Hishinuma T, Kato Y, Itoh K, Suzuki T, Oguri H, Hiramama M, Goto J, Mizugaki M. Characterization of 11-dehydro-thromboxane B2 recombinant antibody obtained by phage display technology. *Prostaglandins Leukot Essent Fatty Acids*. Apr 2003;68(4):273-284.
114. Tao MH, Morrison SL. Studies of aglycosylated chimeric mouse-human IgG. Role of carbohydrate in the structure and effector functions mediated by the human IgG constant region. *J Immunol*. Oct 15 1989;143(8):2595-2601.
115. Yamaguchi Y, Nishimura M, Nagano M, Yagi H, Sasakawa H, Uchida K, Shitara K, Kato K. Glycoform-dependent conformational alteration of the Fc region of human immunoglobulin G1 as revealed by NMR spectroscopy. *Biochim Biophys Acta*. Apr 2006;1760(4):693-700.
116. Mimura Y, Church S, Ghirlando R, Ashton PR, Dong S, Goodall M, Lund J, Jefferis R. The influence of glycosylation on the thermal stability and effector function expression of human IgG1-Fc: properties of a series of truncated glycoforms. *Molecular immunology*. Aug-Sep 2000;37(12-13):697-706.
117. Sethuraman N, Stadheim TA. Challenges in therapeutic glycoprotein production. *Current opinion in biotechnology*. Aug 2006;17(4):341-346.
118. Verma R, Boleti E, George AJ. Antibody engineering: comparison of bacterial, yeast, insect and mammalian expression systems. *Journal of immunological methods*. Jul 1 1998;216(1-2):165-181.
119. Wood CR, Boss MA, Kenten JH, Calvert JE, Roberts NA, Emtage JS. The synthesis and in vivo assembly of functional antibodies in yeast. *Nature*. Apr 4-10 1985;314(6010):446-449.
120. Li H, Sethuraman N, Stadheim TA, Zha D, Prinz B, Ballew N, Bobrowicz P, Choi BK, Cook WJ, Cukan M, Houston-Cummings NR, Davidson R, Gong B, Hamilton SR, Hoopes JP, Jiang Y, Kim N, Mansfield R, Nett JH, Rios S,

- Strawbridge R, Wildt S, Gerngross TU. Optimization of humanized IgGs in glycoengineered *Pichia pastoris*. *Nat Biotechnol*. Feb 2006;24(2):210-215.
121. Boss MA, Kenten JH, Wood CR, Emtage JS. Assembly of functional antibodies from immunoglobulin heavy and light chains synthesised in *E. coli*. *Nucleic acids research*. May 11 1984;12(9):3791-3806.
122. Skerra A. Bacterial expression of immunoglobulin fragments. *Current opinion in immunology*. Apr 1993;5(2):256-262.
123. Schlapschy M, Skerra A. Periplasmic chaperones used to enhance functional secretion of proteins in *E. coli*. *Methods Mol Biol*. 2011;705:211-224.
124. Venturi M, Seifert C, Hunte C. High level production of functional antibody Fab fragments in an oxidizing bacterial cytoplasm. *Journal of molecular biology*. Jan 4 2002;315(1):1-8.
125. Simmons LC, Reilly D, Klimowski L, Raju TS, Meng G, Sims P, Hong K, Shields RL, Damico LA, Rancatore P, Yansura DG. Expression of full-length immunoglobulins in *Escherichia coli*: rapid and efficient production of aglycosylated antibodies. *Journal of immunological methods*. May 1 2002;263(1-2):133-147.
126. Levy R, Weiss R, Chen G, Iverson BL, Georgiou G. Production of correctly folded Fab antibody fragment in the cytoplasm of *Escherichia coli* *trxB* *gor* mutants via the coexpression of molecular chaperones. *Protein Expr Purif*. Nov 2001;23(2):338-347.
127. Brennan PJ. Structure, function, and biogenesis of the cell wall of *Mycobacterium tuberculosis*. *Tuberculosis (Edinburgh, Scotland)*. 2003;83(1-3):91-97.
128. Minnikin DE, Kremer L, Dover LG, Besra GS. The methyl-branched fortifications of *Mycobacterium tuberculosis*. *Chemistry & biology*. May 2002;9(5):545-553.
129. Peter J, Green C, Hoelscher M, Mwaba P, Zumla A, Dheda K. Urine for the diagnosis of tuberculosis: current approaches, clinical applicability, and new

- developments. *Current opinion in pulmonary medicine*. May 2010;16(3):262-270.
- 130.** Gouzy A, Nigou J, Gilleron M, Neyrolles O, Tailleux L, Gordon SV. Tuberculosis 2012: biology, pathogenesis and intervention strategies; an update from the city of light. *Res Microbiol*. Apr 2013;164(3):270-280.
- 131.** Sharma M, Sethi S, Mishra AK, Chatterjee SS, Wanchu A, Nijhawan R. Efficacy of an in-house polymerase chain reaction assay for rapid diagnosis of Mycobacterium tuberculosis in patients with tubercular lymphadenitis: comparison with fine needle aspiration cytology and conventional techniques. *Indian J Pathol Microbiol*. Oct-Dec 2010;53(4):714-717.
- 132.** Moreira LO, Mattos-Guaraldi AL, Andrade AF. Novel lipoarabinomannan-like lipoglycan (CdiLAM) contributes to the adherence of Corynebacterium diphtheriae to epithelial cells. *Archives of microbiology*. Nov 2008;190(5):521-530.
- 133.** Gibson KJ, Gilleron M, Constant P, Puzo G, Nigou J, Besra GS. Structural and functional features of Rhodococcus ruber lipoarabinomannan. *Microbiology*. Jun 2003;149(Pt 6):1437-1445.
- 134.** Gibson KJ, Gilleron M, Constant P, Puzo G, Nigou J, Besra GS. Identification of a novel mannose-capped lipoarabinomannan from Amycolatopsis sulphurea. *The Biochemical journal*. Jun 15 2003;372(Pt 3):821-829.
- 135.** Gibson KJ, Gilleron M, Constant P, Brando T, Puzo G, Besra GS, Nigou J. Tsukamurella paurometabola lipoglycan, a new lipoarabinomannan variant with pro-inflammatory activity. *The Journal of biological chemistry*. May 28 2004;279(22):22973-22982.
- 136.** Hur M, Moon HW, Yun YM, Kang TY, Kim HS, Lee KM, Kang SH, Lee EH. Detection of tuberculosis using artus M. tuberculosis PCR Kit and COBAS AMPLICOR Mycobacterium tuberculosis Test. *The international journal of tuberculosis and lung disease : the official journal of the International Union against Tuberculosis and Lung Disease*. Jun 2011;15(6):795-798.

137. Schlesinger LS, Hull SR, Kaufman TM. Binding of the terminal mannosyl units of lipoarabinomannan from a virulent strain of *Mycobacterium tuberculosis* to human macrophages. *J Immunol.* Apr 15 1994;152(8):4070-4079.
138. Torrelles JB, Knaup R, Kolareth A, Slepishkina T, Kaufman TM, Kang P, Hill PJ, Brennan PJ, Chatterjee D, Belisle JT, Musser JM, Schlesinger LS. Identification of *Mycobacterium tuberculosis* clinical isolates with altered phagocytosis by human macrophages due to a truncated lipoarabinomannan. *The Journal of biological chemistry.* Nov 14 2008;283(46):31417-31428.
139. Rachow A, Zumla A, Heinrich N, Rojas-Ponce G, Mtafya B, Reither K, Ntinginya EN, O'Grady J, Huggett J, Dheda K, Boehme C, Perkins M, Saathoff E, Hoelscher M. Rapid and accurate detection of *Mycobacterium tuberculosis* in sputum samples by Cepheid Xpert MTB/RIF assay--a clinical validation study. *PloS one.* 2011;6(6):e20458.
140. Wojtas B, Fijalkowska B, Wlodarczyk A, Schollenberger A, Niemialtowski M, Hamasur B, Pawlowski A, Krzyzowska M. Mannosylated lipoarabinomannan balances apoptosis and inflammatory state in mycobacteria-infected and uninfected bystander macrophages. *Microbial pathogenesis.* Jul-Aug 2011;51(1-2):9-21.
141. Vergne I, Chua J, Deretic V. Tuberculosis toxin blocking phagosome maturation inhibits a novel Ca²⁺/calmodulin-PI3K hVPS34 cascade. *J Exp Med.* Aug 18 2003;198(4):653-659.
142. Welin A, Winberg ME, Abdalla H, Sarndahl E, Rasmusson B, Stendahl O, Lerm M. Incorporation of *Mycobacterium tuberculosis* lipoarabinomannan into macrophage membrane rafts is a prerequisite for the phagosomal maturation block. *Infection and immunity.* Jul 2008;76(7):2882-2887.
143. Geijtenbeek TB, Van Vliet SJ, Koppel EA, Sanchez-Hernandez M, Vandenbroucke-Grauls CM, Appelmelk B, Van Kooyk Y. Mycobacteria target DC-SIGN to suppress dendritic cell function. *J Exp Med.* Jan 6 2003;197(1):7-17.

144. Varma-Basil M, Garima K, Pathak R, Dwivedi SK, Narang A, Bhatnagar A, Bose M. Development of a novel PCR restriction analysis of the hsp65 gene as a rapid method to screen for the Mycobacterium tuberculosis complex and nontuberculous mycobacteria in high-burden countries. *Journal of clinical microbiology*. Apr 2013;51(4):1165-1170.
145. Mahon RN, Sande OJ, Rojas RE, Levine AD, Harding CV, Boom WH. Mycobacterium tuberculosis ManLAM inhibits T-cell-receptor signaling by interference with ZAP-70, Lck and LAT phosphorylation. *Cellular immunology*. Jan-Feb 2012;275(1-2):98-105.
146. Appelmelk BJ, den Dunnen J, Driessen NN, Ummels R, Pak M, Nigou J, Larrouy-Maumus G, Gurcha SS, Movahedzadeh F, Geurtsen J, Brown EJ, Eysink Smeets MM, Besra GS, Willemsen PT, Lowary TL, van Kooyk Y, Maaskant JJ, Stoker NG, van der Ley P, Puzo G, Vandenbroucke-Grauls CM, Wieland CW, van der Poll T, Geijtenbeek TB, van der Sar AM, Bitter W. The mannose cap of mycobacterial lipoarabinomannan does not dominate the Mycobacterium-host interaction. *Cellular microbiology*. Apr 2008;10(4):930-944.
147. Afonso-Barroso A, Clark SO, Williams A, Rosa GT, Nobrega C, Silva-Gomes S, Vale-Costa S, Ummels R, Stoker N, Movahedzadeh F, van der Ley P, Sloots A, Cot M, Appelmelk BJ, Puzo G, Nigou J, Geurtsen J, Appelberg R. Lipoarabinomannan mannose caps do not affect mycobacterial virulence or the induction of protective immunity in experimental animal models of infection and have minimal impact on in vitro inflammatory responses. *Cellular microbiology*. Nov 2 2012.
148. Hida Y, Hisada K, Shimada A, Yamashita M, Kimura H, Yoshida H, Iwasaki H, Iwano M. Rapid detection of the Mycobacterium tuberculosis complex by use of quenching probe PCR (geneCube). *Journal of clinical microbiology*. Nov 2012;50(11):3604-3608.
149. Gounder CR, Kufa T, Wada NI, Mngomezulu V, Charalambous S, Hanifa Y, Fielding K, Grant A, Dorman S, Chaisson RE, Churchyard GJ. Diagnostic accuracy of a urine lipoarabinomannan enzyme-linked immunosorbent assay

- for screening ambulatory HIV-infected persons for tuberculosis. *J Acquir Immune Defic Syndr.* Oct 1 2011;58(2):219-223.
- 150.** Shah M, Martinson NA, Chaisson RE, Martin DJ, Variava E, Dorman SE. Quantitative analysis of a urine-based assay for detection of lipoarabinomannan in patients with tuberculosis. *Journal of clinical microbiology.* Aug 2010;48(8):2972-2974.
- 151.** Shah M, Variava E, Holmes CB, Coppin A, Golub JE, McCallum J, Wong M, Luke B, Martin DJ, Chaisson RE, Dorman SE, Martinson NA. Diagnostic accuracy of a urine lipoarabinomannan test for tuberculosis in hospitalized patients in a High HIV prevalence setting. *J Acquir Immune Defic Syndr.* Oct 1 2009;52(2):145-151.
- 152.** Mutetwa R, Boehme C, Dimairo M, Bandason T, Munyati SS, Mangwanya D, Mungofa S, Butterworth AE, Mason PR, Corbett EL. Diagnostic accuracy of commercial urinary lipoarabinomannan detection in African tuberculosis suspects and patients. *The international journal of tuberculosis and lung disease : the official journal of the International Union against Tuberculosis and Lung Disease.* Oct 2009;13(10):1253-1259.
- 153.** Daley P, Michael JS, Hmar P, Latha A, Chordia P, Mathai D, John KR, Pai M. Blinded evaluation of commercial urinary lipoarabinomannan for active tuberculosis: a pilot study. *The international journal of tuberculosis and lung disease : the official journal of the International Union against Tuberculosis and Lung Disease.* Aug 2009;13(8):989-995.
- 154.** Dheda K, Davids V, Lenders L, Roberts T, Meldau R, Ling D, Brunet L, van Zyl Smit R, Peter J, Green C, Badri M, Sechi L, Sharma S, Hoelscher M, Dawson R, Whitelaw A, Blackburn J, Pai M, Zumla A. Clinical utility of a commercial LAM-ELISA assay for TB diagnosis in HIV-infected patients using urine and sputum samples. *PloS one.* 2010;5(3):e9848.
- 155.** Peter JG, Cashmore TJ, Meldau R, Theron G, van Zyl-Smit R, Dheda K. Diagnostic accuracy of induced sputum LAM ELISA for tuberculosis diagnosis in sputum-scarce patients. *The international journal of tuberculosis and lung*

- disease : the official journal of the International Union against Tuberculosis and Lung Disease*. Aug 2012;16(8):1108-1112.
- 156.** Wood R, Racow K, Bekker LG, Middelkoop K, Vogt M, Kreiswirth BN, Lawn SD. Lipoarabinomannan in urine during tuberculosis treatment: association with host and pathogen factors and mycobacteriuria. *BMC Infect Dis*. 2012;12:47.
- 157.** Lawn SD, Kerkhoff AD, Vogt M, Wood R. Diagnostic accuracy of a low-cost, urine antigen, point-of-care screening assay for HIV-associated pulmonary tuberculosis before antiretroviral therapy: a descriptive study. *The Lancet infectious diseases*. Mar 2012;12(3):201-209.
- 158.** McNerney R, Maeurer M, Abubakar I, Marais B, McHugh TD, Ford N, Weyer K, Lawn S, Grobusch MP, Memish Z, Squire SB, Pantaleo G, Chakaya J, Casenghi M, Migliori GB, Mwaba P, Zijenah L, Hoelscher M, Cox H, Swaminathan S, Kim PS, Schito M, Harari A, Bates M, Schwank S, O'Grady J, Pletschette M, Ditui L, Atun R, Zumla A. Tuberculosis diagnostics and biomarkers: needs, challenges, recent advances, and opportunities. *The Journal of infectious diseases*. May 15 2012;205 Suppl 2:S147-158.
- 159.** Lawn SD, Kerkhoff AD, Vogt M, Wood R. Clinical significance of lipoarabinomannan detection in urine using a low-cost point-of-care diagnostic assay for HIV-associated tuberculosis. *Aids*. Aug 24 2012;26(13):1635-1643.
- 160.** Butler WR, Guthertz LS. Mycolic acid analysis by high-performance liquid chromatography for identification of Mycobacterium species. *Clinical microbiology reviews*. Oct 2001;14(4):704-726, table of contents.
- 161.** Viader-Salvado JM, Molina-Torres CA, Guerrero-Olazarán M. Detection and identification of mycobacteria by mycolic acid analysis of sputum specimens and young cultures. *Journal of microbiological methods*. Sep 2007;70(3):479-483.
- 162.** Song SH, Park KU, Lee JH, Kim EC, Kim JQ, Song J. Electrospray ionization-tandem mass spectrometry analysis of the mycolic acid profiles for the

- identification of common clinical isolates of mycobacterial species. *Journal of microbiological methods*. May 2009;77(2):165-177.
- 163.** Leite CQ, de Souza CW, Leite SR. Identification of mycobacteria by thin layer chromatographic analysis of mycolic acids and conventional biochemical method: four years of experience. *Memorias do Instituto Oswaldo Cruz*. Nov-Dec 1998;93(6):801-805.
- 164.** Watanabe M, Aoyagi Y, Ridell M, Minnikin DE. Separation and characterization of individual mycolic acids in representative mycobacteria. *Microbiology*. Jul 2001;147(Pt 7):1825-1837.
- 165.** Watanabe M, Aoyagi Y, Mitome H, Fujita T, Naoki H, Ridell M, Minnikin DE. Location of functional groups in mycobacterial meromycolate chains; the recognition of new structural principles in mycolic acids. *Microbiology*. Jun 2002;148(Pt 6):1881-1902.
- 166.** Nishiuchi Y, Baba T, Hotta HH, Yano I. Mycolic acid analysis in *Nocardia* species. The mycolic acid compositions of *Nocardia asteroides*, *N. farcinica*, and *N. nova*. *Journal of microbiological methods*. Aug 1999;37(2):111-122.
- 167.** Verschoor JA, Baird MS, Grooten J. Towards understanding the functional diversity of cell wall mycolic acids of *Mycobacterium tuberculosis*. *Progress in lipid research*. Oct 2012;51(4):325-339.
- 168.** Toney NC, Toney SR, Butler WR. Utility of high-performance liquid chromatography analysis of mycolic acids and partial 16S rRNA gene sequencing for routine identification of *Mycobacterium* spp. in a national reference laboratory. *Diagn Microbiol Infect Dis*. Jun 2010;67(2):143-152.
- 169.** Gebhardt H, Meniche X, Tropis M, Kramer R, Daffe M, Morbach S. The key role of the mycolic acid content in the functionality of the cell wall permeability barrier in *Corynebacterineae*. *Microbiology*. May 2007;153(Pt 5):1424-1434.
- 170.** Herrera-Alcaraz E, Valero-Guillen P, Martin-Luengo F, Canteras-Jordana M. Numerical analysis of fatty and mycolic acid profiles of *Corynebacterium urealyticum* and other related corynebacteria. *Microbiologia*. Apr 1993;9(1):53-62.

171. Ojha AK, Baughn AD, Sambandan D, Hsu T, Trivelli X, Guerardel Y, Alahari A, Kremer L, Jacobs WR, Jr., Hatfull GF. Growth of *Mycobacterium tuberculosis* biofilms containing free mycolic acids and harbouring drug-tolerant bacteria. *Molecular microbiology*. Jul 2008;69(1):164-174.
172. Peyron P, Vaubourgeix J, Poquet Y, Levillain F, Botanch C, Bardou F, Daffe M, Emile JF, Marchou B, Cardona PJ, de Chastellier C, Altare F. Foamy macrophages from tuberculous patients' granulomas constitute a nutrient-rich reservoir for *M. tuberculosis* persistence. *PLoS pathogens*. Nov 2008;4(11):e1000204.
173. Korf J, Stoltz A, Verschoor J, De Baetselier P, Grooten J. The *Mycobacterium tuberculosis* cell wall component mycolic acid elicits pathogen-associated host innate immune responses. *European journal of immunology*. Mar 2005;35(3):890-900.
174. Barkan D, Hedhli D, Yan HG, Huygen K, Glickman MS. *Mycobacterium tuberculosis* lacking all mycolic acid cyclopropanation is viable but highly attenuated and hyperinflammatory in mice. *Infection and immunity*. Jun 2012;80(6):1958-1968.
175. Vander Beken S, Al Dulayymi JR, Naessens T, Koza G, Maza-Iglesias M, Rowles R, Theunissen C, De Medts J, Lanckacker E, Baird MS, Grooten J. Molecular structure of the *Mycobacterium tuberculosis* virulence factor, mycolic acid, determines the elicited inflammatory pattern. *European journal of immunology*. Feb 2011;41(2):450-460.
176. Montamat-Sicotte DJ, Millington KA, Willcox CR, Hingley-Wilson S, Hackforth S, Innes J, Kon OM, Lammas DA, Minnikin DE, Besra GS, Willcox BE, Lalvani A. A mycolic acid-specific CD1-restricted T cell population contributes to acute and memory immune responses in human tuberculosis infection. *The Journal of clinical investigation*. Jun 2011;121(6):2493-2503.
177. Schroeder EK, de Souza N, Santos DS, Blanchard JS, Basso LA. Drugs that inhibit mycolic acid biosynthesis in *Mycobacterium tuberculosis*. *Current pharmaceutical biotechnology*. Sep 2002;3(3):197-225.

178. Lemmer Y, Thanyani ST, Vrey PJ, Driver CH, Venter L, van Wyngaardt S, ten Bokum AM, Ozoemena KI, Pilcher LA, Fernig DG, Stoltz AC, Swai HS, Verschoor JA. Chapter 5 - Detection of antimycolic acid antibodies by liposomal biosensors. *Methods in enzymology*. 2009;464:79-104.
179. Benadie Y, Deysel M, Siko DG, Roberts VV, Van Wyngaardt S, Thanyani ST, Sekanka G, Ten Bokum AM, Collett LA, Grooten J, Baird MS, Verschoor JA. Cholesteroid nature of free mycolic acids from *M. tuberculosis*. *Chemistry and physics of lipids*. Apr 2008;152(2):95-103.
180. Villeneuve M, Kawai M, Watanabe M, Aoyagi Y, Hitotsuyanagi Y, Takeya K, Gouda H, Hirono S, Minnikin DE, Nakahara H. Differential conformational behaviors of alpha-mycolic acids in Langmuir monolayers and computer simulations. *Chemistry and physics of lipids*. Jun 2010;163(6):569-579.
181. Villeneuve M, Kawai M, Kanashima H, Watanabe M, Minnikin DE, Nakahara H. Temperature dependence of the Langmuir monolayer packing of mycolic acids from *Mycobacterium tuberculosis*. *Biochim Biophys Acta*. Sep 15 2005;1715(2):71-80.
182. Beukes M, Lemmer Y, Deysel M, Al Dulayymi JR, Baird MS, Koza G, Iglesias MM, Rowles RR, Theunissen C, Grooten J, Toschi G, Roberts VV, Pilcher L, Van Wyngaardt S, Mathebula N, Balogun M, Stoltz AC, Verschoor JA. Structure-function relationships of the antigenicity of mycolic acids in tuberculosis patients. *Chemistry and physics of lipids*. Nov 2010;163(8):800-808.
183. Simmons LC, Yansura DG. Translational level is a critical factor for the secretion of heterologous proteins in *Escherichia coli*. *Nat Biotechnol*. May 1996;14(5):629-634.
184. Chan CE, Chan AH, Lim AP, Hanson BJ. Comparison of the efficiency of antibody selection from semi-synthetic scFv and non-immune Fab phage display libraries against protein targets for rapid development of diagnostic immunoassays. *Journal of immunological methods*. Oct 28 2011;373(1-2):79-88.

185. Durocher Y, Perret S, Kamen A. High-level and high-throughput recombinant protein production by transient transfection of suspension-growing human 293-EBNA1 cells. *Nucleic acids research*. Jan 15 2002;30(2):E9.
186. Adams EW, Ratner DM, Bokesch HR, McMahon JB, O'Keefe BR, Seeberger PH. Oligosaccharide and glycoprotein microarrays as tools in HIV glycobiology; glycan-dependent gp120/protein interactions. *Chemistry & biology*. Jun 2004;11(6):875-881.
187. Holemann A, Stocker BL, Seeberger PH. Synthesis of a core arabinomannan oligosaccharide of *Mycobacterium tuberculosis*. *J Org Chem*. Oct 13 2006;71(21):8071-8088.
188. Graslund S, Nordlund P, Weigelt J, Hallberg BM, Bray J, Gileadi O, Knapp S, Oppermann U, Arrowsmith C, Hui R, Ming J, dhe-Paganon S, Park HW, Savchenko A, Yee A, Edwards A, Vincentelli R, Cambillau C, Kim R, Kim SH, Rao Z, Shi Y, Terwilliger TC, Kim CY, Hung LW, Waldo GS, Peleg Y, Albeck S, Unger T, Dym O, Prilusky J, Sussman JL, Stevens RC, Lesley SA, Wilson IA, Joachimiak A, Collart F, Dementieva I, Donnelly MI, Eschenfeldt WH, Kim Y, Stols L, Wu R, Zhou M, Burley SK, Emtage JS, Sauder JM, Thompson D, Bain K, Luz J, Gheyi T, Zhang F, Atwell S, Almo SC, Bonanno JB, Fiser A, Swaminathan S, Studier FW, Chance MR, Sali A, Acton TB, Xiao R, Zhao L, Ma LC, Hunt JF, Tong L, Cunningham K, Inouye M, Anderson S, Janjua H, Shastry R, Ho CK, Wang D, Wang H, Jiang M, Montelione GT, Stuart DI, Owens RJ, Daenke S, Schutz A, Heinemann U, Yokoyama S, Bussow K, Gunsalus KC. Protein production and purification. *Nat Methods*. Feb 2008;5(2):135-146.
189. Lee YJ, Kim HS, Ryu AJ, Jeong KJ. Enhanced production of full-length immunoglobulin G via the signal recognition particle (SRP)-dependent pathway in *Escherichia coli*. *J Biotechnol*. May 20 2013;165(2):102-108.
190. Skerra A. Use of the tetracycline promoter for the tightly regulated production of a murine antibody fragment in *Escherichia coli*. *Gene*. Dec 30 1994;151(1-2):131-135.

191. Lutz R, Bujard H. Independent and tight regulation of transcriptional units in *Escherichia coli* via the LacR/O, the TetR/O and AraC/I1-I2 regulatory elements. *Nucleic acids research*. Mar 15 1997;25(6):1203-1210.
192. Ehrt S, Guo XV, Hickey CM, Ryou M, Monteleone M, Riley LW, Schnappinger D. Controlling gene expression in mycobacteria with anhydrotetracycline and Tet repressor. *Nucleic acids research*. 2005;33(2):e21.
193. Lund PA. Multiple chaperonins in bacteria--why so many? *FEMS microbiology reviews*. Jul 2009;33(4):785-800.
194. Kasprowicz VO, Mitchell JE, Chetty S, Govender P, Huang KH, Fletcher HA, Webster DP, Brown S, Kasmar A, Millington K, Day CL, Mkhwanazi N, McClurg C, Chonco F, Lalvani A, Walker BD, Ndung'u T, Klenerman P. A molecular assay for sensitive detection of pathogen-specific T-cells. *PloS one*. 2011;6(8):e20606.
195. Reither K, Saathoff E, Jung J, Minja LT, Kroidl I, Saad E, Huggett JF, Ntinginya EN, Maganga L, Maboko L, Hoelscher M. Low sensitivity of a urine LAM-ELISA in the diagnosis of pulmonary tuberculosis. *BMC Infect Dis*. 2009;9:141.
196. Nigou J, Gilleron M, Puzo G. Lipoarabinomannans: from structure to biosynthesis. *Biochimie*. Jan-Feb 2003;85(1-2):153-166.
197. Kaur D, Lowary TL, Vissa VD, Crick DC, Brennan PJ. Characterization of the epitope of anti-lipoarabinomannan antibodies as the terminal hexaarabinofuranosyl motif of mycobacterial arabinans. *Microbiology*. Oct 2002;148(Pt 10):3049-3057.
198. Lim AP, Chan CE, Wong SK, Chan AH, Ooi EE, Hanson BJ. Neutralizing human monoclonal antibody against H5N1 influenza HA selected from a Fab-phage display library. *Virology*. 2008;5:130.
199. Murase T, Zheng RB, Joe M, Bai Y, Marcus SL, Lowary TL, Ng KK. Structural insights into antibody recognition of mycobacterial polysaccharides. *Journal of molecular biology*. Sep 18 2009;392(2):381-392.

200. Schoonbroodt S, Steukers M, Viswanathan M, Frans N, Timmermans M, Wehnert A, Nguyen M, Ladner RC, Hoet RM. Engineering antibody heavy chain CDR3 to create a phage display Fab library rich in antibodies that bind charged carbohydrates. *J Immunol*. Nov 1 2008;181(9):6213-6221.
201. Mao S, Gao C, Lo CH, Wirsching P, Wong CH, Janda KD. Phage-display library selection of high-affinity human single-chain antibodies to tumor-associated carbohydrate antigens sialyl Lewisx and Lewisx. *Proceedings of the National Academy of Sciences of the United States of America*. Jun 8 1999;96(12):6953-6958.
202. Crowther JR. Systems in ELISA. *Methods in Molecular Biology, The ELISA Guidebook*. Totowa, NJ: Humana Press, Inc.; 2009:9-42.
203. Morrison SL, Johnson MJ, Herzenberg LA, Oi VT. Chimeric human antibody molecules: mouse antigen-binding domains with human constant region domains. *Proceedings of the National Academy of Sciences of the United States of America*. Nov 1984;81(21):6851-6855.
204. Hofman F. Immunohistochemistry. *Current Protocols in Immunology*. 2002;49:21.24.21–21.24.23.
205. Ahmed HG, Nassar AS, Ginawi I. Screening for tuberculosis and its histological pattern in patients with enlarged lymph node. *Pathology research international*. 2011;2011:417635.
206. Seiler P, Ulrichs T, Bandermann S, Pradl L, Jorg S, Krenn V, Morawietz L, Kaufmann SH, Aichele P. Cell-wall alterations as an attribute of Mycobacterium tuberculosis in latent infection. *The Journal of infectious diseases*. Nov 1 2003;188(9):1326-1331.
207. McCloskey N, Turner MW, Steffner P, Owens R, Goldblatt D. Human constant regions influence the antibody binding characteristics of mouse-human chimeric IgG subclasses. *Immunology*. Jun 1996;88(2):169-173.
208. Tischenko VM, Zav'yalov VP. Core hinge of human immunoglobulin G3 as a system of four independent co-operative blocks. *Immunology letters*. May 1 2003;86(3):281-285.

209. Sarkar S, Tang XL, Das D, Spencer JS, Lowary TL, Suresh MR. A bispecific antibody based assay shows potential for detecting tuberculosis in resource constrained laboratory settings. *PloS one*. 2012;7(2):e32340.
210. Sharma K, Sharma A, Modi M, Singh G, Kaur H, Varma S, Sharma M. PCR detection of co-infection with *Mycobacterium tuberculosis* and *Mycobacterium avium* in AIDS patients with meningitis. *J Med Microbiol*. Dec 2012;61(Pt 12):1789-1791.
211. Griffith DE, Aksamit T, Brown-Elliott BA, Catanzaro A, Daley C, Gordin F, Holland SM, Horsburgh R, Huitt G, Iademarco MF, Iseman M, Olivier K, Ruoss S, von Reyn CF, Wallace RJ, Jr., Winthrop K. An official ATS/IDSA statement: diagnosis, treatment, and prevention of nontuberculous mycobacterial diseases. *American journal of respiratory and critical care medicine*. Feb 15 2007;175(4):367-416.
212. Torres M, Casadevall A. The immunoglobulin constant region contributes to affinity and specificity. *Trends Immunol*. Feb 2008;29(2):91-97.
213. Crowther JR. Stages in ELISA. *Methods in Molecular Biology, The ELISA Guidebook*. Totowa, NJ: Humana Press, Inc.; 2009:43-78.
214. Minnikin DE. Isolation and purification of mycobacterial wall lipids. In: Hancock I, Poxton I, eds. *Bacterial Cell Surface Techniques* John Wiley & Sons; 1988:125–135.
215. Shui G, Bendt AK, Pethe K, Dick T, Wenk MR. Sensitive profiling of chemically diverse bioactive lipids. *Journal of lipid research*. Sep 2007;48(9):1976-1984.
216. Pan J, Fujiwara N, Oka S, Maekura R, Ogura T, Yano I. Anti-cord factor (trehalose 6,6'dimycolate) IgG antibody in tuberculosis patients recognizes mycolic acid subclasses. *Microbiology and immunology*. 1999;43(9):863-869.
217. Tiruvilumala P, Reichman LB. Tuberculosis. *Annu Rev Public Health*. 2002;23:403-426.

218. Lawn SD, Edwards DJ, Kranzer K, Vogt M, Bekker LG, Wood R. Urine lipoarabinomannan assay for tuberculosis screening before antiretroviral therapy diagnostic yield and association with immune reconstitution disease. *Aids*. Sep 10 2009;23(14):1875-1880.
219. Savolainen L, Kantele A, Sandboge B, Siren M, Valleala H, Tuompo R, Pusa L, Erkinjuntti-Pekkanen R, Knuutila A, Ku CL, Chi CY, Vasankari T, Tuuminen T. Modification of Clearview(R) TB ELISA for tuberculosis patients without HIV. *Clinical and vaccine immunology : CVI*. Jul 3 2013.
220. Sada E, Aguilar D, Torres M, Herrera T. Detection of lipoarabinomannan as a diagnostic test for tuberculosis. *Journal of clinical microbiology*. Sep 1992;30(9):2415-2418.
221. Schmidt R, Jacak J, Schirwitz C, Stadler V, Michel G, Marme N, Schutz GJ, Hoheisel JD, Knemeyer JP. Single-molecule detection on a protein-array assay platform for the exposure of a tuberculosis antigen. *J Proteome Res*. Mar 4 2011;10(3):1316-1322.
222. de la Rica R, Stevens MM. Plasmonic ELISA for the ultrasensitive detection of disease biomarkers with the naked eye. *Nature nanotechnology*. Dec 2012;7(12):821-824.
223. Liu F, Bergami PL, Duval M, Kuhrt D, Posner M, Cavacini L. Expression and functional activity of isotype and subclass switched human monoclonal antibody reactive with the base of the V3 loop of HIV-1 gp120. *AIDS research and human retroviruses*. Jul 2003;19(7):597-607.
224. Miao X, Li A, Chen W, Qi H, Qiu Z, Zhang Y, Zhang J, Wang M. Optimization and modification of anti-rhTNF-alpha single chain variable fragment antibody: effective in vitro affinity maturation and functional expression of chimeric Fab. *Biomedicine & pharmacotherapy = Biomedecine & pharmacotherapie*. Jun 2013;67(5):437-444.
225. Liu JL, Hu ZQ, Xing S, Xue S, Li HP, Zhang JB, Liao YC. Attainment of 15-fold higher affinity of a *Fusarium*-specific single-chain antibody by directed

molecular evolution coupled to phage display. *Molecular biotechnology*. Oct 2012;52(2):111-122.

- 226.** Oyama H, Yamaguchi S, Nakata S, Niwa T, Kobayashi N. "Breeding" diagnostic antibodies for higher assay performance: a 250-fold affinity-matured antibody mutant targeting a small biomarker. *Analytical chemistry*. May 21 2013;85(10):4930-4937.